ELECTRICAL PROPERTIES OF HETEROPHASE ION-EXCHANGED GLASS FIBRES AND MECHANICAL PROPERTIES OF GLASS FIBRES CONTAINING ALUMINIUM DISPERSOIDS

by

ASHOK SHRIVASTAVA

INTERDISCIPLINARY PROGRAMME OF MATERIALS SCIENCE

INDIAN INSTITUTE OF TECHNOLOGY KANPUR

OCTOBER, 1985

ELECTRICAL PROPERTIES OF HETEROPHASE ION-EXCHANGED GLASS FIBRES AND MECHANICAL PROPERTIES OF GLASS FIBRES CONTAINING ALUMINIUM DISPERSOIDS

A Thesis Submitted
in Partial Fulfilment of the Requirements
for theDegree of

DOCTOR OF PHILOSOPHY

by

ASHOK SHRIVASTAVA

to the

INTERDISCIPLINARY PROGRAMME OF MATERIALS SCIENCE

INDIAN INSTITUTE OF TECHNOLOGY KANPUR

OCTOBER 1985

IPMS-1985-D-SRL-EE

ओ३म्

ॐ भूर्भुव स्व । तत्सवितुवरेण्यम् भर्गो देव य धीमहि । धियो यो न प्रचोदयात ॥

(यजुर्वेद अ० ३६ म ३)

Om Bhoor Bhuvah Swah Tat Savitur Varenyam
Bhargo Devasya Dheemahi Dhiyo Yo Nah Prachodayat

(Yajuerveda ch 36 mantra 3)

—Thou O Supreme Lord The Source of Existence Intelligence and Bliss ! The Creator of The Universe ! May we prove Worthy of Thy choice and acceptance ! May we meet Thy Glorious Grace ! May Thou vouchsafe an unerring guidance to our intellects and may we follow Thy lead unto Righteousness

In the fond memory of

Amma

I dedicate this to my beloved

Father

ACKNOWLEDGEMENTS

Sanity disallows- not, expressing my- deep sense of gratitud and indebtedness to connessieur Professor D Chakravorty for his excellent guidance, lively suggestions and invigourating encouragement, throughout the course of the present research work, which ultimately transformed my unsightly- original into a completed manuscript I sincerely thank Dr D C Agrawal for not less but the same stimulating guidance, inspiration and cooperation during this work

My thanks are due to Professors E C Subbarao, K P Gupta, S Kar and Drs J Kumar, K N Rai, K Shahi, D Saran and S C Sen for their valuable suggestions and encouragement

I thank Drs Devendra Kumar, S Datta, G C Das, Om Prakash, D Bahadur, Shankar Ram, Anil K Srivastava and Kundan L Patel for their cooperation and unassuming help

I thank all my friends particularly Messrs Amar N Sen, Abhitab Verama, G Uniyal, E G Rajan, Gopal Krishna, Iswaria, P S Chauhan, Jayant, Ravi Shankar, P Singh, R.S Verma, Madho Singh, V K Malhotra, V K Srivastava, J C Srivastava, H C Bhattacharya and Miss Parvati, Geeta Ahuja and Mrs Uma Devi for rendering all possible helps whenever needed

Special acknowledgement is credited to Messrs B Sharma, Samar Das S R. Chaurasia, B K Jain, V P Sharma, U S Lal, Nar Singh, I Sharma, A N Prasad, Uma Shankar Singh and R S Sharma for their active technical assistance during this work

I feel great pleasure in thanking Mr Jawar Singh for the excellent typing and S C Barthwal for elegant figure drawings I also thank Mr Laku Lal for neat and clean cyclostylling

The Financial assistance received from Science and Engineering Pesearch Council, Department of Science and Technology Govt of India, is gratefully acknowledged

My parents transmitted to me the quest for knowledge and reverence for learning which inspired my efforts My wife Shashi and children who cheerfully and carefully nurtured these efforts with their forbearance, sacrifice and goodwill Crucially significant intellectual association of Miss Sudha further stimulated the same For them, I have rare words to express my heartify gratitute

To them, my special thanks

c

Ashok Shrivastava

CONTENTS

LIST OF TABLES

--

LIST OF FIGURES

--

LIST OF PRINCIPAL SYMBOLS

a	Flaw size
a_b	Radius of nozzle
a_c	Core radius
a_o	Inter-atomic distance
a_A, a_B	Activity of species A,B
b	Shape parameter of Weibull's distribution
B_1, B_2	Constants
c	Concentration of charge carriers
C_1	Activation energy of electron tunnelling
C	Capacitance
C_o	Surface concentration
C_A, C_B	Ionic concentrations of species A, B
D	Diameter of fibres, self diffusion coefficient
D_c	Calculated Fibre diameter
$\bar{D}$	Interdiffusion coefficient
D_o, $\bar{D}_o$	Pre-exponential factors of self diffusion and inter-diffusion coefficients
d	Grain diameter
d_1	Density
E	Young's modulus
E_R	Regressed Young's modulus
$\bar{E}$	Mean value of E
E_e	Electric field
E_c	Critical electric field
E_c^o	Energy required to create a pair of charged grains

E_o	Maximum value of electric field
E_σ	Activation energy of conductivity
E_g, E_s, E_{ll} E_H, E_D, E_τ	Other activation energies
f	Frequency
f_r, f_c	Correlation factors
F (τ)	Distribution function of relaxation times
G	Conductance
h	Planck's constant
H	Height of the glass in bushing
k	Boltzmann constant
k_e	Gradient energy coefficient
l	Length of nozzle bore
L_1, L_o	Length of fibre sample
M	Mass of sample
N_c	Cation concentration
n	Charge carrier concentration
n_1, n_2, n_3	Constants
p	Polarisation
P	Probability of failure
p_i	Load of ith sample
Q, Q_T	Activation energy for ion migration
R	Average hopping distance
R_o, R_T	D C resistances
S	Strength
S_o	Scaling parameter of Weibull's distribution
S_c	Calculated strength
e, e_i	Strain

s	Inter particle separation
T_g	Glass transition temperature
T_N, T_o, T_c	Other temperatures
V_D	Dimensionless parameter
W	Power dissipation
x	Distance
γ	Fracture energy
δ	Loss angle
$\delta(x)$	Delta Dirac function
ϵ	Dielectric constant
ϵ'	Real part of dielectric constant
ϵ''	Imaginary part of dielectric constant
η_o	Viscosity
η, $\eta_{cladding}$ η_{core}	Refractive indices
ρ	Resistivity
ρ_o, ρ_{OT}	Pre-exponential factors of resistivity
σ	Conductivity
σ_o	Pre-exponential factor of conductivity
σ_s	Stress
σ_m	Theoretical strength of glass
τ	Relexation times
μ	Mobility
μ_o	Pre-exponential factor of mobility
ω	Angular frequency
ω_α, ω_β	Width of α, β phases

SYNOPSIS

1	Name of student	ASHOK SHRIVASTAVA
2	Programme	Ph D
3	Department	Interdisciplinary Programme in Materials Science Indian Institute of Technology Kanpur INDIA
4	Title of Thesis	Electrical Properties of Heterophase Ion-exchanged Glass Fibres and Mechanical Properties of Glass Fibres Containing Aluminium Dispersoids
5	Thesis Supervisors	(i) Professor D Chakravorty (ii) Dr D C Agrawal

Alkali containing oxide glasses have long been known to conduct electricity by the alkali ion migration under the influence of an electric field But only recently with the development of several high conducting glass systems, ionic conduction in glasses have attained new dimensions Such glass systems are known as fast ion conducting glasses (FIC) and they display very high value of ionic conductivity of the order of 10^{-2} $(Ohm\text{-}Cm)^{-1}$ at room temperature These find wide applications as solid electrolytes in various energy devices More than 100 FIC's are reported in the literature and almost all of them have lithium or silver as the migrating species Highest conductivity is exhibited by FIC's based on silver ion migration Most of such FIC s are based upon compositions derived from AgI which itself is FIC in the

crystalline form and very few of these are based on SiO_2 as the network former because of the problem of silver precipitating out as metallic agglomerates during the melting operation In the present thesis large concentration of silver in silica based glass has been achieved by sodium-silver ion exchange treatment As the silver rich layer formed at the glass surface by the ion-exchange treatment is of the order of a few microns, possibility of replacing almost all the alkali ions by silver ions by this treatment has been explored by ion exchanging the base glass in fibre form The average diameter of the fibres used is around 10 microns The effect of such an ion exchange process on electrical conductivity has been studied

Presence of ultrafine metallic granules in glass has a significant effect on its electrical conductivity. Such metal-glass microcomposites with aluminium as a dispersion metal in glass matrix, have been prepared Role of metallic dispersoids on ionic conductivity of alkali containing glasses and that of their ion exchanged versions has been investigated. It has been found that there is a large enhancement in electrical conductivity of glasses by metallic dispersion and ion-exchange treatment It has been further observed for the first time, that high conducting glasses with almost negligible activation energy can be developed with conductivities at room temperature of the order of 10^{-2} $(ohm\ Cm)^{-1}$ It has been further shown that aluminium dispersoids further enhance the conductivity of glass The increase in conductivity is attributed to the microstructural features of

these glasses Presence of aluminium particulates further improves the morphological structure in a desirable way

Effect of aluminium particulates on the mechanical properties of glass fibres has been investigated It has been found that while strength of glass fibres decreases by the incorporation of aluminium particles, the modulus shows an increase with increasing amount of aluminium As strength is a statistical parameter the strength data have been analysed by Weibull's analysis A new technique to analyse the strength data for glass fibres has been developed Fracture surface studies have been made using scanning electron microscopy Corrosion strength of these glass fibres have been found to improve with increasing aluminium concentration

In chapeter I (Introduction), various characteristics of glasses in bulk and fibre form have been reviewed Present state of the art of glass fibre drawing technology is described Electrical and mechanical properties of glasses, both in bulk and fibre form have been discussed Various aspects of ion exchange and phase separation are described alongwith A C and D C responses of glass systems A brief review of FIC glasses is also incorporated

Chapter II (Experimental), describes the experimental techniques used to prepare and characterise glass fibres for their electrical and mechanical properties Details of fibre drawing assembly and conductivity cell designed and fabricated

by the author are also given in this chapter Ion-exchange treatment of glass fibres have been discussed The characterisation techniques include A C and D C electrical conductivity measurements, Chemical analysis, DTA, Transmission electron microscopy and Scanning electron microscopy

In chapter III, results of DC and AC resistivity of some silicate glasses in fibre form containing 10 to 30 mol % of sodium have been described These fibres after ion-exchange show lowering of activation energy and increase of electrical conductivity An optimum combination of electric field and temperature brings about a permanent morphological transformation in ion-exchanged samples inducing a high conducting state in them The newly attained conducting state is characterised by very low activation energy which in some cases is found to be almost tending to zero Such behaviour has been attributed to the microstructural features exhibited by the samples

In chapter IV, results of AC and DC conductivity of glass fibres of glass-metal composites containing aluminium metal dispersoids have been reported Mol % of aluminium has been varied from 0 to 10 Presence of aluminium particulates enhances the electrical conductivity of virgin and ion-exchanged samples In virgin glasses, in the temperature range 20°C to 110°C, the conduction mechanism is shown to be due to electron Tunnelling between the metallic islands in the glass matrix Ion-exchanged glass samples under the influence of electric field and temperature are found to attain a stable high conducting state chara-

cterised by very low activation energy and very high conductivity Presence of aluminium particles brings in some desirable effects in the microstructure such that maximum conductivity at room temperature is obtained for glass composition having 5 mol% of aluminium This behaviour has been supported by corresponding microstructural features

In chapter V mechanical properties of glass fibres containing various amounts of aluminium particles have been described A new technique to process the data of mechanical measurements has been suggested which gives better estimates of strength and Young modulus. As surface flaws dictate the strength of glass fibres, the data have been analysed by the Weibull method Comparision of graphical regression technique and most likelihood estimator technique (MLE) to evaluate the Weibull's parameters have been made Effect of aluminium concentration on Weibull's parameters has been investigated Fracture surface studies have been made by scanning electron microscopy Presence of small pores of the order of 1 micron explains the decrease in strength of the composite glass fibres

Chapter VI (Conclusions) gives a summary of the results of electrical properties of virgin and ion-exchanged glass fibres Similar results for fibres drawn from glass-metal micro composite systems are also described It is inferred that ion-exchanged fibres of the glass systems studied constitute a new set of FIC glasses In their high conducting state, they provide high conducting materials with almost zero activation energy Mechanical strength decreases with increasing amount of aluminium particles

CHAPTER - I

INTRODUCTION

Glass fibre is one of the most important engineering materials of the present space age It exhibits a unique set of optical, mechanical and electrical properties Its applications are enormous and diversified As a reinforcement material, it forms the backbone of G R P (Glass Reinforced Plastic) and G R C (Glass Reinforced Cement) products which have already captured a significant part of the industrial market Their use is continuously increasing GRP's have found diverse applications in space vehicles, air crafts, ships, submarines, boats, radomes, sonar domes, off shore structures, automobiles, protective armours, containers and pipes for chemical industry, corrosion resistant coatings, sporting goods, electronics and appliances (Parkyn Brian, 1970) G R C's main usage includes architectural cladding, walling systems, housing, street furnitures, water transport systems including pipes, sewer linnings, water channels, field drainage components, canal linings, tanks and various other applications in the field of agriculture and as an asbestos replacement (Smith, JW and Walker, TWL, 1980) Glass fibres with some of their characteristic optical properties, have emerged as major transmission media for light and are poised to revolutionize telecommunications (MacChesney, JB 1981) It has been possible to make these optical fibres with power loss even less than 1 dB/Km Flexibility of these optical fibres has been exploited commercially in the form of various medical and enginnering instruments (Kapany 1960, 1967, Allan 1973) In this

wide perspective of glass fibre applications, a potentially new dimension has been added by recent researches carried out to develop electrically conducting glass fibres either by a suitable choice of glass composition (Provance, JD, 1971), or by ion-exchange and reduction technique (Mozhi T Arul and Chakravorty D, 1982), or by the fiberisation of glass-metal particulate system (Chakravorty D, et al, 1979) All these interesting features associated with glass fibres, result from the coupling of innate characteristics associated with the fibre form and other useful properties exhibited by glasses in their bulk form In order to delineate the present trend of glass fibre technology and to contemplate the development of newer materials, a brief review incorporating various aspects of glass fibres and glass fibre technology is presented Various new glass forming systems including those exhibiting fast ion conduction and various technological aspects associated with glass-metal particulate systems are reviewed Dissussions on phase separation in glasses and the ion exchange process are also incorporated because of their technological importance as well as relevance to the present investigation

1 1 Glass Fibres

1.1 1 Historical Survey

Glass fibres in one form or another were known to glass makers in antiquity (Parkyn B, 1963). The Egyptian kings of xviiith Dynasty used small glass vases made of glass fibres for holding cosmetics The earliest use of woven glass fibres was reported to be in 1713 when Rene Reaumur submitted some glass

cloth to Paris Academy of Science, which had been woven by Venetian Carlo Riva In 1860, a woven glass garment was presented to spanish princess, but it was found that the fibre was too coarse to allow the garment to be folded (Parkyn B 1970).

Early in 1930's, the Owens - Illinois Glass Co. of New York, Ohio, made significant improvements to the process of glass fibre manufacture which made it commercially viable Later this company joined with Corning Glass Works of Corning, New York, which was also working in the same field, to form a specialist company namely Owens- Corning Fiber Glass Corporation, which became the undisputed leader in the development marketing and technology of this industry Upto this point, the fibre being manufactured on an industrial scale was discontinuous i e glass wool The need to insulate fine wire at high temperatures paved the way to the development of extremely well chosen formulation of glass which later became known as 'E' glass Under stress of war, economic circumstances or patent restrictions, other type of glasses were tried and for some time, found their market, they did not however gai a major importance in the industry As a result of exhaustive experimentation, some specialized glasses characterised by high chemical strength and extra high strength were also developed such as 'S' and 'HM' 905 glasses

The first patents covering room temperature thermosetting resins e.g polyesters appeared in 1935 Reinforcement of these resins with 'E' glass fibres gave birth to a new reinforced plastic industry and found its first major application in world war II

in the manufacture of radomes for aircrafts Since then, the industry has acquired a significant growth rate of 10 to 15% per annum In 1949 Pittsburgh Plate Glass and Libbey- Owens-Ford acquired licences from Owens- Corning followed by overseas licences to St Gobain in France in 1951 and Pilkington in Great Britain in 1952 New uses, better performance of composites and rapidly improving manufacturing technology have been the hall mark of this industry (Loewenstein, KL 1973)

1 1 2 Basic Features of Glass Fibres .-

Glass fibres are glass filaments usually having their diameters in the range of 3μm-15μm In the case of optical glass fibres the diameter of the cladded fibre is above 100μm Glass fibres differ from bulk glass of the same composition in two major respects first,the rate of cooling from molten state which is of the order of $10^{+5} - 10^{+3}$ °K/Sec (Manfre G, 1967) and secondly the ratio of surface to weight of glass.For an average fibre diameter of 9μm, 10gms of fibre possesses a surface area of 2 m^2 (Loewenstein KL 1973) The effect of rapid quenching on fibre formation is such that the composition and structure related properties are lower for the fibre than for the bulk glass As density,refractive index and Young's modulus are structure sensitive properties i e, they depend on the composition of glass and its configuration temperature (Loewenstein KL 1961), it has been reported that density, refractive index and Young's modulus are 2%, 15 to 40% and 7 to 25% lower respectively than those of bulk glass (Loewenstein KL 1961) This has also been

observed that when fibres of same diameter are drawn from liquid glass at various temperatures, as the temperature of glass rises, so the fibres drawn from it show a progressive decrease in Young's Modulus (Loewenstein KL and Pervin K 1962) These differences in properties between glasses in bulk and fibre form can be eliminated by heating the fibres for a sufficiently long time at temperatures between 100-400°C, the higher the temperature, the more rapid the rate at which the glass fibres become denser and acquire the same properties as the bulk glass

1 1.2 1 Strength of Glass Fibres:

The strength of glass fibres when measured at room temperature and under not an uncommon condition of 60-65% relative humidity is found to depend upon the glass composition, the fibre diameter and the temperature of the glass from which the fibreis drawn (Loewenstein KL and Dowd J 1968) The extent to which each one of these factors influences the strength varies with the composition The alkali-containing 'A' glass shows a very significant strength diameter relationship whereas the strength of nearly alkali free 'E' glass fibres is almost independent of diameter. In fact when 'E' glass fibres are tested at room temperature and at relative humidities of 40% or below, the observed tensile strengths are independent of diameter and consistant to with in a coefficient of variation of about 1% (Thomas WF, 1960) Various basic properties exhibited by some commercial glass fibres along with their chemical composition are shown in Table 1 1.

Table 1 1 : Composition and basic properties of commercial glass fibres

Constituent	E glass	C glass	A glass	S glass	Fused silica	HM 905
SiO_2	55 2	65 0	72 0	65 0	99 97	48 0
Al_2O_3	14 8	4.0	2 5	25 0	015	-
B_2O_3	7 3	5 0	0 5	-	-	8.0
MgO	3 3	3 0	0 9	10 0	-	8 5
CaO	18 7	14 0	9 0	-	0032	11 5
Na_2O	0 3	8 5	12 5	-	0022	-
K_2O	0 2	-	1 5	-	0007	-
Fe_2O_3	0 3	0 5	0 5	-	0010	-
F_2	0 3	-	-	-	-	-
BeO	-	-	-	-	-	0.0
Li_2O	-	-	-	-	-	6.0
V_2O_5	-	-	-	-	-	4.0
MoO_2	-	-	-	-	-	2 0
TiO_2	-	-	-	-	-	4 0
(1) Tensile strength of single fibre at 25°C (Kg/mm^2)	370	310	310	430		
(2) Tensile strength of straind (Kg/mm^2)	175-275	160-235	160-235	210-320		
(3) Young's modulur of fibre at 25°C (Kg/mm^2)	7700	7400	7400	8800		
(4) Density g/Cm^3	2 53	2 46	2 46	2 45		

(5)	Refractive index η_D	1 550	-	1 542	-
(6)	Coefficient of linear thermal expantion per °C x 10^6	5 0	8.0	9 0	5 0
(7)	Dielectric constant at 25°C and 10^{10} Hz	6 11	-	-	5 21
(8)	Loss tangent at 25°C and 10^{10} Hz	004	-	-	009
(9)	Volume resistivity in Ohm-Cm	10^{15}	-	10^{10}	-

The strength of glass fibres is much smaller than the theoretical strength of glasses The latter can be evaluated from the following equation (Orowan, 1949)

$$\sigma_m = \left(\frac{E \gamma}{a_o} \right)^{1/2} \qquad (11)$$

where σ_m is theoretical strength of glass

E is Young's Modulus

γ is the fracture surface energy

and a_o is the inter atomic distance

Fracture surface energies for glasses have been reported and they lie in the range of 3 5 to 4 82 Jm^{-2} at 25°C (Wiederhorn 1966)

By substituting values of E, a_o and γ as 10^{11} Nm^{-2}, 2×10^{-10} m and 3 Jm^{-2} respectively in the above equation, the theoretical strength of glass is found to be 4×10^4 MNm^{-2} which is valid for all glasses of practical interest as none of the variables in the above equation is sensitive to the glass composition

Strengths of this order of magnitude have been measured in pristine glass fibres (Procter et. al 1962) However, strengths of glasses under most conditions are 10-100 times lower than this value. This apparant anamoly in strength value is attributed to the presence of Griffith flaws as mentioned below

1 1 2 2 Griffith Equation

The order of magnitude difference between theoretical and experimental strength values is explained in terms of surface flaws which act as stress concentrators, the stress at the flowtip being much greater than in the matrix The strength S is related to the critical flaw size'a by the following equation (Griffith 1920)

$$S = \sqrt{\frac{2E\gamma}{\pi a}} \qquad (1\ 2)$$

where E is the Young' Modulus

γ is the fracture surface energy

For a fracture stress of 100 MNm^{-2} which is the usual value of S for glasses in bulk form, the critical flaw size as calculated from equation (1 2) turns out to be 20 μm It follows from equation (1 2) that any reduction in 'a' would cause an enhancement of strength (Rawson H 1984) As glass fibres show a strength an order of magnitude more than that for bulk glass, equation (1 2) suggests that surface flaws on glass fibres should be such that $a < 1\ \mu m$ The dependence of strength on surface flaws has been confirmed experimentally when removal of surface damage by etchant consisting of an equeous 15% HF and 15% H_2SO_4 solution shows improvement in the strength of glass (Proctor 1962)

1 1 2 3 Flaw Statistics

The flaws on a glass surface have a distribution of shapes and sizes Its quantitative description is given in terms

of a'flaw distribution function In principle, this function can be used to predict the strength under any specified system of loading The cumulative probability of failure is given by Weibull distribution (Weibull 1951)

$$P = 1 - \exp\left(\left(- \frac{S}{S_o} \right)^b \right) \qquad (1\ 3)$$

where S_o and b are the scaling and shape parameters respectively of the distribution The values of S_o and b are determined experimentally

1 1 2 4 Strength Protection by Surface Treatment

To protect the surface of glass fibres from abrasion and to minimise the surface damage, glass fibres are coated with a sizing material which may be a resin (Roskos T G et al 1962, Eakins WJ 1964), glass (Morley JG 1959), Metal (Morley JG 1963) or graphite (Zvanut C 1965) Recently it has been shown that various factors which contribute towards strength, include glass quality, pretreatment prior to fibre drawing, cleanliness of the heat source, nature of size application and techniques of applying it (Schonhorn H et al 1976) It has been reported that ultimate strength of laser drawn silica fibres is dependent on fibre tension and drawing velocity (Schonhorn et al 1978)

1 1 2 5 Strength Enhancement by the Precipitation of a Heterophase

Alkaliboro silicate glass fibres containing bismuth and or silver have shown marginal improvement in strength but significant enhancement in Young's Modulus (Chakravorty D ,et al 1979) This increase in strength is attributed to the deflection of cracks along the

glass metal interface during the course of crack propagation Similar effects have been observed in alkali alumino borosilicate glasses (Venkateswaran A 1979) Fibres drawn from glasses having compositions similar to that of the blast furnace slag have shown strength values comparable to that of E glass fibres with some improvement in Young's Modulus (Srivastava A and Chakravorty D. 1979) The latter has been ascribed to the presence of a crystalline phase (Srivastava A.1978) within the fibre

1 1.3 Types of Glass Fibres :

On the basis of its applications, glass fibres can be classified as follows

1.1.3.1 Reinforcement Glass Fibres

99% of the total production of glass fibres is being consumed as reinforcements for fabrication of various composite material A wide variety of such composites have been developed These composites are characterised by a matrix which can be either polymer metal or a ceramic based (Mc Creight LR et. al 1965). A suitable combination of matrix and glass fibre defines a unique composite material. A detailed study of such combinations, has resulted in the development of the following group of composites which are being commercially exploited.

(a) Glass Reinforced Plastics : Expoxide resins or polyester resin are used to make GRP's. E glass fibres are used as a reinforcement material Various lengths of fibres have been tried for reinforcement. It has been shown that polymers, reinforced with continuous

fibres exhibit strengths that are 5 times those for composites formed by short lengths In some special applications such as in aerospace industry 'S' glass fibres are used as reinforcement (Parkyn B , 1970,Loewenstein KL, 1973)

(b) Glass Reinforced Cements The invention, development and commercialisation of alkali resist nt glass fibres for glass reinforced cement has introduced a new group of building and construction materials, which is rapidly gaining acceptance around the world (Majumdar AJ and Ryder JF 1968, Proctor BA and Yale, B 1978, Blackman LCF et al 1977) A typical glass composition is 71 3 SiO_2 15 8 ZrO_2 11 5 Na_2O 2Li_2O 1 K_2O 1 MgO 1 CaO, (Bacon 1968) The early work at the U K Building Research Establishment has been commercially exploited by Pilkington Brothers U K , the fibre product being marketted as 'cemfil' (Rawson H , 1984) The ultimate strength of GRC whether it be bending tensile or impact strength is essentially dependent on the glass fibre content and form, orientation and disposition of fibres, the bonding between fibre and matrix (a function of matrix type, porosity and curing of matrix) The Young's Modulus limit of proportionality and creep behaviour of GRC, are strongly dependent on matrix property and are therefore influenced by the type of matrix being used (neat cement, mortar etc) and the degree of curve of the cement (Proctor BA 1980) Behaviour of glass fibres in strong acid and alkaline media have been studied (Ilona Wojnarovitis 1983) in this context

(c) Fibre-Reinforced Metals : Glass fibres have been used as reinforcement for metal matrix in both continuous and discontinuous forms. However the higher Shear strength available in metals permits the efficient use of short fibres, provided they are well bonded to the matrix The highiest strength achieved by using continuous filaments for reinforcing metals have been silica-fibre reinforced aluminium, which has been developed at Rolls-Royce Ltd. and used in making various items such as compressor blades for jet engines (Mc Creight et al 1965)

1 1 3 2 Optical Glass Fibres :

These consist of a core glass surrounded by a cladding layer of lower refractive index When a ray of light enters into the core region of the cladded fibre structure, the portion falling within a certain solid angle is guided by total internal reflection (Niizeki, Nobukazu 1984). The light collecting ability of a fibre is measured by its numerical aperture (NA) which is given by the lollowing relation

$$N A. = \eta_{core}\sqrt{2.\Delta} \qquad . \quad (1.4)$$

$$\text{where } \Delta = \frac{\eta_{core} - \eta_{cladding}}{\eta_{core}}$$

η_{core} = refractive index of the core

$\eta_{cladding}$ = refractive index of the cladding

The number of modes that such a fibre can transmit is related to a dimensionless parameter V_D such that

$$V_D = \frac{2\pi a_c}{\lambda} (NA) \quad .. \quad (1\ 5)$$

$$= \frac{2\pi a_c \eta_{core}}{\lambda} \sqrt{2\Delta} \quad .. \quad (1.6)$$

where a_c = core radius

λ = transmitted ligt wavelength

Depending upon the modes that can be transmitted through optical fibres these can be subdivided into the following two categories:

(a) Mono Mode Fibres: Such fibres are characterized by $V_D \leq 2\ 4$ which implies from (1 6) that for $\lambda = 800$ nm and $\Delta\eta = 01$, core diameter should be of the order of 3 5 μm

(b) Multimode Fibres : The optical glass fibres having $\Delta\eta > 01$ or core diameter $> 3\ 5\mu$m are known as multimode optical fibres These may be either of the multimode step index or the multimode graded index type

One of the stringent conditions which glass fibres have to meet so that they can act as effective optical waveguides is low loss Absorption loss is specifically caused due to the presence of transition metal ions Fe^{3+}, Co^{2+}, Cu^{2+}, Cr^{3+}, Mn^{2+} V^{3+} etc. and OH^- within the glass. Other contributions to the loss arise from Rayleigh scattering and Mie scattering (Mac Chesney 1981). With the improvement and perfection of fabrication technology, glas fibres with power loss as low as 1 dB/Km are now available

1 1 3 3 Electrically conducting glass fibres:

In recent years there has been a spurt in research activiti to develop electrically conducting glass fibres The efforts seem to be directed to three different methods which can be broadly classified as follows :

1 1 3 3.1 Coating of electrically conducting thin films on the surface of glass fibre

Various electrically conducting materials have been applied as a thin coating on the surface of the glass fibres In another technique, thin (3μm) coatings of conducting SnO_2-Sb_2O_3 have been successfully achieved by processing glass fibres with Sn (iso-PrO)$_4$ and Sb(OPr)$_3$ dissolved in iso-PrOH (Nano T and Eguchi T , 1985)

1 1 3 3 2. Glass Fibres Drawn From Glass Metal Composites :

Oxide glasses containing dispersed metallic granules of dimension of the order of a few hundred angstroms show electrical conduction by electron tunnelling mechanism between the metallic islands (Chakravorty et al 1979) Continuous glass fibres have been drawn in the system SiO_2 B_2O_3 K_2O. Al_2O_3 As_2O_3 Bi_2O_3 Ag_2O for various molar fractions of Bi_2O_3(0-3%) and Ag_2O (0-6%) respecti vely. Highiest conductivity of 10^{-8} (Ohm Cm)$^{-1}$ at room temp. has been reported

1.1.3 3.3 Electroconducting Glass Fibres Produced by Ion Exchange Followed by Reduction Treatment :

Suitable metallic particles can be precipitated in

alkali containing glasses subjecting the latter to an ion exchange an reduction treatment (Chakravorty 1975) Preliminary investigations have shown that alkali containing glass fibres subjected to a sodium ⇄silver ion exchange followed by a reduction treatment show higher electrical conductivity as compared to the virgin fibre (Mozhi, T Arul and Chakravorty D , 1982) The lowest resistivity value at room temperature is reported to be 10^5Ω-Cm The conductivity has been ascribed to an electron tunnelling mechanism as described in the previous section.

Electrically conducting glass fibres have also been developed by subjecting glass fibres drawn from a suitable glass compositions to a reduction treatment (Provance 1971). In the fabrication of image intensifier and channel multiplier, similar approach is used where by reduction of the inner surface of hollow glass fibre a conducting layer of Pb is generated An electron entering such a conducting channel kept in vacuum under influence of potential drop across the length of channel, undergoes many collisions with the conducting layers , thereby ejecting more than one electron at each impact Thus for each electron entering one end of the channel, many leave at the other (Eschard and Manley 1971 , Trap 1971, Washington et. al 1971, Mackenzie 1974, Graf and Polaert 1973)

1 1.4 Glass Fibre Drawing Process:

The fibre forming process is highly sensitive to glass melt temperature, viscosity and pulling rate Fibres are produced

as continuous filaments which are mechanically drawn from softened glass under controlled conditions various techniques have been developed. Each of these typically offers some advantages that makes it preferable in a given situation. All of them are improved versions of either of the two techniques as described below.

1.1.4 1 Bushing Technology

Glass fibres are made by rapid attenuation of drops of molten glass exuding through nozzles under gravity and suspended from them The dynamic balance between forces of surface tension and mechanical attenuation results in the drop of glass taking on the shape of a meniscus held at the annular opening of the nozzle and tapering to the diameter of the fibre being drawn. For successful fiberisation glass viscosity should be in the range of 500-1000 poises If viscosity is lower than 500 poises, the glass is too fluid and falls away from nozzle as drops because of the predominance of surface tension forces If the viscosity is higher than 1000 poises, the tension in the fibre is too high and rate of flow of glass through nozzle can become too low to maintain a meniscus (Loewenstein KL 1973)

The rate of fibre production from a given bushing is a function of the rate of flow of glass through the nozzles and is independent of rate of attenuation i.e. of the diameter of fibre mode. It has been reported that the flow rate is independent of the speed of draw and is a function of the temperature only The rate of flow is given by the poiseuille equation

$$V_f = \frac{\pi a_b^4 H d_1 g}{8 \eta_0 l} \qquad (1\ 7)$$

where V_f is rate of flow (in m^3/sec)

a_b is radius of nozzle (m)

H is height of glass above the nozzle (m)

d_1 is density of glass (Kgm/m3)

g is acceleration due to gravity (m/ sec 2)

η_0 is viscosity of glass newton-Sec/ m 2)

l is length of nozzle bore (m)

The fibre diameter is a function of the pulling rate and the bushing temperature

Almost all the fibre manufacturing units the world over employ bushings made of 10% Rhodium-Platinum and 20% Rhodium-Platinum alloys respectively the latter being more resistant to distortion at elevated temperatures Zirconium-stablised platinum, highly resistant to distortion has recently been added to the range of suitable materials. As Pt-Rh is a precious metal involving huge investment, an alternative ceramic bushing technology has been developed ((Chakravorty et al 1981) The material used for making these bushings is either pure alumina or calcia stablised zirconia single nozzle bushings as well as multi-nozzle bushings have been made using slip casting technique followed by a sintering operation

There are two processes which are currently in use depending upon the feeding mechanism of glass into the bushings

(a) Marble Melt Process In this method glass cullet is introduced into the bushing in the form of marbles.

(b) Direct Melt Process:

The raw materials are fed directly into a glass melting tank from which molten glass is led onto different bushings via a long fore hearth

In either of these processes, glass fibre undergoes sizing operation by which a thin polymer coating is applied on the pristine surface of glass fibres, to protect its strength. Glass fibres are collected on the drum through a graphite shoe

1 1 4 2 Rod Technology

The glass which is to be fibanised is taken in the form of a rod or preform. A feed mechanism operates the lowering of the rod into the hot zone of the furnace or heat source where the glass softens The glass is pulled down into a thin fibre which is wound on a drum This rotating drum provides the force for the fibre drawing operation and at the same time stores the fibre neatly by translating as it revolves Modern fibre drawing machines commercially available, are equipped with a laser monitoring device whose output excites the feed back mechanism to control the pulling speed, so as to regulate the diameter of the fibre to a preset value (Mc Chesney 1981). protective coating is applied to the fibre by an applicator placed between furnace and the drum, so as to protect the pristine glass surface of drawn fibre and to preserve the strength Pulling speed varies from a few 100m/minute to 3 Km/minute

Hardly any industry uses this rod technology to draw glass fibres for reinforcement purposes. But almost all the optical glass

fibres are drawn by this technique To meet the stringent conditions of high purity which involve an impurity level of less than a few tens of ppb and to have a cladding, number of techniques have been developed to make preforms with a characteristic structural and optical properties Many such techniques each with a set of distinct advantages are commercially being exploited In all of them a preform is fabricated by the vapour deposition technique All the glass forming elements and the required dopants are taken in vapour form and are made to undergo a chemical reaction under well controlled conditions of temperature and pressure The glass particles so formed are deposited layer by layer. The resultant tube is then collapsed to get the required preform which is subsequently fiberised to obtain the optical fibers. The various techniques to produce required preforms are as follows (Mc Chesney 1981)

1 Outside vapour phase oxidation technique (OVPO)
2 Vapour phase axial deposition technique (VAD)
3 Chemical vapour deposition technique (CVD)
4 Modified chemical vapour deposition technique (MCVD)

1 2 Electrical Properties of Glasses

Glasses exhibit a very wide range of specific resistivities at room temperature While calcium boro aluminate glasses show the highest specific resistivity of 10^{27} Ohm-Cm the metallic alloy glasses are good electronic conductors, having a specific resistivity 10^{-3} Ohm-Cm In between these two extremes are the oxide and chalcogenide semi conducting glasses All the commercial oxide glasses are good

insulators with their resistivities decreasing very rapidly with temperature (Rawson 1984)

The following sections give a brief review of the electrical behaviour of various inorganic glasses

1.2 1. Electronic Conduction :

Many glass systems show electronic conduction A good number of reviews exist concerning these semiconducting materials (Owen 1970, 1977, Owen and Spear 1976, Mott 1968, 1977) Three types of glass systems which show electronic conduction, are as follows

1 2 1 1 Chalcogenide Glasses:

These glasses are primarily based on S, Se and Tl as glass formers. It has been shown that semiconducting glasses are obtained by melting mixtures of As, Se, Te, S, Sb, Bi, Tl and P etc (Kolomiets 1964) Their d c conductivity is given by

$$\sigma = \sigma_o \exp (- E_\sigma / KT) \qquad (1.8)$$

where E_σ is the activation energy which is a constant (Fritzsche 1974) and usually lie in the range (0 5 to 1 0 eV) Although values as low as 0 2 eV and as high as 1 5 eV have also been observed The pre-exponential factor σ_o is of the order of 10^3-10^4 $(\Omega hm\ Cm)^{-1}$ but it can be as low as 10^{-5} $(\Omega hm\ Cm)^{-1}$ and as high as 10^8 $(\Omega hm\ Cm)^{-1}$ They are characterised by a well defined optical absorption edge which for absorption coefficients $\alpha > 10^4$ Cm^{-1} fits to an equation of the type ,

$$\alpha h\nu = B_2 (h\nu - Eg)^{n2} \qquad (1\ 9)$$

where B_2 is a constant, Eg is the optical energy gap which is usually equal to twice the activation energy E_σ (MottDavis 1971)

$$Eg = 2 E_\sigma \qquad (1\ 10)$$

The Seebeck coefficient S_e is a decreasing function of temperature

$$S_e = \frac{K}{e} \left[\frac{E_s}{kT} + A_1 \right] . \qquad (1\ 11)$$

Its value is of the order of millivolts per degree where A_1 is a constant and Es is not equal to E_σ or Eg/2. The difference in E_σ and E_s is in the range of 1 to .15 eV. In most of the cases Seebeck coefficient is found to be positive indicating holes dominate the transport process. The carrier mobility is given by

$$\mu = \mu_0 \exp (- E_\mu/kT) . \qquad (1\ 12)$$

This behaviour is explainable in terms of the following mechanisms

i) Direct phonon-assisted hopping between localised states (Pfister 1976)

ii) Polaron hopping (Quinn & Seager 1975, Seager et al 1973

iii) Transport of carriers in the extended states.

A C. conductivity has been measured in various systems. It has been found that variation of conductivity with frequency is given by the following relation:

$$\sigma(\omega) \propto \omega^{n_3} \quad . \qquad (1\ 13)$$

where $7 \leqslant n_3 \leqslant 1\ 0$

Eq (1 13) has been found to be valid in the case of thin films of As_2Se_3 (Lakatos and Abkowitz 1971), As_2Te_3 (Rockstad 1972), bulk samples of As_2Se_3, As_2S_3 and As_2Se_3-As_2Te_3 (Owen and Robertson 1970, Kitao 1972, Ivkin and Kolomiets 1970, Segawa 1974) and $(As_2Te_3)_{95}Ge_5$ (Lecleach and Palmier 1975) In some systems n_3 is 2(Lakatos and Abkowitz 1971) in the megacycle frequency range It is further reported that the AC component of the total conductivity, with increasing frequency becomes less temperature senstive and measured AC conductivity approaches the D C. value at high temperatures. Conductivity has been found to be insensitive to doping which is ascribed to the fact that in the disordered materials the coordination environment can adjust to satisfy the valency requirement of each atom (Mott 1967, Ovshinsky 1977) . However, electrical conductivity increases by many orders of magnitude by chemically modifying the amorphous semiconductor with relatively large amounts of nickel or other transition metal atoms (Ovshinsky 1977).

Recently it has been found out that many chalcogenide glasses become metallic under pressure with a continuous decrease in band gap and resistivity even as they retain their molecular structure (Sakai and Fritzche 1977, Minomura 1982).

small amounts of reduced ions like V^{4+}, W^{5+} and Mo^{5+} respectively. Reduction process is specially needed for Cu and Ti ions in phosphate glasses (Tsuchiya and Mariya 1975, Vaughan et al 1977) While for glasses containing large amounts of Mn, Co, Ni ions, an oxidation step is necessary as almost all the ions are present in the lower valency state.

The conductivity for these glasses is given by (Mott 1968, Austin and Mott 1969)

$$\sigma = \frac{\nu_{ph}\, e^2 c\,(1-c)}{KTR} \exp(-2\alpha_w R) \exp\left(-\frac{E_H + \frac{E_O}{2}}{KT}\right) \quad 1.14)$$

where ν_{ph} is phonon frequency

α_w is rate of decay of wavefunction

c is ratio of core of ions in lower valency state and total conc of transition metal ion

R is average hopping distance

E_H is polaron hopping energy

E_O is disorder energy

The conduction mechanism in these glasses is diffusion like in nature and the model is based on a random distribution of ions in the glass. Therefore any presence of heterogeneity will cause the conductivity to deviate from that predicted by the above theory. Maximum conductivity in iron phosphate glasses and vanadium phosphate glasses occur at c = 5 (Dozier et al 1972) and between 0.1 - 0 2 (Linnisley et al 1970) respectively. Fe and Ti ions in silicate glasses do not follow this dependence of conductivity on concentration (Rawal and Mac

Crone 1978) A model is proposed by postulating that charge carriers move along paths of relatively highly conducting chains of transition metal ions Usually $E_H \geq E_0/2$ and tends to decrease with decreasing temp. Thus in contrast to chalcogenide glasses, plots of $\log \rho$ vs $\frac{1}{T}$ for transition metal oxide glasses tend to show a continuously decreasing slope over a wide range of temperatures

1 2 1.3 Glass-Metal Particulate Composites

Oxide glasses containing ultrafine metal particles exhibit semi conductivity (Chakravorty 1984) This effect has been ascribed to the tunnelling of electrons from one metal grain to the next (Chakravorty et al 1977) A theoretical model, to analyse the experimental results, has been proposed. According to this, the generation of a charge carrier viz. electron involves creation of a pair of positively and negatively charged grains. The energy E_c^o required to create such a pair is given by

$$E_c^o = \frac{2e^2}{K_1 d} \quad . \qquad (1.15)$$

where e is electronic charge and d the metal grains diameter and

$$k_1 = \varepsilon \left[1 + \frac{d}{2s} \right] \qquad (1.16)$$

ε = dielectric constant for glass

s = interparticle separation

If θ is the effective barrier height, m the electronic mass and h the Planck's constant, the mobility of charge carrier in present system is proportional to tunnelling probability

exp (- 2 x s) where

$$x = \left[\frac{8\pi^2 m\theta}{h^2} \right]^{1/2} \quad . \qquad (1.17)$$

If $\beta(s)$ be the density of percolation paths associated with s then conductivity is given by (Abeles et al 1976)

$$\sigma \propto \int_0^\infty \beta(s) \exp \left[-2xs - \left(\frac{c_1}{2xskT} \right) \right] ds \qquad (1\ 18)$$

where $c_1 = xs\, E_c^o = \left(\frac{8\pi^2 m\theta}{h^2} \right)^{1/2} \frac{s2\, e^2}{d\epsilon \left[1 + \frac{d}{2s} \right]}$

$$= \frac{2\pi e^2 \sqrt{2m\theta}}{\epsilon h \left[\frac{d}{2s} \left(1 + \frac{d}{2s} \right) \right]}$$

under certain approximations (Abeles et al 1976) (1 18 reduces to:

$$\sigma = \sigma_o \exp \left(- 2 \left(\frac{c_1}{kT} \right)^{1/2} \right) \quad . \qquad (1\ 19)$$

Various glass metal particulate composites exhibits conductivity variation with temperature as predicted by eq. (1 19)

Table 1 2 summerises the E_c^o values for different systems as obtained from experimental data. It also includes calculated E_c^o values using average diameters of metal islands as estimated from electron microscopic investigation Table 1 3 summarises the results obtained on some glass fibres subjected to ion exchange followed by reduction, to precipitate silver granules (Arul Mozhi and Chakravorty D , 1982). In all the cases calculated

Table 1 2 E_c^o values for various glass-metal particulate systems

Sl No	Glass composition mol%	Metallic species	Average diameter (Å)	E_c^o (eV) Experimental	E_c^o (eV) Calculated	Reference
1	$64SiO_2$ $18B_2O_3$ $8Bi_2O_3$ $10Na_2O$	Bismuth	50	$4x10^{-2}$	$9x10^{-2}$	Chakravorty et al 1977
2	$80V_2O_5$ $15P_2O_5$ $5Bi_2O_3$	Bismuth	50	$1.2x10^{-2}$	$1.3x10^{-2}$	Chakravorty et al 1979
3	$70V_2O_5$ $15P_2O_5$ $15Bi_2O_3$	Bismuth	100	$4.7x10^{-3}$	$3.9x10^{-2}$	Chakravorty et al 1979
4	$85 B_2O_3 \cdot 5Na_2O$ $10Bi_2O_3$	Bismuth	120	$1.4x10^{-2}$	$1.5x10^{-2}$	Chakravorty and Chakrabarty 1980
5	$75 B_2O_3$ $20PbO$ $5Bi_2O_3$	Bismuth	400	$4.2x10^{-3}$	$3.8x10^{-3}$	Chakravorty and Chakravorty 1980
6	$75V_2O_5$ $15P_2O_5$ $10Ag_2O$	Silver	200	$1.6x10^{-3}$	$1.6x10^{-3}$	Chakravorty et al 1979
7	$46SiO_2$ $25B_2O_3$ $11K_2O$ $9Al_2O_3$ $4Sb_2O_3$ $1As_2O_3$ $4Ag_2O$ (in fibre form)	Silver	500	$1.7x10^{-2}$	$2.2x10^{-2}$	Chakravorty et al 1979b

Table 1.3 E_c^o values for glass metal particulate system produced by ion exchange and reduction treatment.

Sl. No.	Glass Composition	Ion-exchange species	Metallic species	Average particle Diameter	E_c^o (eV) Experimental	E_c^o (eV) Calculated	References
1	Commercial C-glass	$Na^+ \rightleftharpoons Ag^+$	Silver	160	1.5×10^{-2}	1.9×10^{-2}	Arul Mozhi and and Chakravorty D 1982 1982
2.	$64SiO_2 \cdot 26B_2O_3$ $10Na_2O$	$Na^+ \rightleftharpoons Ag^+$	Silver	115	8.7×10^{-3}	2.3×10^{-2}	Arul Mozhi and and Chakravorty D 1982 1982

values of E_c^o are in reasonable agreement with experimental values

1 2 2 Ionic Conduction:

Most of the inorganic oxide glasses exhibit ionic conductivity In various glass systems like silicates, borates phosphates and germenates the presence of modifier oxides induces additional oxygen ions. This results in the degradation of the network structure. Cations, particularly those from I and II groups of the periodic table remain as free ions in these materials. The structure is characterised by large holes which facilitate ionic migration. These holes are surrounded by non-bridging oxygens (NBO) which act as host for the cations The conductivity has Arrehenius like temperature dependence given by (Rawson 1984),

$$\sigma = \sigma_o \exp (- Q / kT) \quad .. \quad (1.20)$$

A number of different transport models (Nakajima 1972), Tomozawa 1977) have been proposed to explain the behaviour given by (1 20) However in a simple model where in ion is supposed to move in a periodic potential barrier of average height E, it can be shown that (Rawson H , 1984)

$$\sigma_o = \frac{n e^2 \nu_c R^2}{2 kT} \quad . \quad (1.21)$$

where n is no of cations per unit volume

ν_c is vibration frequency of cation

R is average distance between adjacent sites.

However the ion a glass experiences a potential barrier of random periodicity and heights, thus Q and R denote some sort of average values for these parameters The correlation factor f_c in Nernst-Einstein equation

$$\frac{\sigma}{D} = f_c \frac{nq^2}{kT} \qquad (1\ 22)$$

where σ = conductivity

D = diffusion coefficient

n = no. of alkali ions per unit volume

q = charge on alkali ion

k = Boltzman constant

T = temperature in °K

The general features of ionic conductivity in alkali containing oxides can be summarised as follows:

(i) The ionic conductivity increases with increase of alkali oxide concentration but this increase is non-linear Thus an increase in alkali content from 15 to 45 mol % increases the conductivity about 100 times (Rawson H 1984)

(ii) The activation energy decreases with increase in the alkali metal ion concentration

(iii) Conductivity is propotional to the square root of the alkali oxide activity in alkali silicates (Ravaine and Souquet 1973, 1977, 1978)

Features (i) and (ii) have led to the concept that some of alkali metal ion are mobile while others are 'trapped' in the structure and can undergo local but no long range motion

Feature (iii) implies that alkali metal ions exist in the structure in such a way that one can think in terms of an association-dissociation equilibrium of alkali oxide in the glass solvent, with the charge carried only by the dissociated cations This approach is analogous to that used in liquid electrolyte solutions This has been exploited to increase the cation activity by the addition of alkali halides in the glass, thereby increasing the concentration of undissociated alkali metal ions In such a case, neither the alkali ion nor the halide ion becomes bound into the macromolecular anionic structure, which consists primarily of shared tetrahedral groups Thus conductivity can be increased substantially be incorporating alkali halides and other simple salts in the glass An increase of about two orders of magnitude in conductivity has been achieved in the case of lithium glasses Conductivity has been found to be greater, the larger the ion with which mobile ion is associated Sulphide analogs of oxide glasses have ionic conductivities about an order of magnitude higher than that for oxide glasses Various glass systems which have been studied can be classified as follows

1 2 2 1 Silica

The d c conductivity of bulk silica glasses is normally attributed to the presence of impurities, particularly sodium (Doremus 1968a) Q lies in the range of 1 3 eV to 1 5 eV Mobilities of Na^+, Li^+ and K^+ in synthetic silica are found to be in the ratio of 1 03: 0007 (Doremus 1969) The activation energy E_{μ} is same for all these ions. Hence 1000 to 1 variation in mobility should be almost entirely due to similar variation in vibrational frequency or some corresponding property

1 2 2 2. Binary Alkali Silicate Systems (R_2O-SiO_2)

conductivity increases monotonically with increasing R_2O content (Hughes and Isard 1972) While activation energy shows a marked reduction (Charles 1966) Q lies in range of 54 eV to 60 eV. The comparision in Table 1 4 of the resistivities of various alkali silicate glasses at the same molecular composition and the same temperature shows that the values increase with increasing cation size. However no simple relationship between Q and the cation size exists which may be valid over the whole range of composition and temperature

Table 1 4 D C resistivity of different alkali silicate glasses at 100°C (Ohm Cm) (Charles, 1966)

Mol % Alkali	Li_2O	Na_2O	K_2O	Rb_2O	Cs_2O
15	1.7×10^7	1.4×10^8	3.1×10^9	1.4×10^{10}	3.3×10^{11}
30	4.2×10^6	3.8×10^6	6.5×10^6	9.7×10^6	1.6×10^8
40	9.7×10^5	1.4×10^5	9.4×10^5	3×10^6	--

1 2 2 3 M_2O- SiO_2- B_2O_3 (M = alkali metal) :

Following observations have been made (Otto 1966)

(i) Q increases linearly with increasing M_2O content ($\leq$ 25 mol %)

(ii) σ_o is almost independent of M_2O content

(iii) σ is enhanced by incorporating lithium salts Li_2SO_4, Li x (x = Cl, Br, F)

Complex impedance analysis has been reported (Tuller et al 1980)

1 2.2 4 B_2O_3-Li_2O-Li x (x = Cl, Br, I)

σ is strongly dependent on polarisability of an ion i e radius of ion (Levasseur et al 1978, 1979) Glasses containing LiI shows a maxim σ (350°C) = 3 4 x 10^{-2} (Ohm Cm)$^{-1}$ and Q = 46eV

1 2 2 5 Li_2O-LiF-Li_2SO_3-Li_2SO_4-B_2O_3 (Smedly and Angell 1978)

Various glasses containing total Li_2x content between 43 to 84 mol % have been studied A glass with 70 mol % of Li_2x shows max. σ (200) = 2 26 x 10^{-3} Ohm Cm^{-1}

σ is function of F/O ratio

1 2 2 6 B_2O_3- Li_2O- Li_nx (n = 1, x= Cl, Br, I, and for n = 2, x = SO_4, n= 3, x = PO_4) have been studied in detail (Levasseur et al 1979a, b, 1980, 1981a, b c , Hagenmuller et al 1979, Irion et al 1980) σ is dependent or Li_2O and Li_nx content.

σ_{max} (300°C) = 10^{-2} (Ohm Cm)$^{-1}$

1 2 2 7 $Li_2Si_2O_5$ - Li_2SO_4 (Kone et al 1979) :

Q (.66 eV) does not change with composition while σ_o changes significantly. Effect of replacing Si by S, shows linear increase in σ with Li_2SO_4 content

1 2 2.8 $LiNbO_3$-SiO_2 (Prasad et al 1980)

The glass with 35 mol % SiO_2 shows σ (200°C) = 10^{-4} (Ohm Cm)$^{-1}$ on doping with 1 mol % of Fe_2O_3 σ increases one order magnitude. Further addition of Fe_2O_3 causes decrease in σ which is ascribed to the onset of nucleation of crystallites within

glass matrix

1 2 2 9 M_2O-MF-$Al(PO_3)_3$(M=Li,Na,V,Co) : (Evastropev et al1974)

Exceptionally high values of σ have been reported Highest σ is obtained in 50LiF. 30 Li_2O 20 $Al(PO_3)_3$ with $\sigma_{max}(300°C) = 10^{-2}$ (Ohm Cm)$^{-1}$ and Q = 52 eV. Mixed alkali effect observed in $Al(PO_3)_3$-NaF-LiF (Pronkin 1978) Detailed A C measurement and analysis have been reported in LiF. Li_2O $Al(PO_3)_3$ system (Jagla and Isard 1980, Kulkarni 1984). The number of effective charge carriers is very low but mobilities are found to be exceptionally high (Kulkarni 1984a)

1 2 2.10 $LiPO_3$-Li_2SO_4 (Malugani et al 1978)

The highest conductivity of 10^{-7} (Ohm Cm)$^{-1}$ at 25°C is reported σ increases with increasing Li_2SO_4 content while T_g and Q decreases continuously

1 2 2 11 $LiPO_3$-Lix (x = Cl, Br, I) (Malugani and Robert 1979)

A linear increase in σ and decrease in T_g and Q is reported with increasing Lix content

1 2 2 12 Li_2O-LiCl-P_2O_5 (Doreau et al 1980)

Maximum conductivity of the order of 5×10^{-7} at 25°C is reported

1 2 2 13 LiI-Li_2S- P_2S_5 (Malugani and Robert 1980)

Various glasses have been made in this system and maximum σ is obtained in 37 Li_2S 18 P_2S_5. 45 LiI with σ (20) = 10^{-3} (Ohm Cm)$^{-1}$ with Q = 31 eV (Mercier et al 1981)

1 2 2 14 M_2S-GeS_2 (M=Li,Na,Ag) :

GeS_2 forms stable glasses with alkali sulphides such that the molar ratio of GeS_2 lies in the range 1 to 5. Maximum σ is found in 50 Li_2S-50 GeS_2 with σ (25°C) = 4×10^{-5} (Ohm Cm)$^{-1}$ and Q = 51 eV. (Malugani et al 1978)

1 2 2 15 Quenched Glasses

High conductivities have been obtained in Li^+ containing specially prepared glass systems in which one normally does not expect glass formation Glasses have been prepared by rapid quenching technique Following systems have been reported

(i) Li_2O-Nb_2O_5 (Glass et al 1978)

(ii) Li_2O- Ta_2O_5 (Nassau et al 1979,a,b, 1981 a)

(iii) Li_2O-Al_2O_3 (Glass and Nassau 1980)

(iv) Li_2O-Ga_2O_3 (Glass and Nassau 1980)

(v) Li_2O-Bi_2O_3 (Glass and Nassau 1980)

(vi) WO_3 (Nassau et al 1980)

(vii) MoO_3 (Nassau and glass 1981 b)

(viii) Li_2SO_4-$SrMg(SO_4)_2$ (Nassau and glass 1981 b)

(IX) Li_2SO_4- $La_2(SO_4)_3$ (Nassau and glass 1981 b)

In all these glasses conductivity values are reported to be greatly enhanced compared to those normally obtained in corresponding crystals for example the enhanced conductivities ($\sigma_{250} \sim 10^{-3}$ (Ohm Cm)$^{-1}$) are almost 10^{20} times greater at room temperature than in single crystal $LiNbO_3$ and are attributed to increased Li^+ mobilities

1 2 2 16 Some other New Glasses :

Various other glass systems have been developed and studied They can be summarized as follows

(i) ZrF_4-BaF_2-ThF_4

(ii) ZrF_4-BaF_2-YF_3 (Chandrashekhar and Shafer 1978)

(iii) PbO-$PbCl_2$ (Rao and Elliott 1981)

(iv) Alkali Tungstate and Alkali Molybdate (Gossink 1971)

(v) K_2SO_4-$ZnSO_4$ (Narasimham and Rao 1978)

(vi) K_2SO_4-Na_2SO_4-$ZnSO_4$ (Sunder and Rao 1980)

1 2 3 Fast Ion Conductors (F I C)

Several glasses containing Li^+ and Ag^+ ions exhibit fast ion conduction Developments in this area has been reviewed recently (Tuller et al 1980) Some important FIC glasses are summarised in Table 1 5 conductivity plots for several such glassy FIC's are also reported . (Tuller et al 1980) After detailed study of these materials, many basic features which have been revealed for these FIC's are as follows:

1. They are formed in glass systems which are known to involve considerable network structures like silicate, Phosphate and borate systems and in molybdate and halide systems where bonding is essentially ionic

2 Preexponential factor σ_o is much smaller in case of FIC's than that for normal ionic conductors This implies that vibrational frequency of charge transporting ion which may by associated with very shallow potential profiles for vibrations is very low This makes the motion of ionic hopping

in FIC's somewhat inconsistent (Tuller 1980)

3 Notion of a molten' or highly disordered sublattice of conducting ions loses much of its significance in glasses while being adequate in crystalline FIC (McGeehin and Hooper 1977)

4 The transport numbers of ions are close to unity (Minami et al 1977)

5 Q for Ag^+ FIC's lie in the range of 15 to 47 eV while Q for Li^+ FIC s lie in range of 31 to 73 eV (Kulkarni 1984)

6 Tg's for Li^+ FIC with anions capable of forming network structure seem to have higher Tg (160° to 280°C) otherwise Tg's are small (52° to 75 °C)

8 AgI which is the component of several glass FIC's is itself a fast ion conductor in its (high temperature) crystalline form

1 2 4 A C Electrical Properties of Oxide Glasses

When an insulator is subjected to an electric field it gets polarised In any particular material the polarisation usually involves several kinds of charge displacements. In oxide glasses polarisation also involves movement of ions over destances of one or two ionic diameters from one equlibrium position to another. These require the surmounting of energy barriers It takes a finite time for all ions capable of this kind of motion to reach their final positions after the field is applied. So polarisation varies with time as shown in Fig 1 1 and can be represented as equation 1 23

$$p(t) = (p_s - p_{to}) \left(1 - \exp\left(\frac{t-t_o}{\tau}\right)\right) \qquad (1\ 23)$$

where τ = relaxation time

Table 1 5 • Some Glassy Fast Ion Conductors

Sl No	Glass Composition (Mol %)	σ(25°C) $(Ohm\text{-}Cm)^{-1}$	σ(I) $(Ohm\ Cm)^{-1}$	Activation Energy (eV)	Reference
1	$Li_2O\ B_2O_3$(42.5-57 5)	7 $1x10^{-8}$	6.$1x10^{-3}$(350)	60	Otto (1966)
2	$Li_2O\ B_2O_3$(63-37)	6 $3x10^{-11}$	-	73	Levasseur et al(1979)
3	$Li_2O\ Li_2Cl_2\ Li_2SO_4\ SiO_2\ B_2O_3$ (35-10-30-12.5-12 5)	3 $3x10^{-6}$	9 $7x10^{-2}$(350)	53	Otto (1966)
4	Li_2O LiCl.B_2O_3 (31 8-12 3-59.9)	3 $2x10^{-6}$	1 $7x10^{-2}$(385)	50	Levasseur et al (1979)
5	Li_2O LiCl $Al_2O_3\ B_2O_3$ (29-24-3-44)	1 $3x10^{-6}$	1 $5x10^{-2}$(350)	49	Takahashi and Yamamoto (1979)
6	Li_2O LiF $Li_2SO_4\ Li_2SO_3\ B_2O_3$ (22.1-12 6-15 8-20 5-28 5)	6 $2x10^{-7}$	2 $3x10^{-3}$(200)	57	Smedly and Angell(1978)
7	$Li_2O.Li_3PO_4\ B_2O_3$.(25-10-65)	7 $44x10^{-9}$	$1x10^{-3}$(330)	62	Basu et al (1983)
8	Li_2O.Lif B_2O_3(20-26-44)	-	3 $14x10^{-4}$(200)	58	Smedly and Angell(1978)
9	$Li_2O\ Li_2SO_4\ B_2O_3$(	-	2 $10x10^{-2}$(300)	58	Levasseur et al (1979)
10	$Li_2O.SiO_2$(40-60)	9 $2x10^{-9}$	$1x10^{-6}$ (100)	63	Otto and Milbert(1968)
11	$Li_2O\ Al_2O_3\ SiO_2$(25-25-50)	6 $2x10^{-10}$	6 $1x10^{-4}$(350)	72	
12	$Li_2O.B_2O_3\ SiO_2$ (29-13-48)	4 $3x10^{-9}$	1 $5x10^{-3}$(350)	67	Biefield et al (1978)

13	$Li_2O.SiO_2$ (33.3-67)	2.8x10	1.9x10 (350)	70	
14	Li_2 Si_2O_5 Li_2SO_4 (71 5-28 5)	1 3x10^{-8}	8 7x10^{-3}(350)	66	Kone et al (1979)
15	Li_2O. Li_2SO_4 SiO_2	-	1x10^{-5}(100)	56- 65	Souquet et al (1980)
16	$LiNbO_3$ SiO_2 (65-35)	-	1x10^{-4} (200)		Prasad et al (1980)
17	$LiPO_3$. LiF (60-40)	6 7x10^{-9}	-	63	Malugani and Report (1979)
18	$LiPO_3$.LiCl (70-30)	1x10^{-7}	1x10^{-3}(220)	63	
19	$LiPO_3$ LiI (67-33)	1x10^{-6}	1x10^{-3}(194)	56	
20	$LiPO_3$.LiBr (67-33)	2 2x10^{-7}	1 3x10^{-3}(220)	57	
21	$LiPO_3$.Li_2SO_4 (67-33)	1x10^{-7}	3 5x10^{-3}(250)	66	Malugani et al (1978)
22	Li_2O.LiF $Al(PO_3)_3$ (30-50-20)	5 8x10^{-7}	1x10^{-2}(300)	56	Evastroper et al (1974) Jagla and Isard (1980)
23	Li_2O LiF $Al(PO_3)_3$ (15-70-15)	-	1 3x10^{-3}(220)	53	Malti et al(1983)
24	Li_2S•P_2S_5 (33-67)	1 1x10^{-4}	-		Ribes et al (1979)
25	Li_2S LiI P_2S_5(37-45-18)	1x10^{-3}	-	31	Malugani and Robert(1980)
26	Li_2S GeS_2(50-50)	4x10^{-5}	-	51	Souquet et al (1981)
27	Li_2S Nb_2O_5(50-50)	1.6x10^{-6}	5 3x10^{-3}(350)	44	Glass et al (1978)
28	Li_2O Ta_2O_5 (50-50)	5x10^{-6}	6 4x10^{-3}(350)	39	Nassau et al (1979 a b 1981)
29	AgI Ag_2SeO_4 (75-25) Tg=75°C	1x10^{-2}	-	20	

30	AgI Ag_2MoO (75-25) Tg=52°C	$1x10^{-2}$	-	22	Minami T et al (1977)
31	AgI Ag_2CrO_4 (80-20) Tg=70°C	$1.5x10^{-2}$	-	15	Borino F et al (1977 1976)
32	AgI $AgPO_3$ (57.5x42.5) Tg=75°C	$1.5x10^{-2}$	-	25	Malugani J P et al (1978)
33	Ag_2SO_4 $AgPO_3$ (30-70) Tg=160 C	$4x10^{-6}$	-	47	Malugani J P et al (1978)
34	Ag_2S Ag_2S_3 (66.6-33.4) Tg=145°C	$9x10^{-5}$	-	36	Kawamoto Y (1976)
35	Ag_2S GeS.GeS_2 (50-5-45) Tg=280°C	$3x10^{-4}$	-	38	K wamoto Y (1976)
36	ZrF_4 BaF_2 ThF_4 (58.7-31.3-10) Tg=300 C	$1.3x10^{-10}$		79	Malugani J P. et al (1978)

As the temperature increases more thermal energy is available and hence the rate at which ions surmount energy barriers to reach their final position is increased Consequently τ decreases with increasing temperature and given by

$$\tau = \tau_o \exp \left(E_\tau / kT \right) \qquad (1\ 24)$$

where E_τ is the activation energy for the relaxation process

If the field alternates, there may be insufficient time in one half cycle for ions to reach their final positions and for polarisation to reach the final value p_s At very high frequencies none of the ions may move in one half cycle and the polarisation will then not exceed the instantaneous value P_∞ Continuous movement backwards and forwards under the action of an AC field results in a continuous absorption of energy by the material The work done on the ions is dissipated as heat The resultant rise in temperature decreases the relaxation time, thus increasing the number of ions which move in one half cycle This can result in a run-away situation of progressively increasing energy loss

If glass is brought into a periodic electric field, there will generally occur a phase angle δ which shows how much the difference in phase between current and applied voltage differs from $\pi/2$ The angle δ is termed as loss angle and tan δ the dissipation factor Significance of tan δ is seen from the expression of power dissipated in the form of heat W

per unit volume per unit time as given by

$$W = \frac{E_o^2 \, f \, \epsilon' \tan\delta}{8\pi} \qquad (1\ 25)$$

where E_o = maximum value of electric field strength

f = frequency of applied field

ϵ' = dielectric constant at the given frequency

Thus, $\epsilon \tan\delta$ (Loss factor) representing the dissipated energy per cycle for unit field strength, is a measure of dielectric losses [Stevels, M 1957]

The conduction losses depend on the resistivity ρ as given by the following equation

$$\tan\delta = \frac{1}{2\pi \, f \, \epsilon' \epsilon_o \rho} \qquad (1\ 26)$$

where $\epsilon_o = 8\ 85 \times 10^{-14}$ F/Cm if ρ is expressed in Ω-Cm

Thus a complex dielectric constant $\epsilon(\omega)$ is conceived as given by eq

$$\epsilon(\omega) = \epsilon'(\omega) + i\epsilon''(\omega) \qquad (1\ 27)$$

such that $\epsilon''(\omega) = \epsilon'(\omega) \tan\delta \qquad (1\ 28)$

The frequency dependence of conductivity and real and imaginary parts of dielectric constant and loss factor are given by Debye equations as shown below (Rawson 1984)

$$\sigma(\omega) = \frac{(\epsilon_s - \epsilon_\infty)\, \omega^2 \tau}{1 + \omega^2 \tau^2} \qquad (1\ 29)$$

$$\epsilon'(\omega) = \epsilon_\infty + \frac{(\epsilon_s - \epsilon_\infty)}{1 + \omega^2 \tau^2} \qquad (1\ 30)$$

$$\epsilon''(\omega) = \frac{(\epsilon_s - \epsilon_\infty)\,\omega\tau}{1 + \omega^2 \tau^2} \qquad (1\ 31)$$

$$\tan\delta = \frac{(\epsilon_s - \epsilon_\infty)\,\omega\tau}{\epsilon_s + \epsilon_\infty \omega^2 \tau^2} \qquad (1\ 32)$$

where ϵ_s and ϵ_∞ are limiting values of low frequency and high frequency dielectric constants corresponding to p_s and p_∞ respectively The solid lines in Fig 1 2 correspond to Debye equations i e they apply to materials having single relaxation time ϵ'' attains a maxima at $\omega = 1/\tau$

While tanδ attains a maxima at $\omega = \frac{1}{\tau}\left(\frac{\epsilon_s}{\epsilon_\infty}\right)^{1/2}$

Dotted line represent the A.C behaviour of a typical glass

A C measurements on a large range of glass corpositions and temperatures exhibit many unifying common features which are as follows:

1 The dielectric loss curves are quite broad, ranging over two to three decade, in frequency and can not be described by a single Debye relaxation rather results require a distribution of relaxation times F (τ)

2 F (τ) in all cases is found to be very asymetric, having a long tail in short relaxation time region

3 F (τ) is found to be independent of temperature.

4 Increase in concentration of alkali ions shifts F (τ) towards shorter relaxation times (Hakim and Uhlman 1973)

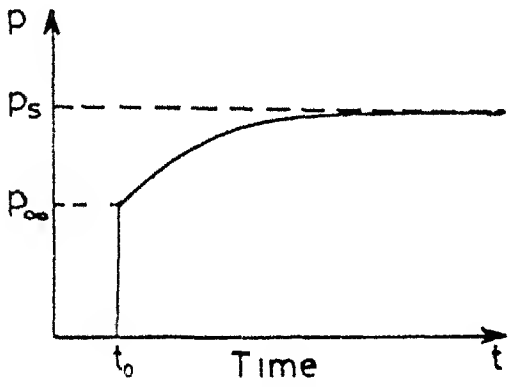

Fig 11 Time dependence of polcrisation after applying a constant D C field at time t_0

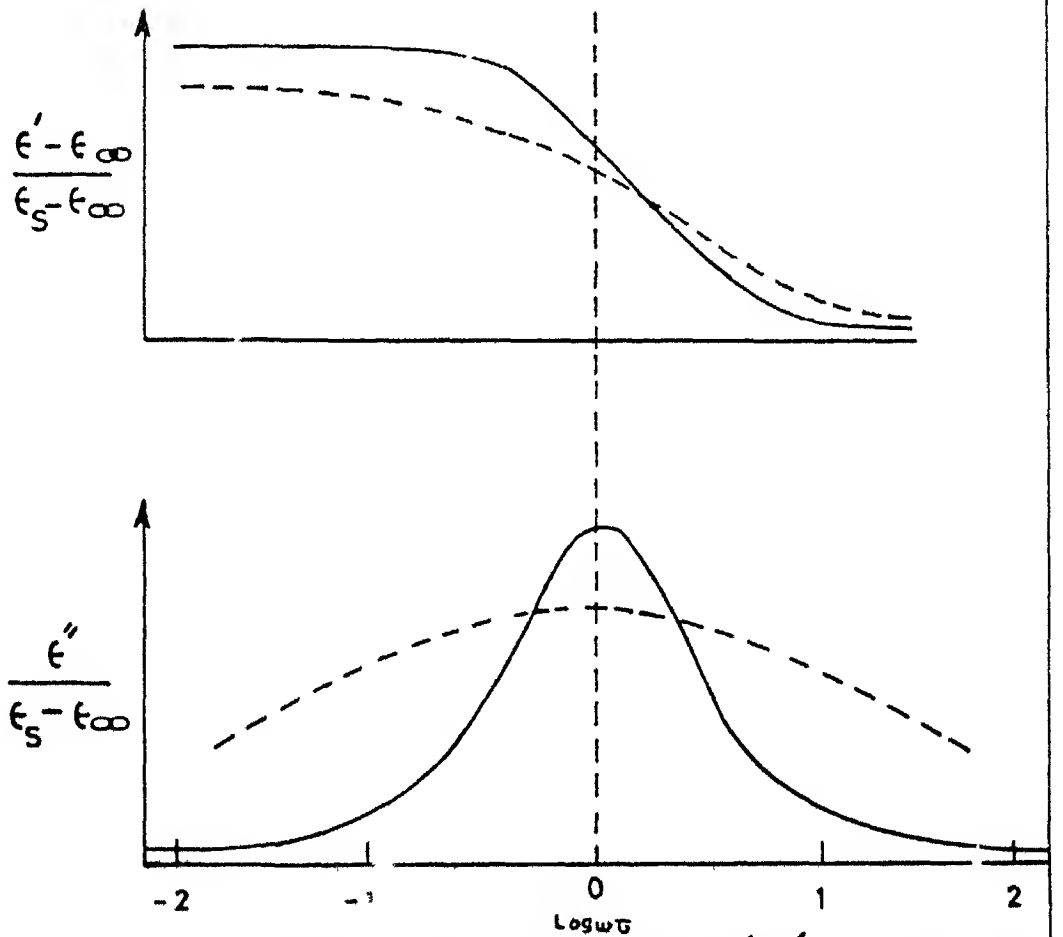

Fig 12 Dependence of normalised ϵ' & ϵ'' on frequency

5 Activation energies for DC & AC conduction are virtually identical at alkali concentrations around 5% (Heroux L 1958) This implies that same process is responsible for both type of conduction

6 At high frequencies variation of ϵ'' becomes much less and usually for a significant range of frequency, dielectric loss is constant

7 In transition metal oxide glasses AC conductivity obeys $\sigma(\omega) = U\omega^{n_4}$ where U is constant increasing with temperature and n_4 is in range .7 to .9

In terms of $F(\tau)$ ϵ' and ϵ' can be written as follows:

$$\epsilon' = \epsilon_\infty + (\epsilon_s - \epsilon_\infty) \int_0^\infty \frac{F(\tau)\, d\tau}{1 + \omega^2\tau^2} \qquad (1\ 33)$$

$$\epsilon'' = (\epsilon_s - \epsilon_\infty) \int_0^\infty \frac{F(\tau)\, \omega\tau}{1 + \omega^2\tau^2}\, d\tau \qquad (1\ 34)$$

Discussion of experimental dielectric behaviour conventionally proceeds through a phenomenological function $F(\tau)$ which fits the data to equations (1 33) and (1 34)

Systematic studies have been made on ionically conducting glasses (Taylor 1956, 1957, 1959) and subsequently discussed (Owen 1963, Isard 1969) Similar results on electronically conducting glasses containing transition metal ions have also been reported (Sayer et al 1971, 1972, Murawski and Gzowski 1974, Namikawa 1975, Man Singh et al 1975 a, b, 1976, Rawal and Mac Crone 1978)

Various models have been proposed to explain this behaviour In limited jump model (Stevels 1957) alkali ion is assumed to be moving through a series of potential wells whose barrier heights vary in a random fashion This model predicts a strong temperature dependence, which is contradicted by experimental results (Isard 1970) In another model, assumption of existence and migration of a defect consisting of two alkali ions attached to a non-bridging oxygen ion, explains the AC and DC activation energy but fails to explain broad destribution in τ without assuming an unrealistically large entropy contribution to the dispersion (Charles 1961). Space charge model has also been developed in which electrode effects play a dominant role to explain the experimental observations (Doremus and Tomozawa 1974) Loss machanisms have been explained on the basis of phase separated regions in the glass These regions give rise to a Wagner-Sillar interfacial polarisation loss mechanism (Isard 1970) But similar characteristic loss curves have been reported in alkali glass systems despite the absence of phase separated regions within them Results have been explained by assuming ions moving preferentially along paths or channels of relatively highconductivity (Hakin and Uhlman 1973) A similar model has been proposed for electronically conducting Pbo-SiO_2-Fe_2O_3 glass (Anderson and Mc Crone 1974). By using the concept of truncated diffusion paths, dielectric relaxation in alkali containing ions, has been explained (Aitken and Mac Crone 1974)

1 3 Ion Exchange .

When a glass containing monovalent cations is placed in a molten salt containing another monovalent cation, ion exchange takes place (Frischat 1975) This reaction can be written as following:

$$\bar{A}\ (glass) + B(Salt) = \bar{B}(glass) + A\ (Salt) \quad (1\ 35\ )$$

where $\bar{A}$ and $\bar{B}$ are the counterions in the exchanger phase and A and B are counterions in liquid phase Molten salts are required because of the temperature range needed before the cations in the glass become mobile with reference to the negatively charged oxygens of rigid, immobile silicate network. Ion - exchange is controlled by the diffusion of ions in the glass Study of diffusion process and the parameters, which influence the mobility of cations reveal the basic mechanism of this transport process Detailed information on exchange kinetics has recently been reviewed (Garfinkel 1972, Frischat 1975)

In binary ion exchange, the diffusing species A and B are charged and tend to diffuse at different rates This results in a build up of electrical charge as one ion tend to move faster than the other However, a gradient in electrical potential along with this charge acts to slow down the faster ion and speed up the slower ion Despite the difference in the mobilities of two ions, the gradient in electrical potential the fluxes of two ions to be equal and opposite, thus preserving the electrical neutrality

The driving force for transport of either species A or B is equal to the negative of its gradient in total chemical potential μ_c which is the sum of gradient in activity and gradient in electrical potential By assuming further that no other pressure or temperature gradient is present in the system and that mobilities of ions are same in self diffusion and inter-diffusion, the flux of diffusing species per unit time in x direction is given by (Doremus 1964) :

$$J_B = -D_A \left[\frac{\partial C_A}{\partial x} \quad \frac{\partial \text{Ln } a_A}{\partial \text{Ln } C_A} + C_A \quad \frac{FE_e}{RT} \right] \quad (1\ 36)$$

where D_A = self diffusion coefficeent of species A

C_A = ionic concentration of species A

a_A = activity of species A

E_e = electric field

Similarly for ion species B

$$J_B = -D_B \left[\frac{\partial C_B}{\partial x} \quad \frac{\partial \text{Ln} a_B}{\partial \text{Ln} C_B} + C_B \quad \frac{FE_e}{RT} \right] \quad (1\ 37$$

The equation J_A and J_B are referred to as Nernst-Planck Equations

The condition of electrical neutrality requires that

$$J_A = - J_B \quad (1\ 38)$$

And since number of negative exchange sites is constant and fixed so

$$\frac{\partial C_A}{\partial x} = \frac{\partial C_B}{\partial x} \quad (1.39)$$

By using 1 36 and 1 37

$$E_e = \frac{RT}{F}\left[\frac{D_B - D_A}{C_A D_A + C_B D_B}\right]\frac{\partial C_A}{\partial x}\quad\frac{\partial \mathrm{Ln}\ a_A}{\partial \mathrm{Ln}\ C_A} \qquad (1\ 40)$$

which by substitution in (1 36) gives

$$J_A = -\frac{D_A D_B}{N_A D_A + N_B D_B}\quad\frac{\partial \mathrm{Ln}\ \bar{a}_A}{\partial \mathrm{Ln}\ C_A}\frac{\partial C_A}{\partial x} \qquad (1\ 41)$$

where N is the cation fraction in the ion exchange As actvity is related to concentration (Karreman and Eisenman 1962) by

$$a_A = C_A^{n_1} \qquad (1\ 42)$$

where n_1 is a constant

$$\text{so } J_A = -\frac{D_A D_B}{N_A D_A + N_B D_B}\quad n_1\frac{\partial C_A}{\partial x} \qquad (1\ 43)$$

which when compared with Fick's first law of diffusion gives the interdiffusion coefficient D

$$\bar{D} = \frac{D_A D_B}{N_A D_A + N_B D_B}\quad n_1 \qquad (1\ 44)$$

for an ideal solution $n_1 = 1$ (Helfferich 1962)

The temperature dependence is given by Arrhenius equatin

$$\bar{D} = \bar{D}_o \exp\ (-E_{\bar{D}}/kT) \qquad (1.45)$$

$$D = D_o \exp\ (-E_D/kT) \qquad (1\ 46)$$

where $\bar{D}$ and D are interdiffusion and self diffused coefficients respectively.

If the electrical current in an exchanger is carried by a single ionic species, then by the Nernst-Einstain equation.

$$D = \frac{\sigma RT}{C(ZF)^2} \qquad (1\ 47)$$

where σ = specific conductivity of exchanger (Ohm Cm)$^{-1}$

R = 8 374 J/ deg mole

C = Concntration of diffusing species in mols/Cm^3

Z = ionic value

F = Faraday or 96500 C/ equiv

The measured σ is usually found to be less than that calculated from the diffusion coefficient (Terai and Hayami 1975) This difference is ascribed to a correlation factor f_r which depends on the structure of exchanger and the transport mechanism

$$f_r = \frac{D_A}{D_\sigma} \qquad (1\ 48)$$

where D_A is the measured self diffusion coefficient and D_σ is the diffusion coefficient as calculated from electrical conductivity

Thus $f_r$is a measure of efficiency of Nernst - Einstein Equation In case of completely random motion

$$f_r = 1 \qquad (1\ 49)$$

While $f_r < 1$ implies that jump direction is not entirely random and next jump dopends upond the direction of the previous jump As these correlations do not arise in electrical conduction (Compean and Haven 1956) the factor $f_v$can be attributed to correlations in diffusion Several possible mechanisms have been proposed to explain the experimental data (Haven and Verkerk 1965, Haven and Stevels 1957)

1.3 1 Experimental Measurements:

Various techniques are used to study self diffusion and interdiffusion kinetics To obtain self diffusion coefficients, radioactive tracers are necessary Weight change, sectioning and electron microprobe data find extensive use for interdiffusion measurements and resistance change to a lesser extent In all these methods diffusion profile is measured and by equating it to theoretically calculated values, self diffusion coefficients and interdiffusion coefficients are evaluated These values are obtained by solving Fick's second law under appropriate boundary conditions Fick's second law is expressed as (Frischat 1976)

$$\frac{\partial C}{\partial t} = \frac{\partial}{\partial x} \left(D \frac{\partial C}{\partial x} \right) \qquad (1\ 50)$$

and if D is constant

$$\frac{\partial C}{\partial t} = D \frac{\partial^2 C}{\partial x^2} \qquad (1\ 51)$$

where C is the concentration of the diffusing species Generally two types of boundary conditions are used which are as follows.

(a) Instantaneous Source

In this case the boundary conditions are

$$C(x,t) = \begin{cases} C_o\, \delta(x) & \text{for } t = o \\ & \text{for } x \to \infty \text{ and } t \geq o \end{cases} \qquad (1\ 52)$$

Where C_o (g/Cm^2) is the initial surface concentration and $\delta(x)$ is the Dirac's delta function Under these conditions solution of (1 51) is given by

$$C(x,t) = \frac{C_o}{\sqrt{\pi Dt}} \exp\left(-\frac{x^2}{4Dt}\right) \qquad (1\ 53)$$

(b) Constant Source

In this case boundary conditions are

$$C(x,t) = \begin{cases} C_o \text{ for } x=0 \text{ and } t \geq 0 \\ 0 \text{ for } x > 0 \text{ and } t = 0 \end{cases} \qquad (1\ 54)$$

and $\frac{\partial C}{\partial x} = 0$ for $x \to \infty$ and $t \geq 0$

where C_o(g/Cm^3) is constant initial concentration Solution of (1 51) is given by

$$C(x,t) = C_o \ \mathrm{erfc}\left(\frac{x}{2\sqrt{Dt}}\right) \qquad (1\ 55)$$

(c) External field

When diffusion takes place under the influence of external electric field E_e

$$\frac{\partial C}{\partial t} = \bar{D} \frac{\partial^2 C}{\partial x^2} - \mu_e E_e \frac{\partial C}{\partial x} \qquad (1\ 56)$$

where μ_e = electrochemical mobility ($Cm^2/V\ s$)

Under the boundary conditions of (1 54) the solution of (1 56) is

$$C(x,t) = \frac{C_o}{2}\left[\mathrm{erfc}\left(\frac{x-\mu_e E_e t}{2\sqrt{Dt}}\right) + \exp\left(\frac{\mu_e E_e x}{\bar{D}}\right) \cdot \mathrm{erfc}\left(\frac{x+\mu_e E_e t}{2\sqrt{Dt}}\right)\right] \qquad (1\ 57$$

1.3.2 Type of Ion- exchanges

The entire gamut of alkali exchanges can be classified into two categories

i Alkali exchanges: The species entering and leaving the glass are alkali metal ions

ii Cementation exchanges: This term has been earlier used for silver and copper staining but now includes the ion exchange of any metal ion other than alkalis or alkaline earths

During all these exchanges Si-O network is almost stable. The mobilities of both cations in the melt are high compared with those in the glass and phase boundary reaction between melt and glass is very fast Interdiffusion of ions in the glass is the rate-determining factor and interdiffusion coefficient $\bar{D}$ describing the binary diffusion process, is in general a function of composition.

Diffusion studies have been made by tracer technique in many glass systems Diffusion of Na, K, Rb and C_s is reported in glasses R_2O $3SiO_2$ where R = Na,K,Rb,Cs, respectively (Malinin et al, 1972) Diffusion measurements of Na have been carried out in glasses having the following composition (Pavlovskii 1970)

(i) $x\,Li_2O$ $(100-x)$ SiO_2

(ii) $x\,K_2O$ $(100-x)$ SiO_2

(iii) $x\,Li_2O$ $(20-x)$ K_2O $80SiO_2$

(iv) $x\,Li_2O$ $(30-x)$ K_2O $70SiO_2$

These results show that the interdiffusion process is energetically less favourable than corresponding self-diffusion process Much work on alkali-ion exchange of glasses have been done at temperatures below and above T_g. However most of this work has been devoted to technical aspects than kinetics of interdiffusion process (Frischat 1976)

When small Li^+ ions (r_c = 78 A°) of a salt melt are exchanged for larger Na^+ ions (r_c = 96 A°) of glasses at temperatures above T_g, a lower surface expansion glass is produced which after cooling generates a compression at the surface In addition, in some compositions very low expansion crystalline phases can be precipitated in surface layer therby increasing the compressive stress in the surface upto 100 Kp/mm^2 (Varshneya 1975, Cooper and Krohn 1969 ,Garfinkel and King 1970, Schaeffer and Heinze 1974). Glass Ceramics have also been ion exchanged in a similar way (Barthalomew and Garfinkel 1977) Diffusion rates are about a factor of 3 slower in the glass ceramic in comparison with the glass (Bartholomew and Garfinkel 1980) Another possibility to generate high compressive stress in the glass surface is exchange of larger ions from melt for smaller ones in the glass at temperatures below T_g i.e. K^+ (r_c = 1 33 A°) for Na^+ (r_c = 96 A°) In this process called as crowding or ion stuffing , the larger ions occupy the site of smaller ones. To a first approximation the build up of integral compressive stresses, σ_s can be characterised by the equation (Hahnert M 1971)

$$\frac{d\sigma_s}{dt} = \frac{m_1}{\sqrt{t}} - \frac{\sigma_s}{\tau_s} \qquad (1.58)$$

where m_1 = constant

$\tau_s = \eta/K_B$ = relaxation time

η = viscosity of the glass

K_B = Bulk modulus

At lower temperatures τ_s is large therefore σ increases with $\sqrt{t}$ If however t is comparable with τ_s or if temperature is increased, stress relaxation occurs It has been found that exchange temperature should be $\lesssim$ 100°C below T_g and for $t = (8 - .9)\tau_s$ the maximum stress build up can be obtained As far as technical applicability is concerned this exchange process acquires increasing importance (Ernsberger 1966, Garfinikel 1969)

Cementation exchange is similar in its early steps to that of alkali exchange However two further steps are added namely reduction of ions Ag^+ and/ or Cu^+ to metals and aggregation of these metals to (crystalline) centres of colour ($\simeq$ 100 Å) Reduction of silver ions occurs with out special special treatment by an electron transfer process:

$$Ag^+ + Fe^{2+} \rightarrow Ag^o + Fe^{3+}$$

or for the case of a simultaneous Ag^+/Cu^+ exchange by

$$Ag^+ + Cu^+ \rightarrow Ag^o + Cu^{2+}$$

As Fe is a common impurity in the glass, the exchange has to be done in oxidising or neutral atmosphere otherwise an undesired metallic mirror is precipitated at the glass surface. Exhaustive literature is available on Ag^+-alkali exchange

(Frischat 1976). Tracer diffusion studies Matousek 1973 , Malinin 1972) have been carried out using ^{110}Ag Electron microprobe analysis has been used for $Ag^{+} \rightleftharpoons Na^{+}$ exchange (Garfinkal 1972) Strengthening of glasses by $Ag^{+} \rightleftharpoons Na^{+}$ ion exchange has been reported (Brungs and McCartney 1975)

1 4 Phase Separation in Glasses

It has been observed that many glasses in their molten states form homogeneous liquids which on cooling separate into two liquids or glass phases (Stookey 1959a) In many cases, one of the phases, possessing higher surface tension, exhibit itself in the form of droplets or emulsion. If by rapid cooling a glass is made to retain its homogeneous form, it will show this phase separation during reheating However, in most of the cases a two phase separation occurs very rapidly once the glass is cooled below a critical immiscibility temperature This is initiated by a process of homogeneous nucleation and is more probable than homogeneous nucleation of a crystal phase within the glass, because the interfacial energy between two liquids is very small and may be almost zero wheras that between a glass and a crystalline substance is quite significant (Mc Millan 1979)

Phase separation is exhibited by glasses, which show both stable and metastable liquid immiscibility. The general features of immiscibility are represented in binary phase diagrams for a hypothetical two-component system involving A and B, Two types of situation may arise as has been depicted in Fig 1 3 and Fig 1.4 respectively Examples of glass systems

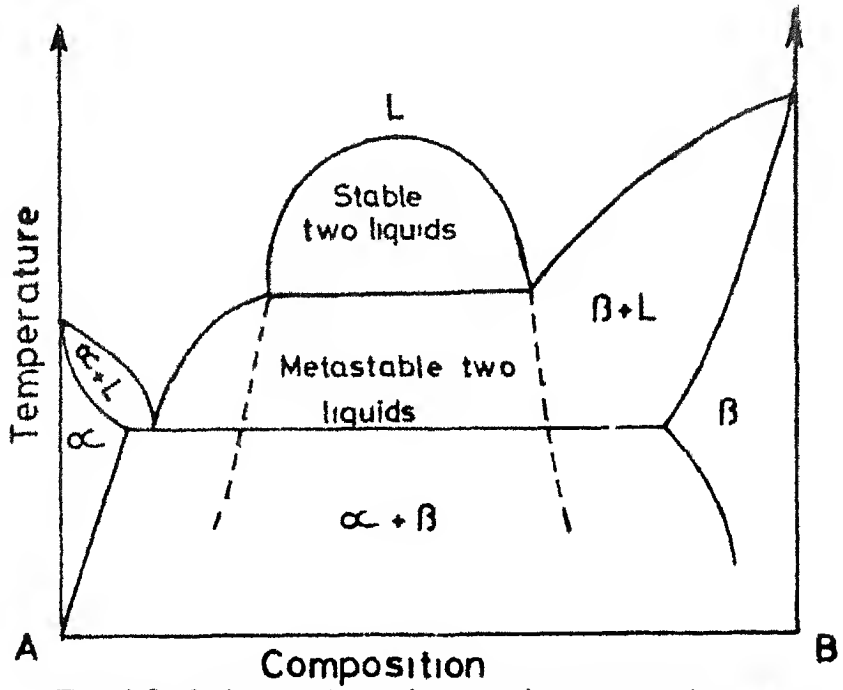

Fig 1 3 Schematic phase diagram showing stable and metastable liquid immiscibility

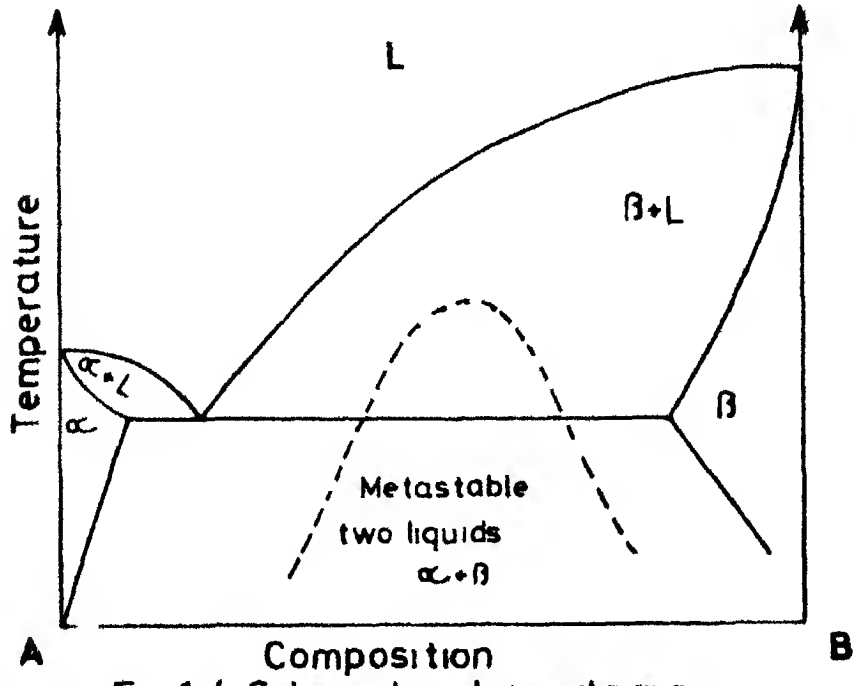

Fig 1 4 Schematic phase diagram showing metastable immiscibility

which show a behaviour typical of fig 1 3 are MO-SiO_2(M= Mg, Ca, Pb) (James 1975 , Doremus 1973) and ZrO_2, SiO_2(Evans et al 1980) Features characteristic of Fig 1.4 have been found in many systems including BaO-SiO_2, R_2O-SiO_2(R = Li, Na), Al_2O_3-SiO_2(Dong Hi and Mc Pherson 1980) The crystalline phases and the metastable immiscibility regions of phase diagrams are obtained by quenching experiments (Evans et al 1980)

The tendency of phase separation, both above and below the liquidus line has been observed The result of immiscibility can be amorphous phase decomposition or glass-in-glass separation Initial state of the material i e whether it is thermodynamically metastable or unstable, is the prime factor to decide the mechanism of decomposition In case of metastable region, decomposition occurs by the classical nucleation and growth mechanism The typical microstructure of such a sysyem is characterised by discrete particles dispersed throughout a continuous matrix In unstable region, the phases formed during decomposition grow by increasing compositional contrast Microstructure developed by this mechanism are typified by irregular diffuse phase boundaries and both faces are continuously interconnected In a hypothetical two component system immiscibility region is represented by a dome as shown in Fig 1 5 The free energy configurations at various compositions have a typical variation as shown in Fig 1 6, at two temperatures T_1 and T_2 respectively.

At temperature T_2 which is below the liquidus line, the presence of two minima in the free energy curve, leads to

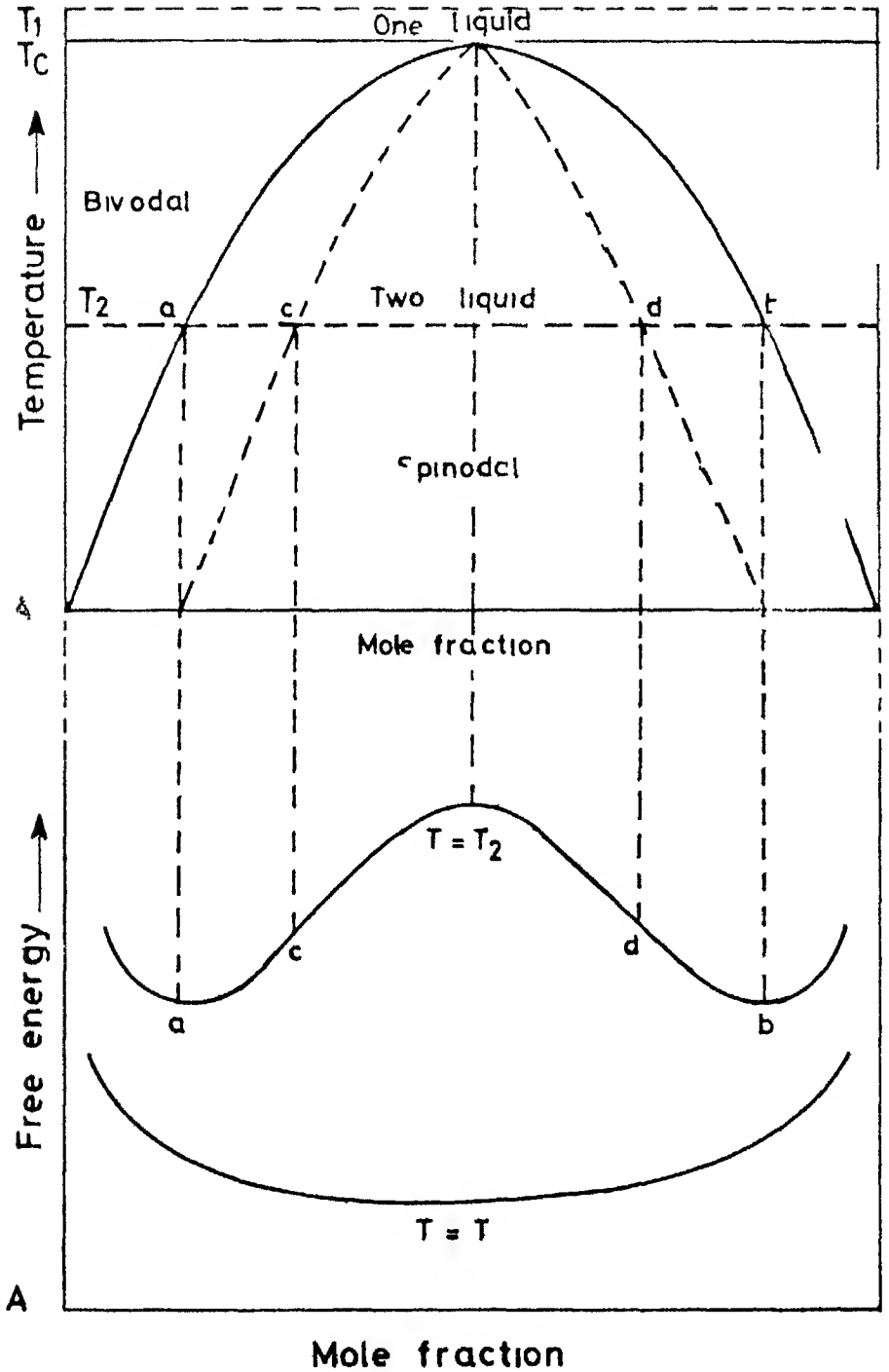

Fig 15 Immiscibility dome for hypothetical two component system

Fig 16 Free energy verses composition of hypothetical two component system

separation into two phases for compositions lying between A and B as the free energy gets minimised by such a conversion The loci of free energy minima, as the temperature is varied forms the immiscibility dome as marked in Fig 1 5 Two minima, coincede at T_c which is referred as the upper consolute temperature within the immiscibility dome The dotted curve covers the composition range in which phase separation occurs by spinodal decomposition. This curve is the loci of points for which $\frac{\partial^2 G}{\partial c^2} = 0$ at different temperatures (Cahn 1968) In this region a small fluctuation in composition is associated with a reduction of a free energy so that the fluctuation is stablised and separate phases grow In the regions between a and c and between b and d $\frac{\partial^2 G}{\partial c^2}$ = positive and hence any composition fluctuation here is associated with an increase of energy Therefore in these ranges of composition phase separation arises due to a nucleation and growth (Cahn 1968) mechanism

In a widely applicable-theory (Cahn and Hilliard 1959) the variation of free energy with spatial variation of composition is considered Total free energy of such a system is given by

$$F = \int_V [\, f_c(c) + k_c (\nabla c)^2] \, dv \qquad (1\ 59)$$

where $f_c(c)$ is free energy per unit volume of uniform composition c and k_c is the gradient energy coefficient

It has been shown that at very low supersaturations the properties of nucleus in metastable region (between binodal and spinodal) approach those predicted by the classical

theory of homogeneous nucleation (Russel 1970) Equation (1 59) is also used to analyse the spontaneous decomposition inside spinodal (Chakravorty 1981)

The reason for phase separation is basically structural and is determined by effects of network forming and network modifying cations an the final structure of glass system (Mc Millan 1979) Silicate glasses are built up of units of SiO_4 tetrahedra in which some 'foreign structural units have been incorporated At low concentration of foreign unit, the structure may be stable, resulting in a single-phase glass, at higher concentrations, the disruptive effect can lead to separation into two phases, one of which is rich in silica while the other is rich in oxide containing the foreign element At still higher concentration the added oxide forms the major component such that a single phase system results in which SiO_4 tetrahedra can be regarded as being dissolved in the network of the second oxide

Various techniques have been used to characterise phase separated glasses Table 1 6 summarises the glass system investigated and the technique used for characterisation

The effect of phase separation on mechanical properties is significant Young's Modulus decreases by 3% as the texture of structure coarsens from 400 to 1500 $\AA$ (Zarzycki 1974) . This is significant but quite small when compared to 10^5 fold change in viscosity that can occur during phase separation (Simmons et al 1970) It has been reported that poisson's ratio is the property most senstive to structural changes (Nimilov & Gilev 1972)

Table 1 6 Various glass systems exhibiting phase separation and the techniques for characterisation

Sl No	Glass Composition	Technique of Characterisation	References
1	Li_2O SiO_2	Electrical Conductivity	Charles (1963)
2	Na_2O B_2O_3 SiO_2	Electrical Conductivity	Charles (1964)
3	SiO_2 B_2O_3 Al_2O_3 K_2O Li_2O	Electrical Conductivity	Tomozawa (1978)
4	Na_2O SiO_2	Electron Microscopy	Moriya et al (1967)
5	Li_2O SiO_2	Electron Microscopy	Moriya et al (1967)
6	Na_2O CaO SiO_2	Electron Microscopy	James and Mc Millan (1968,1970)
7	Na_2O B_2O_3 SiO_2	Electron Microscopy	Haller et al (1970) Srinivasan et al (1971)
8	Na_2O BaO SiO_2	Electron Microscopy	Seward et al(1968), Mc Dowell and Beale (1969)
9	Na_2O SiO_2	Small Angle X-ray Scattering	Neilson (1969), Tomozawa et al (1970) Weinberg and Neilson (1978)
10	PbO B_2O_3	Small Angle X-ray Scattering	Zarzycki and Naudin (1967), Neilson(1972)
11	PbO B_2O_3 Al_2O_3	Small Angle X-ray Scattering	Zarzycki and Naudin (1969), Srinivasan et al (1973)
12	Na_2O B_2O_3 SiO_2	Small Angle X-ray Scattering	Tomozawa and Takamori (1977)

13	K_2O CaO B_2O_3	Electron Spin Resonance	Kawazoe et al(1978), Kokumai andKKanazawa (1979)
14	K_2O BaO B_2O_3	Electron Spin Resonance	Kawazoe et al (1978) Kokumai and Kanazawa (1979)
15	CaO Al_2O_3 B_2O_3 SiO_2	Light Scattering	Hammel and Ohlberg (1965)
16	SiO_2 B_2O_3 Al_2O_3 K_2O Li_2O Na_2O	Light Scattering	Takamori and Tomozawa (1976) Kerwawyez and Tomozawa (1980) Tomozawa and Takamori (1980)
17	TeO_2 P_2O_5	Neutron Diffraction	Neov et al (1980)
18	Na_2O B_2O_3 SiO_2	Chemical Durability	Takamori and Tomozawa (1978), Tomozawa and Takamori (1977)
19	Na_2O B_2O_3 SiO_2	Viscosity	Mazurin and Strettsina (1972), Simmons et al (1974), Tomozawa (1978) Takamori and Tomozawa (1979)

hence to phase separation Various models to calculate Young's modulus for such system are reported in literature (Hashin and Shtrikman 1963, Shaw and Uhlman 1971)

Phase separated glasses can be leatched out to obtain microporous glasses having an interconnected microstructure Such porous glasses have enormous potential to be used in various applications (Mc Millan 1976) Their important applications include enzymes immobilising substrates (Weatall 1969) carbon deposited resistance thermometers (Lawless 1972), high 'H_c' superconducting materials by impregnating it with Pb-Bi alloy and molecular stuffing by index modifier like CeO_2 to make preforms for optical waveguides

1 5 Statement of Problem

From the discussion given in the previous sections it becomes apparent that most of the fast ion conducting glasses contain silver as the migrating species. However, very few of these glasses are based on SiO_2 as the network former The reason is that it is difficult to incorporate silver ions in such a network in a large concentration because of the problem of silver precipitating out as metallic agglomerates during the melting operation [Riebling 1971] It is possible to incorporate silver ions into a silicate glass by an alkali $\rightleftharpoons$ silver exchange reaction at a temperature much below the glass transition point [Frischat 1976] However, such an exchange mechanism is controlled by the interdiffusion coefficient between silver and the alkali ion concerned [Doremus 1964] Under ordinary ion exchange conditions viz , temperature around 300°C and duration extending to 36 hours the silver-rich layer is found to be only a few tens of microns thick [Matousek 1973, Garfinkel 1972] Hence, one way to study the effect of replacing most of the alkali ions in a silicate glass by silver ions will be to carry out such experiments on glass fibres having diameters of the order of 10 microns In the latter case, it will be possible to substitute most of the alkali ions by silver within the glass by an ion-exchange process. The present work has been undertaken to investigate the effect of sodium $\rightleftharpoons$ silver exchange on the electrical properties of suitably chosen silicate glass fibres

Presence of metallic granules may also affect the ionic conductivity of glass fibres It has been reported that the

strength of bulk glasses can be improved by the incorporation of metallic particles within them [Krestic et al 1981] Investigation on the effect of metallic micro granules on the electrical conductivity as well as mechanical properties of glass fibres has also been included in the present study

The objectives of the present thesis may be summarised as follows:

(1) To design and fabricate a semiautomatic fibre drawing assembly incorporating various facilities e.g , monitoring and controlling the temperatures, temperature gradient and drawing velocities

(2) To draw glass fibres from various glasses and glass-metal composite systems.

(3) To subject all the above fibres to a sodium⇌silver ion exchange under suitable conditions of temperature for reasonable period of time & to chemically analyse the ion-exchanged glass fibres for their silver content so as to correlate this with the resulting electrical conductivity

(4) To characterize the electrical properties of both virgin and ion-exchanged glass fibres

(5) To characterise the microstructure of all glass fibres by transmission electron microscopy

(6) To measure the strength and young s Modulus of metal containing glass fibres

(7) To study fracture surface of the metal containing fibres by scanning electron microscope (SEM) and correlate with observed strength

(8) To analyse the strength data of metal containing glass fibres by Weibull analysis

CHAPTER II

EXPERIMENTAL TECHNIQUES

In this chapter various aspects of preparation of glasses in both bulk and fibre form are being discussed The details of the fibre drawing assembly used in the present work are described Different characterisation techniques employed are delineated

2.1 Preparation of Glass

All glasses are prepared from reagent grade chemicals Two base glass systems chosen for the present investigation are referred as N and A Their compositions are described in Table 3 1 and Table 4 1 respectively

Proportionate amounts of various oxides (e g SiO_2 Al_2O_3) or compounds (e g Na_2CO_3 for Na_2O, $CaCO_3$ for CaO, and H_3BO_3 for B_2O_3) or metal powder (e g Al) are thoroughly mixed using acetone as grinding medium in FRITSCHE Ball Mill to prepare batch mixtures of various glasses in each system Each mixture is melted in pure alumina crucible in a temperature controlled electrically heated furnace All these glasses

have been melted at temperatures in the range of 1300°C to 1450°C They have been kept at this temperature for two hours each and are mechanically stirred so as to make it bubble free and homogeneous The melt is poured in an aluminium mould to get a rectangular glass block which is immediately taken inside an annealing furnace maintained at 500 C where it is annealed for 6 hours After taking it out from the annealing furnace, it is kept inside a desiccator The fibre form of these glasses is obtained by fibre drawing assembly (FDA)

2 2 Fibre Drawing Assembly (FDA)

Fig 2 1 shows the photograph of this assembly Fig 2 2 gives a schematic view of the same unit The salient features of this system are as follows

(i) The unit is based on bushing technology where the bushings are made of pure alumina indigeneously developed and fabricated in this laboratory [Chakravorty et al 1981

(ii) The bushings are heated externally by a temperature controlled electrically heated semi cylindrical furnace (13 5 KVA) The heating chamber contains eight globar rods to which power is fed from transformers

Upper section of FDA with v
ous facilities (
conditions of this drawing

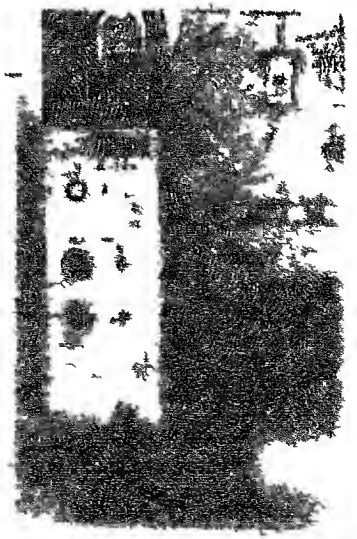

r r view of furnace assembly
porting arrangements for
and its accessories

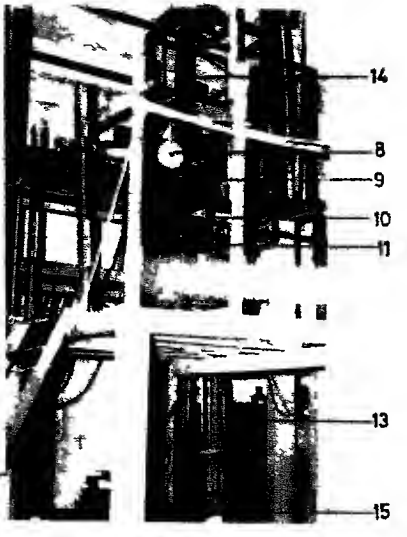

Upper section of FDA with various facilities to maintain optional conditions of fibre drawing

Characteristic parameters of FDA
(a) Furnace power 13 5 KVA
(b) Furnace temperature (max) 15
(c) Bushing tip temperature 1
(d) Temperature gradient t
tip (100 5 C
(e) Velocity of draw)

1 On line display show nr c c
state of F D A
2 Digital display for measureme
temperatures of various p t
F D A
3 Temperature controller
4 Velocity monitor
5 Manual control
6 Dyno drive motor
7 Drum
8 System to move hor zontal pl
separating vertical nam
heating chamber
9 Furnace assembly
10 Location of bush ng and te
erature gradient ont
angement
11 Assembly to measure e
ture profile in f b s
12 Transformer
13 - Virgin sample cell c
14 System to move u
embly in and u
chamber
15 Graphite shoe

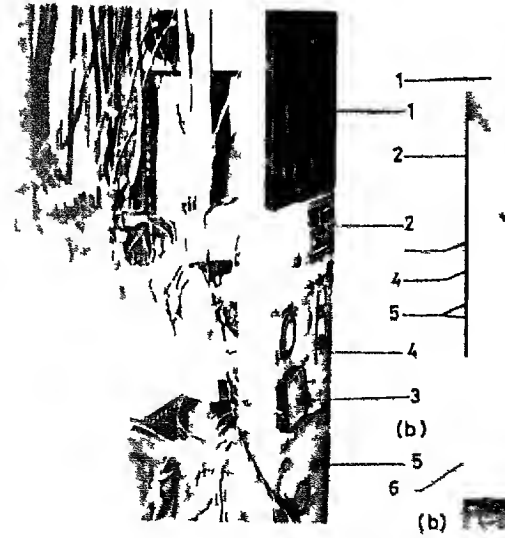

ontrol panel

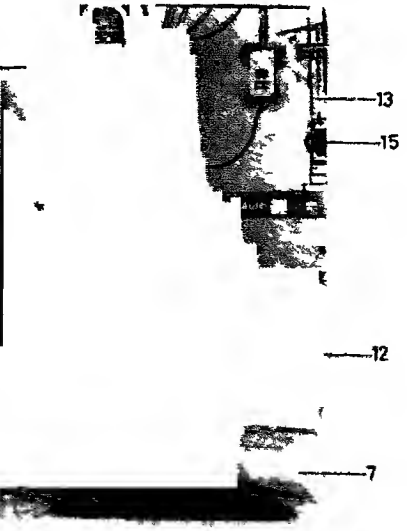

Lower section of FDA with control panel

Fig 2 emi automatic fibre drawing assembly (FDA) indigenously designed and fabricated by the author

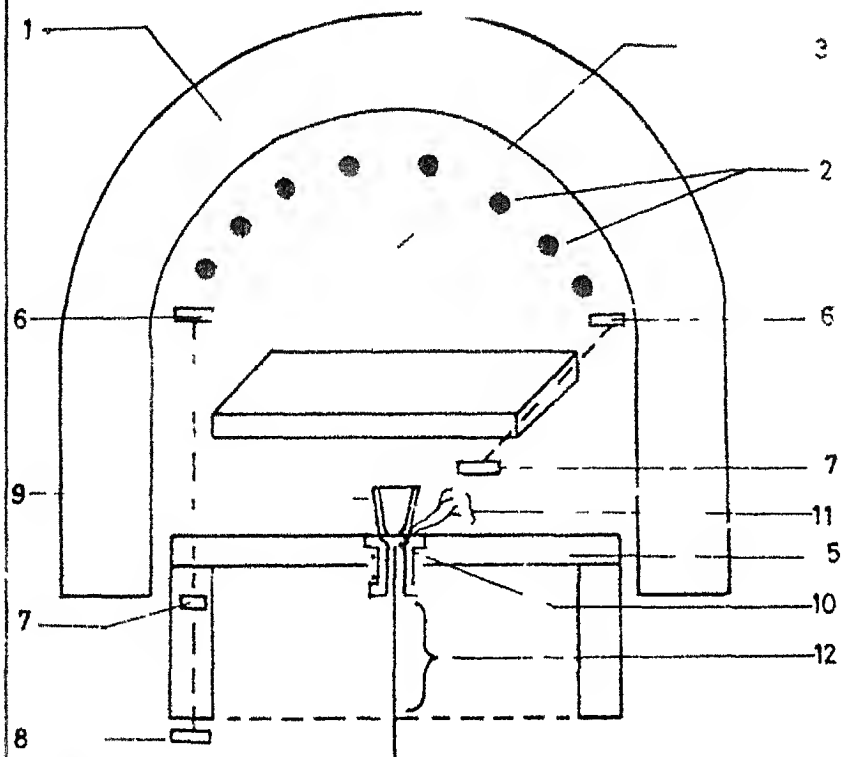

1-Thermal insulations
2-Globar rods
3 H C
4-P H
5 P V
6 7 8 Displacement limits for PH PV
9-Alumina bushing
10-T G C U
11-Thermocouples
12-T P U
13-V S U
14-Drum
15-Motor
16-S F
17-Sample holder
18-Glass fibre

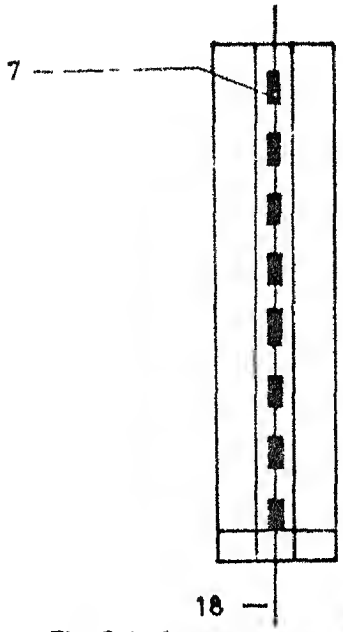

Fig 24 Schematic view of V S U

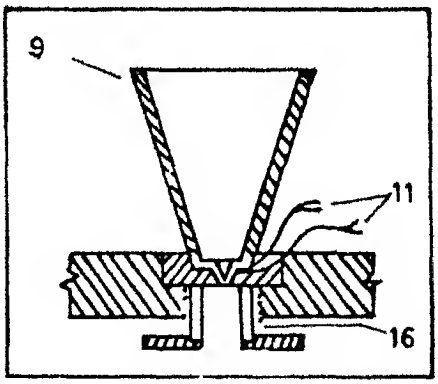

Fig 23 Schematic view of T G C U

Fig. 22 Schematic view of fibre drawing assembly (F D A)

(iii) The furnace temperature is controlled by a suitable temperature controller (APLAB 7152) using Pt-Rh thermocouples which are placed at different furnace zones The temperature in the furnace can be maintained upto 1550°C with an accurcy of $\pm$ 10°C

(iv) The heating chamber (HC) is separated from a vertical one by a horizontal ceramic plate(PH) The temperature gradient in the vertical chamber (VC) can be varied by moving the horizontal plate in or out

(v) An alumina bushing with a single nozzle is placed in the opening of a ceramic base plate (PV) which moves vertically in and out of vertical chamber (VC) Around this opening there is a small furnace (SF) which carries bushing The temperature and temperature gradient at the bushingtip may be varied and maintained to a specific set of values by combination of movement of ceramic plates PH,PV and temperature in HC and SF TGCU represents the arrangement to monitor and control the temperature gradient at the bushing tip Within this, SF is located The bushing tip temp can be varied upto 1200°C while temperature gradient may vary in range of 100°C/Cm to 500°C/Cm (Fig 2 3)

(vi) Glass is kept in the bushing and melted. At optimum conditions of temperature and temperature gradient, a glass meniscus is formed at the bushing tip, which is drawn in fibre form by a variable velocity motor 'DYNO DRIVE' at the required pulling rate. The velocity of draw may be

varied in the range of 3m/sec to 20 0 m/sec The fibre is wound on a drum

(vi) The incoming fibre before being wound on the drum passes through VSU unit (Fig 2 4) to collect virgin fibre samples for mechanical characterisation As described in section 1 1 2 4 strength of glass fibres is quite sensitive to surface damage Hence to measure the strength of glass fibres before they come into contact with any other surface, virgin samples may be collected in situe of fibre drawing process by VSU unit

(vii) The temperature distribution along the fibre, during fibersing operation is recorded by TPU unit which measures temperatures along a length of 30 Cm at an interval of 1 Cm each

2 2 1 Optimal conditions of fibre drawing:

Viscosity temperature characteristics of a glass determine its optimal conditions of fiberisation This itself is decided by the chemical composition of glass For a given glass two parameters need a stringent control and monitoring They are

(i) The temperature at the bushing tip (T_B)
(ii) The temperature gradient at the bushing tip (TG_B)
(iii) The temperature of glass melt (T_M)

Usually T_B, TG_B and T_M have a narrow zone of variation within which fibre can be drawn continuously without encountering fibre breakage If because of any perturbation, either of these parameters attains a value beyond the critical range, fiberisation

process ceases and either of the following situation may arise

(1) Glass inside the bushing may be very fluid but yet no meniscus be formed at the bushing tip This implies that either of (2 1) and (2 2) or both together are true

$$T_B < T_B \text{ (critical)} \qquad (2\ 1)$$

$$TG_B > TG_B \text{ (critical)} \qquad (2\ 2)$$

This situation is termed as bushing being situated in 'Cold Zone' In such a case, optimal conditions are regained in this FDA by (i) moving base plate inside the vertical chamber and / or (ii) opening of horizontal plate and/or (iii) increasing current in minifurnace

(2) Glass is so fluid that glass starts pouring out through the bushing tip and no fiberisation is possible as glass meniscus drops to the ground before it can be attenuated to fibre form by the pulling force This situation may be described by bushing situated in 'Hot Zone' In such a case

$$T_B > T_B \text{ (critical)} \qquad (2\ 3)$$

$$TG_B < TG_B \text{ (critical)} \qquad (2\ 4)$$

$$T_M > T_M \text{ (critical)} \qquad (2\ 5)$$

The situation is brought back to normal one by (i) reducing current in minifurnace and/or (ii) moving base plate down in the vertical chamber and/or (iii) closing of horizontal plate

Many times due to variation in local composition of glass or due to irregualr power supply, such perturbation do arise

which brings the once attained optimal conditions to either of 'Cold Zone' or 'Hot Zone' state thereby needing resetting of the conditions In this present set up, this is done automatically by a series of control mechanisms activated by a temperature sensitive feed back circuit

2 3 Preparation of Ion Exchanged Glass Fibres

Glass fibres drawn from FDA are subjected to $Na^{+} \rightleftharpoons Ag^{+}$ ion exchange, in order to produce ion-exchanged glass fibres Bunches of glass fibers of 10 Cm length are cut from the fibre cake wound on the drum These are immersed in liquid $AgNO_3$ bath which is made of a pyrex boat of semi-circular section. This boat is maintained at the required temperature within a temperature controlled electrically heated furnace with an accuracy of $\pm$ 1°C After fibres have been subjected to ion-exchange treatment for the reasonable time (36 hours) boat is taken out of the furnace bunch of ion exchanged glass fibres taken out from $AgNO_3$ melt and cooled in a petri dish These fibres are treated in boiling water thrice for 1 hr duration each and then washed throughly in acetone to remove any silver nitrate adhering to their surfaces

The fibres are taken out of acetone bath and kept in a desiccator

2.4 Electrical Resistivity Measurement

2 4 1 Sample Preparation:

A piece of 2 Cm length is cut from the bunch of glass fibres for both virgin as well as ion exchanged fibres They are weighed by a electronic weighing balance (least count 10ugm)

A length of 0 5 Cm from each side of this bunch of fibres is coated by silver paste This bunch is placed between two stainless steel electrodes of conducting cell and pasted at the electrodes by silver paint

2 4 2 Conductivity Cell

Fig. 2 5 shows the schematic view of the cell used for electrical measurements It consists of a stainless steel jacket J, 300 mm long having a diameter of 50 mm E_1 and E_2 are two stainless steel electrodes These electrodes consist of a screw and nut arrangement having two small stainless steel bushes which are used to hold the sample The bushes are tightented by a spring attached to it by the nut so as to always keep it in a compressed state These electrodes are supported on an alumina substrate which itself is attached rigidly to the main structure of the cell The centre to centre distance between the two electrodes is 22 mm , while the diameter of each of bushes is 1 2 mm. Thus the free distance between the two bushes is 10 mm The sample of length 20 mm , coated on both ends by silver paste (NPL, New Delhi) upto 5 mm length, is clamped between these spring supported bushes Silver paste is also applied to these bushes before placing the specimen, so as to assure good ohmic contact between the specimen and the bushes The spring supported mechanism ensures good ohmic contact even at higher temperature

The main structure of the cell consists of three stainless steel rods fixed to a bronze flange The alumina substrate supporting the electrode assembly is rigidly attached to this main structure

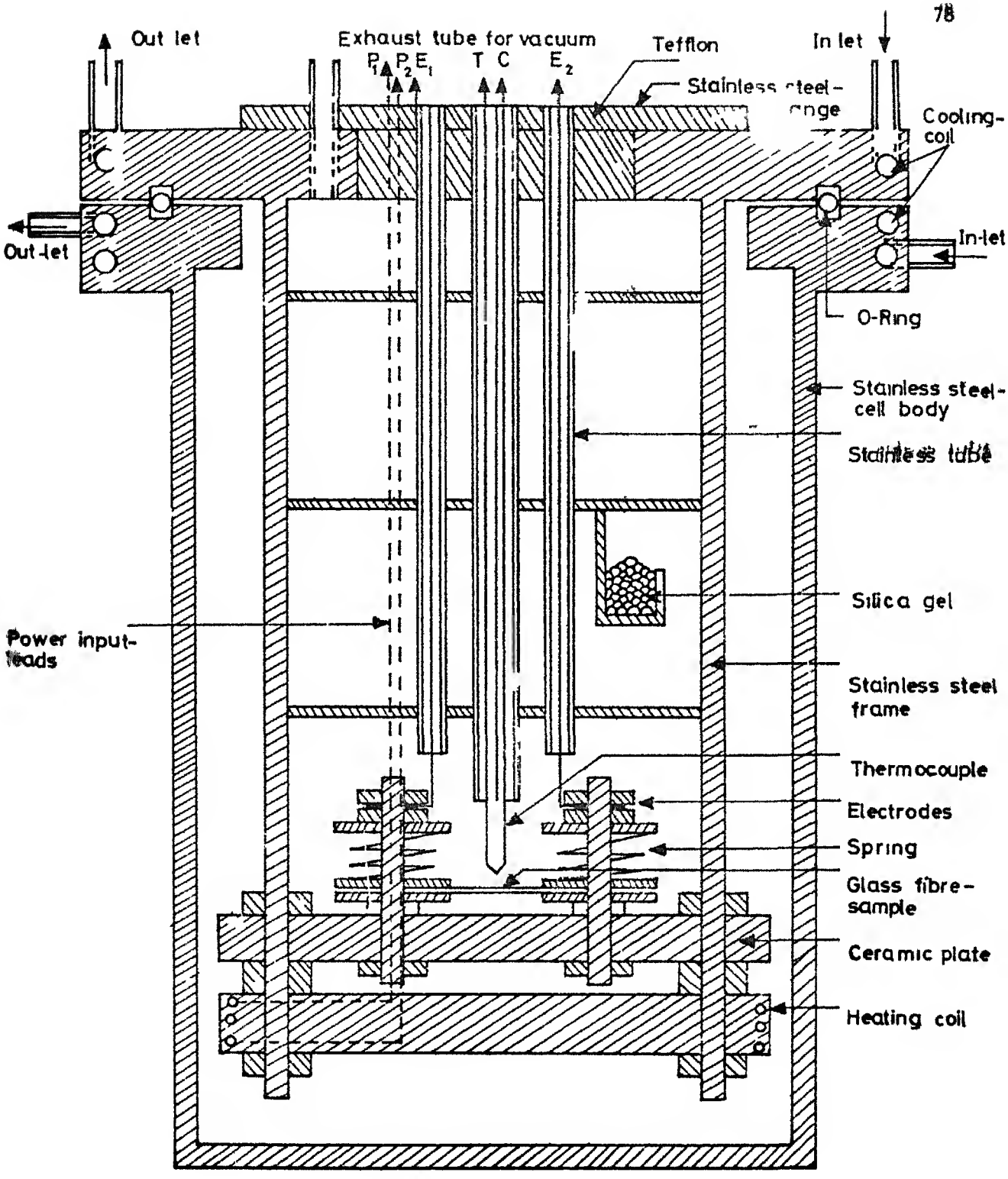

Fig 2.5 Schematic view of the conductivity cell

The electrodes are connected to the BNC connectors B with shielded wires A chromel-alumel thermocouple is placed near the electrode assembly its other end taken out through the teflon disc fitted onto the flenge H_C is a non-inductive heating coil wound on a porcelain tube This is connected to a 30 volts 2 amperes regulated power supply , through the shielded wires passing through the teflon disc The flange is brazed with a cooling coil and clamped to the jacket through O ring The jacket also has cooling coil assembly attached at its top D contains the desiccant, silica gel for keeping the chamber moisture free The sample holder can also be flushed with a dry gas After loading the sample, the entire assembly, properly connected and clamped is placed inside an electrically heated temperature controlled assembly By this set up the temperature can be varied from room temperature to 500°K with an accuracy of $\pm$ 1°K

2 4 3 D C Resistivity

Fig 2.6 represents the schematic view of circuit used for measurement of current-voltage characteristics of different samples The sample and the standard resistance are in series with a 30 V 2 amp DC regulated power supply (APLAB Model 7152) The potential drop across the standard resistance is fed to Y axis of XY recorder (No 2000 made by Digital Electronics Ltd India) The potential drop across the sample is fed to Keithley Electrometer (model 610) whose out put is fed to X axis of the XY recroder Use of electrometer is necessary because of the impedance mismatch of sample ($\simeq 10^{10}\Omega$) with that of

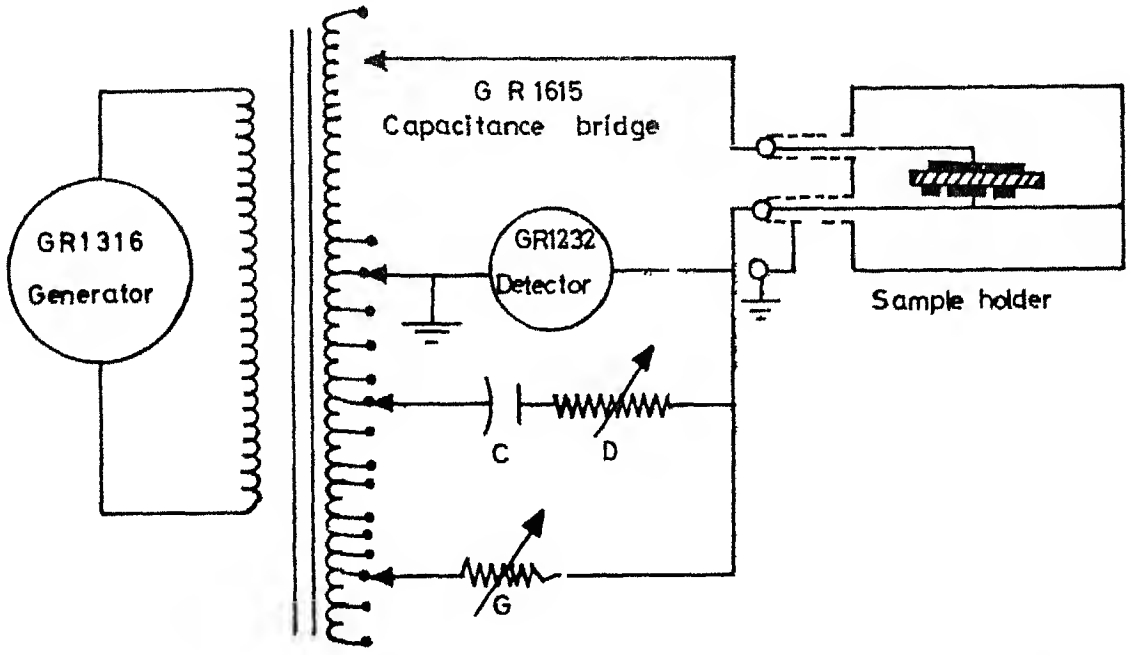

Fig 27 Schematic circuit diagram for A C resistivity measurement

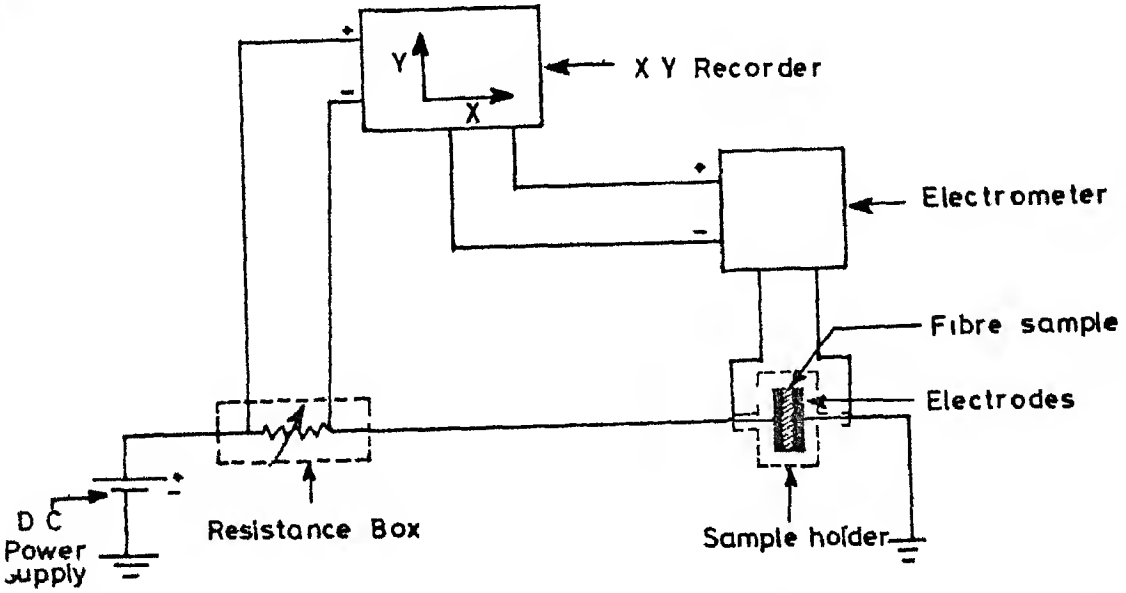

Fig 26 Schematic circuit diagram for D C resistivity measurement

the XY recorder ($10^6\Omega$) The applied voltage is varied by the power supply and this is recorded as I-V characteristic on the X-Y recorder at a given temperature The sample consists of number of fibres parallel to each other If ith fibre has a resistance r_1 the total resistance (R_o) of the sample is given by

$$\frac{1}{R_o} = \Sigma \frac{1}{r_1} \qquad (2\ 6)$$

$$\text{as } r_1 = \rho \frac{l_i}{A_1} \qquad (2\ 7)$$

$$\text{so } \frac{1}{R_o} = \rho\Sigma \frac{A_i}{l_1} = \rho\Sigma \frac{A_1\ l_1}{l_1^2\ d_1} \frac{d_1}{} = \rho\Sigma \frac{m_i}{l_1^2 d_1}$$

As all lengths are equal to L so

$$\frac{1}{R_o} = \frac{\rho}{L^2 d_1} \Sigma m_1 = \frac{m_o \sigma}{L^2 d_1} \qquad (2\ 8)$$

where m_o and L are the mass and length of uncoated length of specimen If M and L_1 are the mass and length of sample

$$m_o = \frac{M}{L_1} L \qquad (2\ 9)$$

from equations (2 8) and (2 9)

$$\rho = \frac{M}{L\ L_1\ d_1} R_o \qquad (2\ 10)$$

where R_o is the resistance determined by the slope of (I-V) curve

Before each measurement, the temperature of the system is maintained constant for sufficient time (approx 20 minutes) to attain equalibrium by the arrangements described earlier

2 4 4 A C Resistivity

A schematic circuit diagram for AC resistivity measurement is shown in Fig 2 7 A General Radio GR 1615 transformer ratio arm capacitance bridge with GR 13136 oscillator bench and GR 1232 tuned amplifier and null detector are used to measure capacitance c and conductance G at various frequencies At each temperature the a c resistivity is determined by measuring capacitance and conductance G at frequencies (f) 02, 12, 1 0, 5 0, 10 0, 50 0 and 100 KHz respectively The a c resistivity is obtained from the following equation,

$$\rho_{AC} = \frac{M}{LL_1 d_1} \quad \frac{1}{G} \qquad (2\ 11)$$

where m k s units are used for M ,L,L_1 and d_1

The real and imaginary parts of the dielectric permittivities are calculated using the relations

$$\epsilon' = \frac{d_1 L L_1}{M} \quad \frac{C}{\epsilon_o} \qquad (2\ 12)$$

$$\epsilon'' = \epsilon' D \qquad (2\ 13)$$

$$D = \frac{\omega C}{G} \qquad (2.14)$$

where $\omega = 2\pi f$

and $\epsilon_o = 8.54 \times 10^{-12}$ farads/m is the dielectric constant of free space

2.4 4 1 Complex Impedance Analysis of A-C Data

Conductance G(ω) and capacitance C(ω) contain all the information regarding electrical relaxation at a given temperature For various reasons, these variables are transformed to complex resistivities (ρ*) complex modulus (M*), complex permittivity (ϵ^*) or some other formalism (Böttcher and Bordewijk 1978 Wong and Angell 1976) It is important to note that such transformations may emphasize and therefore, help resolve one particular aspect of relaxation process, but no new information which is not contained in G(ω) and C(ω) can be extracted For a specimen of unit thickness and unit area of across section

$$\rho^* = \rho' - i\rho'' = \frac{G}{G^2+\omega^2C^2} - i\frac{\omega C}{G^2+\omega^2C^2} \qquad (2\ 15)$$

$$M^* = M' + iM'' = \frac{\omega^2 C}{G^2+\omega^2C^2} + i\frac{\omega^2 G}{G^2+\omega^2C^2} \qquad (1\ 16)$$

$$\epsilon^* = \frac{1}{M^*} \qquad (2\ 17)$$

complex conductivity $\sigma^* = \frac{1}{\rho^*}$ (2.18)

and loss tangent

$$\tan\delta = \frac{\epsilon''}{\epsilon'} = \frac{\omega C}{G} \qquad (2\ 19)$$

These equations imply that a plot of ρ'' or M'' vs log ω will show Debye peak at $\omega\tau = 1$ where $\tau (= C/G_{D\ C})$ is the time constant The ρ' or M vs log ωτ will be a sigmoidal curve with

a point of inflexion at $\omega\tau = 1$ On a complex plane ρ' vs ρ' will be a semi circle passing through origin. However, the experimental data for any glass rarely agree with the above description This implies that specimen can not be simply treated as a parallel combination of a resistive and capacitative element This departure in behaviour from that of an ideal capacitor is due to that fact that a real sample usually consists of a discontinuity at the electrode glass interface which has different polarisation properties than the bulk specimen In most cases this can be approximated by a series combination of two parallel R-C elements

The electrode interface polarisation is a highly capacitive phenomenon, exhibiting a much larger time constant than the bulk phenomenon. Complex resistivity plots (ρ'' vs ρ') are generally used to separate these two effects, each appearing as an arc of a circle(Hodge et al 1976, Jain H and Nagi K L 1983). The D C. conductivity of the glass is given by the high frequency intersection of the semicircle with the real axis This procedure has been used in the analysis of data so as to check whether there is any effect of the electrode polarisation on the data collected by either D C or A C resistivity measurements.

2.5 Differential Thermal Analysis (DTA)

To determine various transformation temperatures characteristic of a glass system, DTA analysis is undertaken for all the virgin glass fibre samples The fibres are ground and then sieved out in the range of -14 mesh to 20 mesh (particle

size ≃ 10um) Pure alumina is taken as a reference These powders (100 mg) are taken in alumina crucibles and heated at a rate of 10°C/minute upto 1000°C Temperature, DTA and weight loss are recorded photographically by a MOM Derivatograph, Hungary

2 6 Electron Microscopic Analysis (TEM)

Both virgin as well as ion exchanged fibres are subjected to electron microscopic analysis Their microstructures and selected Area Diffraction (SAD) are recorded by Phillips EM 301 electron microscope operating at 100 kV For this purpose the electron microscopic samplesare prepared in the following manner

2 6 1 Preparation of Electron Micropic Sample:

A thin film of carbon is deposited on a cleaned glass slide Cuts in form of squares of approx sizes of 2 mm x 2 mm are made on this film formed at the glass slides The glass slide is dipped into deionised water and small pieces of carbon films peel off from the surface of glass slide and float on the surface of water Electron microscopic copper grid (EMG) is made to cover itself by one of these small pieces by dipping it into the water below the floating piece and taking it out along with the film This carbon coated grid is kept on a cleaned glass slide Glass fibres are crushed to very fine powder form and a very dilute suspension of this powder is made in acetone A drop of such suspension is poured on the carbon coated EMG A thin film of callodion is floated on the surface of deionised water and this sample containing EMG is placed on the surface of this film in such a way that glass particles re sandwiched below the carbon and callodion films respectively

The EMG is fished out of water and dried in an oven at 100°C for 1 hour

2 6 2 Analysis of S A D

The diameters of diffraction rings are measured from the negtive by using a graduated eye-piece with an accuracy of 01 Cm The interplaner spacings are calculated from the relation given below

$$R_s\, d_{hkl} = \text{Camera Constant} \qquad (2\ 20)$$

where R_s is radius of diffraction ring and d_{hkl} the corresponding interplaner spacing The camera constant is determined from the standard gold diffraction pattern obtained at 100 kV (Srivastava A and Chakravorty D 1978)

2 7 Chemical Analysis

To estimate the concentration of silver ions in the ion exchanged glass fibres a weighed amount of these fibres is dissolved in dilute HF and a few drops of HNO_3 added so as to dissolve silver in the form of silver-nitrate The resulting solution is analysed for silver by an IL/751 atomic absorption spectrophotometer, which is calibrated by standard solutions of silver in the form of silver nitrate

2 8 Density Measurement

Density of glass is measured by bouyancy method A known weight w_1 of glass is dipped into the water and weighed

giving its value W_2 Density is calculated by following formulae,

$$d_1 = \frac{W_1}{W_1 - W_2} \qquad (2\ 21)$$

2 9 Diameter Measurement

Diameters of glass fibres are measured by an electronic comparator 'Sheffield ACCUTRON' U S.A. with an accuracy of 254 micron The fibre is held between two heads of a pressure transducer which is calibrated for the desplacement First the scale of accutron is calibrated by slip gauges

2 10 Measurements of Strength and Young's Modulus of Glass Fibres

2 10 1 Sample Preparation

To measure the strength(S) and Young's (E) modulus of glass fibres samples of length 10 Cm each are cut and pasted on fibre mounts which are fairly stiff smooth rectangular bits of paper of dimensions 10 Cm x 1 5 Cm x 25 Cm, having a rectangular slot of width 1 0 Cm and length equal to the gauge length, in the centre of paper (Fig 2 4). The fibres are mounted in a line through the centre of each slot and parallel to it Fibres are held firmly to the mount by pasting an adhesive (Quick Fix) at the mounts of this slot. The extra lengths of fibre extending for about 2 Cm each beyond the slot are either side are fixed to the ends of mounts by using cellotape These extra ends may be used for diameter measurements in cases where the bits of fibres remaining within the gauge length after breaking is too small to be of any use The mounts are

stored in a desiccator In case of determining the virgin strength of fibres, the samples are collected in situ during fibre drawing by the VSU unit of FDA (Fig 2 4) In case of non-virgin samples, fibres drawn and collected from the drum are used and single filaments are taken out from the bunch of fibres They are cut to proper size and mounted on the fibre mounts as described above

2 10 2 Testing of Fibres :

Instron Machine is used for the determination of S and E Fibre mount is firmly held between the two grips of Instron and load is adjusted to the zero value The sides of the mount are cut, leaving the fibre intact, so that when the crosshead is made to move, the entire load is taken by the fibre itself Fibre is pulled till it breaks The breaking load as well as the elongation in the fibre are directly read from the chart traced on the x-y recorder attached to Instron The load cell used has a range 0-50 gms with a least count of 1 gm A uniform chart speed of 2 Cm /min, 5 Cm/min & 10 Cm/min have been tried but for the accuracy of results chart speed of 10 Cm/min has been used Crosshead speed has been maintained at 0 05 Cm/min and a gauge length of 5 Cm has been used

2 10 3 Calculation of Strength and Strain

Strength of ith specimen is evaluated by measuring the breaking load P_i from the Instron chart and diameter (D_i) of fibre as described in Section 2.9 by the following

$$S_i = \frac{4 P_1}{\pi D_i^2} \qquad (2\ 22)$$

strain is given by e_i,

$$e_i = \frac{\text{Crosshead Speed} \cdot \text{Time Taken for Breaking}}{\text{Original Gauge Length of Fibre}}$$

$$= \frac{\text{Cross Head Speed} \cdot \text{Total distance Covered by Chart Upto Point of Breaking } (x_1)}{\text{Original Gauge Length of Fibre} \cdot \text{Chart Speed}} \qquad (2\ 23)$$

which under present conditions becomes

$$e_i = 10^{-3}\ x_i \qquad (2\ 24)$$

2 10 4 Determination of Young's Modulus:

For a single measurement Young's Modulus may be estimated by the ratio of strength to strain i e

$$E_i = \frac{S_i}{e_i} \qquad (2\ 25)$$

But it is seen that for a set of such measurements taken on N number of fibres ($N \geq 30$), E_i show a wide destribution Usually the mean of E_i found by equation (2 22) has been taken as an estimator for Youngsmodulus of glass fibres i.e

$$\overline{E} = \frac{\sum_{1=1}^{N}}{} E_i/N \qquad (2.26)$$

But it is being proposed that a better estimate of Young's Modulus can be made by regressing a straight line

between strength and strain, passing through the origin in the strength-strain plane The slope of this line gives the best estimater for young's modulus of the glass fibre, as the regression line approximates the actual stress-strain relationship for a given set of glass fibres If the regression line is given by

$$S = E_R \quad e \qquad (2\ 27)$$

where E_R is the slope obtained by the least square fit of the strength versus strain data then according to this proposition

$$\hat{E}(E) \quad = E_R \qquad (2\ 28)$$

where $\hat{E}(X)$ is the estimator of variable X.

2 10 5 Determination of Strength

Strength, especially in the case of glass fibres is a statistical quantity It arises due to the distribution of surface flaws existing on the surface of the fibres as have been described in section (1 1 2.1) Two estimators of strength $\hat{E}_1(S)$ and $\hat{E}_2(S)$ are being evaluated Either of them is found out by taking the mean value of strength for individual fibres

Two sets of strength data are available to represent the sample. One of them is found as per the equation (2 22), while the other set is found by using eq (2 27) This calculated strength S_c is found as

$$S_{c_i} \quad = E_R \quad e_i \qquad (2\ 29)$$

and two estimates of strength are given by

$$E_1 (S) = \bar{S} = \sum_{1}^{N} S_i / N \qquad (2\ 30)$$

$$E_2 (S) = \bar{S}_c = \sum_{1}^{N} S_{c_1} / N \qquad (2\ 31)$$

Where $\bar{S}$ and $\bar{S}_c$ are the mean of distributions of S_i and S_{c_1} respectively It is shown by variance and Weibull analysis respectively that $E_2(S)$ is a better estimator of strength than $E_1(S)$ for a given glass fibre

2 10 6 Weibull Analysis

It has been shown in section 1 1 2 3 that strength distribution is given by Weibull distribution as described by equation (1 3) This equation contains two parameters S_o and b Specification of strength value in terms of these parameters is the best way of representing the entire set of data These parameters contain all the information about the distribution. Two techniques are being used to evaluate S_o and b, which are as follows

2 10 6 1 Graphical Regression Technique (GRE)

In this method a least square fit line is regressed between Log S_i and Log (Log $(1-P_i)$) If J_1 and J_2 are the slope and intercept of (Log S_i) axis for Log (Log $(1-P_i)$) being zero, then equation (1 3) can be rewritten as

$$\text{Log } S = \frac{1}{b} \text{ Log } (\text{Log } (1-P)) + \text{Log } S_o \qquad (2\ 32)$$

So $b = 1/J_1$ (2 33)

and $S_o = \exp(J_2)$ (2 34)

To get P_i the probability of failure for strength $S \geqslant S_i$, the strength data are arranged in ascending order of values The cumulative probability P_i is found out from this table as

$$P_i = i/(N + 1) \quad (2\ 35)$$

Where i is the sequence number for strength P_i

2 10 6 2 Maximum Likelihood Technique (MLE)

In this technique, the likelihood function is minimised with respect to two parameters (Cohen 1951) The likelihood function for failured censored sample with failure strength of r fibres that failed out of n fibres is given by

$$L \propto \left(\frac{b}{A}\right)^r \left(\prod_{i=1}^{r} S_i^{b-1}\right) \exp\left(-\frac{\sum_{i=1}^{r} S_i^b}{A}\right) \left[\int_{sr}^{\infty} \frac{b}{A} S_1^{b-1} \exp\left(-\frac{S_i^b}{A}\right) ds\right]^{n-r} \quad (2\ 36)$$

Where $A = S_o^b$

Or $S_o = (A)^{\frac{1}{b}}$ (2 37)

Taking Log_e of L and differentiating equation (2 36) w r t A and b respectively one gets

$$\frac{\partial}{\partial A} \text{Log}_e L = -\frac{r}{A} + \frac{\sum_{i}^{r} s_i^b + (n-r)\, s_r^b}{A^2} \qquad (2\ 38)$$

$$\frac{\partial}{\partial b} \text{Log}_e L = \frac{r}{b} + \sum_{i=1}^{r} \text{Log}_e S_i - \frac{1}{A}\left[\sum s_i^b \text{Log}_e S_i + (n-r)\, s_r^b \text{Log}_e S_r \right] \qquad (2\ 39)$$

and for MLE $\frac{\partial}{\partial A} \text{Log}_e L = \frac{\partial}{\partial b} \text{Log}_e L = 0 \qquad (2\ 40)$

As in this work, complete sample is being analysed so

$$r = n \qquad (2\ 41)$$

Hence values of $\hat{b}$ and $\hat{A}$, which are the estimators of b and A respectively are obtained from above, are as follows

$$\frac{\sum_{1}^{n} s_i^{\hat{b}} \text{Log}_e S_i}{\sum_{1}^{n} s_i^{\hat{b}}} - \frac{1}{\hat{b}} = \frac{1}{n} \sum_{1}^{n} \text{Log}_e S_i \qquad (2\ 42)$$

$$\hat{A} = \frac{1}{n} \sum_{1}^{n} s_i^{\hat{b}} \qquad (2\ 43)$$

Eq. (2.42) is solved by Newton-Raphson iterative method to get $\hat{b}$ and when this value is substituted in eq. (2 43) $\hat{A}$ is determined

By general theory of MLE (Cohen 1951) it has been shown that ($\hat{b}$, $\hat{A}$) is a bivariate normal with mean (b,A) and variance, co-variance matrix given by

$$\begin{bmatrix} E\left(-\frac{\partial^2 \text{Log}_e L}{\partial b^2}\right) & E\left(-\frac{\partial^2 \text{Log}_e L}{\partial b\, \partial A}\right) \\ E\left(-\frac{\partial^2 \text{Log}_2 L}{\partial A\, \partial b}\right) & E\left(-\frac{\partial^2 \text{Log}_e L}{\partial A^2}\right) \end{bmatrix}^{-1} \quad (2\ 44)$$

Where E(Z) is the expected value of Z

It can be shown that variance (b), variance (A) and co-variance of (b,A) are given by

$$\text{Var}(\hat{b}) = \frac{1}{U}\left(-\frac{\partial^2 \text{Log}_e L}{\partial A^2}\right)_{\hat{b},\hat{A}} \quad (2\ 45)$$

$$\text{Var}(\hat{A}) = \frac{1}{U}\left(-\frac{\partial^2 \text{Log}_e L}{\partial b^2}\right)_{\hat{b},\hat{A}} \quad (2\ 46)$$

$$\text{Co-Var}(\hat{b},\hat{A}) = \frac{1}{U}\left(\frac{\partial^2 \text{Log}_e L}{\partial A\, \partial b}\right)_{\hat{b},\hat{A}} \quad (2\ 47)$$

$$\text{Where } U = \left[\left(\frac{\partial^2 \text{Log}_e L}{\partial b^2}\right)\left(\frac{\partial^2 \text{Log}_e L}{\partial A^2}\right) - \left(\frac{\partial^2 \text{Log}_e L}{\partial b\, \partial A}\right)^2\right]_{\hat{b},\hat{A}} \quad (2\ 48)$$

$$- \left. \frac{\partial^2 \text{Log}_e L}{\partial b^2} \right|_{\hat{b},\hat{A}} = \frac{n}{\hat{b}^2} + \frac{1}{\hat{A}} \left[\sum_1^n s_i^{\hat{b}} (\text{Log}_e S_i)^2 \right] \qquad (2\ 49)$$

$$- \left. \frac{\partial^2 \text{Log}_e L}{\partial A^2} \right|_{\hat{b},\hat{A}} = \frac{n}{\hat{A}^2} + \frac{2}{\hat{A}^3} \left[\sum_1^n s_i^{\hat{b}} \right] \qquad (2\ 50)$$

$$- \left. \frac{\partial^2 \text{Log}_e L}{\partial A\, \partial b} \right|_{\hat{b}\ \hat{A}} = \frac{\sum_1^n s_1^{\hat{b}} \text{Log}_e S_1}{\hat{A}^2} \qquad (2\ 53)$$

For Weibull distribution mean and varance are calculated by

$$\bar{S} = \frac{\lceil \hat{b}+1}{\hat{b}} \, S_o \qquad (2\ 52)$$

$$\text{Var}\ (S) = S_o^2 \left[\frac{\lceil \hat{b} + 2}{\hat{b}} - \left(\frac{\lceil \hat{b} + 1}{\hat{b}} \right)^2 \right] \qquad (2\ 53)$$

and coefficient of variation, V_p which is independent of $\hat{A}$, is obtained by

$$\frac{\text{Var}\ (S)}{\bar{S}^2} = \sqrt{\frac{\lceil(\hat{b} + 2)/\hat{b} - \lceil(\hat{b} + 1)/\hat{b}}{\lceil(\hat{b} + 1)/\hat{b}}^2} \qquad (2\ 54)$$

By using above equations $\hat{b}$ and $\hat{S}_o$ are evaluated for both sets of strength i e S_i and S_{c_1}

2 10 6 3 Regression of Line

As has been described in earlier sections linear relationship is regressed between two variables (X_i, Y_i) to evaluate slope m and intercept C in the following form

$$Y = mX + C \qquad (2\ 65)$$

This is employed to find activation energy and pre-exponential factos in case of D C resistivity, Young's modulus from strength (S), strain (e) data and Weibull parameters b and S_o from probability (P) and strength (S) To do this analysis condition of least square fit is used which is as follows The error is given by a function F_e such that

$$F_e = \sum_1^n (Y_i - mX_i - C)^2 \qquad (2\ 56)$$

for condition of minimum error,

$$\frac{\partial F_e}{\partial m} = 0 \quad \text{and} \quad \frac{\partial F_e}{\partial C} = 0 \qquad (2\ 57)$$

By solving one gets

$$m = \frac{\bar{X}\ \bar{Y} - \overline{XY}}{(\bar{X})^2 - \overline{(X^2)}} \qquad (2\ 58)$$

$$\text{and} \quad C = \frac{\bar{X}\ \overline{XY} - \bar{Y}\ \overline{X^2}}{(\bar{X})^2 - \overline{(X^2)}} \qquad (2\ 59)$$

Such that $\bar{Z} = \frac{1}{n} \sum_{1}^{n} Z_i$

where $\bar{Z}$ is the mean of Z_i

$$\text{Var (m)} = \frac{F_k^2}{\left[\Sigma Y_i^2 - n (\bar{Y})^2 \right]} \qquad (2\ 60)$$

$$\text{Var (C)} = F_k^2 \left[\frac{1}{n} + \frac{\bar{X}^2}{\left[\Sigma X_i^2 - n(\bar{Y})^2 \right]} \right] \qquad (2\ 61)$$

$$\text{Where } F_k^2 = \frac{1}{n-2} \left[\Sigma \left(Y_i - C - mX_i \right)^2 \right]$$

$$= \frac{1}{n-2} \left[\Sigma Y_i^2 - n\bar{Y}^2 - \frac{\left(\Sigma X_i Y_i - n\bar{X}\bar{Y} \right)}{\left(\Sigma X_i^2 - n\bar{X}^2 \right)} \right] \qquad (2\ 62)$$

Thus from above equations m and C are evaluated and a line fitted by above method provides these parameters with a range such that m and C lies between $m \pm \Delta m$ and $C \pm \Delta C$ respectively such that

$$\Delta m = \sqrt{\text{var (m)}} \qquad (2\ 63)$$

$$\Delta C = \sqrt{\text{var (C)}} \qquad (2\ 64)$$

In case $C = \text{Log}_e B$ where B is a parameter to be determined so

$$B = \exp(C) \qquad (2\ 65)$$

$$\Delta B = \exp(C)\ \Delta C = B\ \Delta C \qquad (2\ 66)$$

Thus B as well as ΔB are obtained

In case of line passing through the origin the above equations simplify to the following

$$m = \Sigma X_1 Y_1 / \Sigma X_1^2 \qquad (2\ 67)$$

$$\text{Var}(m) = \frac{F_k^2}{\Sigma X_1^2} \qquad (2\ 68)$$

$$\text{Where } F_k^2 = \frac{1}{n-1}\left[\Sigma Y_1^2 - \frac{(\Sigma Y_1 X_i)^2}{\Sigma X_i^2}\right] \qquad (2\ 69)$$

$$\Delta m = \sqrt{\text{var}(m)} \qquad (2\ 70)$$

2 110 7 Determination of Fracture Surface:

The fracture surface has been studied by a scanning electron microscope (SEM), ISI-60 U K The glass fibres fractured under tensile test are mounted on cylindrical aluminum base (1 Cm x 1 Cm) with their fracture surface showing upwards The length of such specimens is kept at about 5 Cm Their

lower ends are pasted with silver paint to the aluminium base The entire assembly is placed in a vacuum unit and a thin ≃ 50 Å thick film of gold is deposited on the fractured surface of the specimen. This aluminium base loaded with gold coated glass fibres is observed in scanning electron microscope and fracture surface morphology is photographed The same method has been used to study the corrosion resistance behaviour of these glass fibres to dilute hydrofluoric acid

CHAPTER III

Electrical conduction in ion exchanged glass fibres

3 1 INTRODUCTION

Electrical conduction in alkali containing glasses arises due to the long range migration of alkali ions under the influence of an electric field Ionic conduction in glasses has become important because of its technological importance The possible use of ionic glasses as solid electrolytes has drawn attention of many research workers to this field [Tuller et al 1980] Various glasses so far investigated for fast ion conduction, have high alkali content or silver ion content ranging from 40 to 70 mol% Almost all of such fast ion conducting glass compositions are derived from Lithium based glass systems or AgI based glass systems [Kulkarni AR et al 1984] It has been known from $Na^+ \rightleftharpoons Ag^+$ ion exchange studies in some glasses that activation energy for silver self diffusion is low [Frischat G H 1976] This has prompted us to study the effect of replacing sodium ions by silver ions in an oxide glass on its ionic conductivity As silver rich layer so produced is usually a few microns thick [Chakravorty D et al 1972 , Collins DR et al 1966] it is possible to enrich glasses by silver ions to more than 90% of their sodium concentration by subjecting the glass fibres with diameters around 10μm, of the said glass to a $Na^+ \rightleftharpoons Ag^+$ ion exchange

It is to be noted further that by changing the sodium ion concentration in the base glass a significant change in the ionic conductivity of virgin glass fibres can be brought about This change in alkali concentration is also expected to bring about drastic changes in the electrical conductivity of ion exchanged fibres because of corresponding variation in silver ion concentration in their fibres

In this chapter we describe the results obtained with ion exchanged glass fibres having different initial concentrations of sodium ions

3 2 Results

The composition of glass fibres which have been investigated are referred to as glass system N Table 3 1 gives the compositions as well as the density of these glasses

3 2 1 Glass Preparation and Fiberization

The glass batch is prepared with the compositions described as above in which Na_2O and CaO are added as carbonates The glass is melted in an alumina crubible at 1450°C for two hours The melt when free of air bubbles is poured into aluminium mould to be cast as thin rectangular plates which are later annealed at 500°C for 6 hours These plates are powdered and the glass powder so obtained is used to draw glass fibres as described in section 2 2 The fiberisation parameters are described in table 3 2

3 2 2 Ion Exchange:

A bunch of fibres of length 10 Cm of each composition have

Table 3 1 Composition and density in glass system N

Sl No	Glass	Na_2O	SiO_2	CaO	B_2O_3	Al_2O_3	Density (gm/cc) d_1
1	N1	10	64	14	8	4	2 62
2	N2	20	60	13	4	3	2 63
3	N3	30	55	12	-	3	2 62

Table 3 2 Fiberisation parameters of glass system N

Sl No	Glass	Melt Temp T_M(°C)	Bushing Temp T_B(°C)	Bushing Tip Temp Tp(°C)	Velocity of draw m/sec
1	N1	1390	975	900	15,13,11,10
2	N2	1335	940	870	16,13,11,10
3	N3	1300	920	820	20,16,13,11

Table 3 3 Molar fraction of silver in glass system IN

Sl No	Glass	Concentration of glass in solution [G] µgm/cc	Conc of silver in solution [Ag] µgm/cc	Weight fraction of Ag (ω_{Ag})	Molar fraction of Ag
1	IN1	4 2	1 10	0 262	95%
2	IN2	3 5	1 56	0 446	98%
3	IN3	2 3	1 30	0 565	96%

been ion exchanged in a pyrex boat containing molten $AgNo_3$ at 330°C for 36 hours as described in section 2 3 The Ion-exchanged glass fibres are being referred to as constituting in glass system

3 2 3 Chemical analysis

IN glass system has been chemically analysed for silver by an IL/751 atomic absorption spectrophotometer as described in section 2 4 The results of chemical analysis are being summarized in Table 3 3

3 2 4 D T A Analysis

Fig 3 1, 3 2 and 3 3 represent the DTA curves obtained for N glass system The glass transition temperature Tg, nucleation temperature T_N and growth temperature T_o for these glasses are being summarized in table 3 4 (D Bahadur et al 1982)

3 2 5 Electrical Measurements:

D C and A.C resistivity measurements for these fibres have been carried out as discussed in section 2 4 A bunch of fibres cut to required size (1 6 Cm) are loaded in the conductivity cell between two electrodes Silver paste is used to make contact of fibres and electrodes I-V plots are obtained on x-y recorder by the circuit described in section 2 4 3 The slope of these plots gives D C resistance (R_o) of te sample. Resistances have been found by such slopes of I-V curves obtained at various temperatures All these plots have been found to be straight lines passing through the origin. Typical representative plots for N and IN samples are shown in figs 3.4 and 3 5 respectively

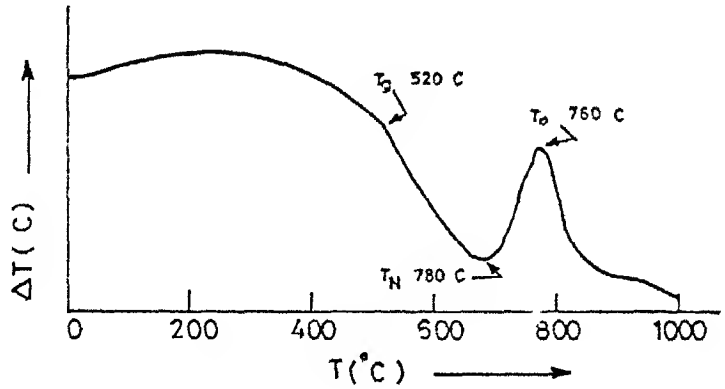

Fig 3 1 D T A Curve for glass N_1

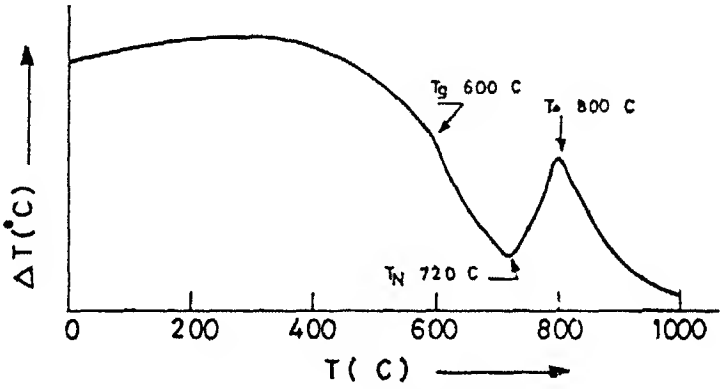

Fig 3 2 D T A Curve for glass N_2

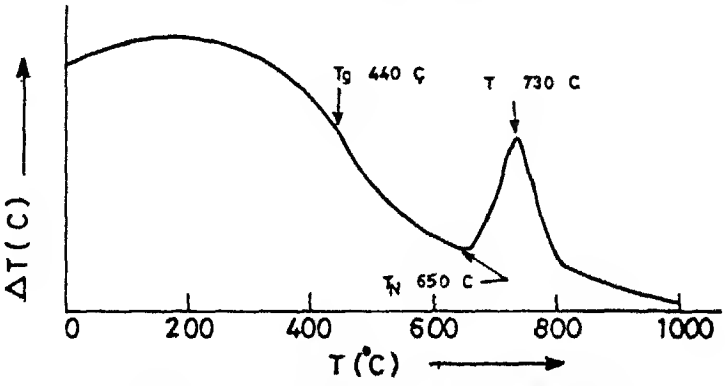

Fig 3 3 D T A Curve for glass N_3

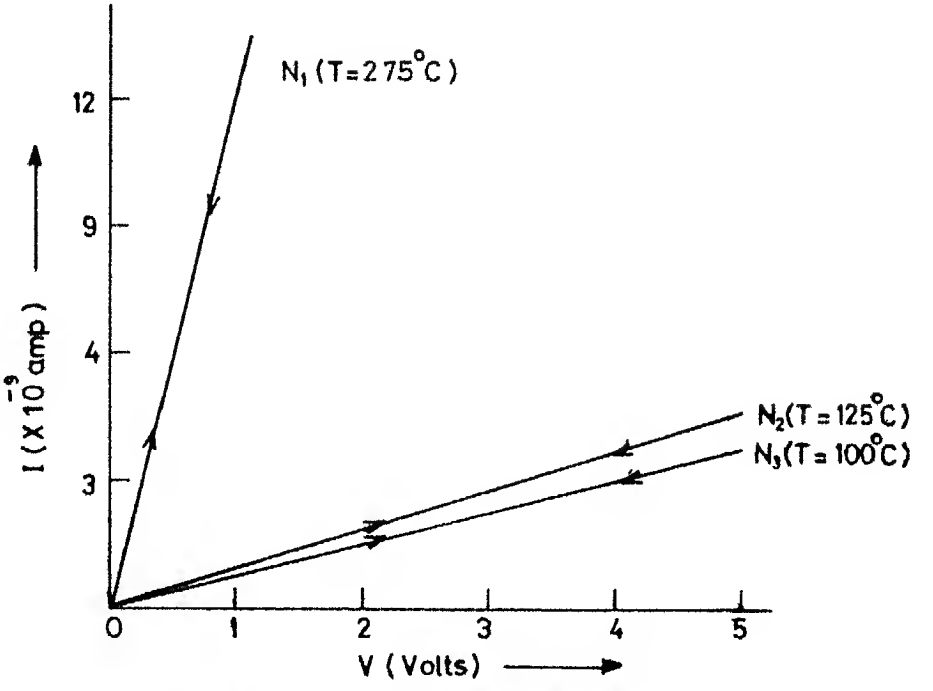

Fig 34 I V Plot for glass system N

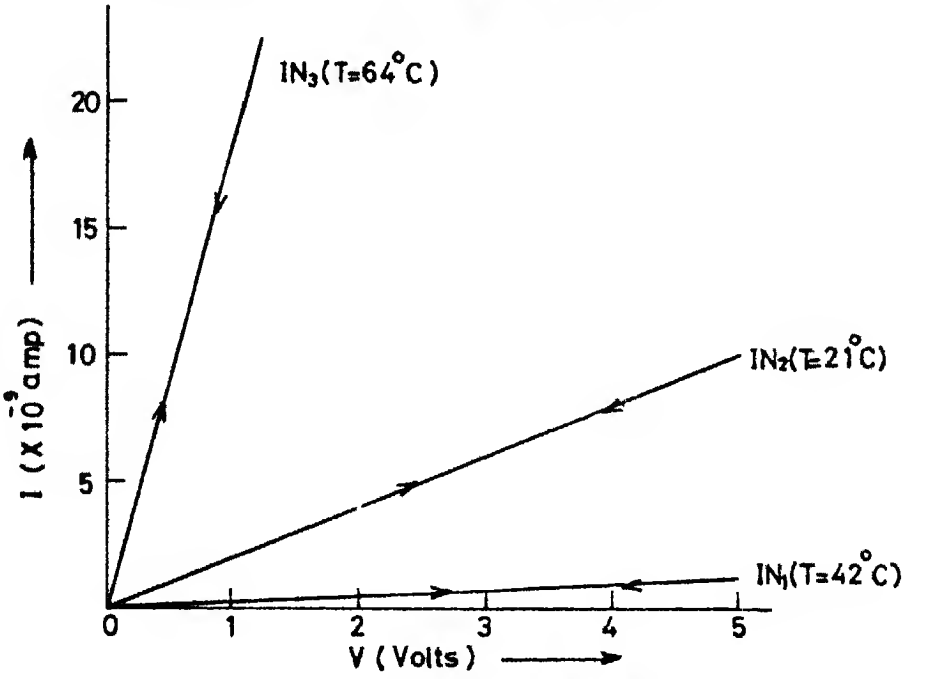

Fig 35 I-V Plot for glass system IN

3 2 5 1 A C Measurements and Complex Impedance Analysis

A C measurements yield the values for conductance (G) and capacitance (C) as a function of frequency (f) The frequency has been varied from 20 Hz to 100 kHz Impedance analysis have been carried out for all these glasses at various temperatures The real (Z') and imaginary (Z') parts of impedance are calculated by equations 3 1 and 3 2

$$Z' = \frac{G}{G^2+\omega^2C^2} \qquad (3\ 1)$$

$$Z' = \frac{\omega C}{G^2+\omega^2C^2} \qquad (3\ 2)$$

where $\omega = 2\pi f$

Various points in the Z -Z'' plane are found to lie on the arc of a circle The intersection of this arc on the real (Z) axis yields the D C resistance (R_T) of the sample Figs 3 6, 3 7, 3 8 are typical Z''-Z' plats for N glass system while figs 3 9, 3 10 and 3 11 represent the similar behaviour of IN glasses system Table 3 5 summarizes a typical set of results of complex impedance analysis It also includes the percentage error (e_r) in D C measurement (R_O) as compared to the values obtained by impedance analysis Error (e_r) is given by equation 3 3

$$e = \frac{R_T - R_O}{R_O} \times 100 \qquad (3\ 3)$$

As evident from the table 3 5 error in D C measurements is within 2% of that estimated from the complex impedance analysis. Hence resistances as obtained from I-V plots have been taken

Table 3 4 T_g T_N and T_o for glass system N

Sl No	Glass	T_g(°C)	T_N(°C)	T_o (°C)
1	N1	520	680	760
2	N2	600	720	800
3	N3	440	650	730

Table 3 5 Comparison of R_O and R_T for glass systems N and IN

Sl No	Glass	T(°K)	R_O (Ω)	R_T (Ω)	e_r
1	N1	548	8 3 x 10^7	8 4 x 10^7	1 2
2	N2	398	1 10 x 10^9	1 08x 10^9	- 1 82
3	N3	373	1 33 x 10^9	1 31x 10^9	- 1 50
4	IN1	315	4 5 x 10^9	4 56x 10^9	1 33
5	IN2	294	5 0 x 10^8	5 1 x 10^8	2 00
6	IN3	337	5 4 x 10^7	5 46x 10^7	1 11

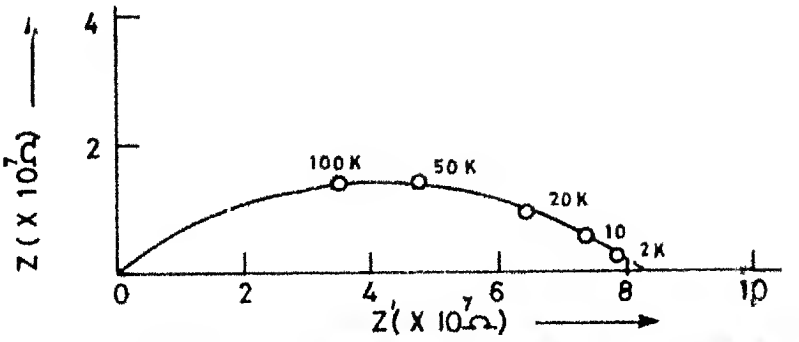

Fig 3 6 Complex impedance plot for glass N_1 (T= 275°C)

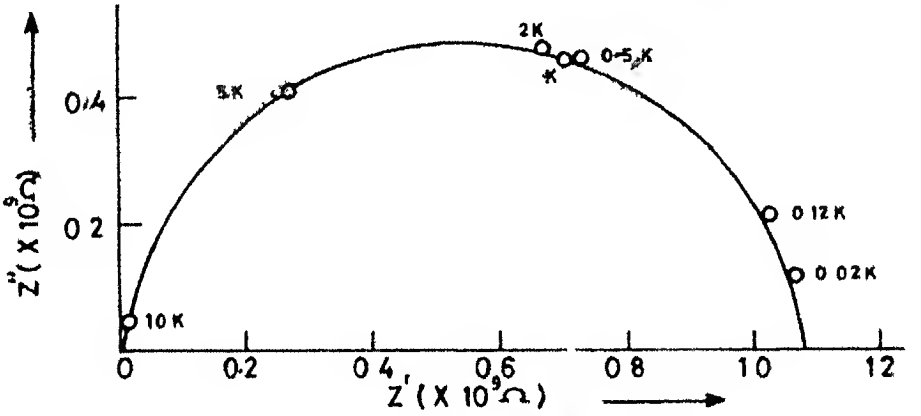

Fig 3 7 Complex impedance plot for glass N_2 (T=125°C)

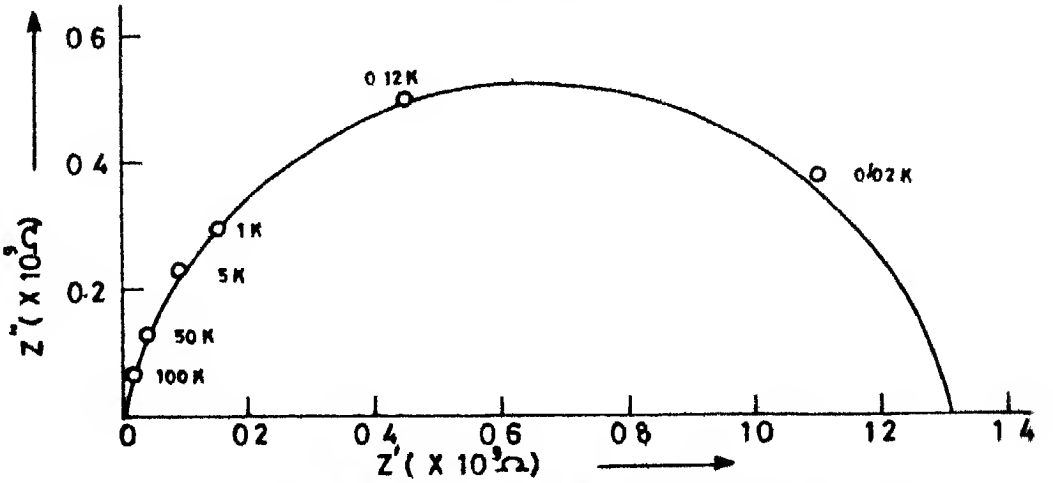

Fig 3 8 Complex impedance plot for glass N_3 (T=100°C)

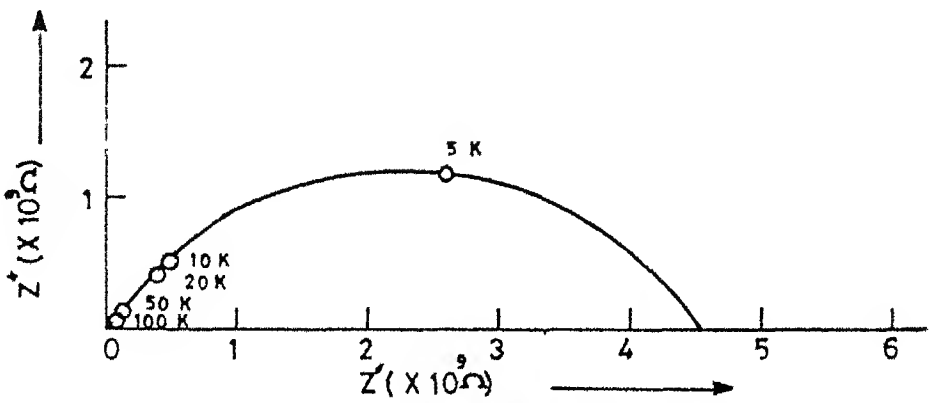

Fig 3 9 Complex impedance plot for glass IN_1 (T = 42°C)

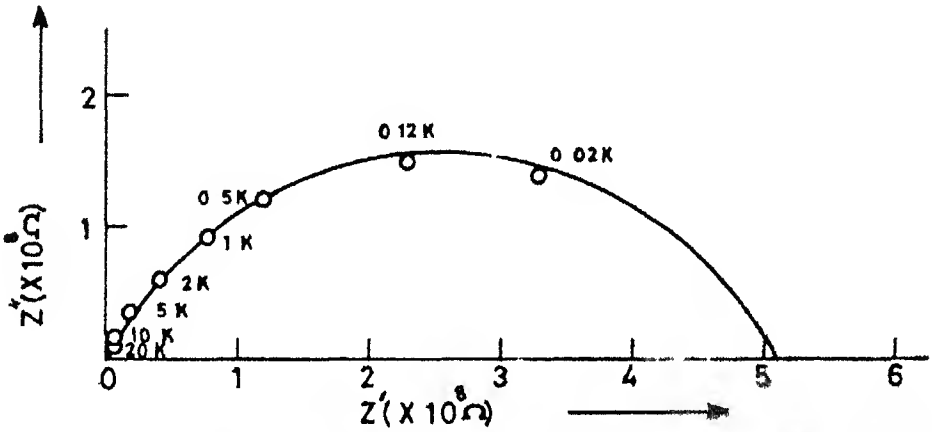

Fig 3 10 Complex impedance plot for glass IN_2 (T = 21°C)

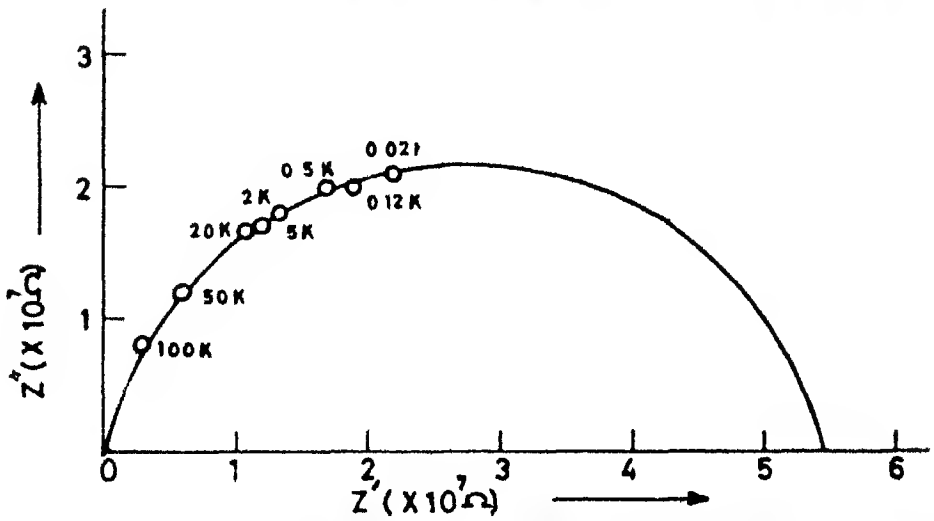

Fig 3 11 Complex impedance plot for glass IN_3 (T = 64°C)

as true representative values for D C resistance of glass systems N and IN

3 2 5 2 Temperature Dependence of resistivity

Resistivity for various glass samples has been calculated by equation 2 7 from the measured value of D.C. resistance R_O Such measurements have been carried out at various temperatures in the range of 20°C to 330°C for glass systems N and IN During such investigations it has been found that IN glass samples invariably show a sudden surge of current when the applied electric field (E_e) exceeds a critical value (E_c) The value of E_c is dependent upon the temperature (T_c) for a given glass composition Thus an optimum combination of E_c and T_c brings about a permanent change in the resistivity of glass The newly attained state has resistivities many orders of magnitude lower than that of the ion-exchanged glass system IN Once IN glass system attains this highly conducting state, it is being referred to have formed HIN glass system The typical switching behaviour (I-V plots) of IN glass to HIN glasses has been shown in Figs 3.12, 3 13 and 3 14 respectively In these figs both IN state and HIN state have been shown These plots are characterised by negative resistance region shown by arrow in these Figs H C S is a stable state and HIN glass system is a new material characterised by high conductivity Variation of E_c with T_c for IN glass system is shown in Fig 3 15

Figs 3 16, 3 17 and 3 18 show the variation of log (ρ/T) with $1/T$ for (N1, IN1, HIN1), (N2, IN2, HIN2) and (N3, IN3, HIN3) respectively In each figure there are three curves indi-

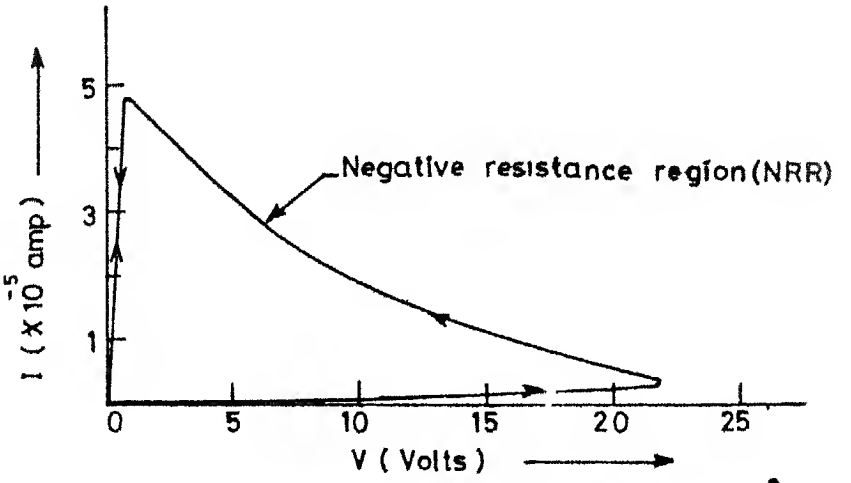

Fig 3 12 Switching of IN_1 glass to HIN_1 glass (T_c=320°C)

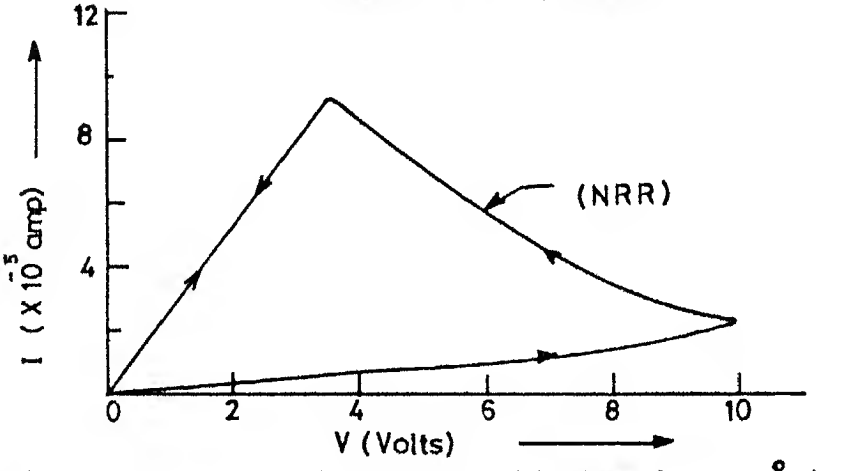

Fig 3 13 Switching of IN_2 glass to HIN_2 glass (T_c=300°C)

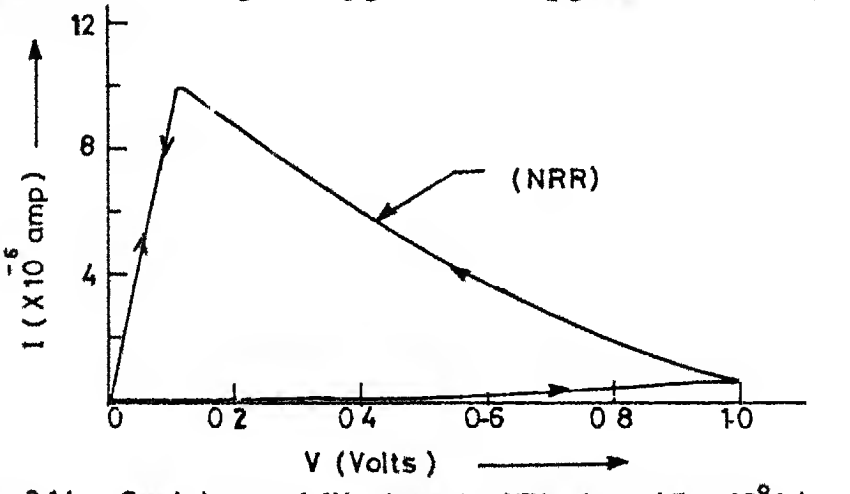

Fig 3 14 Switching of IN_3 glass to HIN_3 glass (T_c=160°C)

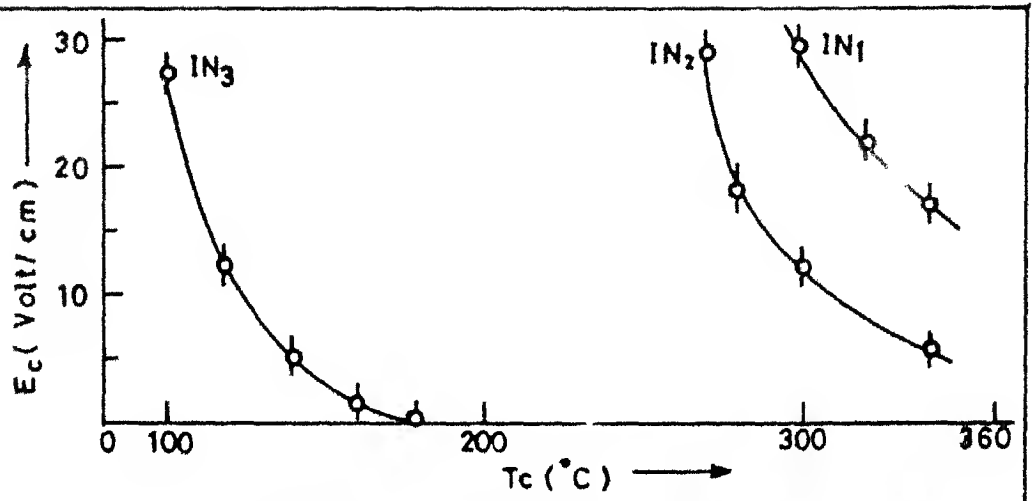

Fig 3.15 Temperature variation of critical electric field (E_c) for glass system IN

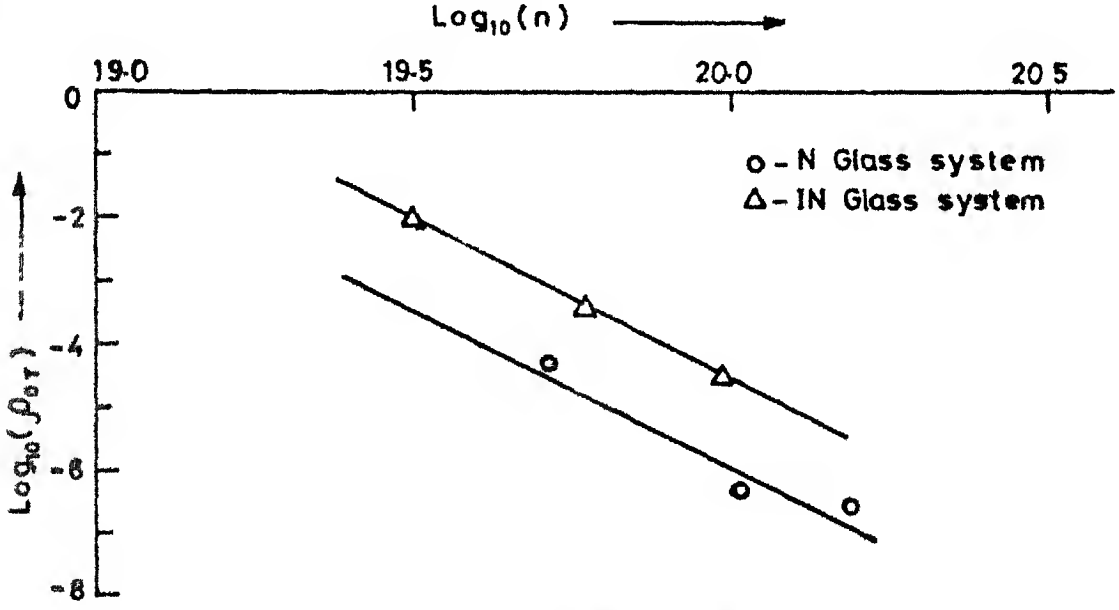

Fig 3.40 Variation of pre-exponential factor (ρ_{0T}) with cation concentration (n) for glass system N and IN

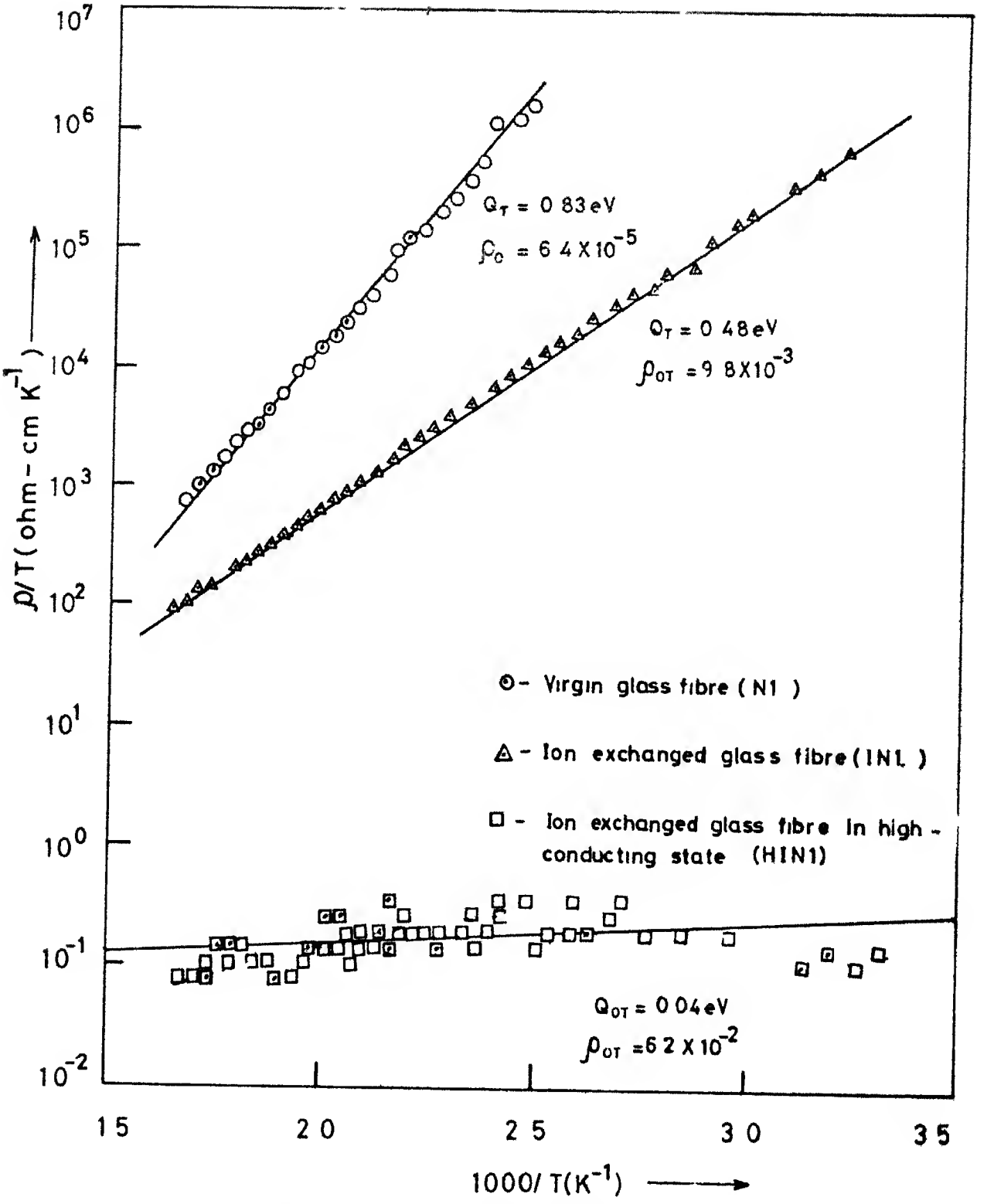

Fig 3 16 Temperature variation of (D C resistivity / temperature) for N1, IN1 and HIN1 glass fibres

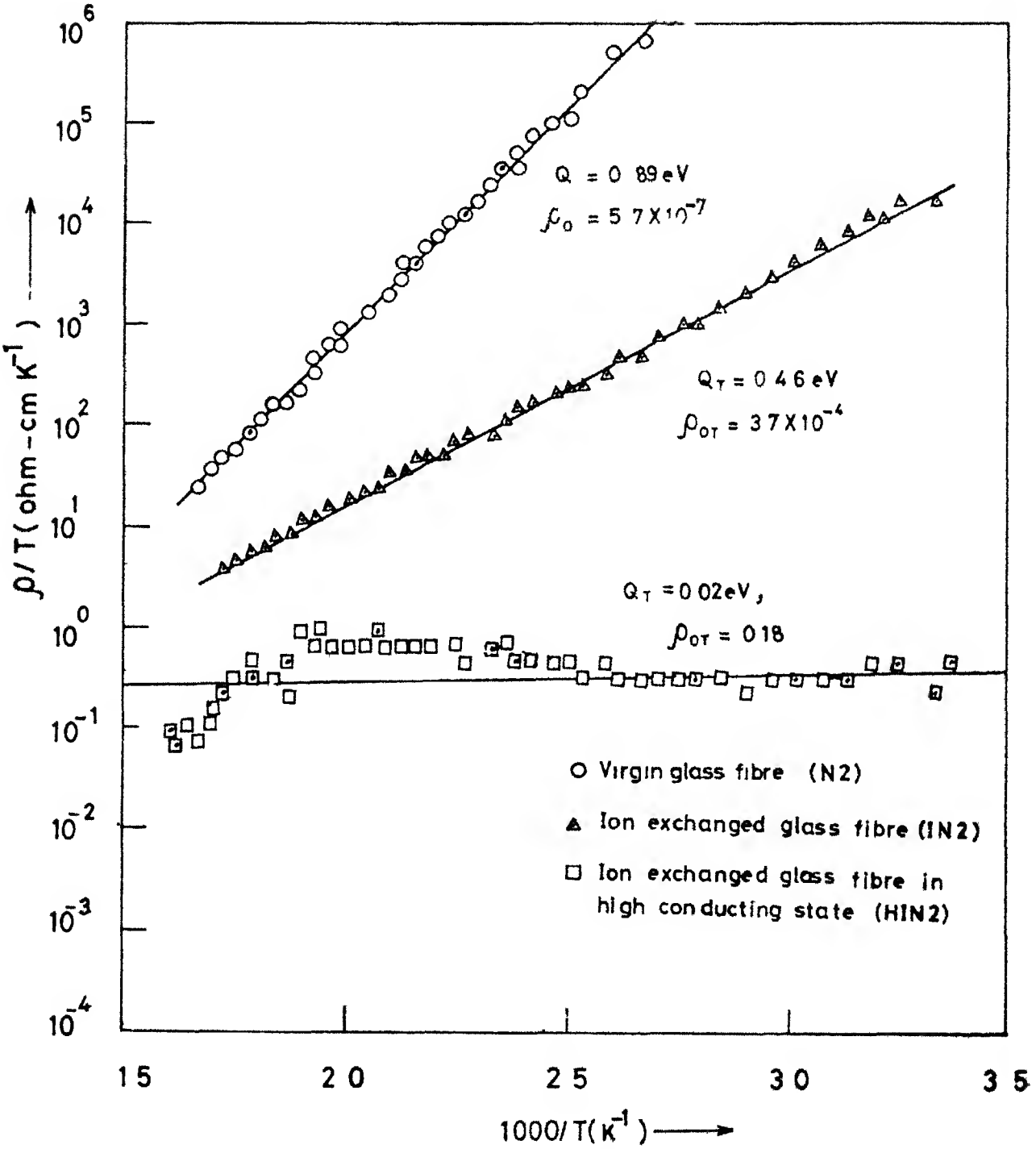

Fig 3 17 Temperature variation of(D C resistivity/ temperature) for N2, IN2 and HIN2 glass fibres

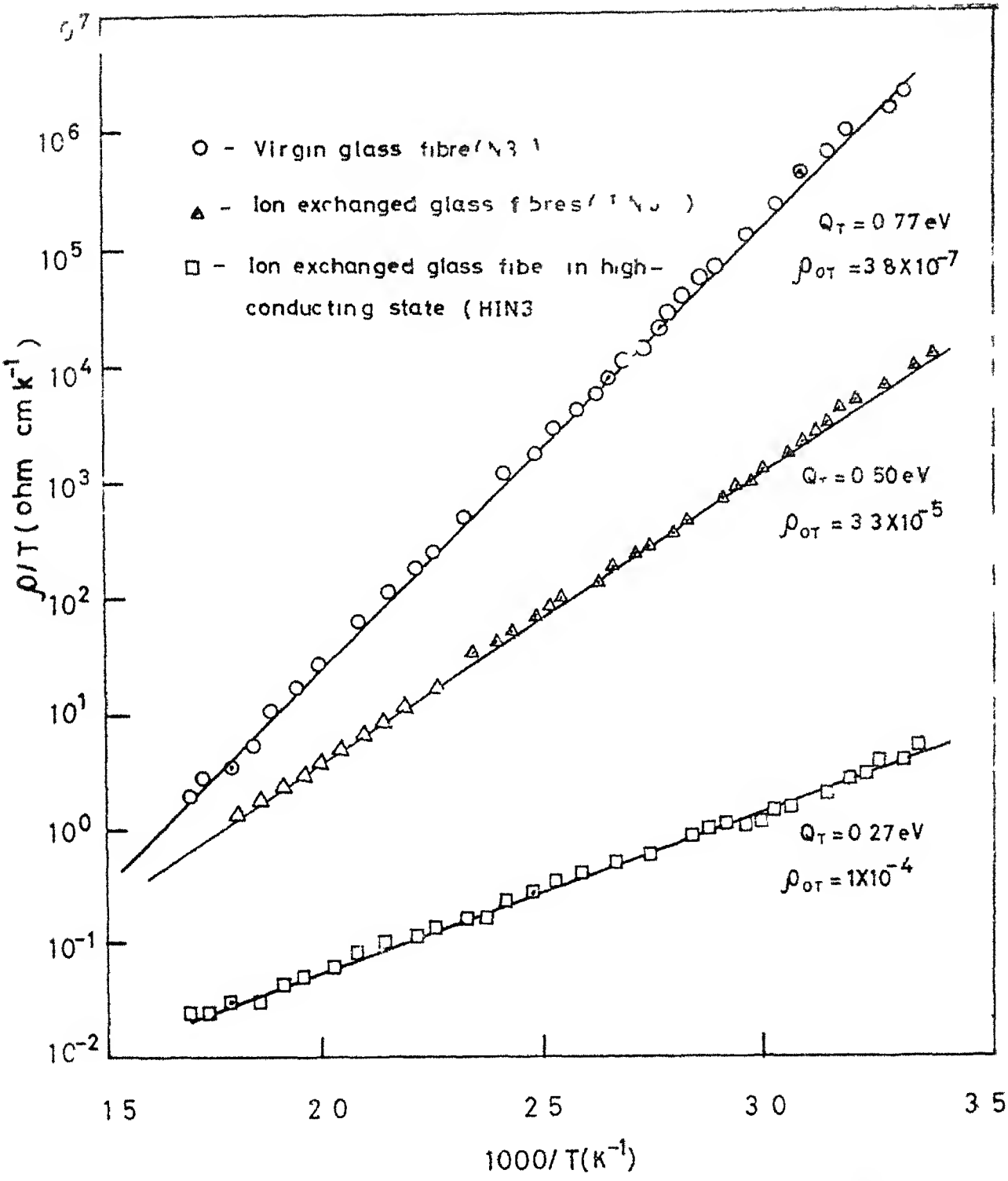

Fig 3.18 Temperature variation of D C resistivity/ temperature) for N3 IN3 and HIN3 glass fibres

cating the temperature dependence of resistivity for three sets of materials belonging to N,IN and HIN glass systems respectively. Figs 3 19, 3 20 and 3 21 show the comparative variation of Log(ρ) with $1/T$ for glass system N, IN and HIN respectively The data have been analysed in two ways The temperature dependence of resistivity in each case, being assumed to follow relationships given by equations 3 4, 3 5

$$\rho = \rho_{OT}\, T \exp\left(\frac{Q_T}{KT}\right) \qquad (3\ 4)$$

$$\sigma = \rho_O \exp\left(\frac{Q}{kT}\right) \qquad (3\ 5)$$

Table 3 6 summarizes the results of this analysis for glass system N As values of ρ_{OT}, Q_T, ρ_O and Q are calculated by least square fitting of a straight line hence each of these parameters will have a scatter which is estimated by the variance of each of them Thus dQ_T, $d\rho_{OT}$, dQ and $d\rho_O$ represent the scatter in the values of Q_T, ρ_{OT}, Q and ρ_O respectively Thus each of these parameters is being provided with the corresponding scatter Similar analysis have been carried out on IN glass system The results are shown in Table 3 7 Table 3 8 shows results of similar anaysis carried out for HIN glass system

3 2 6 TEM Analysis

As described in section 2 6, samples have been characterised by transmission electron microscopy Basic features associated with each of them are described in the following sections.

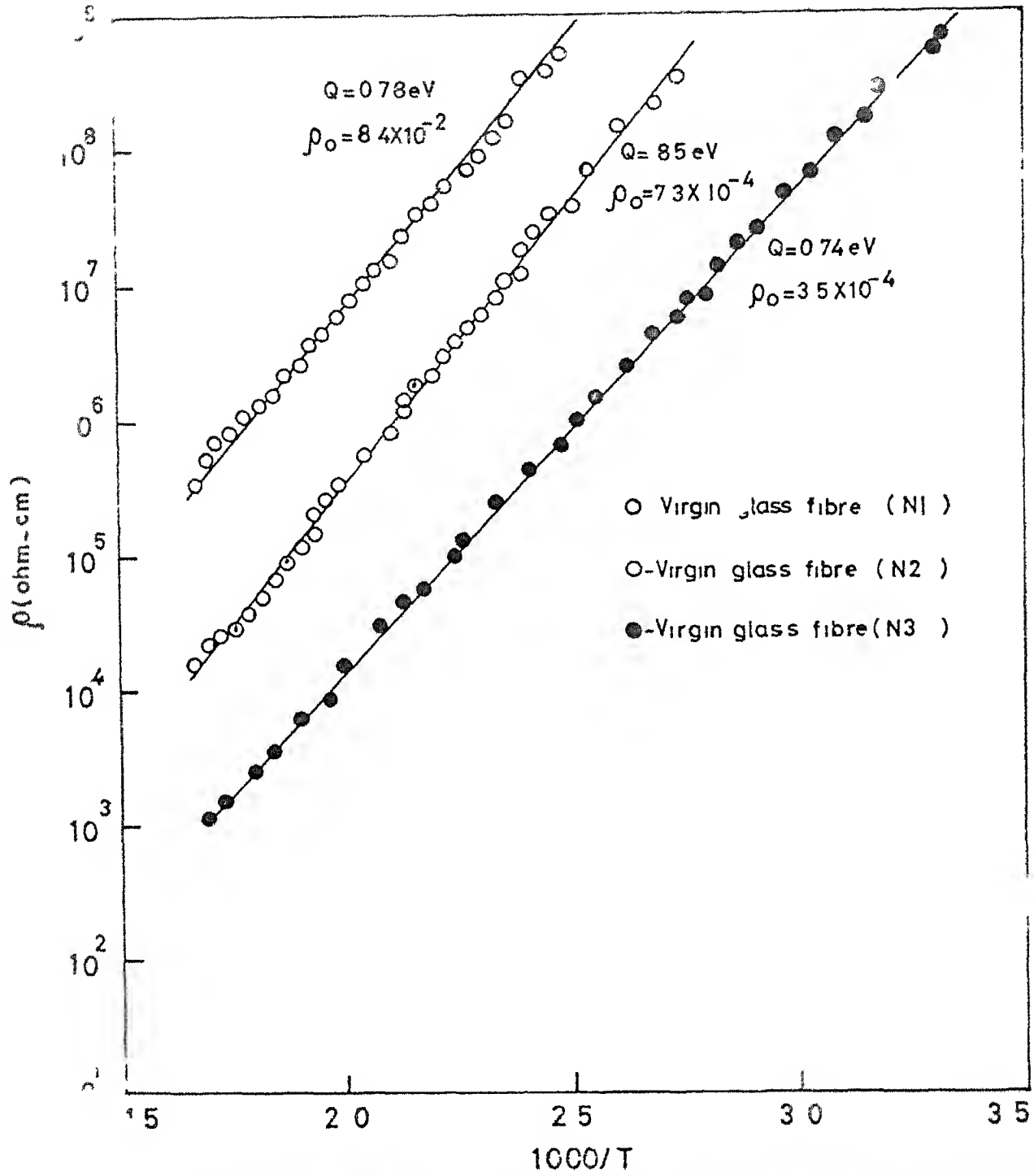

F,g3 9Temperature variation of D C resistivity for glass system N

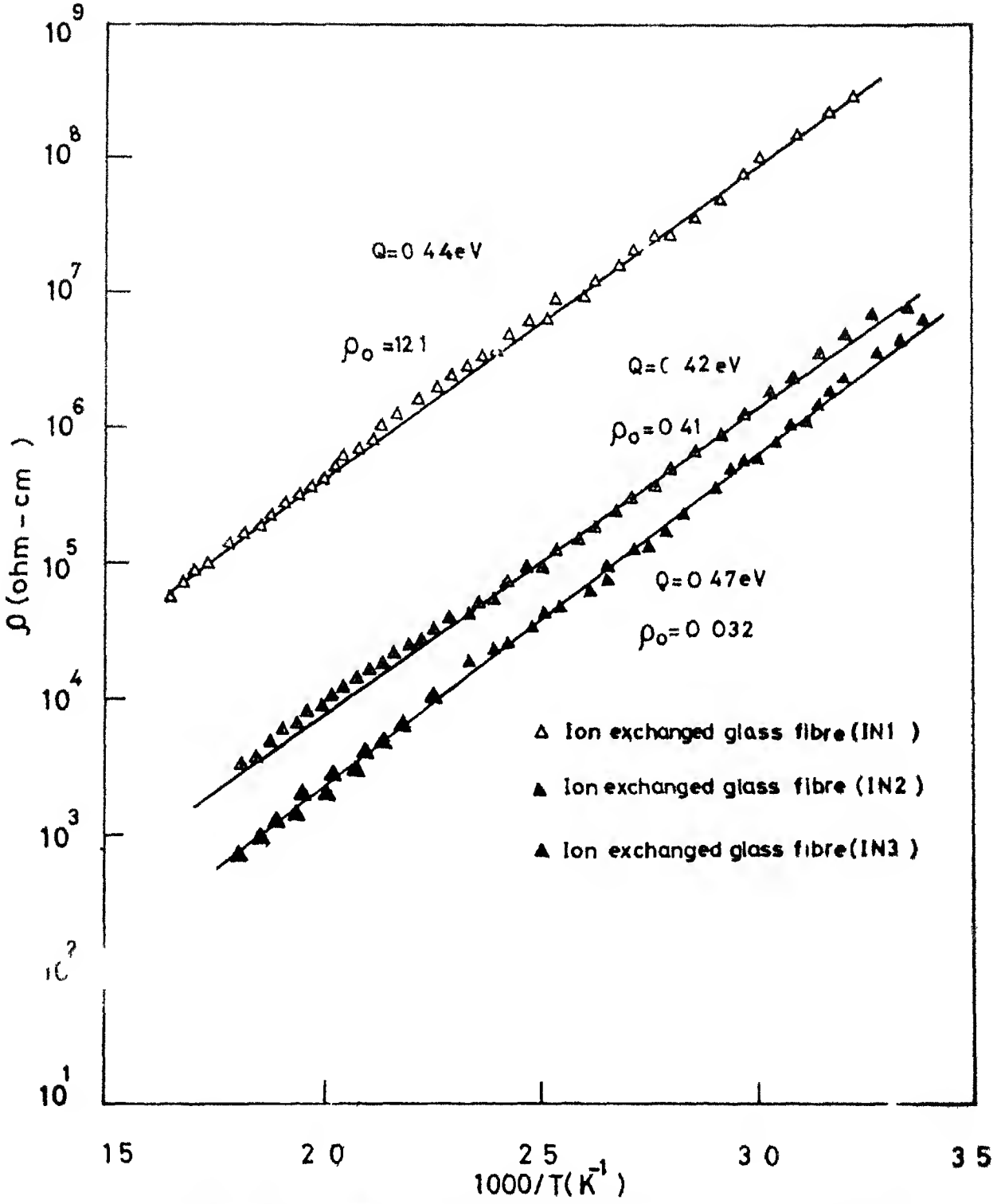

Fig 320 Temperature variation of D C resistivity for glass system IN

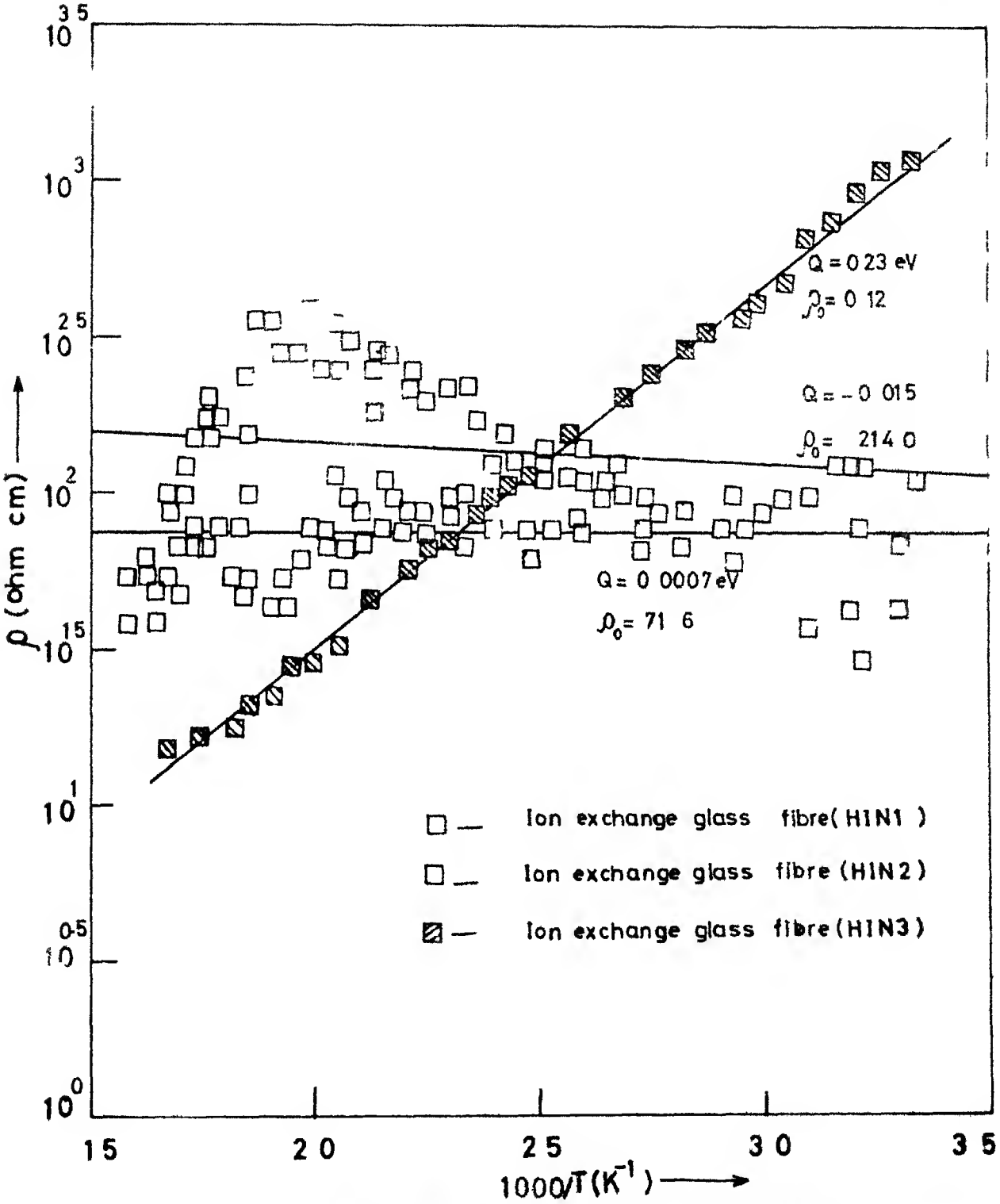

Fig 3 21 Temperature variation of resistivities for glass system HIN

Table 3 6 Activation energy and pre-exponential factors for glass system N

Sl No	Glass	$Q_T \pm dQ_T$ (eV)	$\rho_{OT} \pm d\rho_{OT}$ (Ohm CmK^{-1})	$Q \pm dQ$ (eV)	$\rho_O + d\rho_O$ (Ohm-Cm)
1	N1	83 ± 01	$6\ 4\times10^{-5} \pm 1\times10^{-5}$	78± 01	$8\ 4\times10^{-2} \pm 2\times10^{-2}$
2	N2	89 ± 01	$5\ 7\times10^{-7} \pm 3\times10^{-7}$	85± 01	$7\ 3\times10^{-4} \pm 4\times10^{-4}$
3	N3	77 ± 01	$3\ 8\times10^{-7} \pm 2\times10^{-7}$	74± 01	$3\ 5\times10^{-4} \pm 2\times10^{-4}$

Table 3 7 Activation energy and pre-exponential factors for glass system IN

Sl No	Glass	$Q_T \pm dQ_T$ (eV)	$\rho_{OT} \pm d\rho_{OT}$ (Ohm-Cm-k^{-1})	$Q \pm dQ$ (eV)	$\rho_O \pm d\rho_O$ (Ohm-Cm)
1	IN1	48± 01	$9\ 8\times10^{-3} \pm 2\times10^{-3}$	44± 01	12 1±2 7
2	IN2	46_ 01	$3\ 7\times10^{-4} \pm 4\times10^{-5}$	42± 01	0 41± 0^5
3	IN3	50±.01	$3\ 3\times10^{-5} \pm 1\times10^{-5}$	47± 01	0 032± 01

3 2 6 1 N glass System

Figs 3 22, 3 24 and 3 26 are representative micrographs of N1, N2 and N3 respectively It is evident from them that N1 and N2 exhibit phase separation while N3 is a single phase system The inhomogeneity of glasses N1 and N2 at microlevel causes one of the two phases of glass to be sodium rich, the other phase containing a smaller amount of sodium Both of these phases are interconnected throughout the glass matrix The darker regions in these micrographs represent silica rich phase Corresponding S A D's (Selected Area Diffraction) are shown in Figs 3 23, 3 25 and 3 27 respectively All of them show rings, characteristic of amorphous material

3 2 6 2 IN glass System

Figs 3 28 3 30 and 3 32 reveal the microstructure of glasses IN1, IN2 and IN3 respectively and their corresponding SAD's are shown in Figs 3 29, 3 31 and 3 33 respectively It is clear from these micrographs that IN glass system consists of a two phase structure The darker phase (α) is silver rich while the lighter (β) one has less amount of silver While α shows broken interconnectivity, β is interconnected throughout the glass matrix The average widths ω_α and ω_β of the α and β phases are given in Table 3 9 As none of the SAD's shows any diffraction rings, both of these phases are amorphous

3 2 6 3 HIN glass systems

Figs 3 34, 3 36 and 3 38 give the typical microstructures of HIN1,HIN2 and HIN3 respectively Figs 3 35, 3 37 and 3 39

Table 3 8 Activation energy and pre-exponential factors for glass system HIN

Sl No	Glass	$Q_T \pm dQT$ (eV)	$\rho_{OT} \pm d\rho_O$ (Ohm-CmK^{-1})	$Q \pm dQ$ (eV)	$\rho_O \pm d\rho_O$ (Ohm-Cm)
1	HIN1	04 ± 01	6 2x10^{-2} ± 1 6x10^{-2}	0007 ± 0095	71 6 ± 18 3
2	HIN2	02 ± 014	182 ± 07	015 ± 014	214 ± 80.2
3	HIN3	27 ± 01	1x10^{-4} ± 15x10^{-4}	23 ± 01	1 2 ± 02

Table 3 9 Widths of the interconnected phases in IN glass system

Sl No	Glass	ω_α (Å) (Phase with broken interconnectivity)	ω_β (Å) (Interconnected phase)
1	IN1	320	85
2	IN2	480	62
3	IN3	275	112

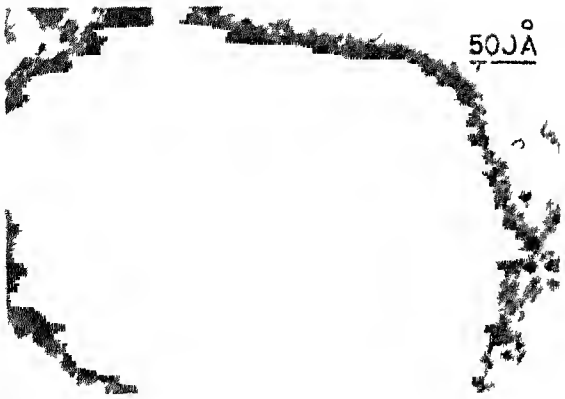

Fig 322 TEM micrograph of glass N1

Fig 323 SAD

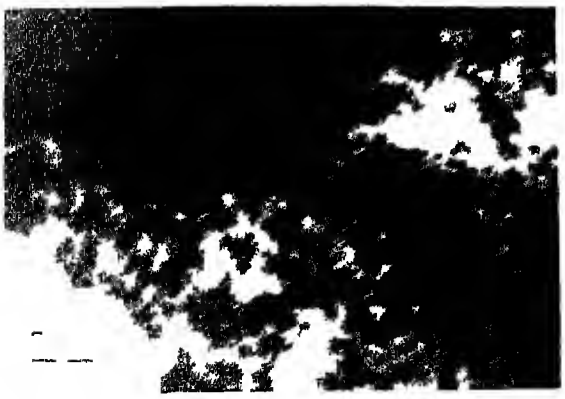

TEM micrograph of glass N2

Fig 325 SAD of glass

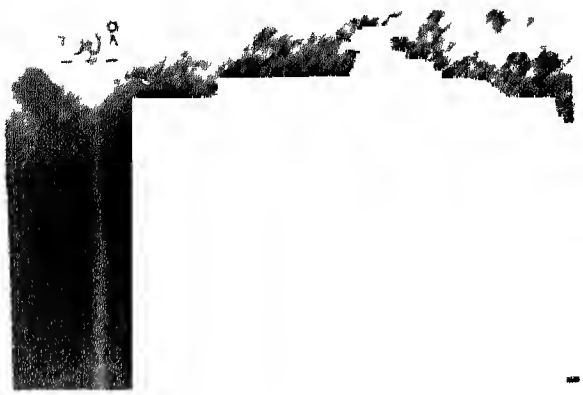

Fig TEM micrograph of glass N3

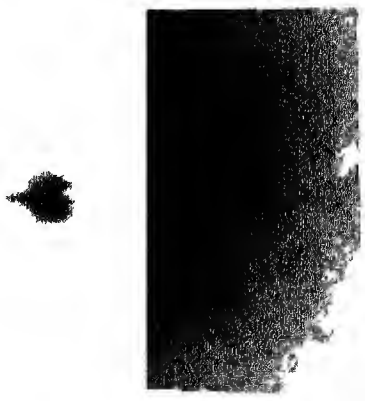

Fig 327 SAD of glass

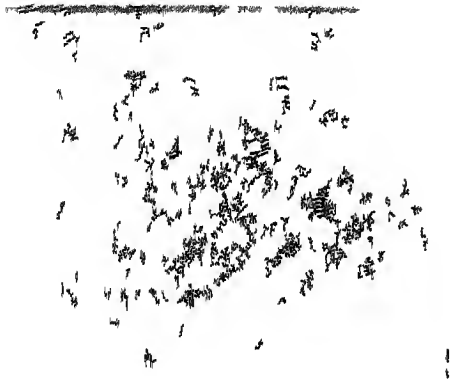

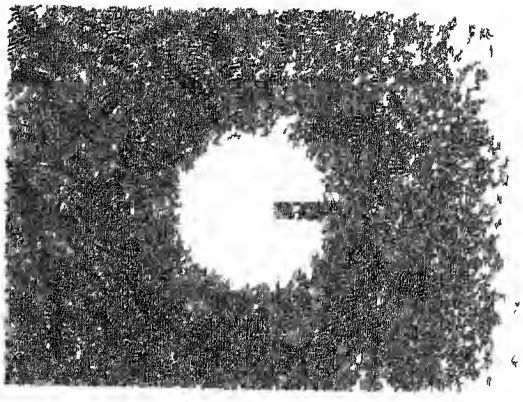

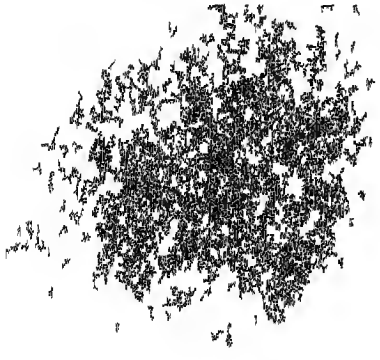

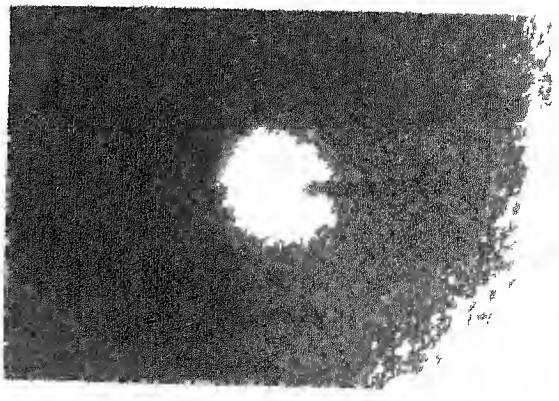

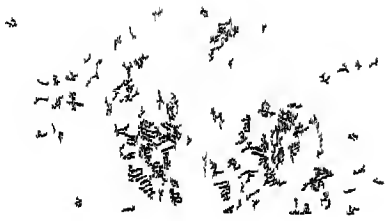

[illegible] micrograph of glass [illegible]

[illegible]

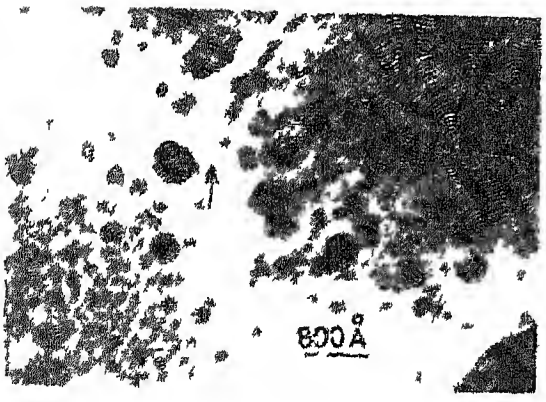

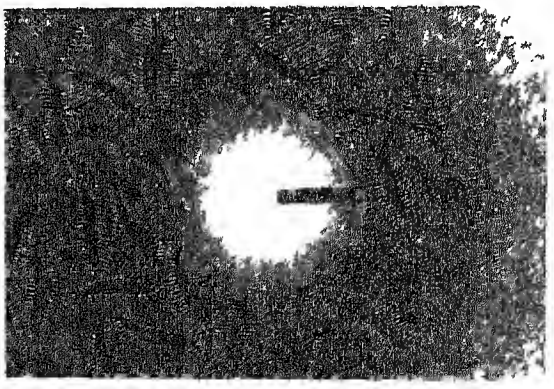

[illegible] micrograph of glass HIN[illegible]

Fig 337 SAD of glass HIN2

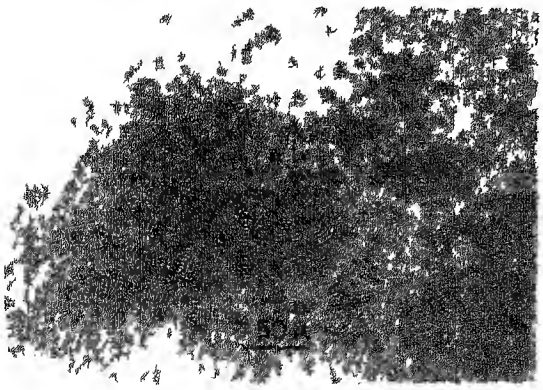

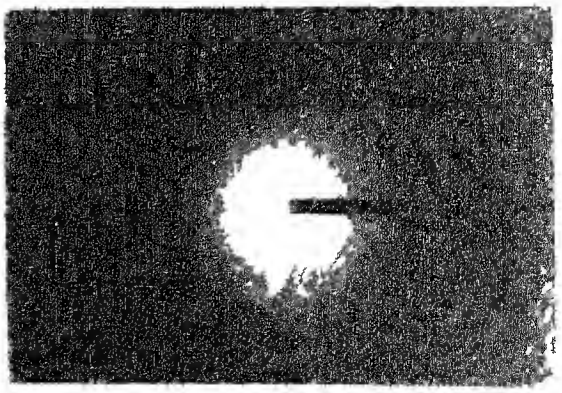

[illegible] micrograph of glass HIN3

Fig 339 SAD of glass, HI[illegible]

are corresponding SAD's These SAD's show very faint rings These have been characterised Table 3 10 shows the comparison between calculated d_{hkl} values for these rings and d_{hkl} (ASTM) for silver metal

The results imply that a small fraction of silver ions get reduced to silver metal These silver metal particles are precipitated in the silver rich phase which is shown as the dark region in the two phased microstructure of HIN glass system There are indications as shown by arrows in Figs. 3 34, 3 36 and 3 38, that as compared to microstructure of IN glass system,links have been formed between the disjointed portions of the α phase Thus in HIN system both silver rich (α) and silver depleted (β) phases are interconnected The average widths (ω_α, ω_β) of these two phases in the HIN system are summarised in Table 3 11

3 3 Discussion

Glass transition temperature T_g for N2 is found to be higher than those for N1 and N3 It is expected that addition of increasing amount of Na_2O should lower the T_g value as the SiO_4 tetrahedral structure is broken up by the formation of non-bridging oxygen ions (Rawson) Thus T_g for N3 should have been lower than that of N2 and N1 Simlarly T_g of N2 should be lower than that of N1. But as is clear from table 3 4, this is not the case This anomaly may be explained by the morphological differences as evident from the microstructures of N1 and N2 Though both N1 and N2 show phase separation, the interconnectivity of

Table 3 10 Comparison of d_{hkl} values of silver with that for HIN glass system

Sl No	(hkl)	d_{hkl}(Ag) (ASTM)	d_{hkl} (Calculated)		
			HIN1	HIN2	HIN3
1	111	2 359	2 35	2 31	2 32
2	200	2 044	2 06	1 99	2 02
3	220	1 445	1 4[illegible]	1 40	1 43
4	311	1 231	1 24	1 22	1 21
5	222	1 180	1 16	1 19	1.17

Table 3 11 Microstructural features of HIN glass system

Sl No	Glass	ω_α (Å)	ω_β(Å)
1	HIN1	215	122
2	HIN2	200	136
3	HIN3	125	140

sodium rich phase is more frequent in case of N1 than that of N2 This implies that N1 has a relatively more open structure than that of N2 and this seems to be responsible for higher T_g of N2 as compared to that of N1

In the case of N glass system, conduction is due to migration of sodium ions as discribed in section 1 2 2The activation energies for sodium migration in the present study are found to be of the same order as reported earlier (Owen 1963, Hughes and Isard 1972)

The resistivities for N glass system decrease with increase of sodium concentration while the activation energy shows a maximum for N2 The slight increase of activation energy for N2 with respect to that of N1 is explainable in terms of its structural characteristics The trend of T_g for N glass system is exactly similar to that observed in the variation of activation energy Thereby suggesting the same mechanism being responsible for both these effects The relative openness of structure of N1 compared to that of N2 makes Q_T for N1 to be less than that of N2 The open single phase structure of N3 is responsible for the lowest value of Q_T in the present series of glasses The pre-exponential factors in the glass system N and IN are consistent with stevel's model of Ionic migration in glass, viz value of pre-exponential factor decreases with increasing number of charge carriers

As evident from Fig. 3 40, plots of $\log_{10} \rho_{OT}$ vs Log η show a linear behaviour for both N and IN glass systems. Both

of these lines are approximately equal to each other The slopes of the least square fit lines are estimated to be $.5 \pm .05$ This implies an empirical relationship between ρ_{OT} and concentration n of the mobile change carriers as follows

$$\rho_{OT} = \frac{C}{n^5} \qquad (3\ 6)$$

where C (N) $= 10^{94}$ for N glass (3 7)

and C (IN) $= 10^{95\ 5}$ for IN glass (3 8)

As per stevel s model, $\rho_{OT} = \frac{6k}{ne^2 \nu R^2}$ (3 9)

where n = no of cations/unit vol

ν = vibration freq of cations

R = average distance between adjascent sites

$$n = \frac{2d_1}{M_o} \frac{N_c}{100} N_o \qquad (3\ 10)$$

where d_1 = Density of glass

N_o = Avogadro number

M_o = Molecular wt of glass

N_c = molar fraction of cation

from eq 3 6 it is obvious that

$$\frac{\rho_{OT}\ (IN)}{\rho_{OT}\ (N)} = \frac{C(IN)}{C(N)} = 10^{1\ 5} \qquad (3\ 11)$$

substituting expressions from eq 3 9

$$\left(\frac{6k}{ne^2 \nu R^2}\right)_{IN} \left(\frac{ne^2 \nu R^2}{6k}\right)_{N} = 10^{1\ 5}$$

assuming

$$\nu_{IN} \cong \nu_N \qquad (3\ 12$$

and

$$d_{IN} \cong d_N \qquad (3\ 13)$$

we get

$$\frac{n_N}{n_{IN}} = 10^{1\ 5}$$

or $$n_{IN} = 10^{-1\ 5}\ n_N$$

$$= 3\ 16 \times 10^{-2}\ n_N \qquad (3\ 14)$$

Thus it is evident from that charge carrier concentration in IN glass system is about 3% of that of N glass system The assumptions given by (3 12 and (3 13) are reasonable in the present case because the ion-exchange process involves only one to one substitution of Na^+ by Ag^+ and no drastic structural change is likely

As evident from equation (3 14) the number of charge carriers effective in determining electrical conductivity in IN glass system is about 3 % of that present in N glass system This is explainable in terms of the microstructure of IN glass system which consists of an interconnected silver-deficient phase (β in section 3 2 6 2) and a silver-rich phase (α in section 3 2 6 2) which has a broken interconnectivity The conductivity is therefore controlled by the carrier concentration in the silver-deficient phase Hence it can be concluded that the charge carrier concentration in the β phase is about 3 % that in the α-phase

From Tables 3 6 and 3 7 it is seen that the values of activation energies for IN glass system are lower as compared to those for N glass system Such decrease in the activation energy for diffusion of silver ions as compared to that of sodium ions has been observed in oxide glass systems (Frischat 1976) This has been explained on the basis of the ionic radii of sodium and silver respectively It has been shown (Stevels JM 1957) that the activation barrier to ionic transport in oxide glasses is usually comprised of two parts, electrostatic and mechanical energies If the glass network is sufficiently open (which is the case when enough alkali ions are present) the mechanical energy can be neglected Under these circumstances, the larger ions should have lower activation energies

The values of activation energies and resistivity at room temperature for IN system are found to be in agreement with values for silver FIC glass systems reported earlier in the literature (Table 1 5)

The activation energies Q_T and Q for N glass system has been found to follow a relationship given by equations 3 19 and 3 20 within an accuracy of $\pm$ 4%

$$\frac{Q_T}{N_C} = 2014 - 1194 \ \mathrm{Log}_{10} N_C \qquad (3\ 19)$$

$$\frac{Q}{N_C} = 1892 - 1116 \ \mathrm{Log}_{10} N_C \qquad (3\ 20)$$

where N_C is the molar concentration of sodium ions

Similar functional relationship in IN glass system is untenable as error is ± 16% The relationship valid in IN glass system is given by equations 3 21 and 3 22 with the accuracy of ± 6%

$$Q_T = 001 N_c + 46 \qquad (3\ 21)$$

$$Q = = 0015 N_c + 413 \qquad (3\ 22)$$

where N_c is molar fraction of silver ions

Difference in functional forms for dependence of activation energy on the concentration of cations in N and IN glass systems, reflects the difference in the mechanisms responsible for giving rise to corresponding activation energies This suggests that during ion exchange process, alongwith one to one substitution of sodium ions by silver ions, some morphological transformation also takes place This is expected as the ionic radii for sodium and silver ions are different

As reported in section 3 2 5 2 an optimum combined influence of E_c and T_c switches the IN glass system to HIN system This effect of E_c and T_c is reflected in the microstructures of IN and HIN glass systems as mentioned in section 3 2 6 2 and 3 2 6 3 The activation energies and preexponential factors of HIN systems are given in Table 3 8 HIN system is characterised by very small activation energies HIN1 and HIN2 show a activation energy barriers which are negligibly small This extraordinary behaviour of HIN glass system can be explained in terms of its microstructural features Switching of IN to HIN system is a

diffusion controlled phenomenon Under combined influence of E_c and T_c silver ions from the silver rich phase ( ) diffuse to the silver dipleted phase ( ) so as to form links among the disjointed portions of the phase Thus a continuous path of phase is created throughout the glass matrix It is this interconnected microstructure of silver rich phase which is responsible for the extremely high conductivity of HIN glass system As silver ions are highly mobile and silver rich phase ( ) is relatively more open as compared to phase, hence very low activation energy for this state is expected

As evident from the fig 3 15, E_c dicreases with increasing T_c This is expected for diffusion controlled phenomenon, as higher the temperature, the higher is the rate of diffusion Only temperature does not seem to be sufficient to bring about this change It is most likely that the presence of electric field is helpful for directional diffusion of silver ions through the phase separating the nearest disjointed portions of phase, so as to make a continuous interconnection of phase As phase is supposed to have almost all the silver ions (99%) present in the glass and structure of phase is quite open, This HIN system has high electrical conductivity Possibility of reduction of a tiny fraction of silver ions to silver atoms as shown by SAD's of HIN system, can not be ruled out during the morphological transformation of IN glass system to HIN glass system These small fractions of silver atoms are most likely to be located in the phase

From the present studies it has been established that a new class of glasses based on silica network can be prepared with a high silver concentration upto molar fractions of 29% by subjecting high-soda containing silica based glass fibres to a sodium silver ion-exchange reaction The ion exchanged glass fibres so prepared show electrical conductivity and activation energy which are similar to those exhibited by fast ion conducting glasses

Another interesting out come of the present investigation is the development of a new group of materials consisting of the HIN glass systems Special metion is to be made of HIN1 and HIN2 glasses which have almost negligible activation energy and exhibit very high conductivity of $2\ 5 \times 10^{-2}$ $(Ohm\text{-}Cm)^{-1}$ and $1\ 7 \times 10^{-2}$ $(Ohm\text{-}Cm)^{-1}$ at room temperature respectively As is obvious from the comparis with Table 1 5, both HIN1 and HIN2 glasses have the highest conductivity so far reported in the literature with almost 0 activation energy It is worth mentioning that highest conducting glassy FIC (from Table 1 5) are A_gI based and contain 70 to 80 mol% of silver and none of them is silica based, whereas HIN1 and HIN2 systems contain only 9 5 and 19 6 mol% silver, respectively and are based on silica network. Hence HIN glass system has potential for futuristic applications in energy devices

CHAPTER IV

Electrical conduction in ion exchanged glass fibres containing aluminium dispersoids

4 1 INTRODUCTION

Oxide glasses with ultrafine dispersion of metallic granules of dimension of the order of few hundred angstroms show electrical conduction by electron tunnelling mechanism between the metallic islands (D Chakravorty et al 1977, D Chakravorty et al 1979) Such microstructures, consisting of dispersion of metallic granules has been induced in glasses by either choosing the mixture of oxides for melting purposes properly (D Chakravorty et al 1977) or by subjecting the glasses to an ion exchange and reduction treatment (T Arul Mozhi, D Chakravorty 1982) The lowest resistivity values obtained by the latter technique is reported to be 10^5 Ω Cm at room temperature

Another method for preparing such glass-metal particulate system may be to use metal in fine powder form and mix it into the batch itself which is then melted If proper blending could be achieved at the batch level of preparation, it is possible to obtain required microstructure As this is a potentially straight forward technique the method may be exploited to prepare such, glass-metal particulate systems on a large scale

As reported and discussed in chapter III, by subjecting the glass fibres of certain composition to $Na^+ \rightleftharpoons Ag^+$ ion exchange the resistivity of glass may be reduced by many orders of magnitude and under the influence of temperature and voltage, such a material may be brought to a high conducting state (HCS) The material in HCS is still an ionic conductor and it is most likely that such ion exchanged glass fibres in HCS state constitute a family of new glasses which are fast ion conductors

Thus it becomes highly interesting to look for the effect of the presence of metal despersoids on the virgin as well as ion exchanged specimens and to explore the possibility of preparing newer material with improved conductivity behaviour

In the present chapter we have explored the possibility of dispersing aluminium particles in glass matrix by directly melting fine aluminium powder with the glass batch The base glass system chosen for such exploration has been N3 containing 30% of sodium We, describe the results obtained during this investigation in the following sections

4 2 Results

The composition and density of glasses which have been investigated are summarised in Table 4 1 The glass system in virgin state is being referred to as A The initial particle distribution of aluminium powder is given in Table 4 2

4 2 1 Glass Preparation and Fiberisation.

The glass batch is prepared with the compositions described in Table 4 1 in which Na_2O and CaO have been added as

Table 4 1 Composition (in mole %) and density of glasses in system A

Sl.No	Glass	Na_2O	SiO_2	CaO	B_2O_3	Al	Density (Gm/cc)
1	A1	30 0	55	12 00	3	0	2 62
2	A2	29 9	54 7	11 9	3	0 5	2 62
3	A3	28 5	52 3	11 4	2 8	5 0	2 61
4	A4	27 8	50 9	11 0	2 8	7 5	2 53
5	A5	27 0	49 5	10 8	2 7	10 0	2 50

Table 4 2 Particle size distribution of aluminium powder used in making the glass-metal composite

Particle diameter (μm)	Weight %
1 0 - 2 0	32
2 0 - 2 5	16
2 5 - 3 0	11
3 0 - 3 5	11
3 5 - 4 0	12
4 0 - 4 5	18

carbonates The glass is melted in an alumina crucible at 1450°C for two hours The melt when free of air bubbles is poured into aluminium mould to be cast as thin rectangular plates which are later annealed at 500°C for 6 hours The plates are powdered and the glass powder so obtained is used to draw glass fibres as discussed in section 2 2 The fiberisation parameters are described in Table 4.3

4 2 2 Ion Exchange

A bunch of fibres cut to 10 Cm length, have been ion exchanged in a pyrex boat containing molten $AgNO_3$ at 330°C for 36 hours as described in section 2 3 This has been done for all the glass compositions The ion-exchanged glass fibres are being referred to as constituting IA glass system

4 2 3 Chemical Analysis

In order to know the molar fraction of silver present in the glass fibres after the ion exchange process, chemical analysis has been performed for IA glass samples by IL/751 atomic absorption spectrometer as described in section 2 4 The results of chemical analysis are summarised in Table 4 4

4 2 4 D T.A. Analysis:

Figs 4 1, 4 2, 4 3, 4 4 and 4 5 represent the DTA curves obtained for different compositions in the A glass system The glass transition temperature T_g, nucleation temperature T_N and growth temperature T_o for these glasses are summarised in Table 4 5 Details of these terms may be seen elsewhere (D Bahadur et al 1982)

Table 4 3 Fiberisation parameters of glass system A

Sl No	Glass	Melt Temp T_M (°C)	Bushing Temp T_B (°C)	Bushing Tip Temp T_P (°C)	Velocity of draw v(m/sec)
1	A1	1300	920	820	20,16,13,11
2	A2	1320	950	830	20,16,13 11
3	A3	1360	960	850	16,13 11 10
4	A4	1400	985	876	14,13,11,10
5	A5	1450	1020	890	13 11,10,9

Table 4 4 Molar fraction of silver in IA glass system

Sl No	Glass	Conc of glass in solution [G] (g/cc)	Conc of silver in sol [Ag] (µg/cc)	Weight fraction of Ag= W_{Ag}	Molar fraction of Ag
1	IN1	2 3	1 30	565	96
2	IN2	3 5	1 97	563	96%
3	IN3	2 8	1 57	561	97%
4	IN4	3 2	1 76	55	95%
5	IN5	2 9	1 60	552	97%

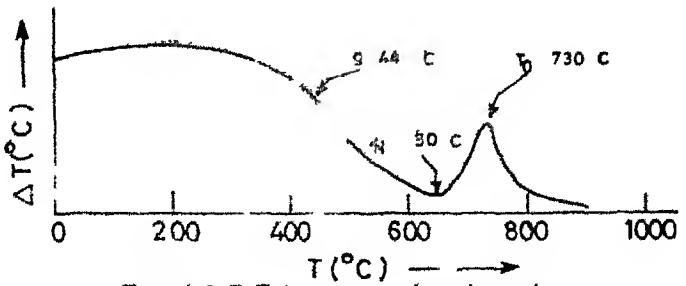

Fig 4 1 D T A curve for glass A_1

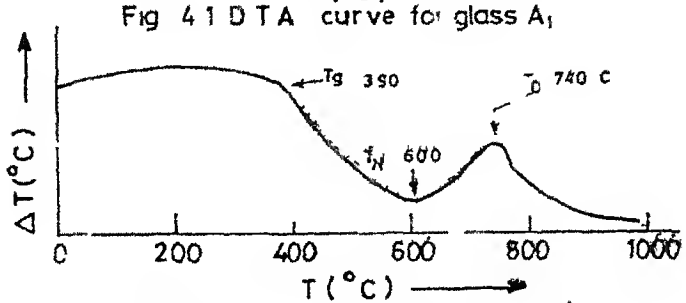

Fig 4 2 D T A curve for glass A_2

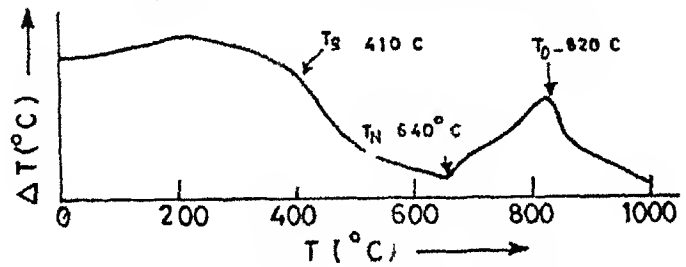

Fig 4 3 D T A curve for glass A_3

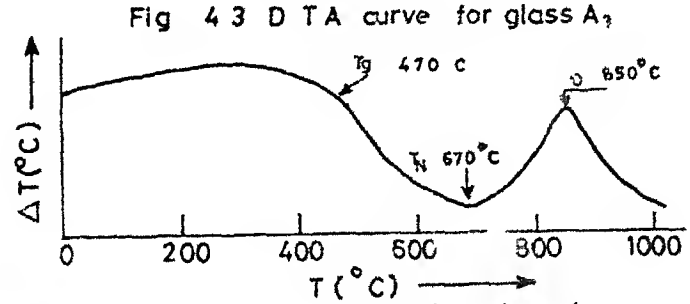

Fig 4 4 D T A curve for glass A_4

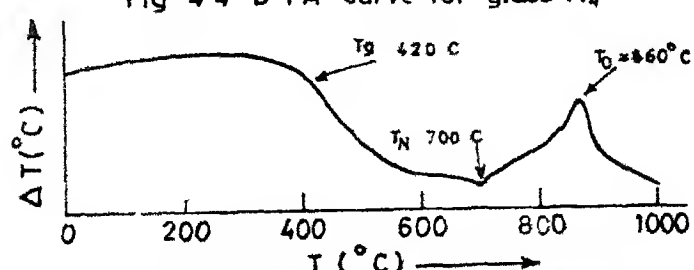

Fig 4 5 D T A curve for glass A_5

4 2 5 Electrical Measurements

D C and A C resistivity measurements for these fibres have been carried out as discussed in section 3 2 5 D C. resistance (R_o) is obtained from the slope of I-V plots Typical representative plots for A and IA samples are shown in Figs 4 6 and 4 7 respectively

4 2 5 1 A C measurement and Impedance Analysis

Conductance (G) and capacitance (C) as a function of frequency (f) have been measured and complex impedance analysis similar to section 3 2 5 1 has been carried out for glass systems A and IA for measurements taken at various temperatures Figs 4 8, 4 9, 4 10, 4 11 and 4 12 are representative Z' -Z' plots for different samples in A glass system Similarly Figs 4 13, 4 14, 4 15, 4 16 and 4 17 show complex impedance analysis for samples of the IA glass system

The D C resistance (R_T) of the sample has been calculated from the intersection of the arc on the real (Z') axis Comparison of R_o and R_T for a typical respresentative set of data is summarised in Table 4 6 Error (e_r) as calculated by equation (3 3) is also shown in this table

It is obvious from Table 4 6 that errors in D C measurements is within 2% of that estimated from complex impedance analysis Hence resistances as obtained from I-V plots have been taken as true representative values for D.C resistance of glass systems A and IA

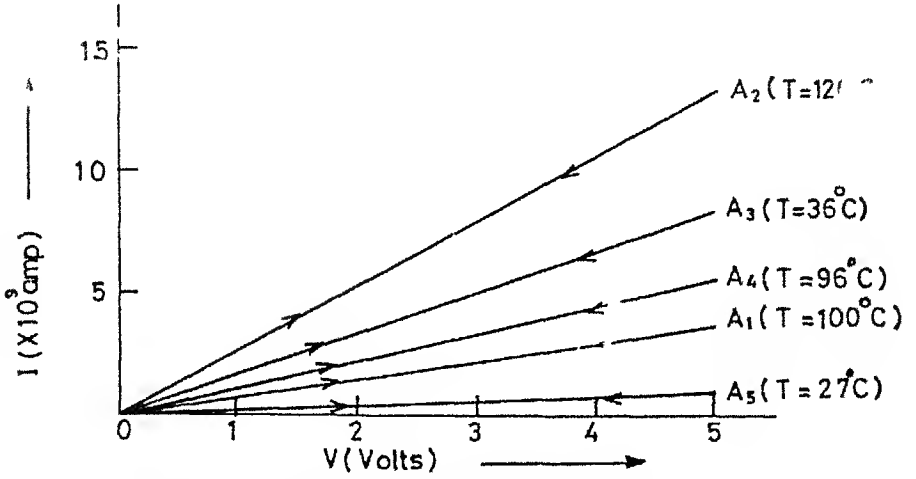

Fig 4 6 I-V Plot for glass system A

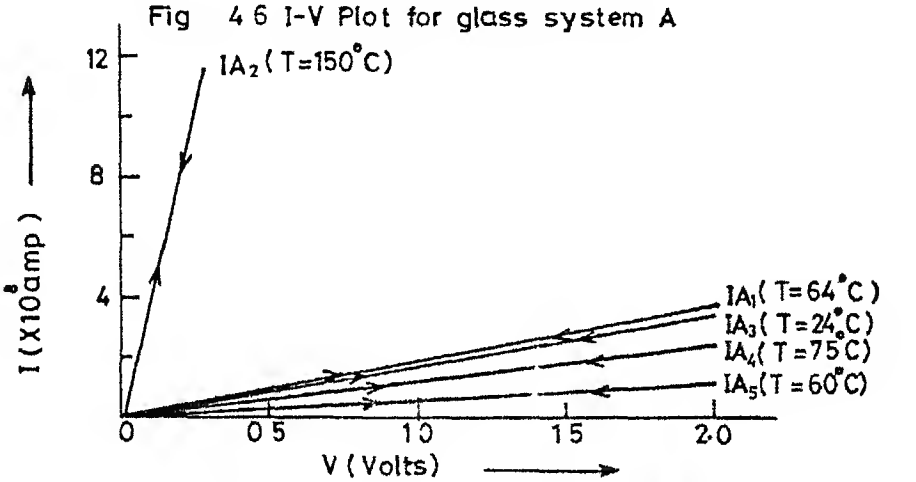

Fig 4 7 I-V Plot for glass system IA

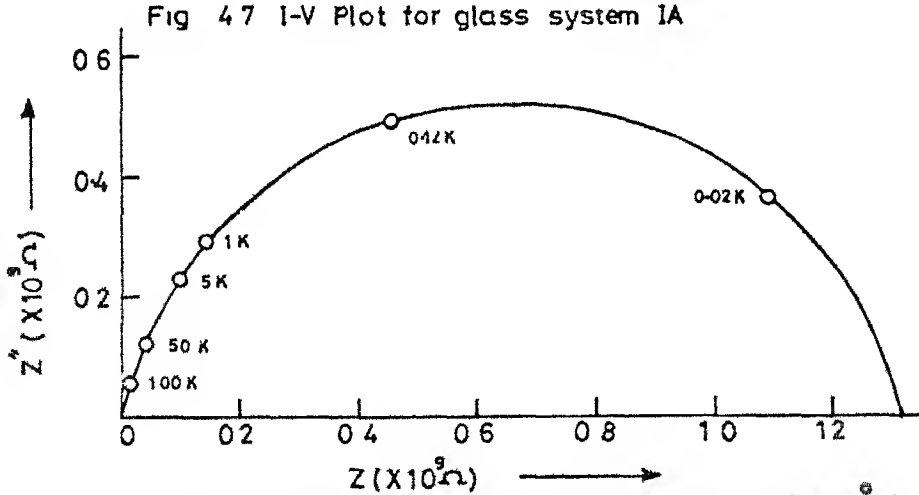

Fig 4 8 Complex impedance plot for glass A_1 (T=100°C)

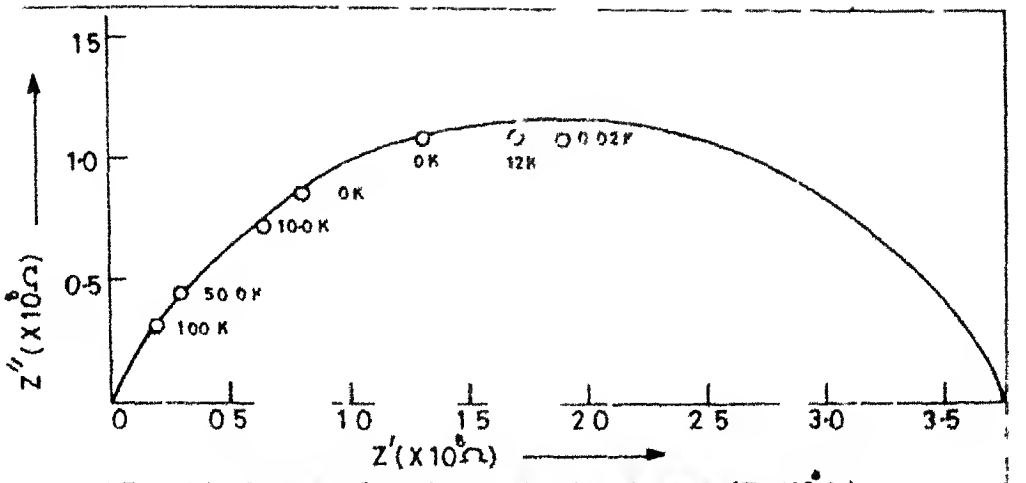

Fig 4 9 Complex impedance plot for glass A_2 (T = 126°C)

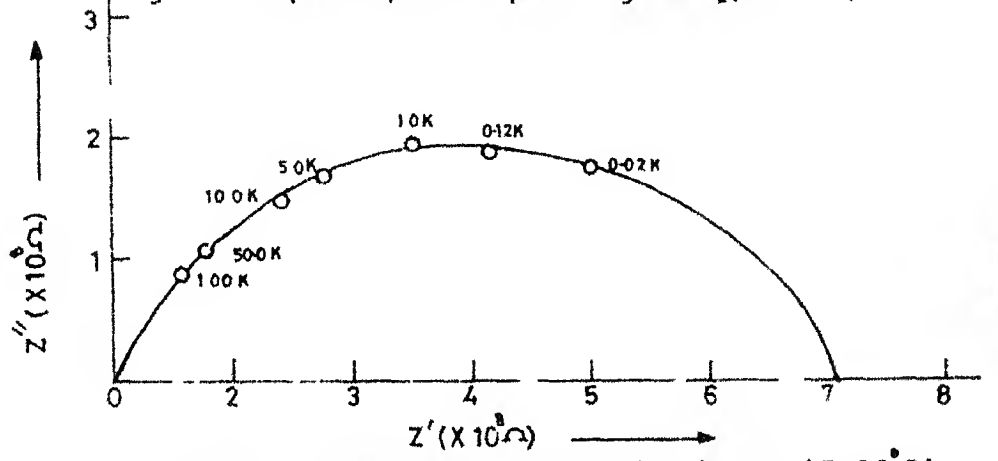

Fig 4 10 Complex impedance plot for glass A_3 (T = 36°C)

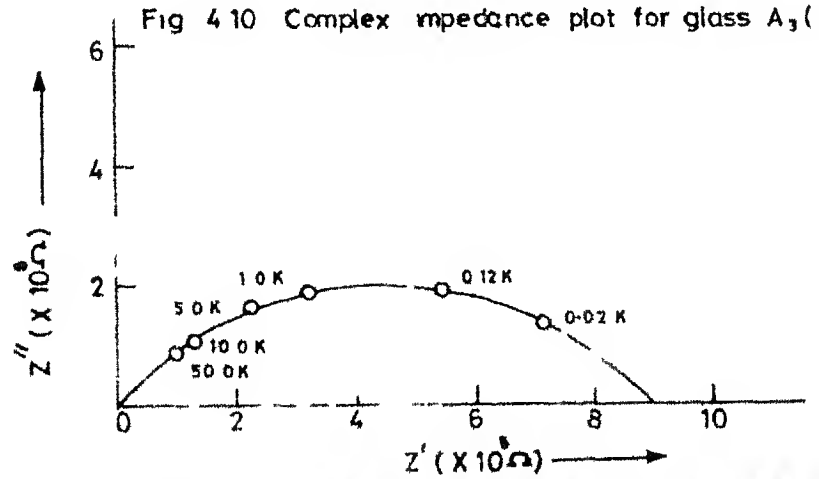

Fig 4 11 Complex impedance plot for glass A_4 (T = 96 C)

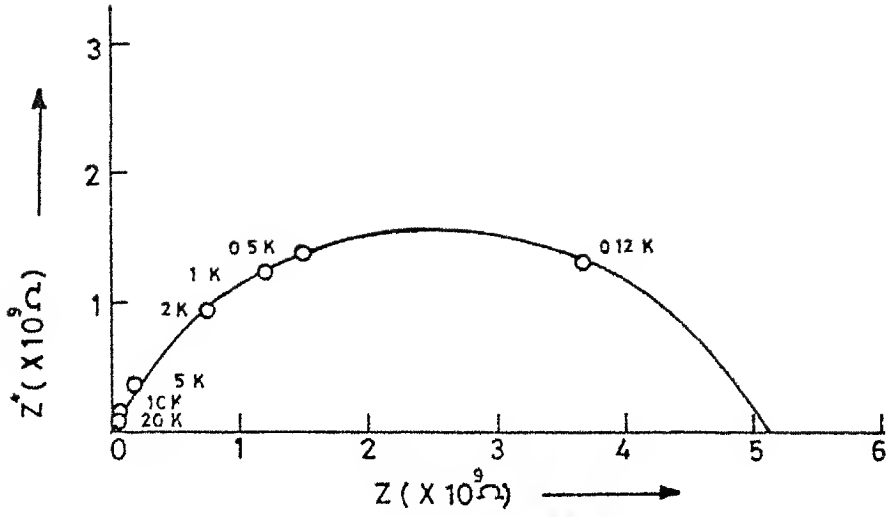

Fig 4.12 Complex impedance plot for glass A_5 ($T = 27^{\circ}C$)

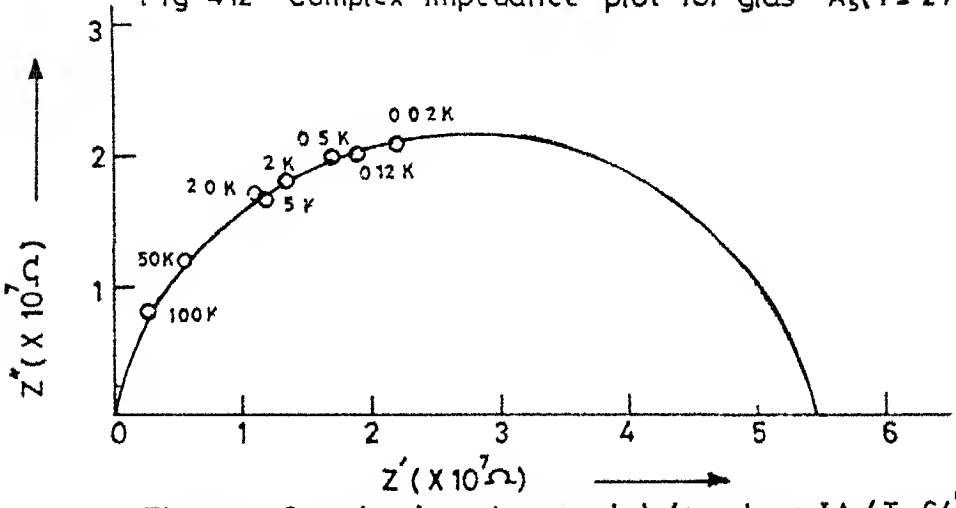

Fig 4.13 Complex impedance plot for glass IA_1 ($T = 64^{\circ}C$)

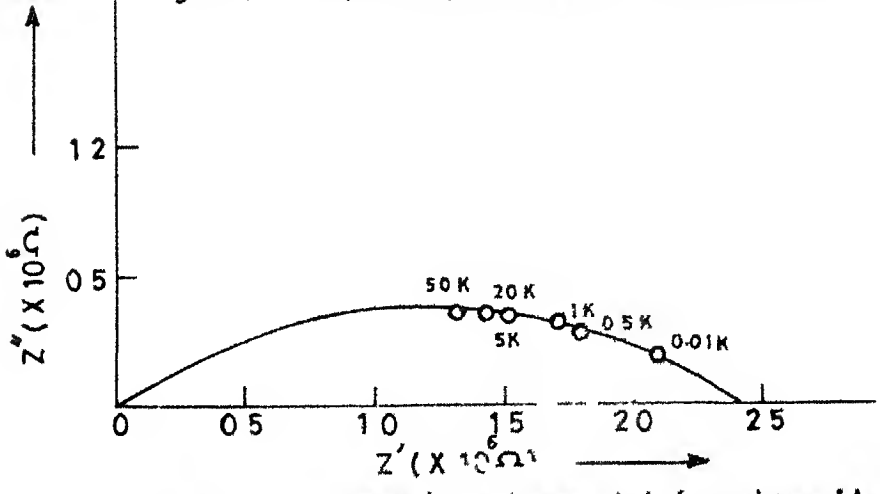

Fig 4.14 Complex impedance plot for glass IA_2 ($T = 150^{\circ}C$)

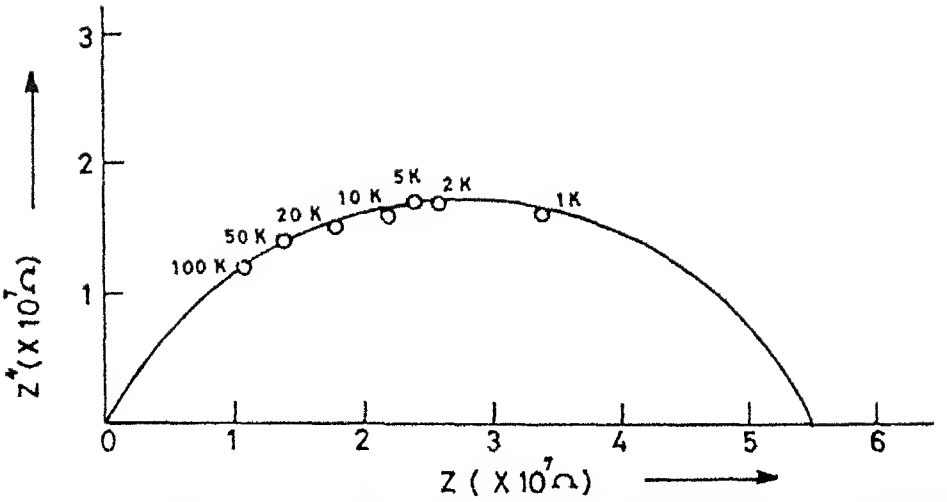

Fig 415 Complex impedance plot for glas $1A_3$ ($T=24^{\circ}C$)

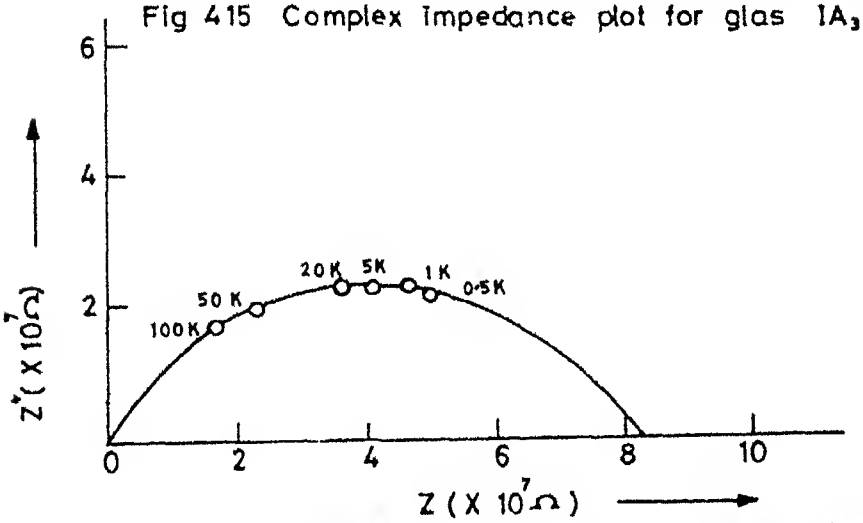

Fig 416 Complex impedance plot for glass $1A_4$ ($T=75^{\circ}C$)

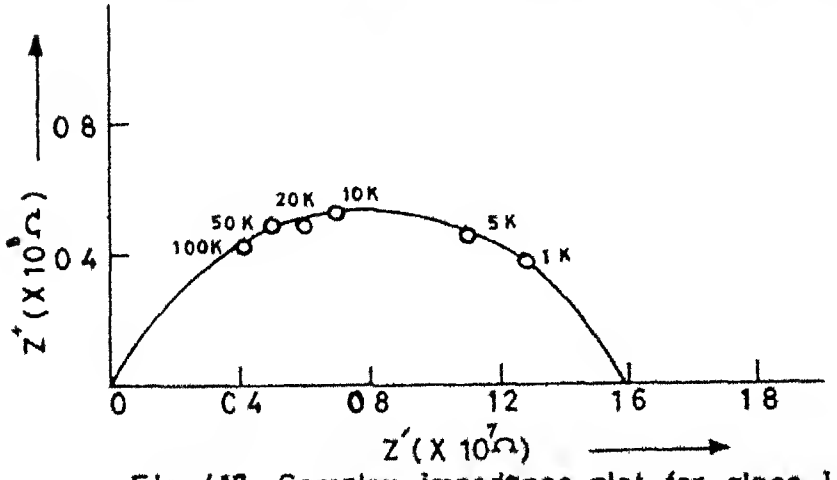

Fig 417 Complex impedance plot for glass 1A5 ($T=60^{\circ}C$)

Table 4.5 T_g, T_N and T_o for glass system A

Sl No	Glass	T_g (°C)	T_N (°C)	T_o (°C)
1	A1	440	650	730
2	A2	390	600	740
3	A3	410	640	820
4	A4	470	670	850
5	A5	420	700	860

Table 4.6 Comparison of R_v and R_T for glass systems A and IA

Sl No	Class	T	R_o (Ω)	R_T (Ω)	e_r (%)
1	A1	100 C	1.37×10^9	1.31×10^9	-1.50
2	A2	126 C	3.7×10^9	3.75×10^8	1.4
3	A3	36°C	6.0×10^8	6.1×10^8	1.7
4	A4	96°C	9.0×10^8	8.9×10^8	-1.1
5	A5	27 C	5.0×10^9	5.1×10^9	2.0
6	IA1	64°C	5.40×10^7	5.46×10^7	1.11
7	IA2	150 C	2.36×10^6	2.4×10^6	1.7
8	IA3	24°C	5.45×10^7	5.5×10^7	0.9
9	IA4	75°C	8.2×10^7	8.3×10^7	1.2
10	IA5	60°C	1.6×10^8	1.58×10^8	-1.3

4 2 5 2 Temperature Dependence of resistivity

The resistivity values for various glass samples have been calculated by eq 2 7 from the measured value of D.C. resistance R_0 determined at various temperatures in the range of 20°C to 330°C for glass systems A and IA The glass system IA has been found to exhibit switching behaviour similar to that shown by glass system IN, described in section 3 2 5 2 Under the combined influence of critical electric fields (E_c) and critical temperature (T_c) a decrease in resistivities by many orders of magnitude is brought about Glass fibres in this highly conducting state are referred to as HIA glass system The newly attained high conducting state is found to be permanent and stable

The typical I-V plots pertaining to the switching of IA to HIA glass system are shown in Figs 4 18,4 19,4 20,4 21 and 4 22 respectively In each figure both IA and HIA states have been shown These plots have a negative resistance region as shown by arrows in these figures Variation of E_c and T_c for IA system is shown in fig 4 23

Figs 4 24,4 25,4 26,4 27 and 4 28 show the variation of log (ρ/T) with $1/T$ for (A1,IA1,HIA1), (A2,IA2,HIA2) (A3 IA3, HIA3), (A4,IA4,HIA4) and (A5,IA5,HIA5) systems respectively Each figure shows three curves representing dependence of resistivity on temperature for three sets of materials belonging to A, IA and HIA glass systems respectively IN figs 4 29, 4 31 and 4 32, comparison of Log ρ with $1/T$ for A,IA and HIA glass systems respectively has been shown

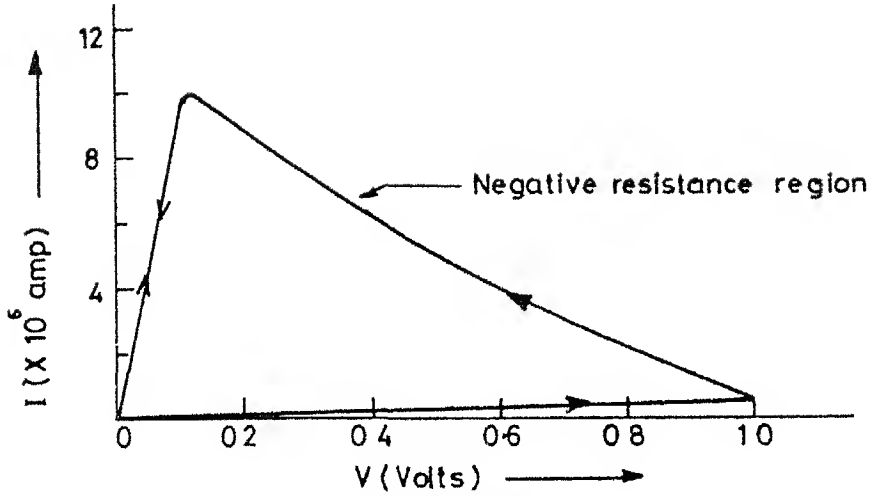

Fig 418 Switching of IA_1 glas to HIA_1 glass (T_c=160°C)

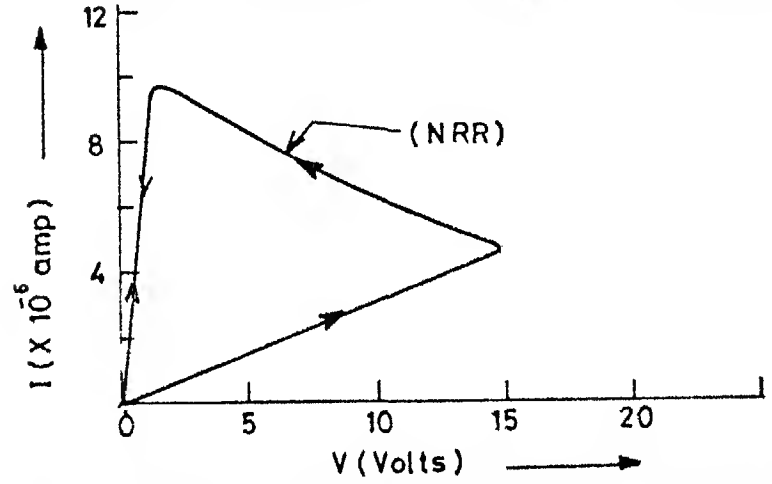

Fig 419 Switching of IA_2 glass to HIA_2 glass (T_c=140°C)

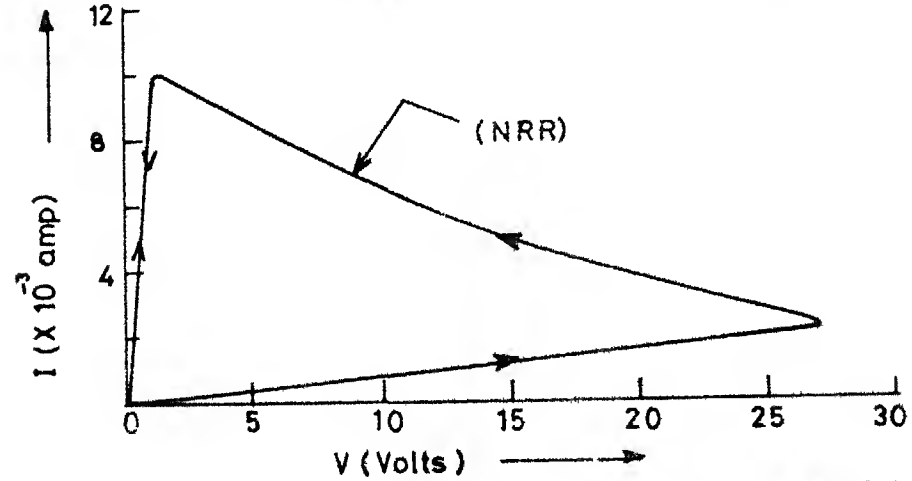

Fig 420 Switching of IA_3 glass to HIA_3 glass (T_c=280°C)

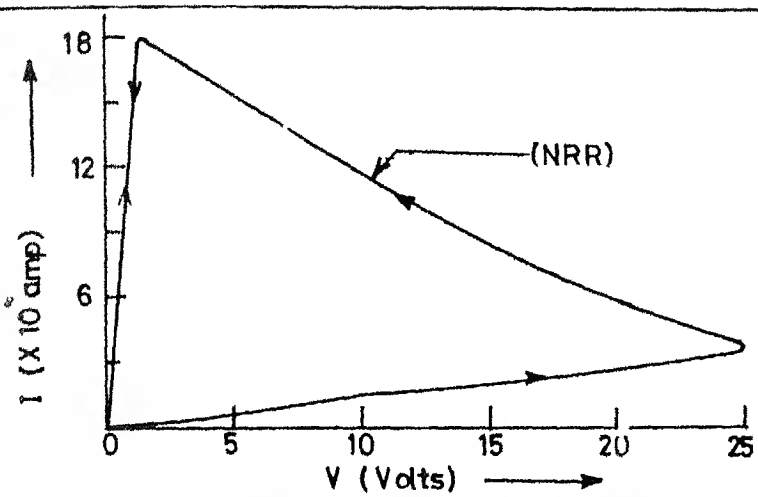

Fig 4 21 Switching of IA_4glass to HIA_4glass (T_c=300°C)

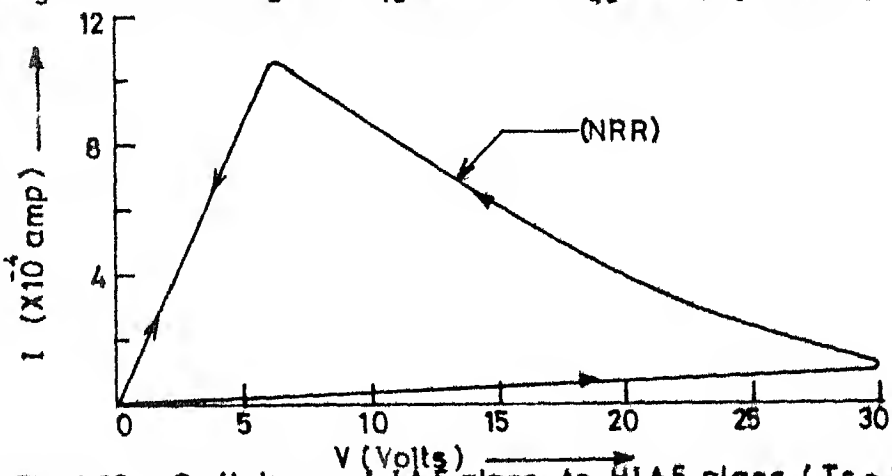

Fig 4 22 Switching of IA 5 glass to HIA 5 glass (Tc = 310°C)

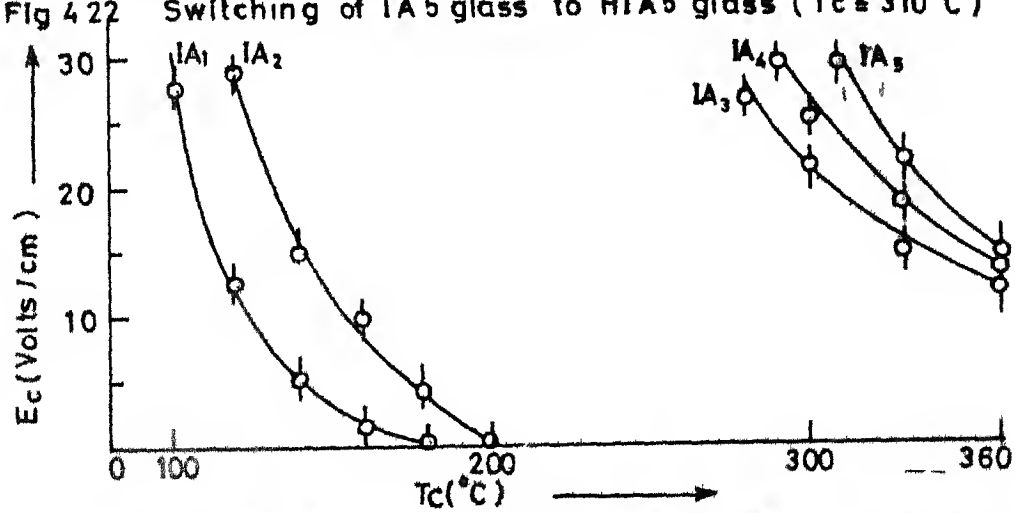

Fig 4 23 Temperature variation of critical electric field (E_c) for glass system IA

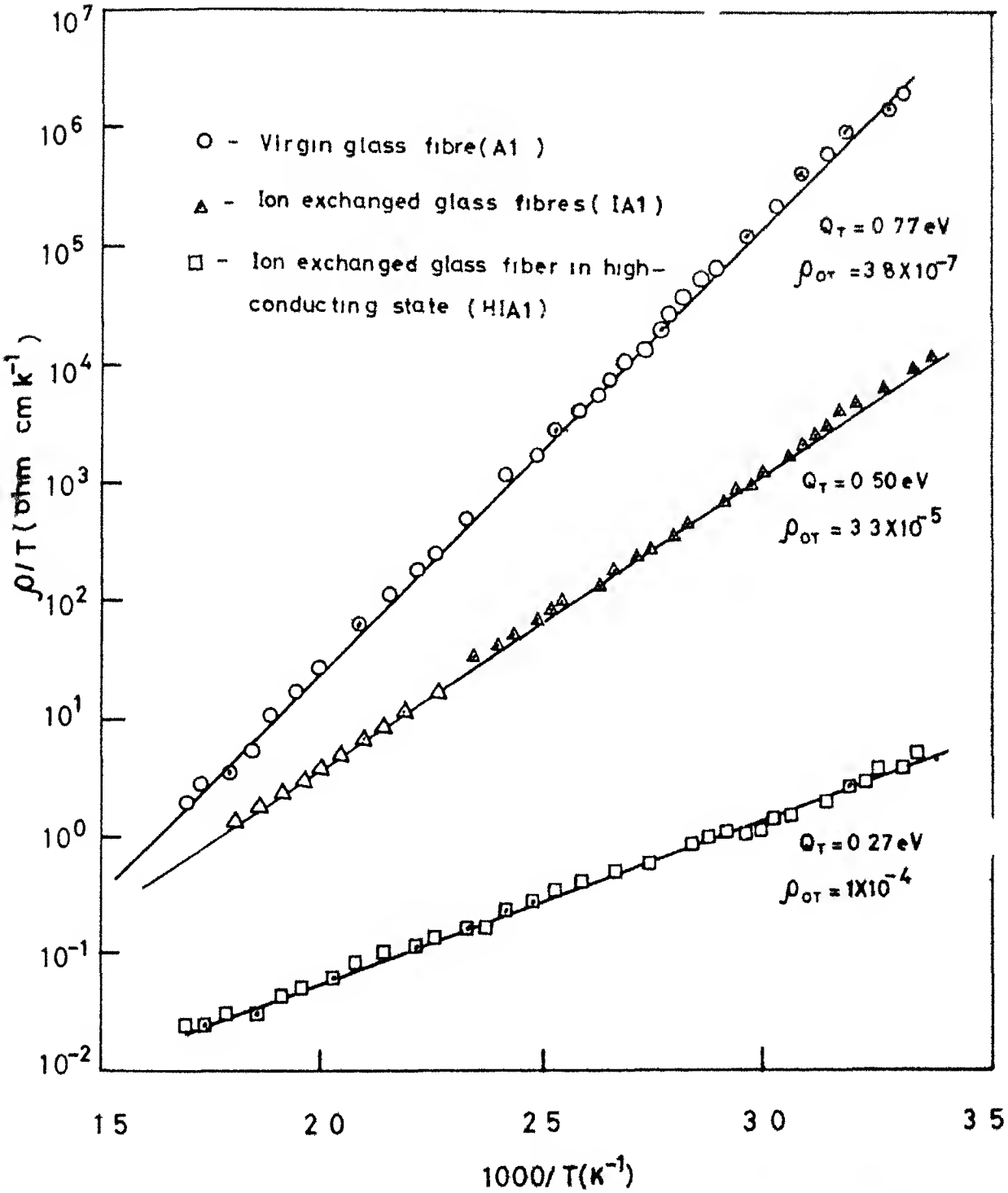

Fig 4.24 Temperature variation of(D C resistivity/ temperature)for A1 IA1 and HIA1 glass fibres

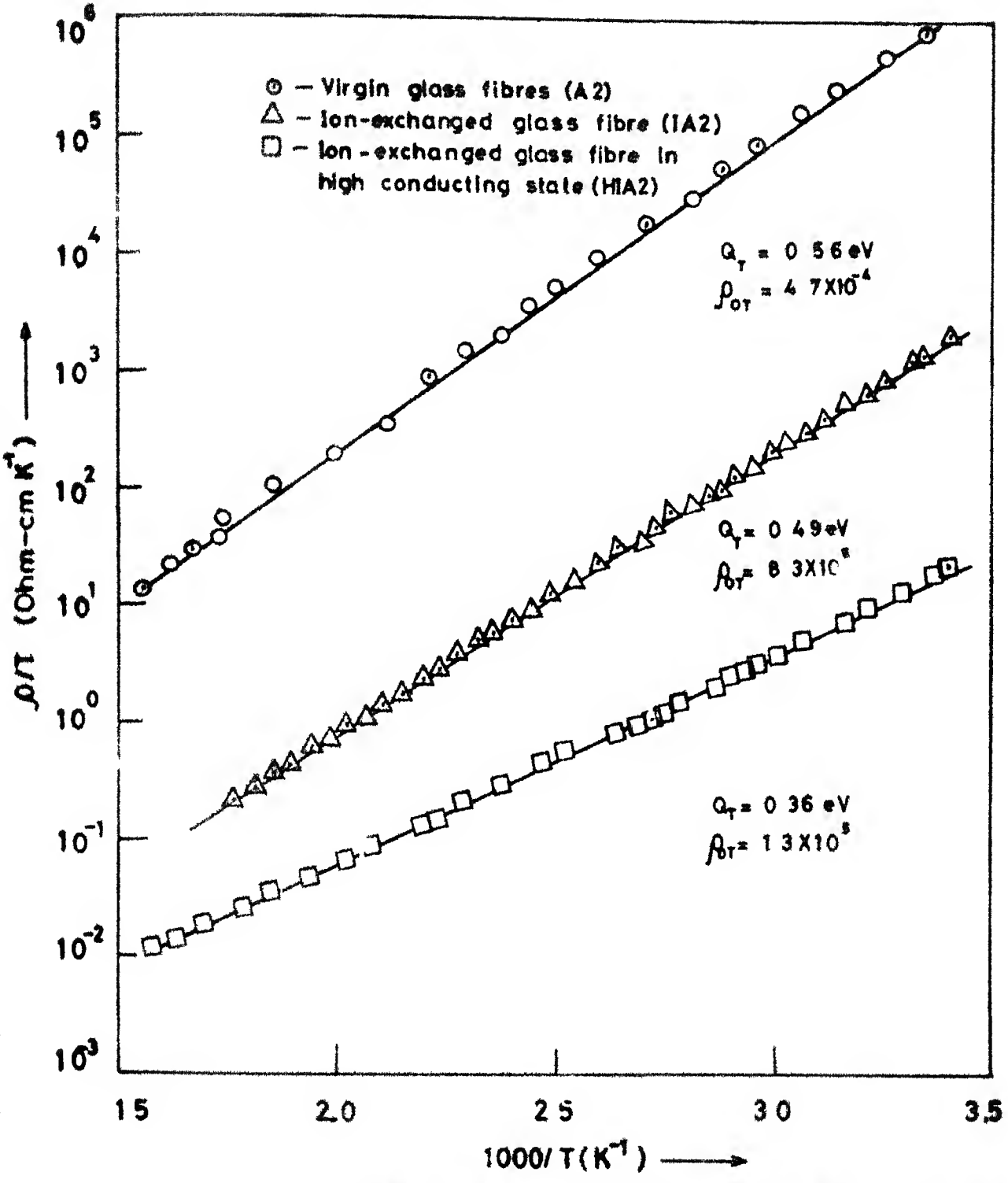

Fig 4 25 Temperature variation of(D C resistivity/ temperature/ for A2, IA2 and H'A2 glass fibres

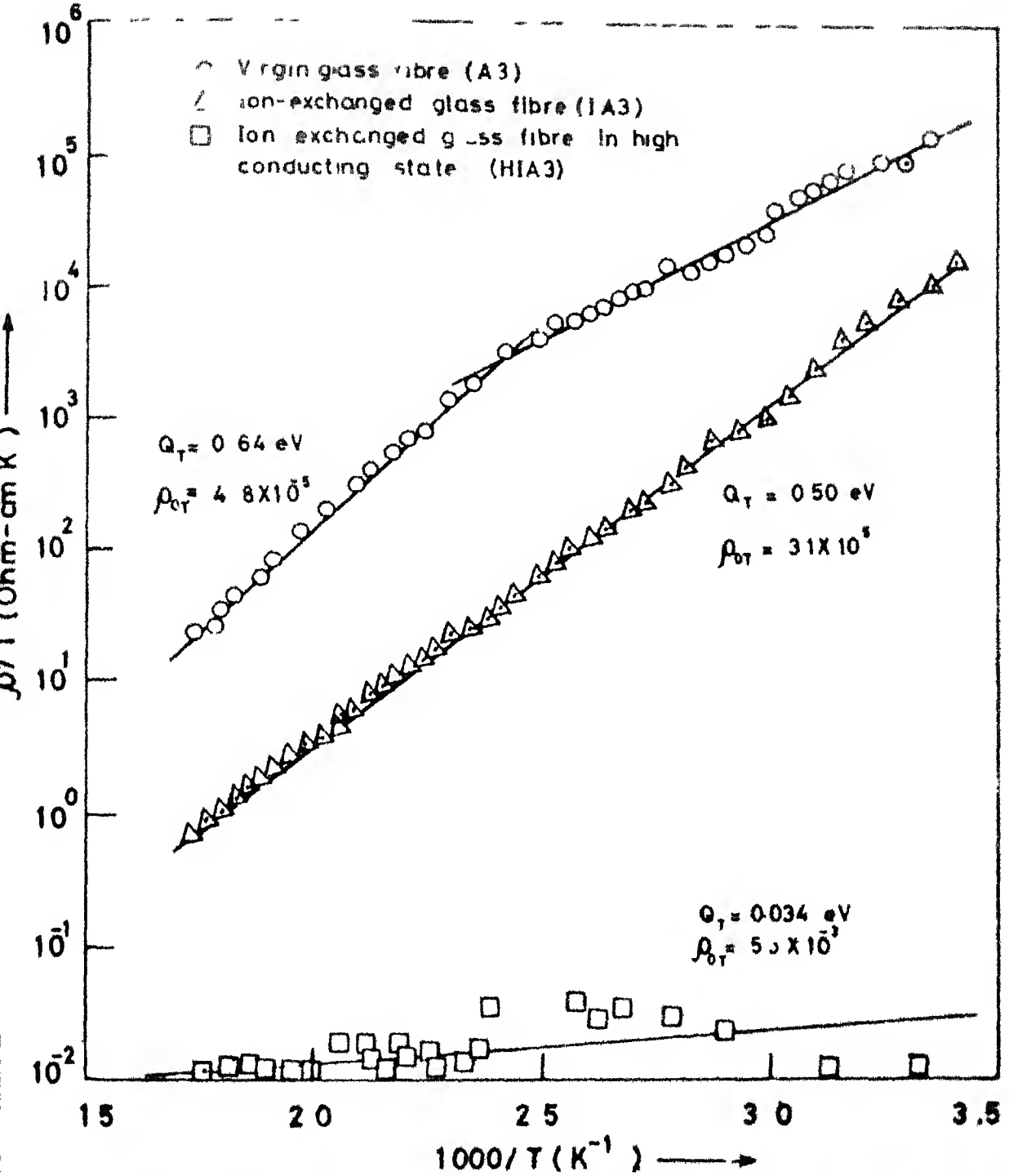

Fig 4 26 Temperature variation of(D C resistivity / temperature)for A3 , IA3 and HIA3 glass fibres

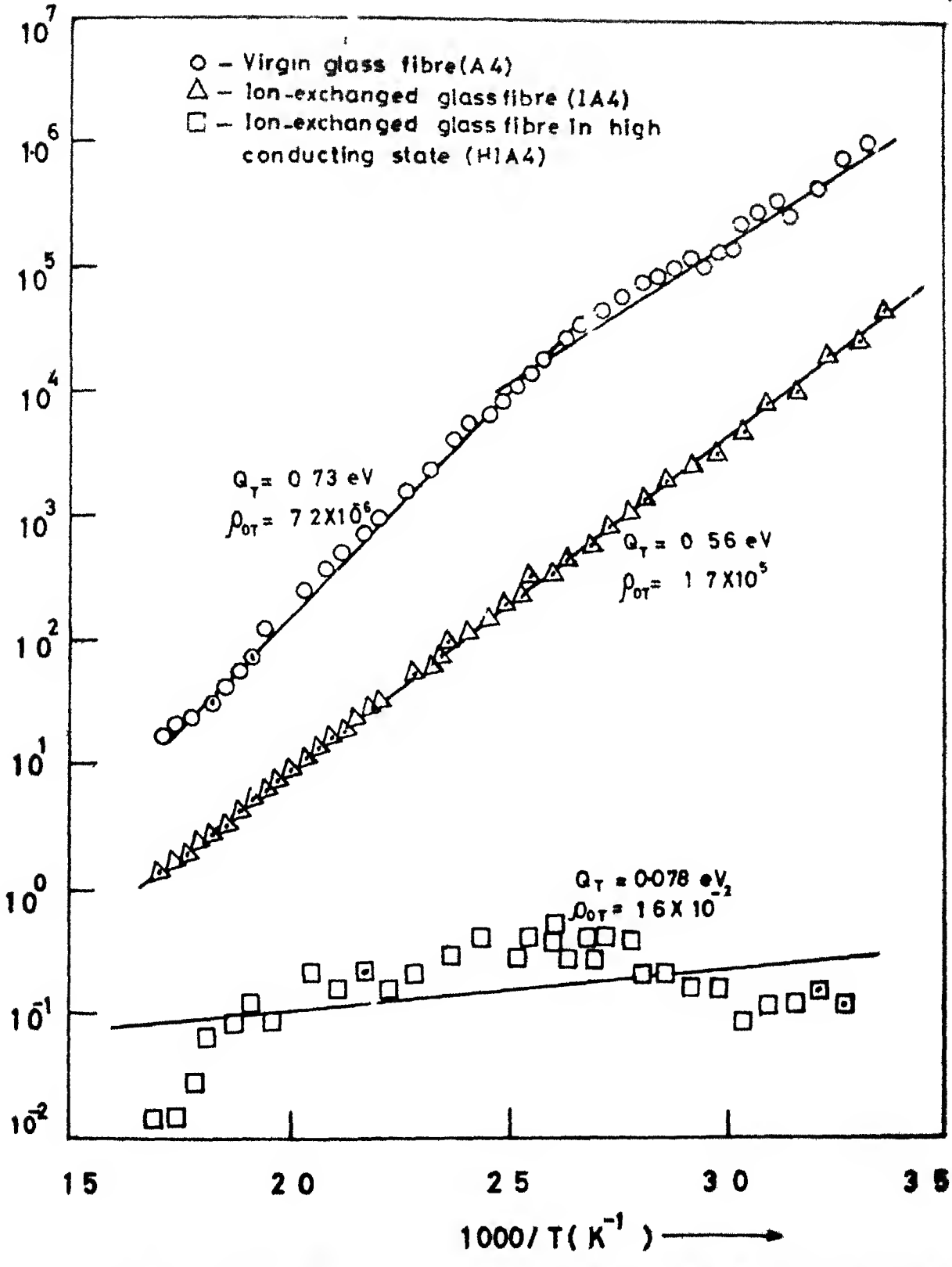

Fig 4 27 Temperature variation of(D C resistivity/ temperature) for A4, IA4 and HIA4 glass fibres.

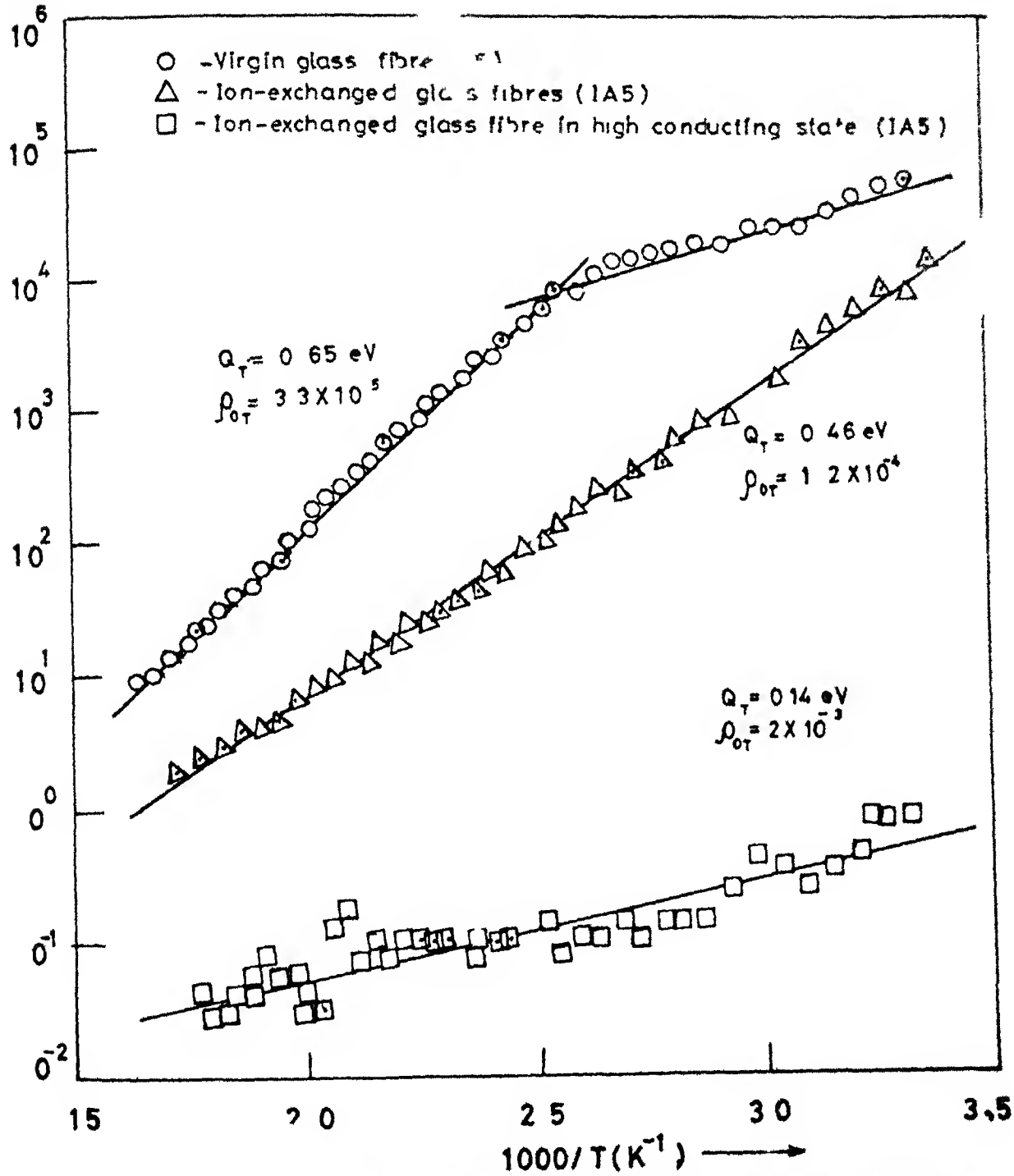

Fig· 4 28 Temperature variation of(D C resistivity/temperature) for A5, IA5 and HIA5 glass fibres

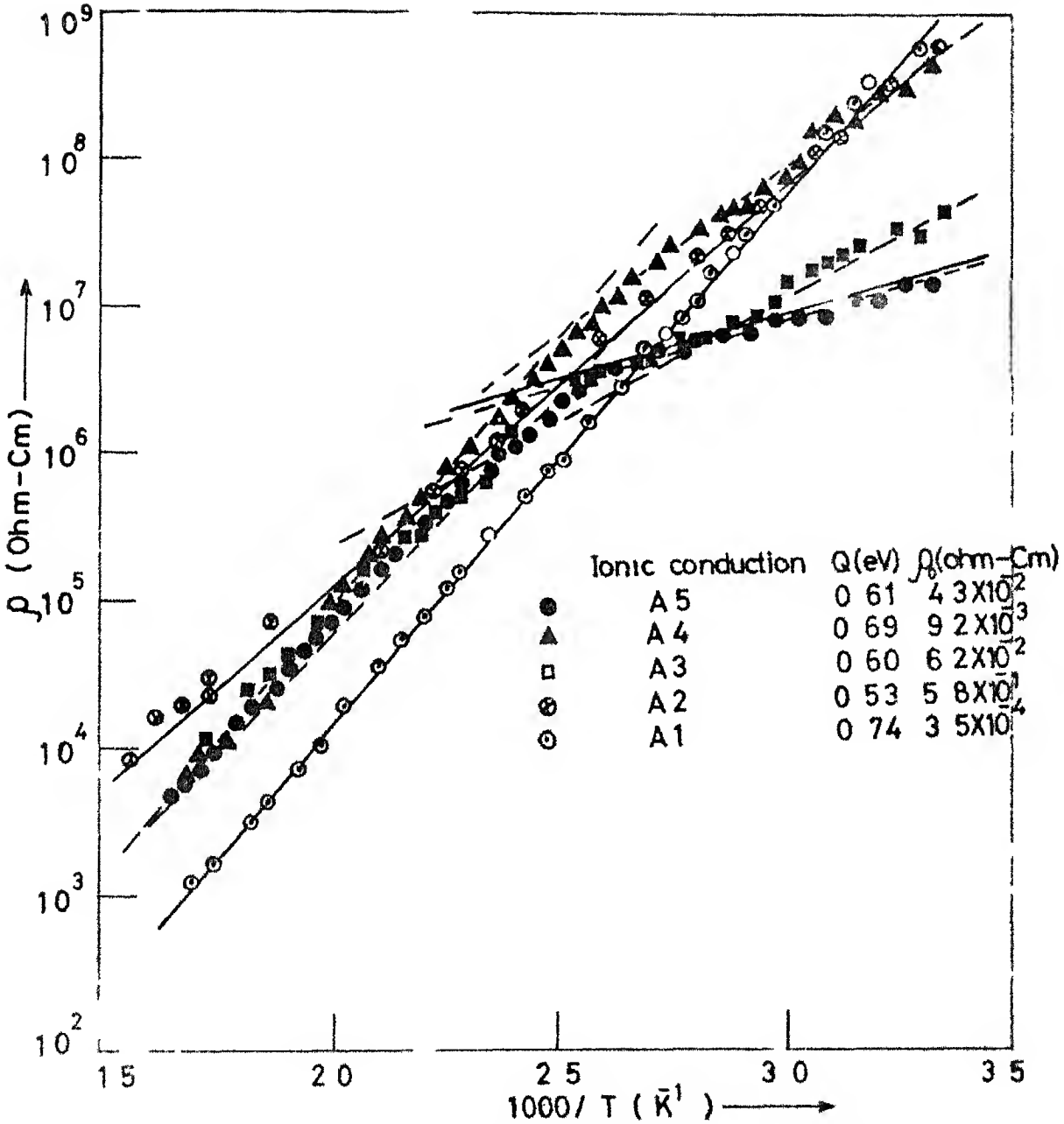

Fig 4 29 Temperature variation of D C restivities for glass system A

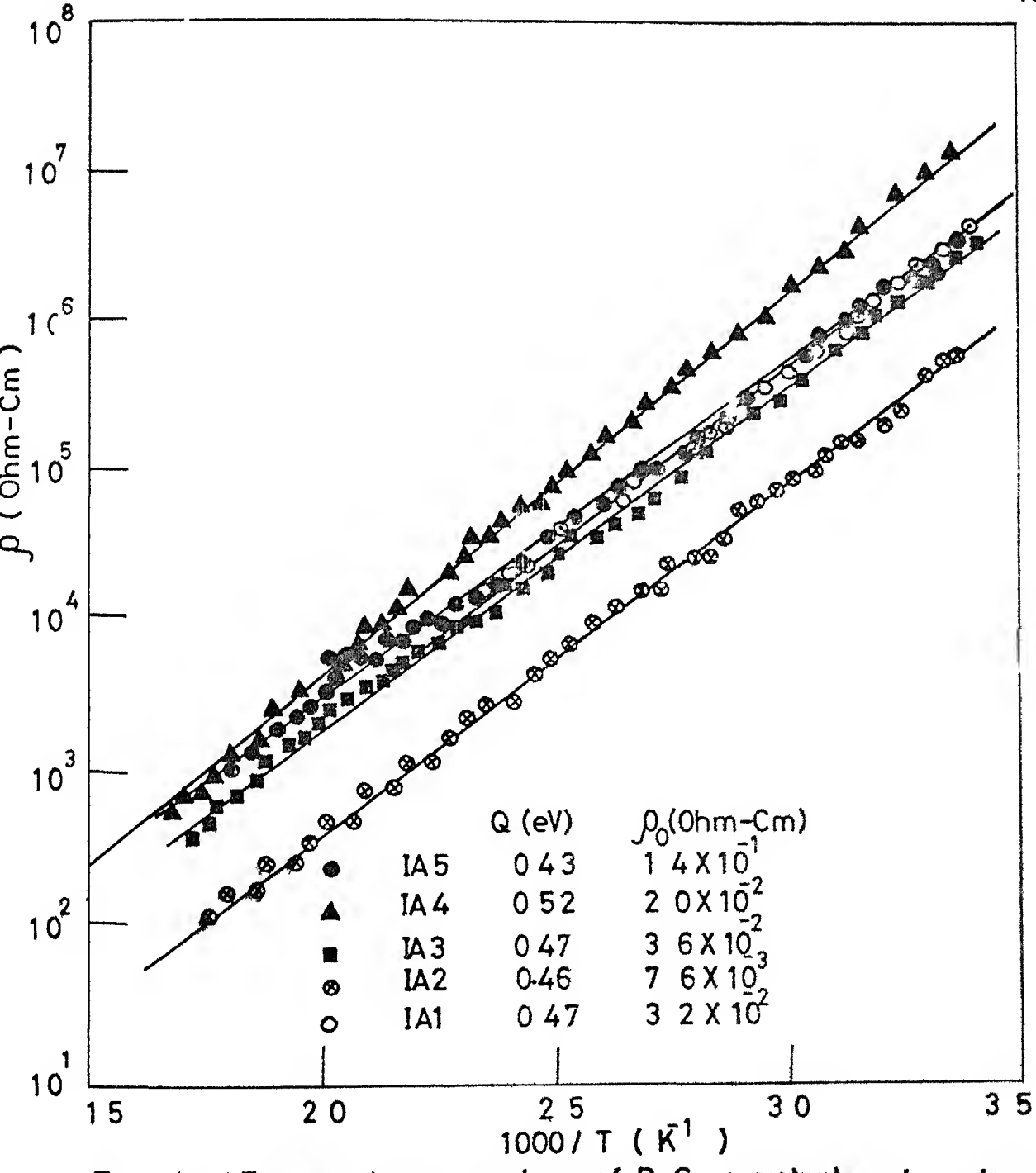

Fig 4 30Temperature variation of D C resistivities for glass system IA

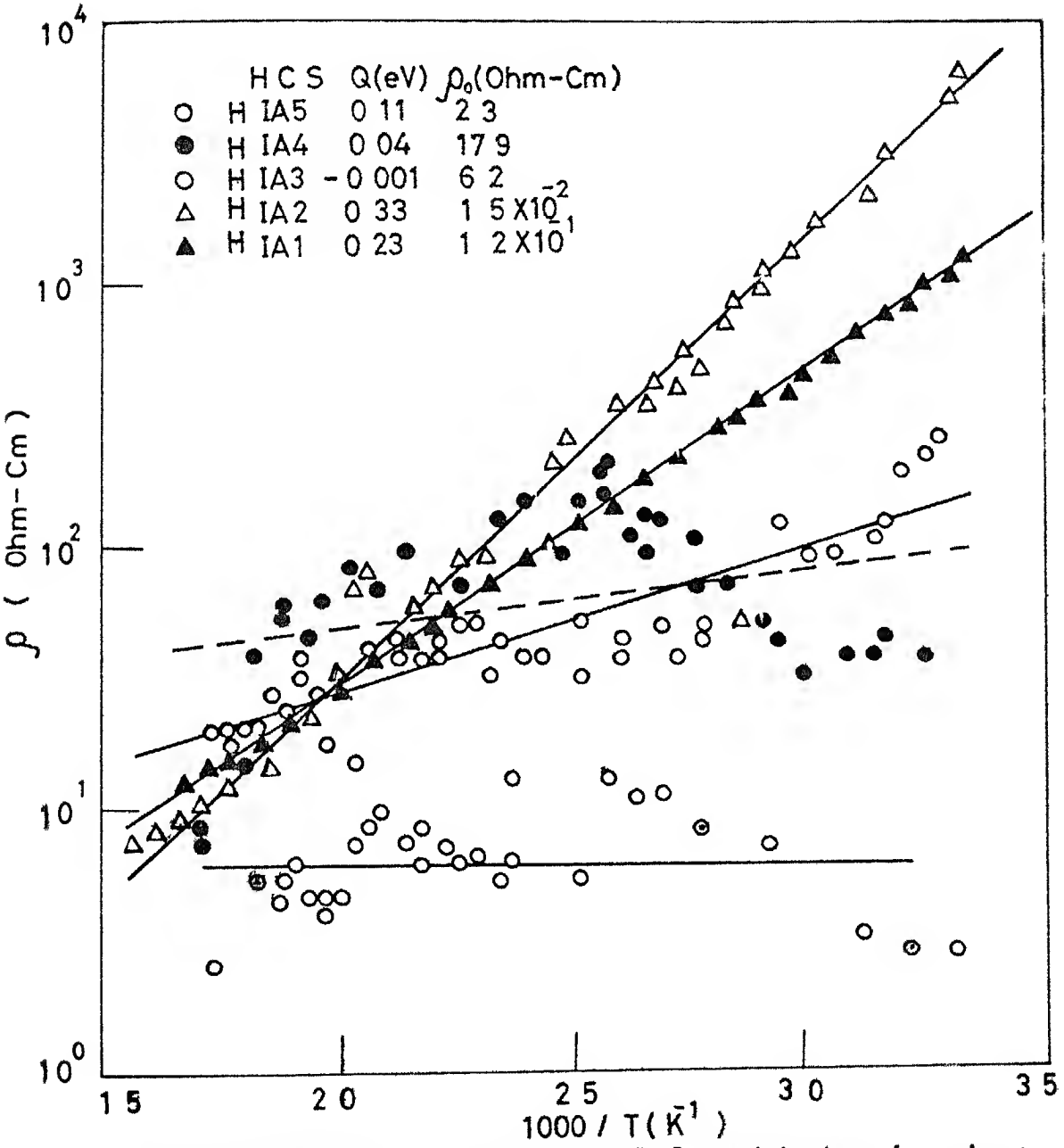

Fig 4 31 Temperature variation of D C resistivities for glass system HIA

As evident from these figures, for glass system A, or compositions corresponding to A3,A4 and A5, resistivity ariation with temperature comprises of two branches characteri-ed by different slopes In the lower temperature range the onductivity arises due to electron tunnelling between the aluminium ranules [Chakravorty 1984] while in the higher temperature range t is due to the migration of alkali ions For electron tunnelling he analysis of data has been shown in figure 4 32 where varia-ion of log ρ with $1/_T$ has been shown

The temperature dependence of resistivity in each case s assumed to follow the relationship given by equations (3 4) nd (3 5) and for electron tunnelling relationship given by equa-ion (4 1) has been assumed (Section 1 2 1 3)

$$\rho = \rho_e \exp \left(\frac{Q_e}{kT} \right)^{1/2} \qquad (4\ 1)$$

Various values of pre-exponential factors and activation nergies for both virgin and ion-exchanged glass systems have been nalysed Each calculated parameter has been assigned its variance oo Table 4 7 summarises the results of this analysis for glass ystem A, for ion migration corresponding to higher temperature egion (110°C-330°C)

Similar analysis carried out for electron tunnelling echanism in the temperature region from 20°C to 110°C for lass compositions A_3, A_4 and A_5 is presented in Table 4 8

Pre-exponential factors and activation energies alculated for IA and HIA glass systems are presented in Table 4 9 nd 4 10 respectively

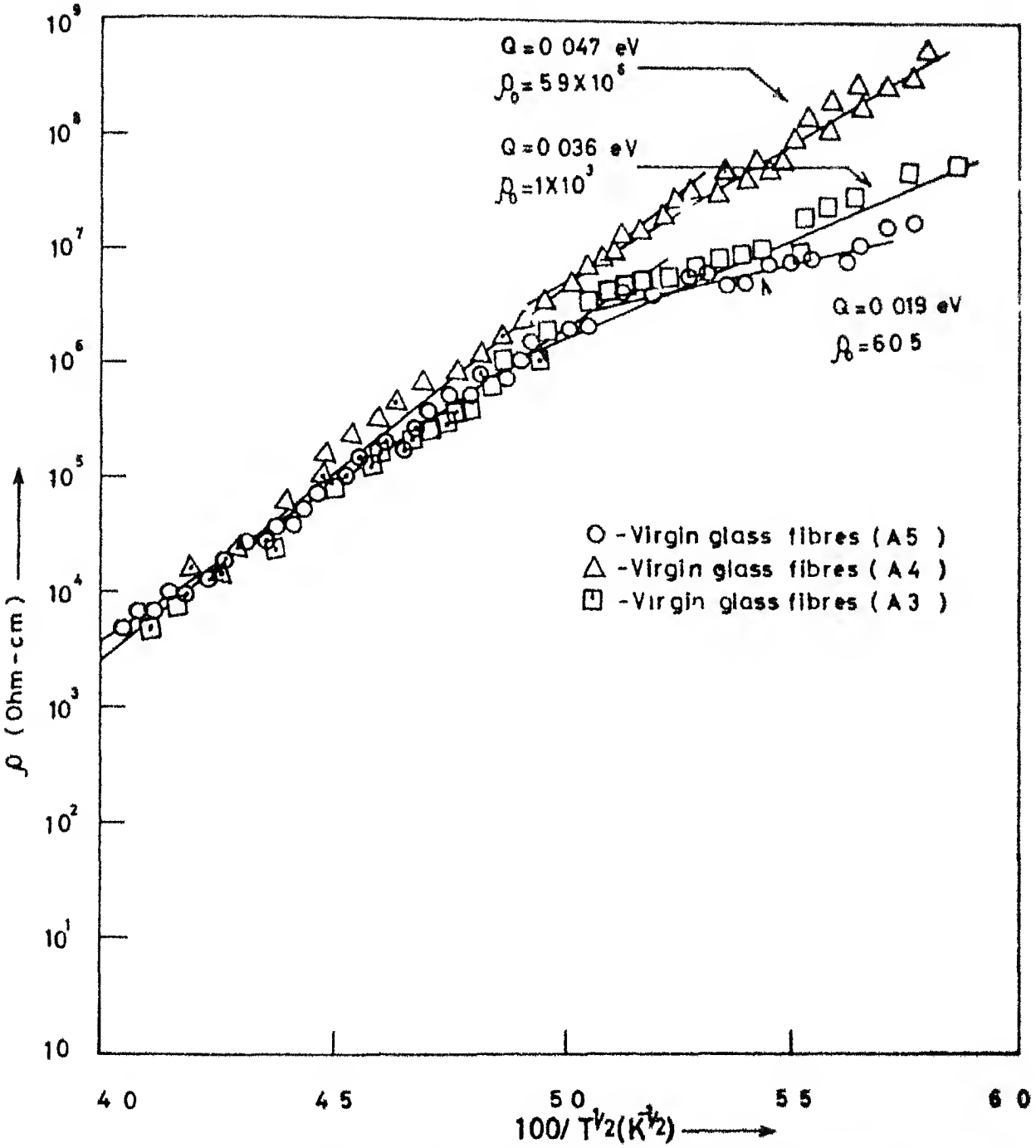

Fig 432Variation of resistivity with ($T^{-1/2}$) for virgin glass - fibres (A3, A4, A5)

Table 4 7 Activation energy and pre-exponential factor for glass system A

Sl No.	Glass	$Q_T \pm dQ_T$ (eV)	$\rho_{OT} \pm d\rho_{OT}$ (Ohm-Cm-K^{-1})	$Q \pm dQ$ (eV)	$\rho_O \pm d\rho_O$ (Ohm-Cm)
1	A1	77 ± 01	$3\ 8\times10^{-7} \pm 2\ 4\times10^{-7}$	$74 \pm .01$	$3\ 5\times10^{-4} \pm 2\ 2\times10^{-4}$
2	A2	56 ± 01	$4\ 7\times10^{-4} \pm 1\ 9\times10^{-4}$	53 ± 01	$5\ 8\times10^{-1} \pm 2\ 3\times10^{-1}$
3	A3	64 ± 01	$4\ 8\times10^{-5} \pm 1\ 4\times10^{-4}$	60 ± 01	$6\ 2\times10^{-2} \pm 1\ 8\times10^{-2}$
4	A4	$.73 \pm 01$	$7\ 2\times10^{-6} \pm 2\ 1\times10^{-6}$	69 ± 01	$9\ 2\times10^{-3} \pm 2\ 6\times10^{-3}$
5	A5	65 ± 01	$3\ 3\times10^{-5} \pm 6\ 3\times10^{-6}$	61 ± 01	$4\ 3\times10^{-2} \pm 8\ 1\times10^{-3}$

Table 4 8 Q_e and ρ_e for A^3, A^4 and A^5 glasses

Sl No	Glass	$Q_e \pm dQ_e$ (eV)	$\rho_e \pm d\rho_e$ (Ohm Cm)
1	A3	036 ± 003	$1\times10^{-3} \pm 1\ 9\times10^{-3}$
2	A4	047 ± 002	$5\ 2\times10^{-6} \pm 7\ 7\times10^{-6}$
3	A_5	019 ± 001	$60\ 5 \pm 28\ 5$

Table 4 9 Pre-exponential factors and activation energies for glass system IA

Sl No	Glass	$Q_T \pm dQ_T$ (eV)	$\rho_{OT} \pm d\rho_{OT}$ (Ohm-Cm-K^{-1})	$Q \pm dQ$ (eV)	$\rho_O \pm d\rho_O$ (Ohm-Cm)
1	IA1	50 ± 01	$3\ 3\times10^{-5} \pm 1\times10^{-5}$	47 ± 01	$3\ 2\times10^{-2} \pm 1\times10^{-2}$
2	IA2	49 ± 01	$8\ 3\times10^{-6} \pm 3\ 4\times10^{-6}$	46 ± 01	$7\ 6\times10^{-3} \pm 3\ 1\times10^{-3}$
3	IA3	50 ± 01	$3\ 1\times10^{-5} \pm 6\times10^{-5}$	47 ± 01	$3\ 6\times10^{-2} \pm .6\times10^{-2}$
4	IA4	56 ± 01	$1\ 7\times10^{-5} \pm 2\times10^{-5}$	52 ± 01	$2\times10^{-2} \pm 2\times10^{-2}$
5	IA5	46 ± 01	$1\ 2\times10^{-4} \pm 2\times10^{-4}$	43 ± 01	$1\ 4\times10^{-1} \pm 2\times10^{-1}$

4 2 6 TEM Analysis

Detailed microstructural studies have been carried out by transmission electron microscopy as described in section 2 6 Basic features associated with each of them are described in the following sections

4 2 6 1 A Glass System

Figures 4 33, 4 35, 4 37, 4 39 and 4 41 are representative micrographs of A1, A2, A3, A4 and A5 respectively Corresponding SAD's are shown in figures 4 34, 4 36, 4 38, 4 40 and 4 42 respectively It is evident that A1 does not exhibit any phase separation Corresponding SAD also confirms the amorphous character of A1 The glasses A2, A3 A4 and A5 show phase separation All of them consist of two phases-darker regions constitute the phase containing metallic aluminium Separation of two phases is maximum in A2. A3 exhibits two phases which are thoroughly interconnected Corresponding SAD's shows characteristic rings corresponding to metallic aluminium This also confirms the uniform fine dispersion of aluminium particulates Both the phases seem to be interconnected in A3 The glasses A4 and A5 besides exhibiting a two phase structure indicate the presence of some bigger particles of aluminium Both the phases seem to be interlinked in these two glass systems

d_{hkl} values calculated from these SAD's are compared with d_{hkl}(ASTM) values of aluminium in Table 4 11

Table 4 10 Pre-exponential factors and activation energies ofor glass system HIA

Sl No	Glass	$Q_T \pm dQ_T$ (eV)	$\rho_{OT} \pm d\rho_{OT}$ (Ohm Cm K^{-1})	$Q \pm dQ$ (eV)	$\rho_O \pm d\rho_O$ (Ohm Cm)
1	HIA1	27 ± 005	$(1 \pm 2) \times 10^{-4}$	23 ± 005	$1\ 2 \times 10^{-1} \pm 2 \times 10^{-1}$
2	HIA2	36 ± 003	$(1\ 3 \pm 1) \times 10^{-5}$	33 ± 003	$(1\ 5 \pm 1) \times 10^{-2}$
3	HIA3	034 ± 016	$(5\ 5 \pm 2\ 5) \times 10^{-3}$	-,001 ± 016	6 2±2 7
4	HIA4	07? ± 025	$(1\ 6 \pm 1\ 2) \times 10^{-2}$	04 ± 02	17 9±1 2 8
5	HIA5	14 ± 01	$(2\ 0 \pm 6) \times 10^{3}$	11 ± 01	2 3± 7

Table 4 11 Comparison of d_{hkl} values of aluminium with those obtained from SAD's of Glass System A

Sl No	(hkl)	d_{hkl} (Al) (ASTM)	d_{hkl} (Calculated)				
			A1	A2	A3	A4	A5
1	111	2 34	-	2 34	2 34	2 34	2 34
2	200	2 02	-	2 02	2 03	2 02	2 03
3	220	1 43	-	1 42	1 42	1 42	1 43
4	311	1 22	-	1 21	1 22	1 21	1 22

4 2 6 2 IA Glass System .

Figs 4 43, 4 45 4 47, 4 49 and 4 51 represent the typical microstructure of glasses IA1, IA2, IA3, IA4 and IA5 respectively Corresponding SAD's are shown in figures 4 44, 4 46, 4 48, 4 50 and 4 52 respectively It is evident that IA glass system consists of two phases The darker phase (α) is the silver rich phase which shows broken interconnectivity The lighter phase (β) is interconnected through out the glass matrix and has less amount of silver The average width of α and β phases denoted by ω_α and ω_β are given in Table 4 12

The rings observed in SAD's of IA2, IA3, IA4 and IA5 confirm the presence of aluminium metal dispersion.Comparison of d_{hkl} values (ASTM) of aluminium with those calculated from SAD's of IA glass system is shown in Table 4 13

4 2 6 3 HIA Glass System

Figs 4 53, 4 55, 4 57, 4 59 and 4 61 give the representative microstructures of AIA1, AIA2, HIA3, HIA4 and HIA5 respectively while Figs 4 54, 4 56, 4 58, 4 60 and 4 62 are corresponding SAD's The rings in SAD's of HIA1, HIA2, HIA3, HIA4 and HIA5 have been analysed and summarised in Table 4 14 The calculated d_{hkl} values for these SAD's have been compared to d_{hkl} (ASTM) values corresponding to silver and aluminium metal As it is not possible to resolve the difference in d_{hkl} of silver and aluminium by SAD's the presence of faint rings in SAD of

Fig 4 33 TEM micrograph of glass A1

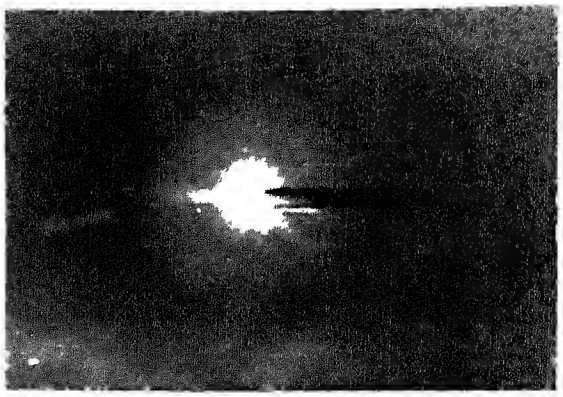

Fig 4 34

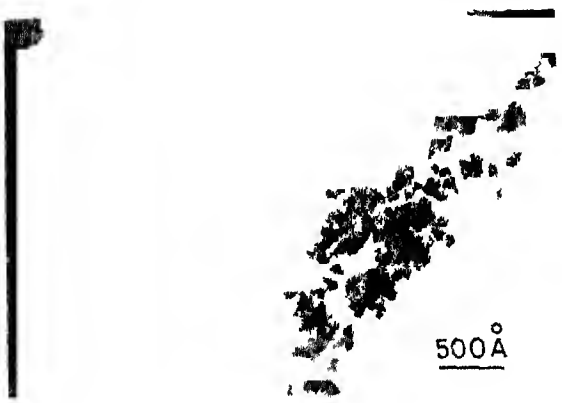

Fig 4 35 TEM micrograph of glass A2

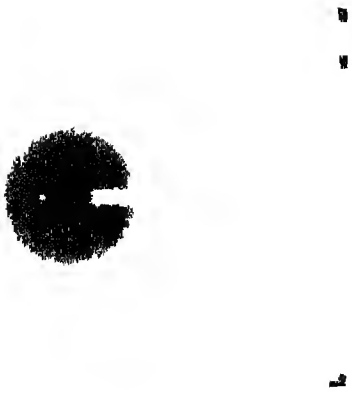

Fig 4 36 SAD of glass A2

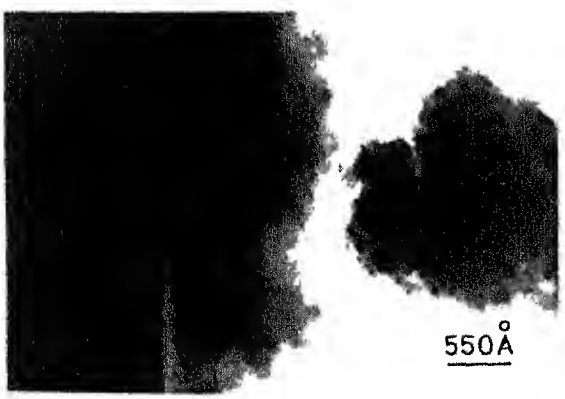

Fig 4 37 TEM micrograph of glass A3

Fig 4 38 SAD of glass A3

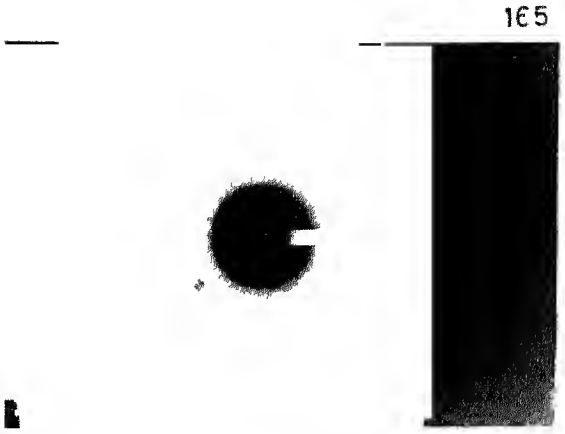

Fig 4 39 TEM micrograph of glass A4

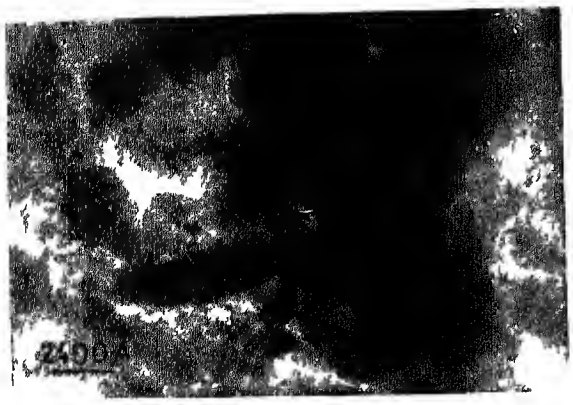

Fig 4 41 TEM micrograph of glass A5

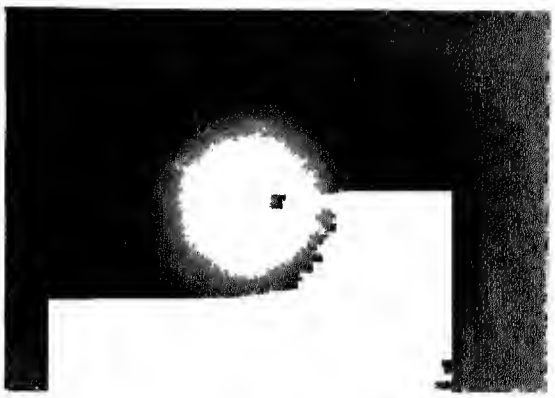

Fig 4 42 SAD of glass A5

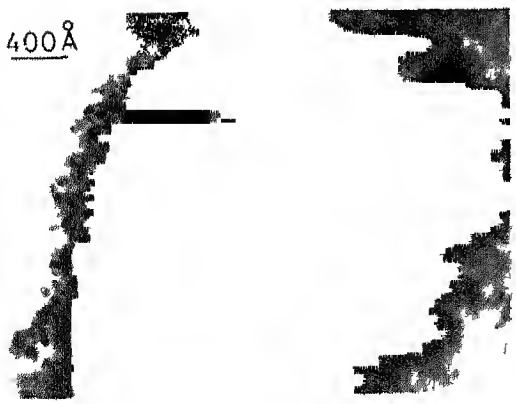

Fig 4 43 TEM micrograph of glass 1A1

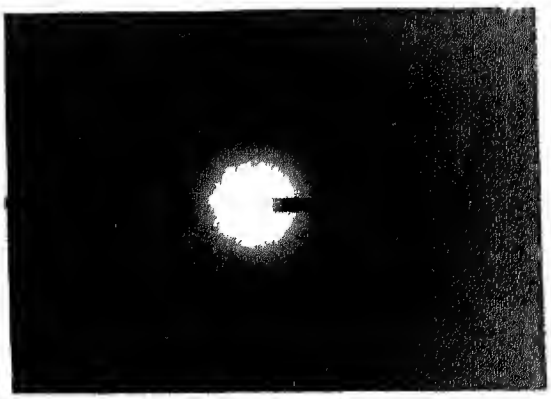

Fig 4 44 SAD of glass 1A1

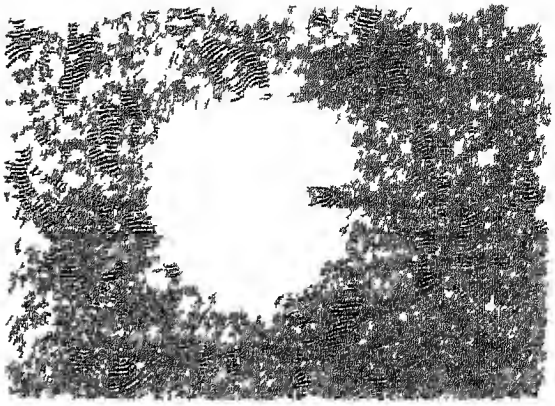

F 1 ⋅ 5(TEM micrograph of

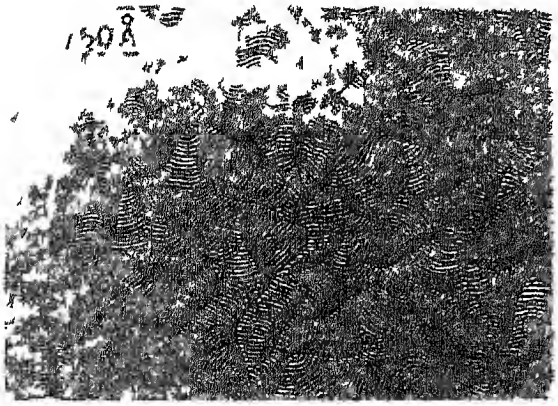

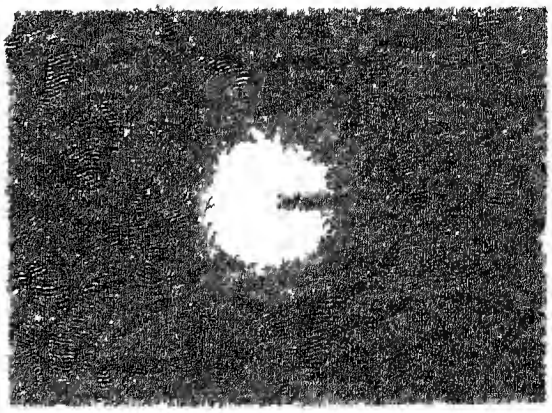

Fig 4 ⋅3 TEM micrograph of

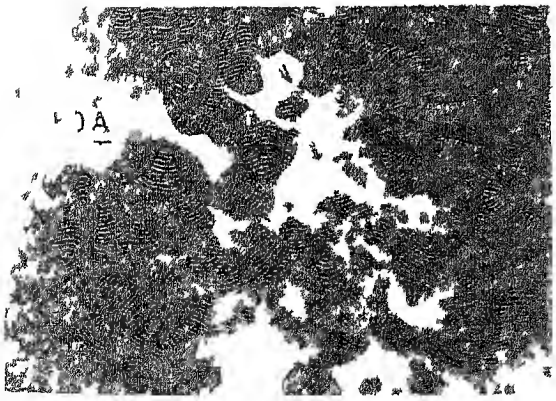

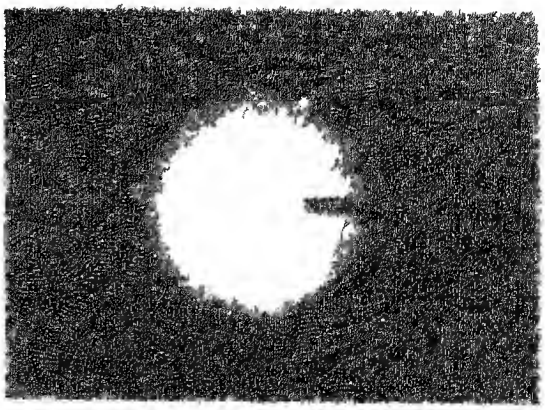

TEM micrograph of cla HtA Fi 4 ⋅ SA

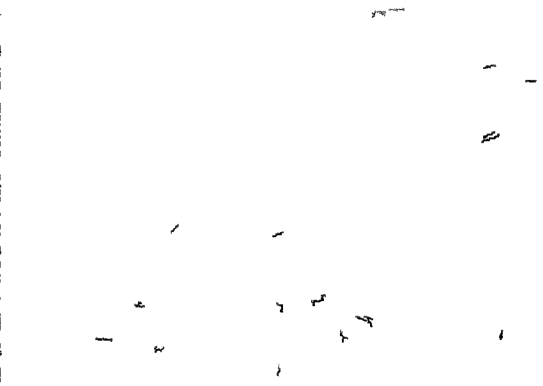

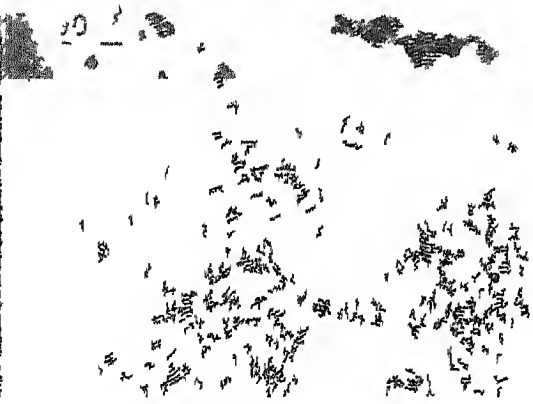

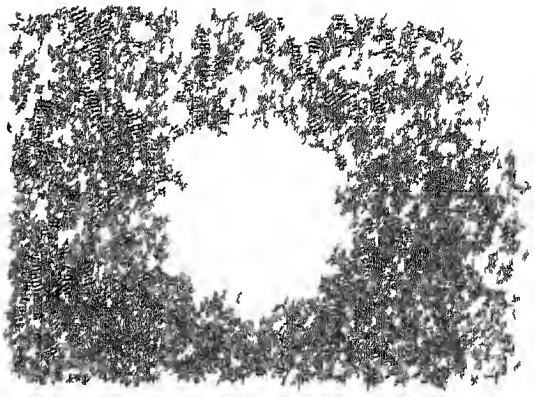

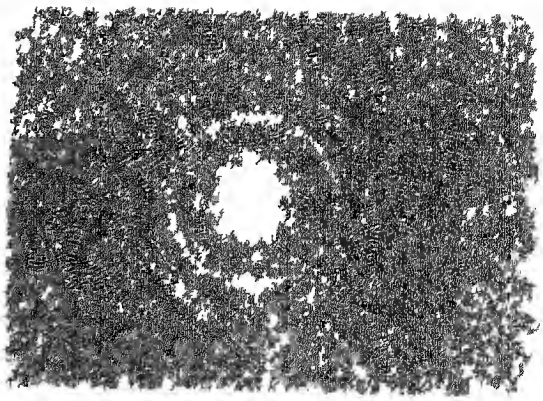

able 4 12 Widths of the interconnected phases in IA Glass system

Sl No	Glass	W_α (Å) (Phase with broken interconnectivity)	W_β (Å) (Interconnected Phase)	W_β / W_α
1	IA1	275	85	31
2	IA2	435	402	92
3	IA3	251	135	54
4	IA4	396	115	34
5	IA5	275	263	96

Table 4 13 Comparison of d_{hkl} values of aluminium with those obtained from SAD's of Glass System IA

Sl No	(hkl)	d_{hkl} (Al) (ASTM)	d_{hkl} (Calculated)				
			IA1	IA2	IA3	IA4	IA5
1	111	2 34	-	2 35	2 34	2 35	2 34
2	200	2 02	-	2 03	2 02	2 03	2 02
3	220	1 43	-	1 42	1 42	1 43	1 42
4	311	1 22	-	1 21	1 22	1 22	1 21

HI-1, imply that some silver ions are reduced to their atomic state

From the micrographs it is evident that the microstructure of HIA glass system is diphasic The darker regions containing high amount of silver denote the α phase while the lighter phase (β) has less amount of silver There are indications as shown by arrows in the micrographs as compared to microstructure of IA glass system that links have formed between the disjointed portions of the α phase so as to make a completely interconnected network of α phase Thus in HIA glass system both α and β phases are interconnected The average width (ω_α) and (ω_β) for α and β phases in HIA glass system are summarised in Table 4 15

4.3-Discussion

As seen from table 4 5, maximum value of Tg is for A_4 while minimum is for A_2 Small addition of aluminium powder (5%) in A_2, shows phase separation while A_1 with no aluminium is a single phased system Darker portions of micrograph for A2 correspond to aluminium rich phase It is most likely that openness of the microstructure which increases by the addition of small amount of aluminium as is the case with A_2 due to phase separation is responsible for lower value of Tg for A_2 as compared to that of A_1

Further addition of aluminium increases Tg as is evident for the compositions A_3, A_1 and A_5 This is explainable in

Table 4 14 Comparison of d_{hkl} values of aluminium and silver with those obtained from SAD's of Glass System HIA

Sl No	(hkl)	d_{hkl} (ASTM)		d_{hkl} (Calculated)				
		Ag	Al	HIA1	HIA2	HIA3	HIA4	HIA5
1	111	2 36	2 34	2 32	2 35	2 35	2 34	2 36
2	200	2 04	2 02	2 02	2 03	2 02	2 02	2 01
3	220	1 44	1 43	1 43	1 43	1 43	1 44	1 43
4	311	1 23	1 22	1 21	1 23	1 22	1 22	1 21

Table 4 15 Microstructural features of Glass System HIA

Sl No	Glass	W_α (Å)	W_β (Å)
1	HIA1	125	140
2	HIA2	169	502
3	HIA3	182	69
4	HIA4	357	415
5	HIA5	78	112

terms of an increase of alumina content in the glass due to oxidation of aluminium particles during glass melting and fiberisation process Aluminium, during melting of the glass is oxidised partially, thereby, increasing alumina content in the glass As alumina is a network former and its action in glass is that of stabilisation [Rawson 1984] due to its inclusion in silica network, the viscosity and Tg of these glasses are bound to be higher than that for A_1 or A_2 The anomalous increase of Tg for A_4 as compared to A_3 or A_5 may be understood in terms of their microstructural features Presence of larger aluminium particulates in A_4 as compared to A_3 and A_5 and lesser uniformity of distribution of the two phases are the most likely reasons for this variation of Tg

In case of A glass system for A_1 and A_2 in the entire temperature range of 20°C to 330 C, conduction is due to migration of sodium ions For A_3, A_4 and A_5, two mechanisms for conduction are operative In the temperature range of 20°C to 110°C, it is the electron-tunnelling between the aluminium islands dispersed in the glass matrix The activation energies of electron tunnelling as shown in Table 4 8 are of the same order as those , reported in the literature (Section 1 2 1 3) As evident from the equation (1 18) the activation energy for formation of a charged pair of grains is a function of the ratio s/d where, d is the particle diameter and s is the interparticle separation The variation of s/d reflecting morphological characteristics of A_3,

$_4$ and A_5, is manifest in the trend of Q_e as summarised in
able 4 8 The pre-exponential factor, too, reflects the same
echanism

For A_3, A_1 and A_5 in the temperature range of 110°C to
30 C, the mode of conduction is migration of sodium ions The
ctivation energies and pre-exponential factors for glass systems
, for ionic migration are summarised in Table 4 7 Highest
ctivation energy (Q_T) is 77eV for A1 while the minimum is 56 eV
or A_2 Further increase of Al concentration, increases the value
f Q_T as compared to that of A_2 This trend is similar as obtained
or Tg Phase separation of aluminium rich phase in A_2 helps to
educe the value of Q_T Both aluminium rich and aluminium deplected
hases will have sodium ions, it is most likely that both the
hases will be responsible for conduction in proportion to the
mount of sodium ions present within them The pre-exponential
actor for A_1 is three orders of magnitude less than that for A_2
his is ecpected due to change of charge carrier concentration(N_c)
nd average distance between adjacent sites (R) by phase separation
rom equation (3 9) such a change will give rise to the observed
rend of the pre-exponential factor The variation of activation
hergies and pre-exponential factors for A_3, A_4 and A_5 shows the
ole played by increasing amount of alumina due to partial
xidation of aluminium particles during glass melting

In IA glass system the conduction is due to migration of
ilver ions The IA glass system shows Q_T to lie in the range of

'6 eV to 56eV For IA_1, IA_2 and IA_3, activation energies are almost identical (50 eV) Q_T for IA_4 is maximum being equal to 56eV while that for IA_5 is minimum being equal to 46 eV The pre-exponential factor ρ_{01} varies in the range of 83 $x10^{-5}$ to 12 x 10^{-5} Ω CmK^{-1} The maximum value is for IA_5 while minimum for I_2 These features may be explained in terms of the two phase microstructure of IA glass system

In I' glass system the silver rich phase (α) has broken interconnectivity while β phase having less amount of silver is thoroughly interconnected Evidently β phase controls the electrical conductivity The variation of ρ_{0T} for A_1 and IA_1 implies that carrier concentration in β phase is about 3 % of that is the α phase, as explained in Section 3 3 for N_3 and IN3 glass system (N3,IN3 being identical to A_1 and IA_1 especti-vely) This implies absence of any drastic structural change brought about by the ion-exchange treatment

The comparison of ρ_{0T} values for A_2, A_3, A A 5 with those of IA_2, IA_3, IA_4, IA_5 respectively suggests that the presence of aluminium has a crucial effect on the average distance bet-ween adjacent sites (R) in ion exchanged samples The changes incurred in the values of R , are reflected in the variation of pre-exponential factors of these glasses The maximum effect is observed in case of IA_2 It is most likely that drastic structural changes take place during ion-exchange of A_2 and A5 samples to form IA_2 and IA_5 respectively

As ρ_{OT} values for IA_3 and IA_4 are almost identical to those for A_3 and A_4 respectively, it is inferred that ion-exchange does not change the relative distribution of carrier concentration in aluminium rich and aluminium depleted phases As is evident from table 4 12 $\frac{\omega_\beta}{\omega_\alpha} \leq 1$ for IA_2 and IA_5 while for IA_3 and IA_4 this ratio is < 5

As mentioned in section 4 2 5 2, under the influence of an optimum combination of E_c and T_c, IA glass system switches to form HIA glass system, characterised by very low activation energies as is evident from Table 4 10 It is remarkable that HIA_3 has almost zero activation energy Switching of IA to HIA glass system is a diffusion controlled phenomenon, continuous links are formed among the disjointed portions of α phase by diffusion of silver ions from α phase under the influence of E_c and T_c to β phase This interconnection of α phase induces high electrical conductivity to the glass system High mobility of silver ions and relatively open structure of α phase as compared to β phase are responsible for very low activation energy for the HIA glass system

Presence of aluminium particles have improved the conductivity of glass in its high conducting state. This may be explained on the basis of microstructural features brought about by the presence of aluminium particles As mentioned above, during melting of glasses, aluminium particles are partially oxidised to form alumina This alumina most likely forms a

ribbon type, three dimentional network and provides a continuous path for silver ions to move along it as alumina is four coordinated in the silica network [Doremus 1984]

E_c decreases with increasing T_c This is natural for any diffusion controlled phenomenon It is expected that electric field causes directional diffusion of silver ions from α' phase to β phase so as to form continuous links between disjointed portion of the α' phase as α' phase contains almost all (97%) of silver ions present, once these links are formed, the conductivity improves by many order of magnitude

From the present investigation it has been found that metal-glass microcomposites having aluminium as metal phase may be prepared by directly melting aluminium powder with the glass batch Glass fibres may be drawn from such microcomposites The presence of aluminium has a significant effect on the conductivity of base glass When added in smaller portion (5%) it lowers the activation energy of sodium ion migration and improves the conductivity When aluminium is present in more than 5 mol %, electron-tunnelling is the mechanism of charge conduction in the temperature range of 20°C to 110 C Above this temperature sodium ion migration is the major mode of conduction

It has been further established that after ion-exchanging of those glass fibres, a new set of microcomposites having high concentration of silver ions may be prepared By an

ɔtɪmum combɪnatɪon of E_c and σ_c a desɪred morphology ɪs created
ɪ the IA glass system to form HIA glɪss system resultɪng ɪn
tremely hɪgh values of conductɪvɪty The actɪvatɪon energy
ɪd conductɪvɪty values of IA and HIA glass systems compare well
th those FIC's as mentɪoned ɪn Table 1 5 Thus for the fɪrst
me ɔ new clɔss of FIC materɪɔl hɔs been prepɔred from ɔ glass-
tɔl mɪcrocomposɪte The most sɪgnɪfɪcɔnt result of the present
ɔrk ɪs thc feɔsɪbɪlɪtv of HI_3 wɪth ɔlmost negligɪble actɪvɔtɪon
ɪergy ɔnd e-tremely hɪgh conductɪvɪty of 3×10^{-1} (Ohm Cm).$^{-1}$
ɪe other bɔsɪc feɔtures of IA ɔnd HIA glɔss system ɔre thɔt
ɪey ɔre sɪlɪcɔ bɔsed ɔnd ɔre not dcrɪved from AgI The mɔxɪmum
ɪlue of totɔl sɪlvcr content ɪn these systems ɪs ɔbout 29 mol %
ɪly Becɔuse of theɪr unɪque feɔtures, IA ɔnd HIA glɔss systems
ve enormous potɔntɪɔl for futurɪstɪc ɔpplɪcɔtɪons ɪn enɔrgy
vɪces

CHAPTER - V

Mechanical Properties of Glass Fibres Containing Aluminium Particles

5 1 Introduction

Glass fibres are characterized by high strength and superior modulus values as compared to bulk glasses This unique combination of various mechanical properties makes them as a very useful group of strength giving materials The latter are used widely as structural composites in different military and civilian applications In case of optical fibres too, alongwith other specific optical properties, the strength of optical fibre is a critical parameter which ultimately decides its limitation for any practical application

The study of metal-glass composites has become very significant in recent years because of the technological importance of these materials [Abeles B et al 1975, Granqvist C G and Buhrman R A 1976] These composites have been developed through various techniques such as by r f sputtering a suitable composite metal-insulator target to a suitable substrate, ion-exchange followed by a reduction treatment [Chakravorty D 1974, Chakravorty D et al 1975], by melting an organo-metallic compound in the glass batch [Datta S and Chakravorty D , 1983] and by melting a suitable choice of mixtures of oxides [Chakravorty D et al 1977, Chakravorty et al 1979] In photosenstive glasses fine dispersions of gold and silver granules have been obtained by nucleation induced by UV irradiation followed by a suitable

heat treatment (Smithard M A and Dupreer 1972)

The mechanical properties of such composite systems have been found to be very promising Aluminium particulates have been shown to increase the strength of bulk glass 64 times while nickel reduces the strength (ristic V D et al 1981, Stephanie C Kunz 1983, Kristic V D and Nicholson P S 1983) mechanism for the toughening of brittle matrices with ductile particles has been proposed (Kristic V D 1983)

Various techniques have been developed for strengthening glasses (La Course 1972) This includes microcrack healing (Niederhorn 1970) etching of glass surface by HF (Ryabov and Kupfer 1970) or etching by steam (Ryabor et al 1972), peripheral clamping (Markov and Kopylov 1970), thermal tempering (Robert Gardon 1980) and chemical strengthening (R F Bartholomew and H M Garfinkel 1980)

The present investigations have been envisaged to incorporate metal particles in glass matrix in fibre form i e development of glass metal composite fibres As various metallic species have shown to improve the mechanical properties of the glasses in bulk form, it is interesting to know whether a similar trend persists when the micro-glass metal composites are drawn in the fibre form

5 2 Results

The composition and density of glasses which have been used in the present study are shown in Table 4 1 The initial

particle distribution of aluminium powder incorporated in the glass matrix has been given in Table 4 2 These glasses have been prepared as described in section 4 2 1 The fiberisation parameters of these glasses are included in Table 4 3 Both sets of glass fibres viz fibres collected in situ in the fibre drawing process, being referred to as virgin fibres and those collected from the drum, being referred to as non-virgin fibres have been used for mechanical characterisation Sets of virgin and non-virgin samples have been prepared as described in section 2 10 1

For testing of fibres on INSTRON, samples are prepared as described in section 2 10 2 Cross head speed has been adjusted to 0·5Cm/minute Diameter of fibres have been measured by Accutron (section 2 9) an electronic comparator Load cell for measuring load on the fibres has a range of 0-50 gms Five sets of glass fibres have been used for the present study It includes a set of virgin fibre samples of glasses A1, A2 and A4 and another set of non virgin fibres of glasses A1 and A2 The chart speed has been fixed to 10 Cm/minute

5 2 1 Strength(S) strain(e) and young modulus (E) of virgin and non-virgin glass fibres

Observed strength (S_i) for ith specimen is calculated by equation (2 22) while strain by equation (2 24) The load (P_i) and extension (x_i) corresponding to fracture are determined by x-y chart recorder attached to INSTRON such that y axis, calibrated to load, and connected to the load cell provides value of Pi while x-axis monitoring displacement by cross head movement gives values of x_i

For each measurement, youngs modulus has been calculated by equation (2 25) and in a given set of such measurements, wide scatter in the values of E_1 are found and youngs' modulus for a given glass fibre is obtained by the average of such E_1's as given by equation (? 26) As proposed in section 2 10 2, a better estimate of young s modulus is obtained by regression of stress versus strain by a straight line passing through origin Figures 5 1, 5 2 and 5 3 show this regression analysis for virgin glass fibres A1, A2 and A4 respectively Non-virgin sample set of A1 and A2 have been similarly analysed in figures 5 4 and 5 5 respectively The values of E_R The estimator of young's modulus as obtained by regression analysis and $\bar{E}$, the estimator of young's modulus as obtained by equation (2 26) are summarised in Table 5 1 Prefixes of V and NV are being used to denote virgin and non-virgin state of fibres $d\bar{E}$ and dE_R denote the variance of $\bar{E}$ and E_R and are measure of scatter

The observed diameters (D) of fibres in each set show a distribution Figures 5 6, 5 8, 5 10, 5 12 and 5 14 represent the histograms of observed diameters of VA1, VA2, VA4, NVA1 and NVA2 respectively The observed strength(S) as calculated by equation (2 22) for each set has been plotted as histogram so as to represent distribution of strength values Figures 5 16, 5 18, 5 20, 5 22 and 5 24 exhibit the histograms of observed strength(S) for VA1, VA2, VA3, NVA1 and NVA2 respectively

Corresponding to each set of observed strength(S) values, another set of strength, referred to as calculated

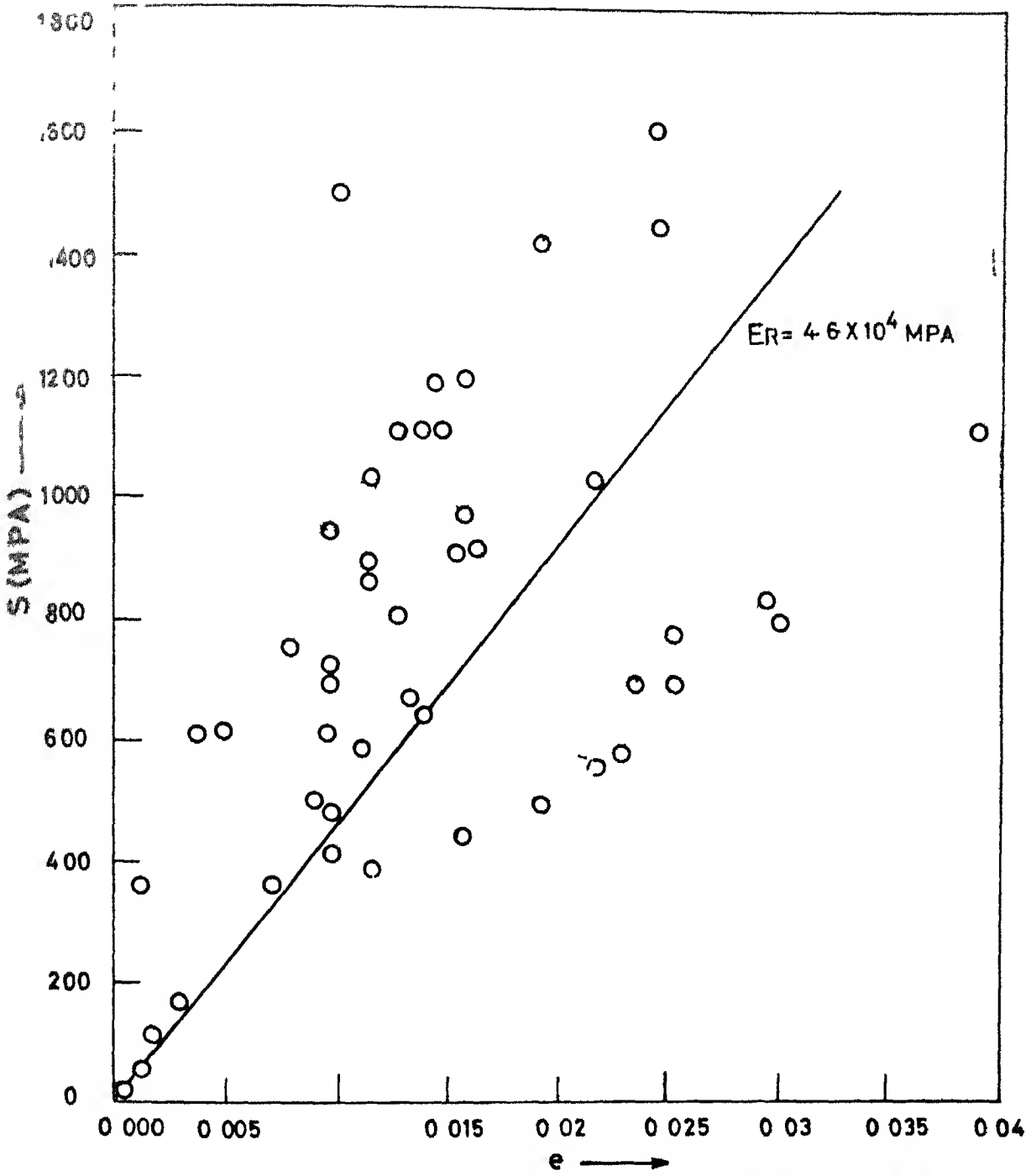

Fig 5 1 Regression of strength(S) with strain(e) for virgin glass-fibres (A1)

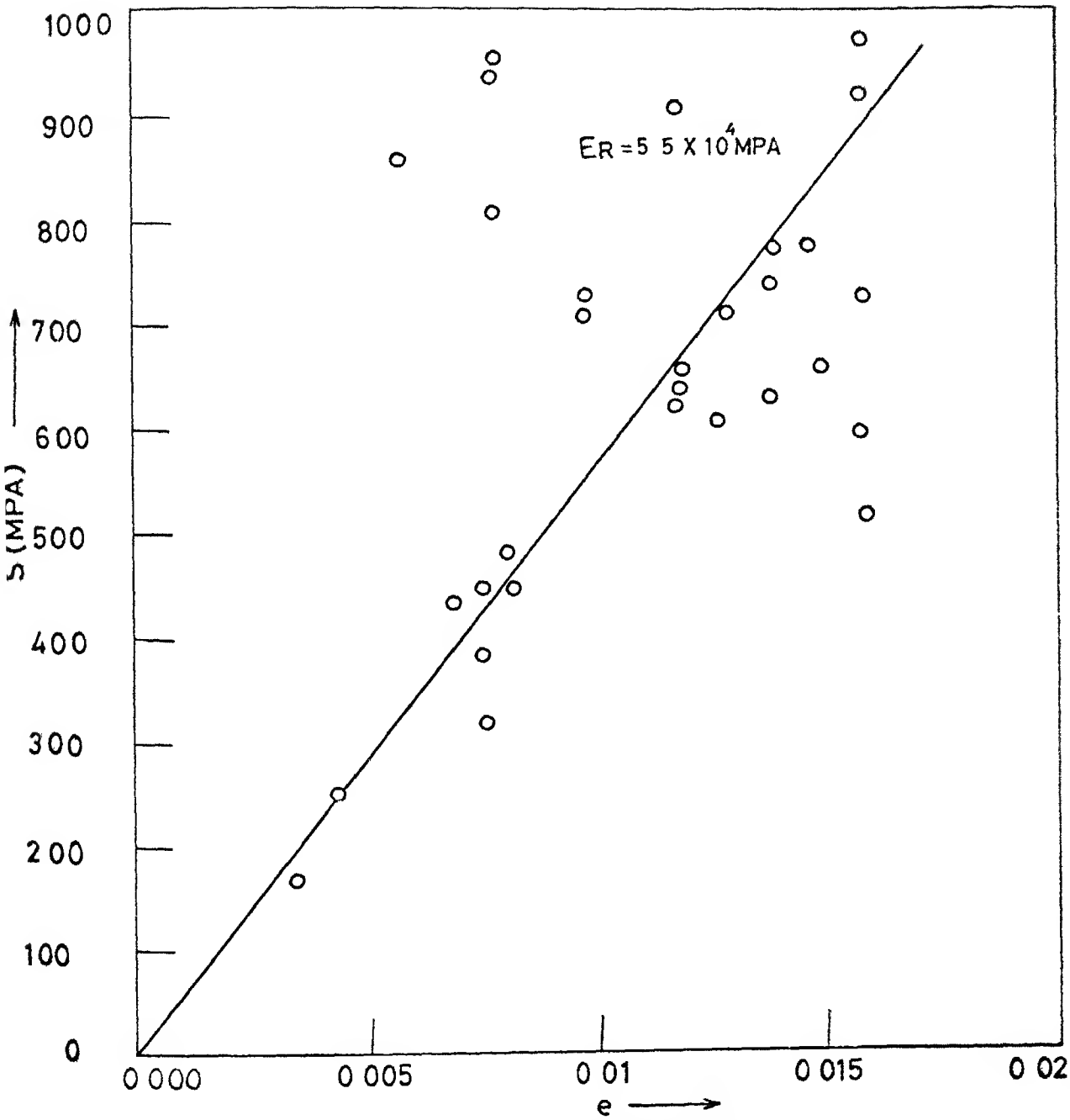

Fig 5 2 Regression of strength (S) with strain (e) for virgin glass fibres (A2)

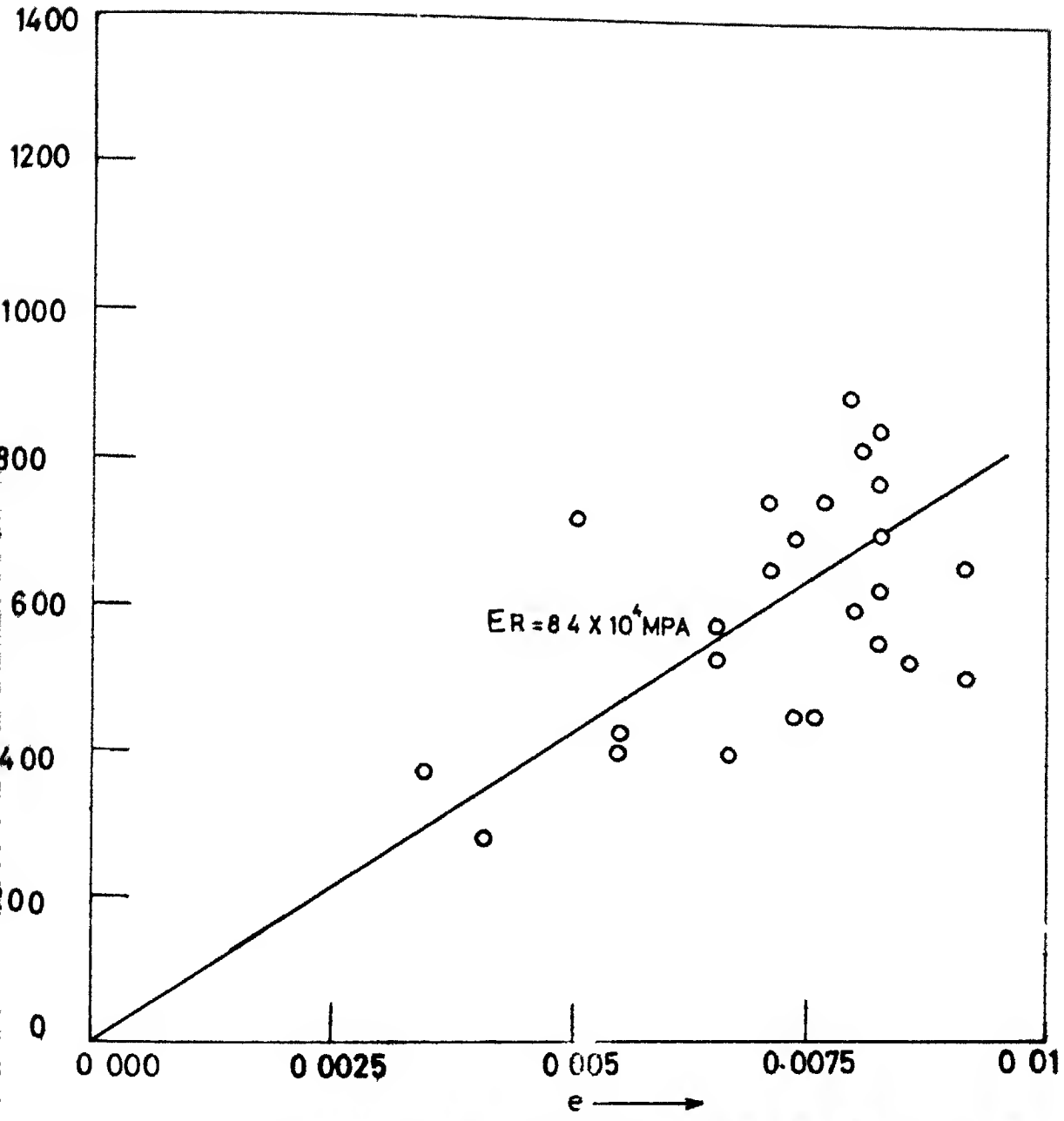

Fig 5 3 Regression of strength (S) with strain (e) for virgin glass fibres (A 4)

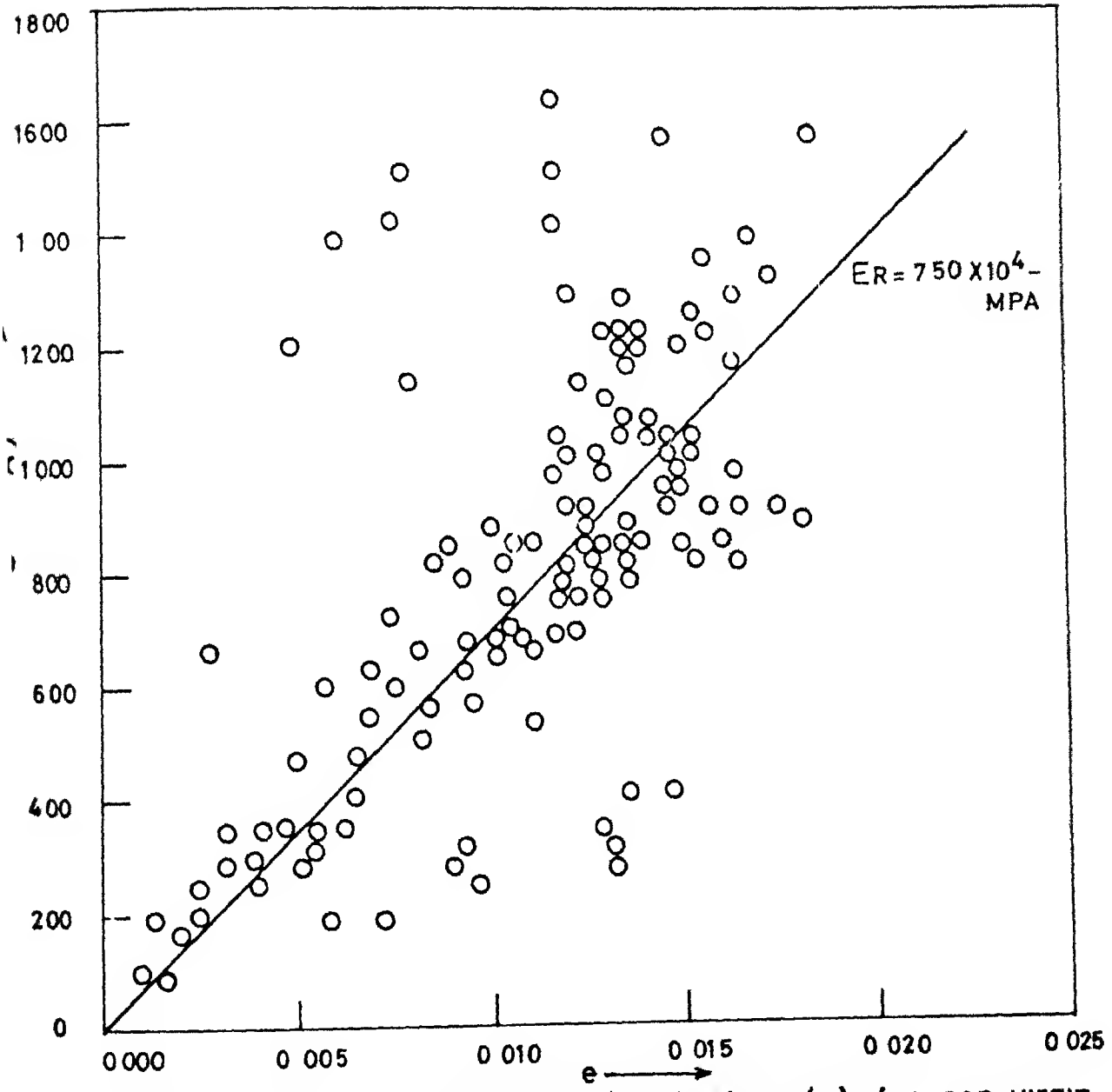

Fig 5 4Regression of strength(S) with strain(e) for non-virgin glass fibres(A1)

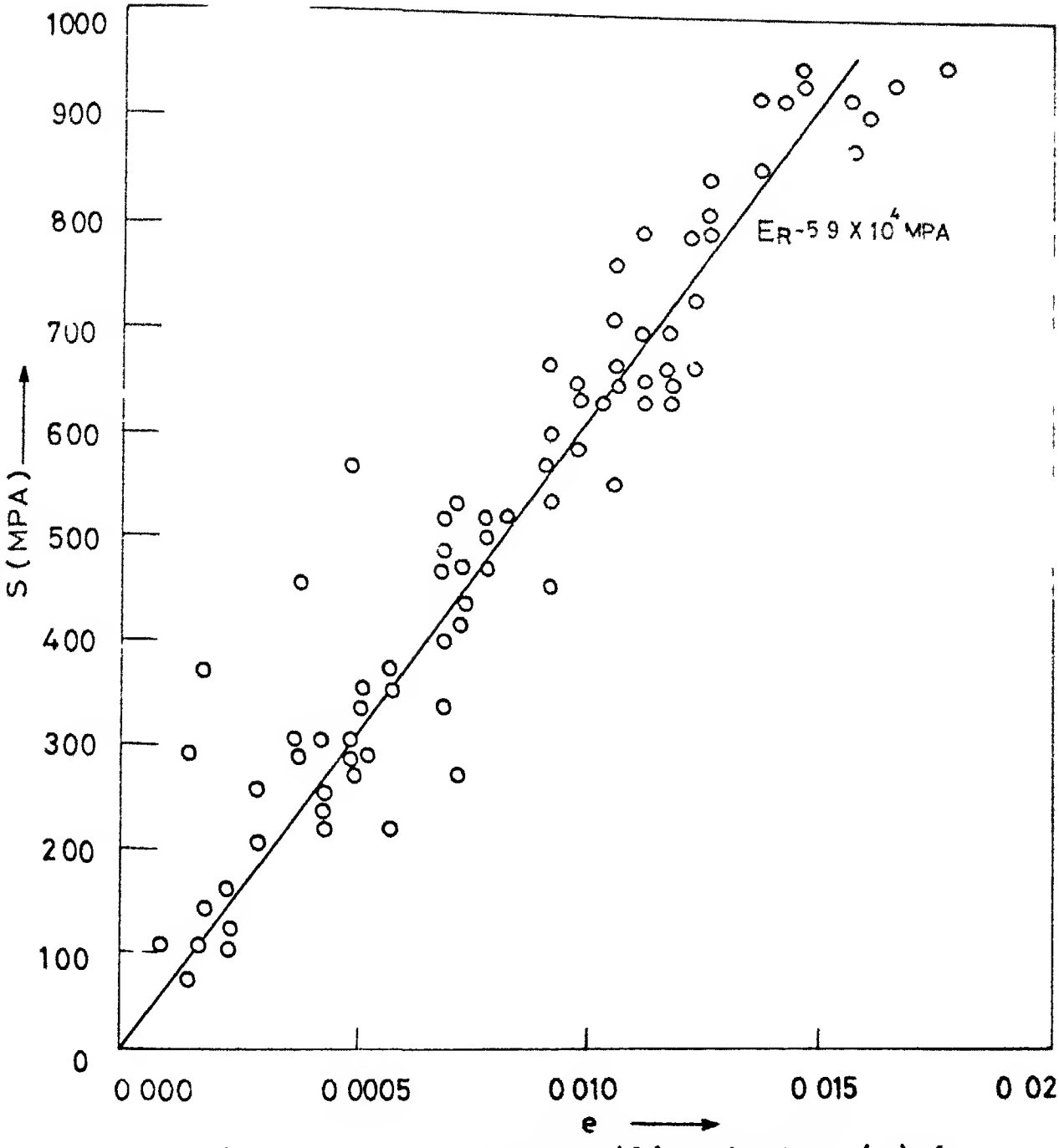

Fig 5 5 Regression of strength (S) with strain (e) for non virgin glass fibres (A2)

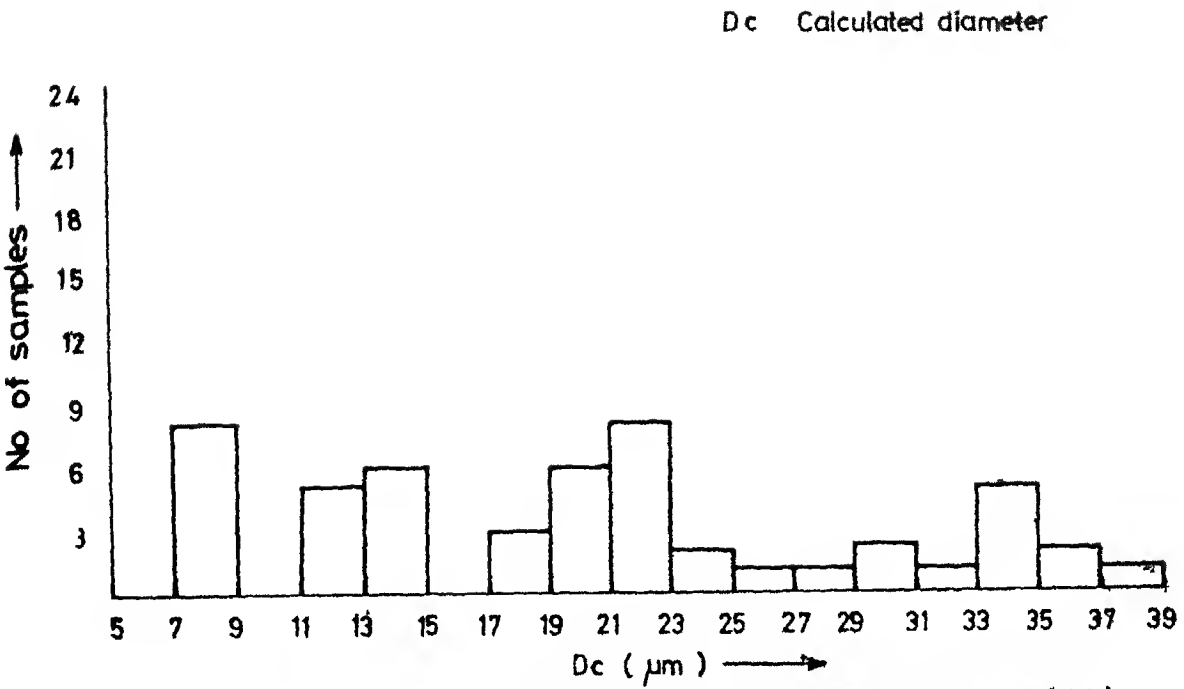

Fig 5 7 Diameter histogram for virgin glass fibres (A1)

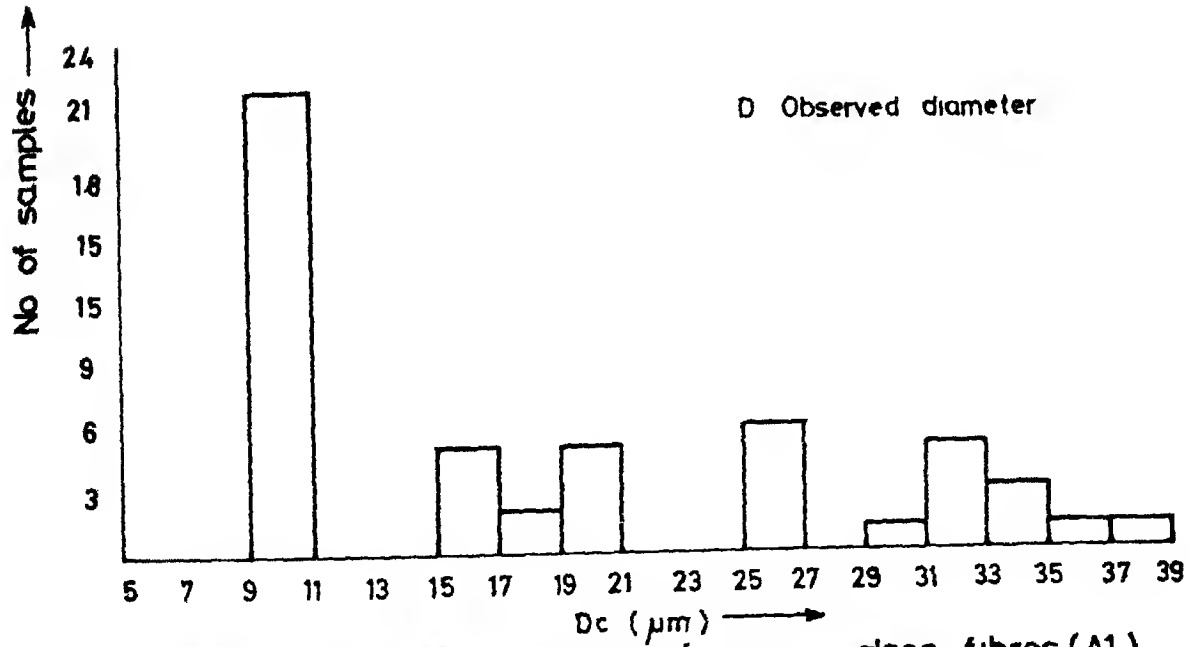

Fig 5 6 Diameter histogram for virgin glass fibres (A1)

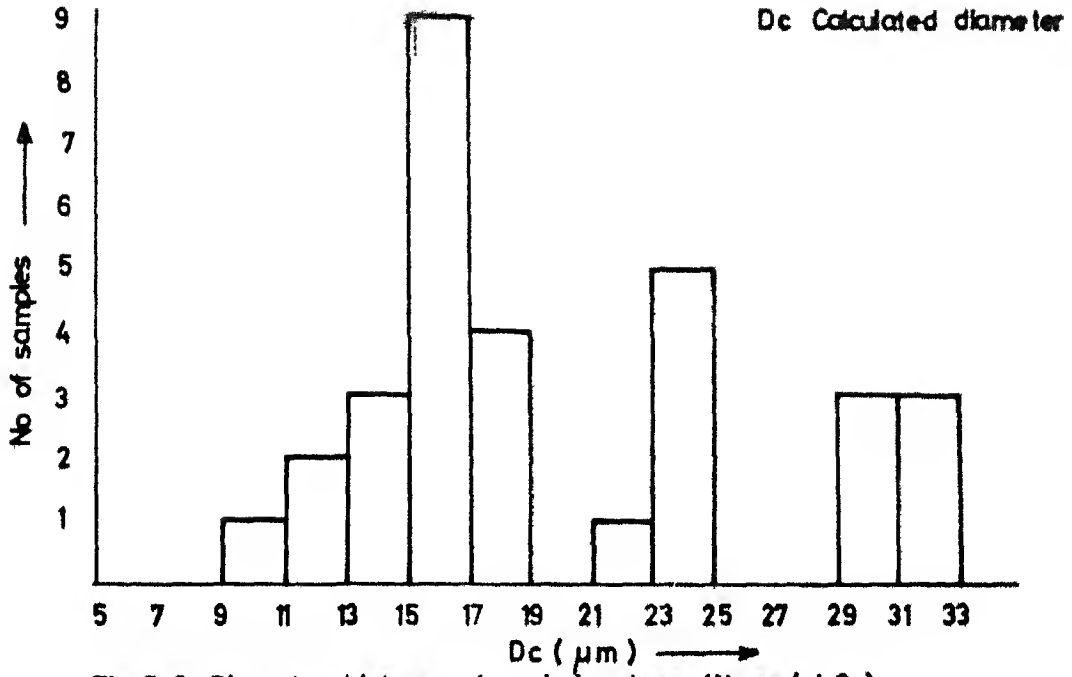

Fig 5 9 Diameter histogram for virgin glass fibres (A 2)

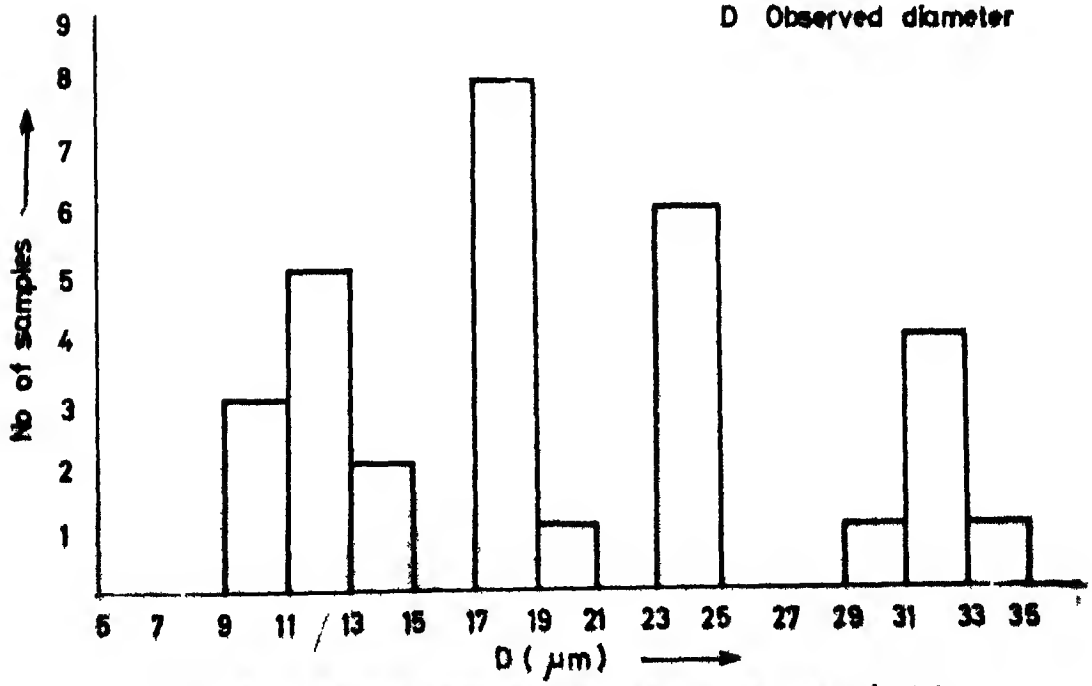

Fig 5 8 Diameter histogram for virgin glass fibres(A 2)

Dc Calculated diameter

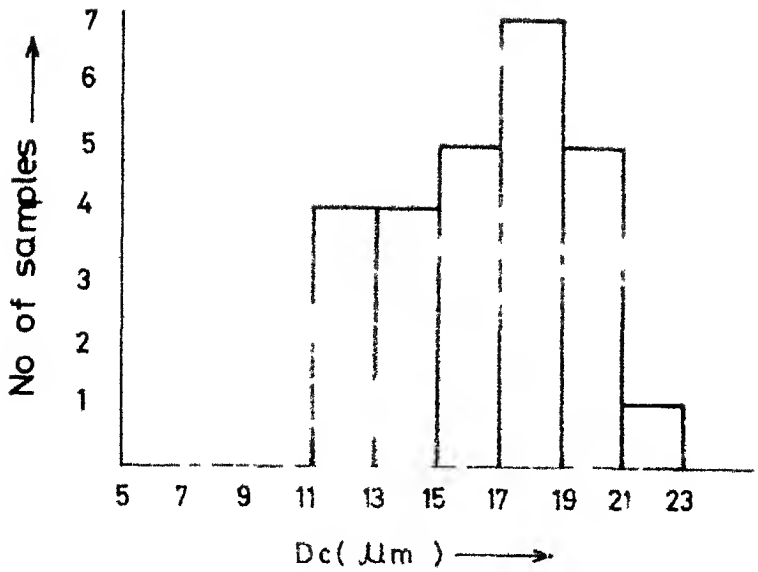

Fig 5.11 Diameter histogram for virgin glass fibres (A4)

D Observed diameter

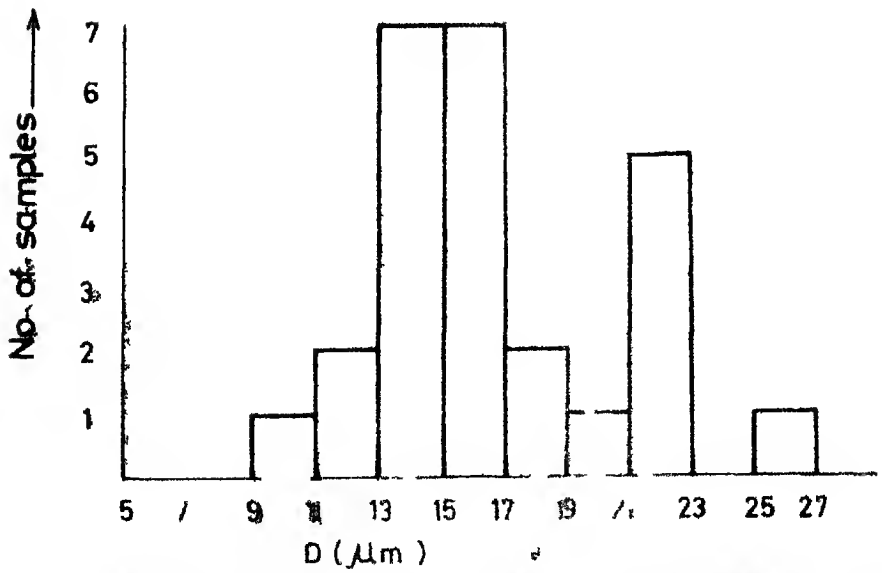

Fig 5.10 Diameter distribution for virgin glass fibres (A4)

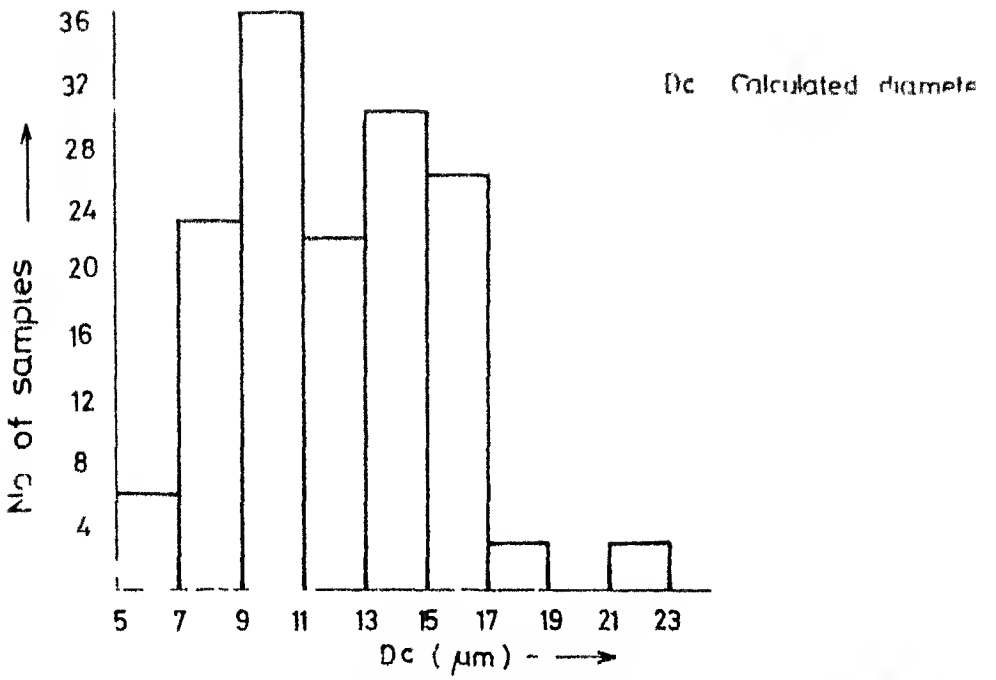

Fig 513 Diameter histogram for non-virgin glass fibres (A1)

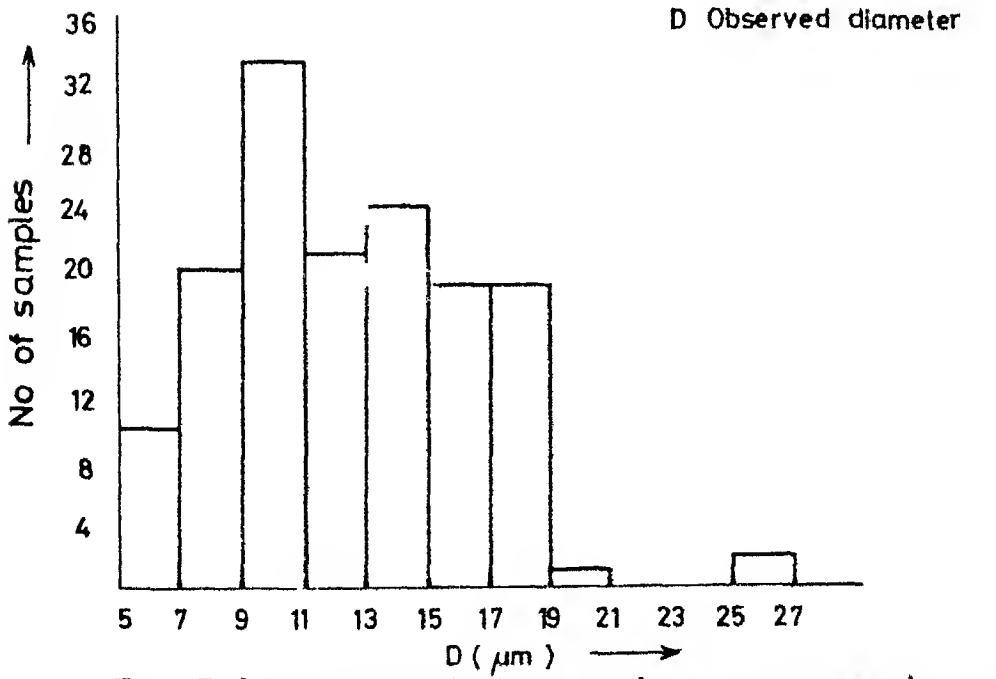

Fig 512 Diameter histogram for non-virgin glass fibres (A1)

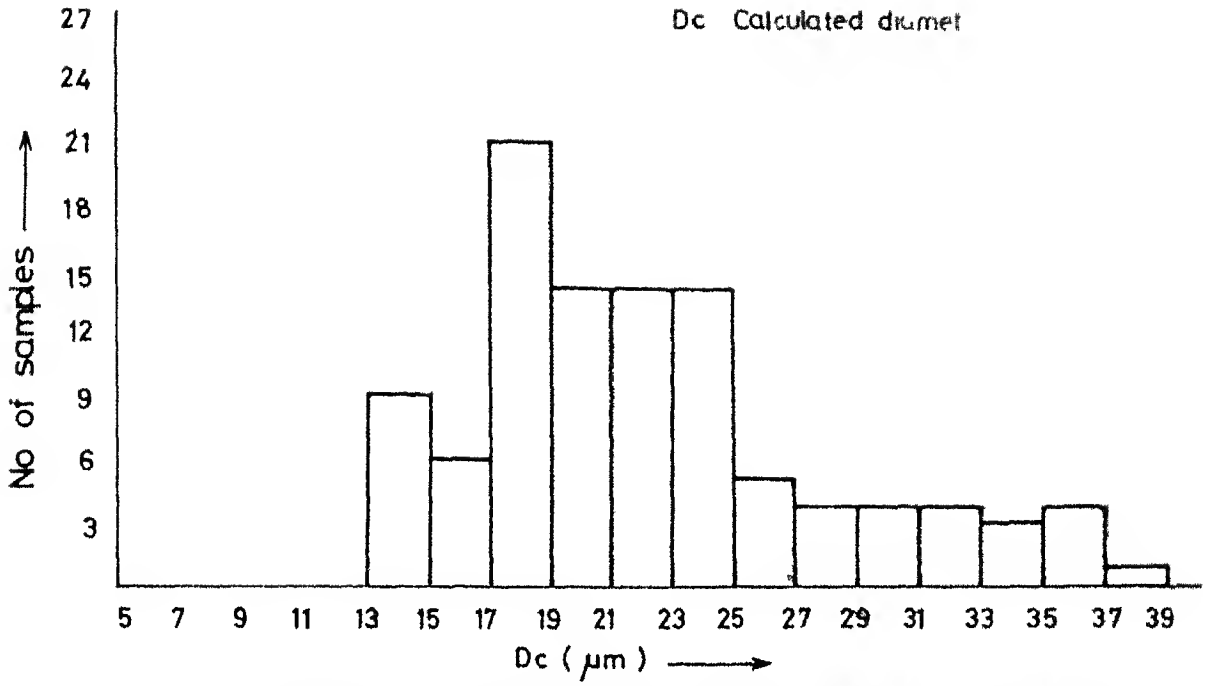

Fig 5 15 Diameter histogram for non-virgin glass fibres(A 2)

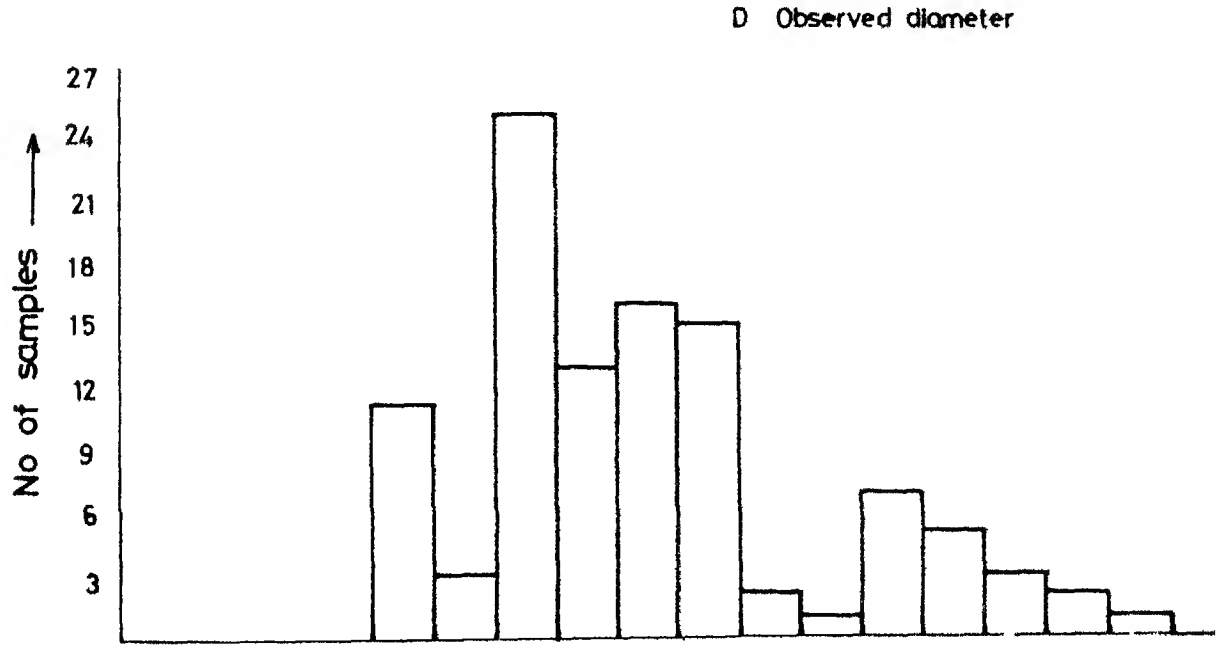

Fig 5 14 Diameter histogram for non-virgin glass fibres (A2)

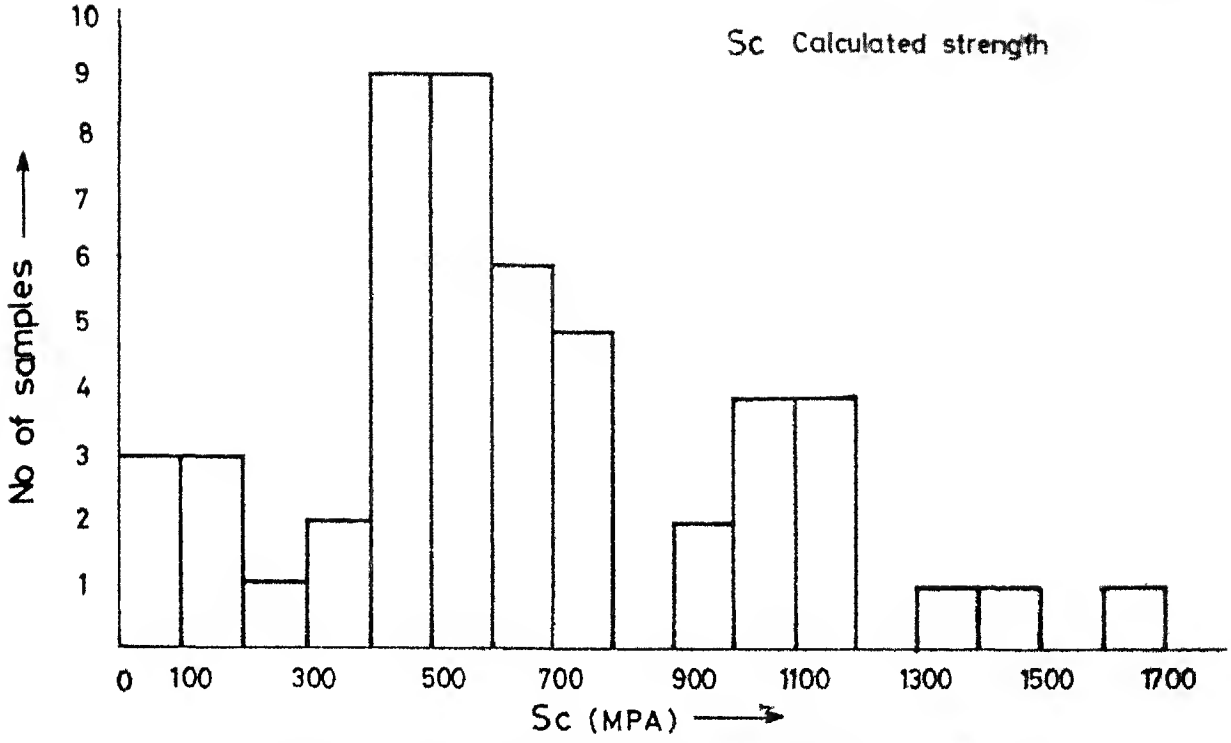

Fig 517 Strength histogram for virgin glass fibres (A1)

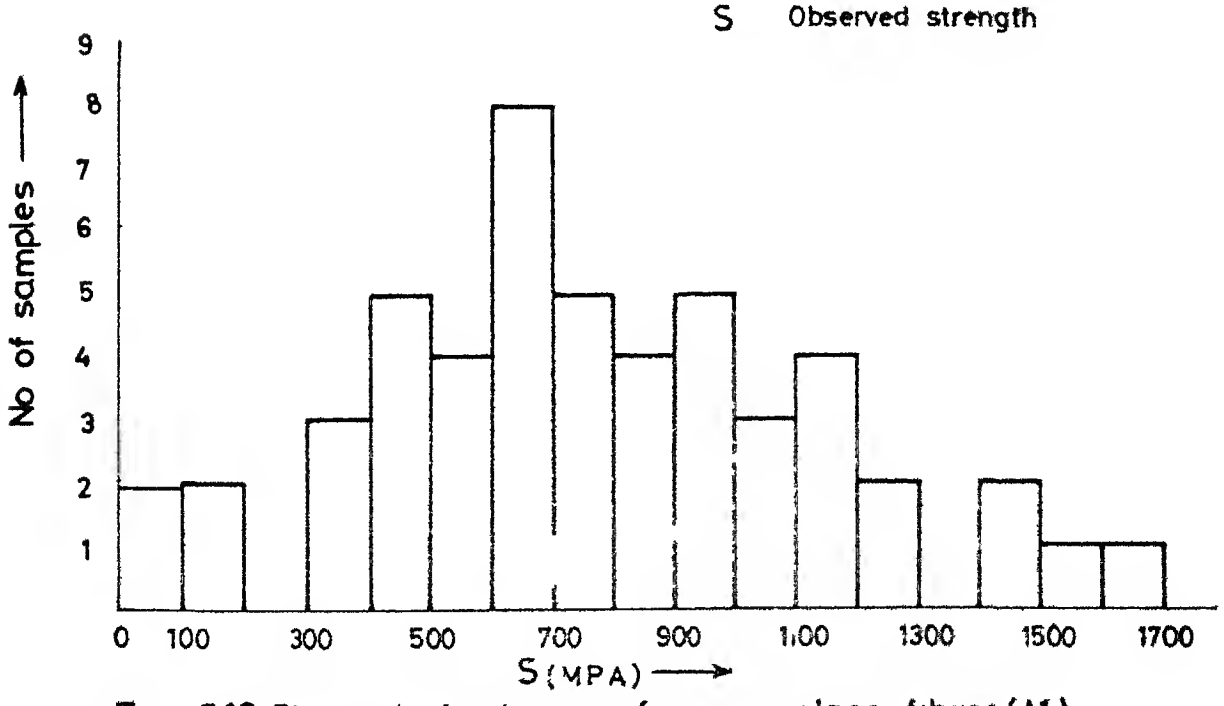

Fig 516 Strenc h histogram for virgin glass fibres (A1)

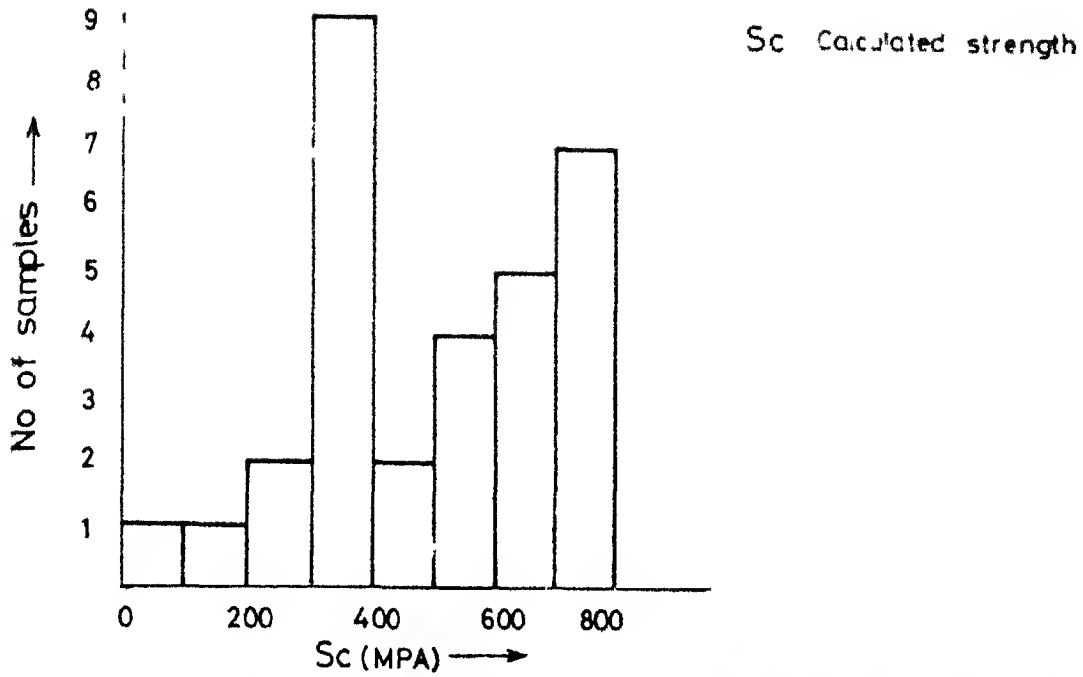

Fig 519 Strength histogram for virgin glass fibres (A2)

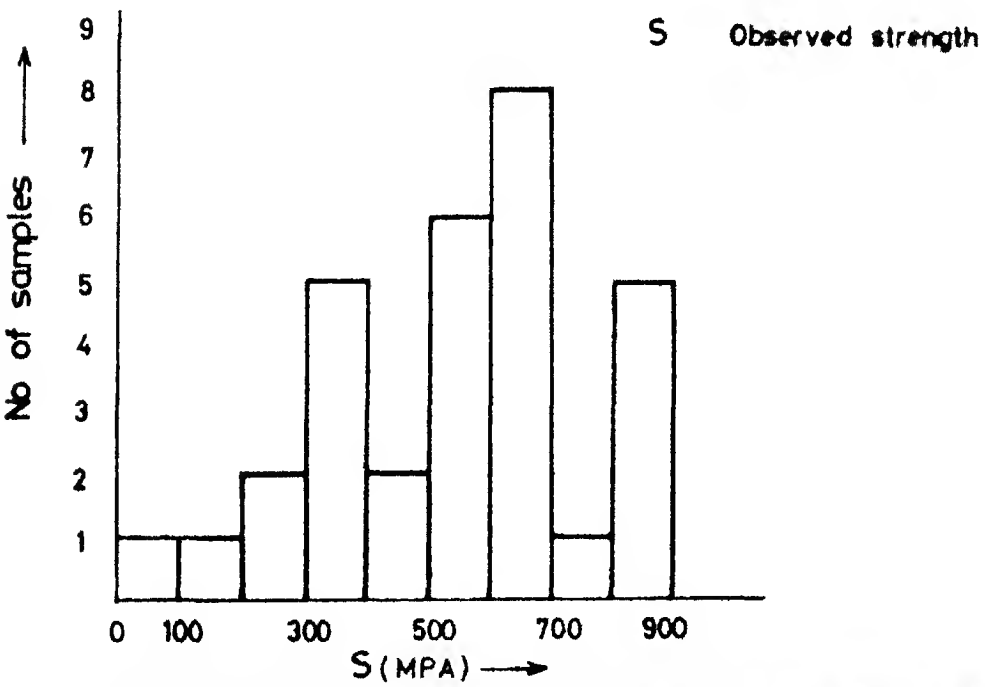

Fig 518 Strength histogram for virgin glass fibres (A2)

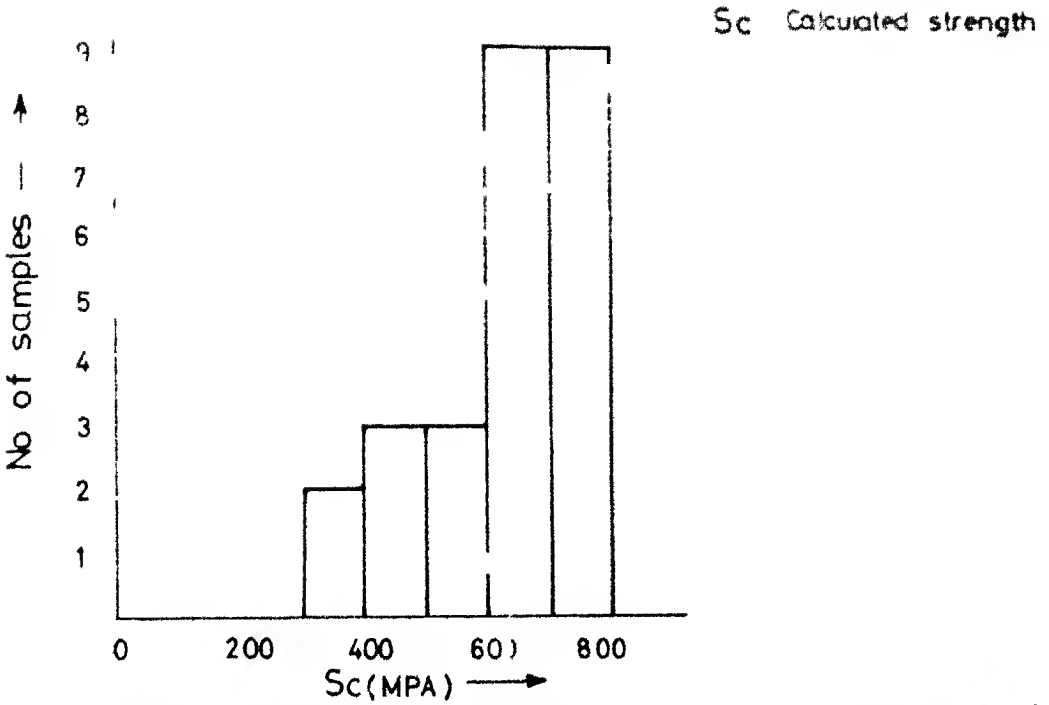

Fig 5 21 Strength histogram for virgin glass fibres (A 4)

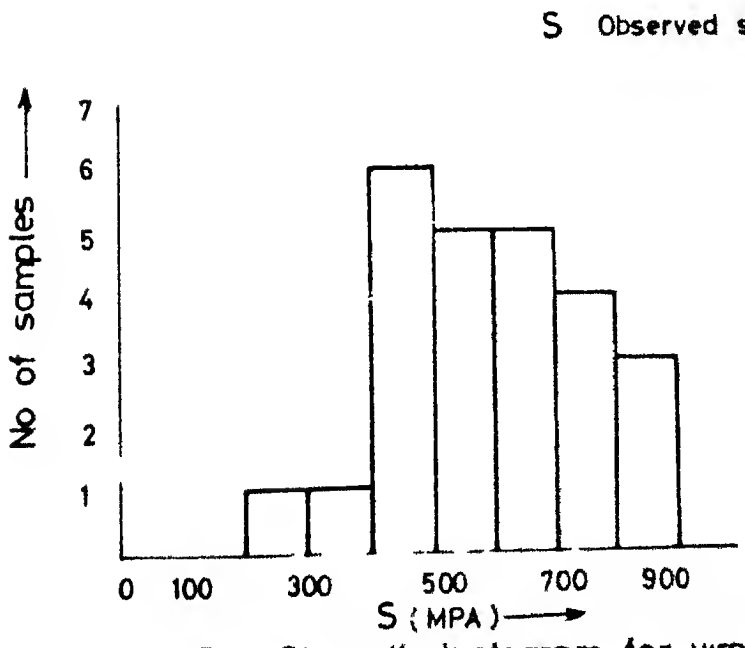

Fig 5 20 Strength histogram for virgin glass fibres (A4)

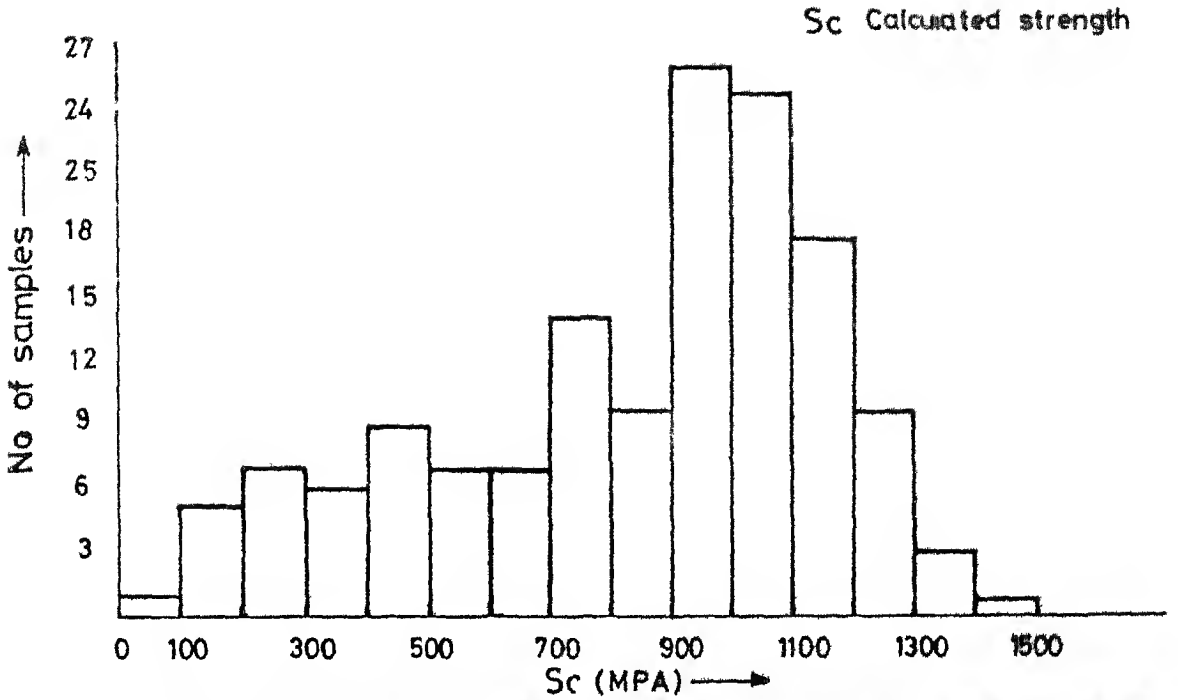

Fig 5 23 Strength histogram for non-virgin glass fibres (A1)

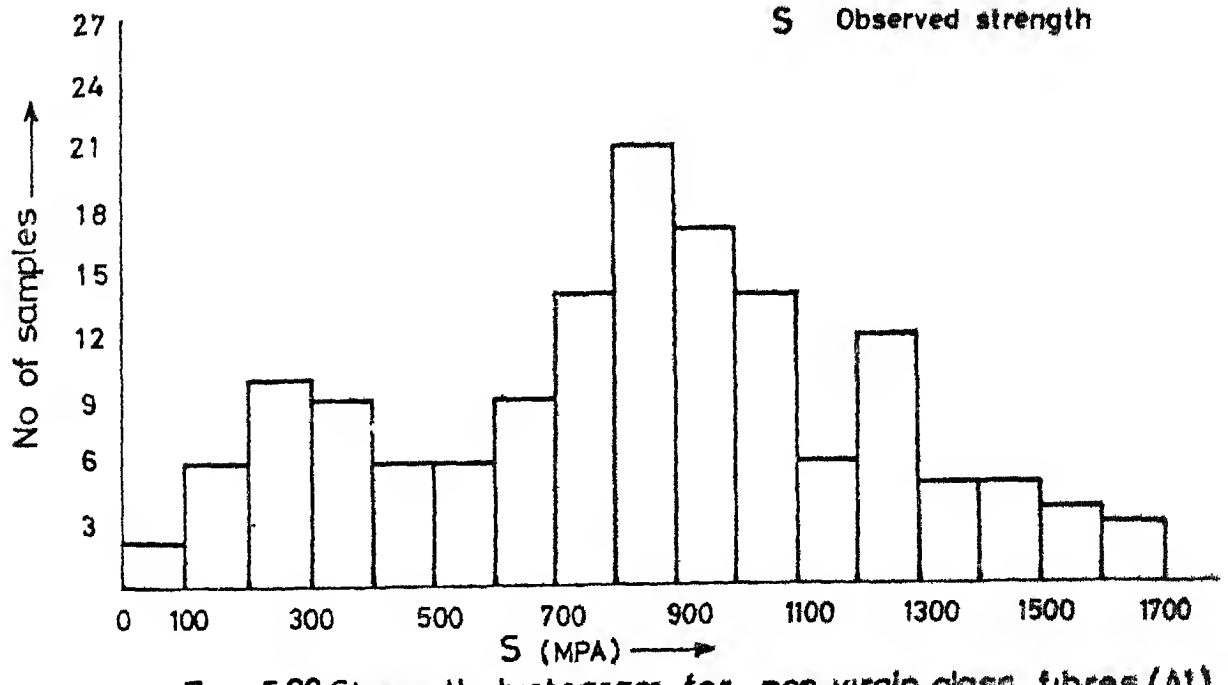

Fig 5 22 Strength histogram for non-virgin glass fibres (A1)

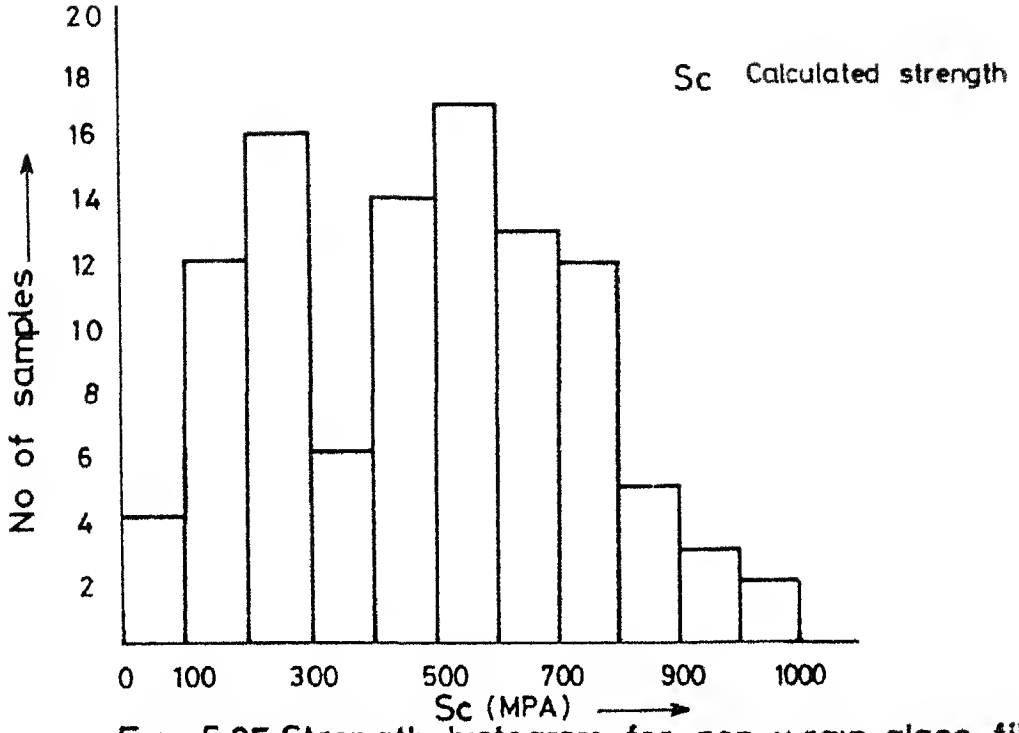

Fig 5 25 Strength histogram for non-v rgin glass fibres (A2)

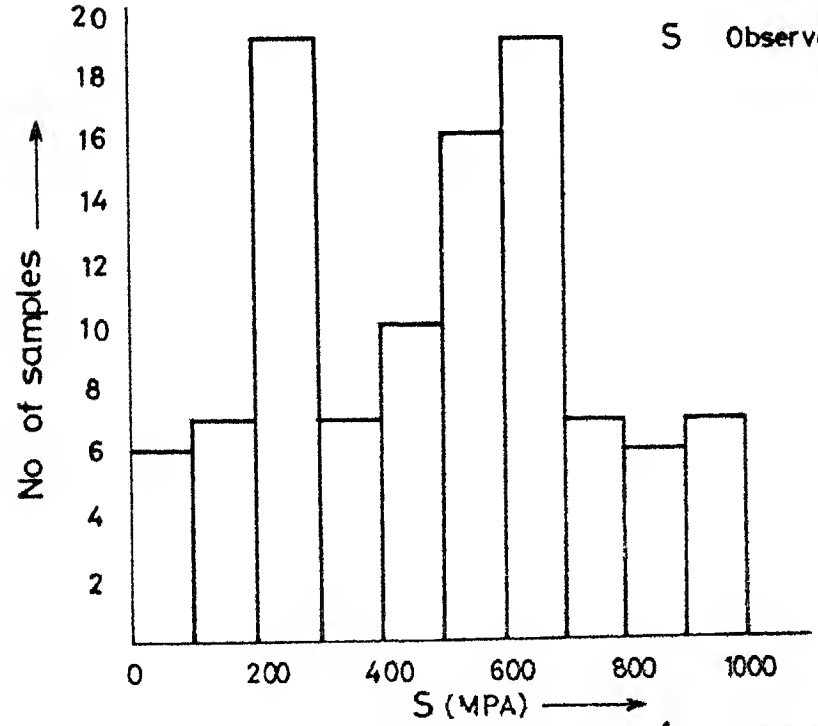

Fig 5 24 Strength histogram for non-virgin glass fibres (A2)

strength (S_c) may be obtained by equation (5 1 by using equation (2 27)

$$S_{c_1} = E_R \; e_1 \qquad (5\ 1)$$

where Sc_1 is the calculated strength for ith specimen in a given set which is characterised by young modulus E_R, as obtained by regression of stress versus strain and e_1 is the strain for that specimen Figures 5 17, 5 19, 5 21, 5 23 and 5 25 show the histograms of Sc for VA1, VA2, VA4, NVA1, NVA2 respectively Significance of S_c will be discussed in section 5 2 Corresponding to each set of Sc, a new set of calculated diameters, hereby referred as D_c is generated by equation (5 2)

$$D_{c_1} = D_1 \sqrt{\frac{S_1}{S_{c_1}}} \qquad (5\ 2)$$

where ith subscript denotes values corresponding to ith sample for a given set

The implications of set of D_c will be discussed in section 5 3 Figures 5 7, 5 9, 5 11, 5 13 and 5 15 represent the histograms of calculated diameters D_c for VA1, VA2, VA4, NVA1 and NVA2 respectively

5 2 2 Strength and Weibull Parameters

As described in section 1 1 2 2, strength of glass fibres is dictated by the flaws present on the surface of glass fibres

The flaw size has a distribution represented by weibull's distribution as given by equation (1 3) The scaling parameter S_o and shape parameter b of this distribution, corresponding to a given set of strength data are obtained by graphical regression technique (GRE) (section 2 10 6 1) and MLE technique (section 2 10 6 2) Figures 5 26, 5 28, 5 30, 5 32 and 5 34 represent regression analysis for weibull s parameters for observed strength(s) corresponding to VA1, VA2, VA4, NVA1, and NVA2 respectively Similar analysis for calculated strength (S_c) for VA1, VA2, VA4, NVA1 and NVA2 have been given in figures 5 27, 5 29, 5 31, 5 33 and 5 35 respectively Table 5 2 summarises the values of weibull's parameters corresponding to observed strength(s) and calculated strength S_c for virgin and non-virgin samples

Table 5 3 summarises the results of weibull analysis by MLE Technique The analysis has been performed for both observed strength S and Calculated strength S_c

Comparison of weibull's distribution as obtained by regression technique and MLE technique with the experimental data has been shown in figures 5 36, 5 38, 5 40, 5 42 and 5 44 for VA1, VA2, VA4, NVA1 and NVA2 respectively Similar comparison of weibull's distributions corresponding to calculated strength S_c has been given in figures 5 37, 5 39, 5 41, 5 43 and 5 45 for VA1, VA2, VA4, NVA1 and NVA2 respectively

Relative variation of failure probability P with S and S_c for virgin and non-virgin samples as evaluated by regression

Table 5 1 Young's modulus estimators for virgin and non-virgin glass fibres.

Sl.No	Set	$\bar{E}$ (MPa)	$d\bar{F}$(MPa)	$\bar{F}_R$ (MPa)	DE_R (MPa)
1	VA1	$2\ 95 \times 10^4$	$1\ 38 \times 10^4$	$4\ 58 \times 10^4$	$2\ 28 \times 10^4$
2	VA2	$2\ 45 \times 10^4$	$0\ 81 \times 10^4$	$5\ 52 \times 10^4$	$1\ 82 \times 10^4$
3	VA4	$2\ 37 \times 10^4$	$0\ 82 \times 10^4$	$8\ 36 \times 10^4$	$2\ 31 \times 10^4$
4	NVA1	$3\ 34 \times 10^4$	$1\ 82 \times 10^4$	$7\ 48 \times 10^4$	$3\ 36 \times 10^4$
5	NVA2	$1\ 90 \times 10^4$	$0\ 96 \times 10^4$	$5\ 92 \times 10^4$	$0\ 74 \times 10^4$

Table 5.2 Weibull's parameters by GRE Technique

Sl.No	Set	S		S_c	
		b	S_o(MPa)	b	S_o(MPa)
1	VA1	1 69	892	1 55	734
2	VA2	2 94	719	3 02	666
3	VA4	3 50	681	4 65	666
4	NVA1	2 04	953	2 29	897
	NVA2	1 82	562	1 92	526

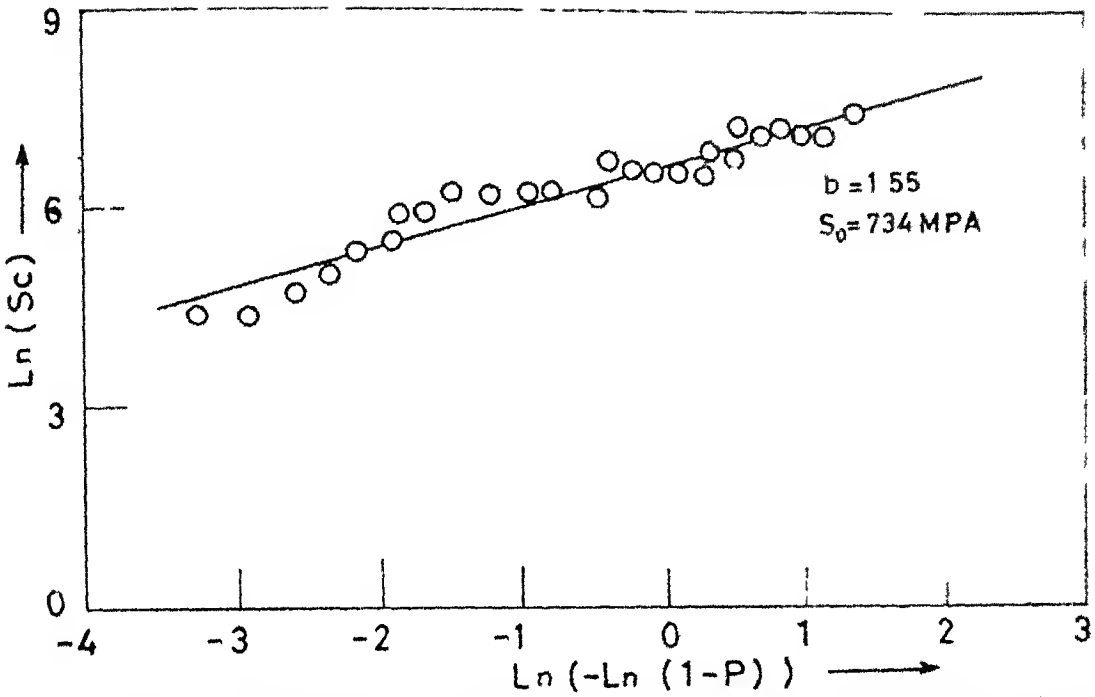

Fig 5 27 Regression analysis of calculated strength (Sc) with failure probability (P) for virgin glass fibres (A1)

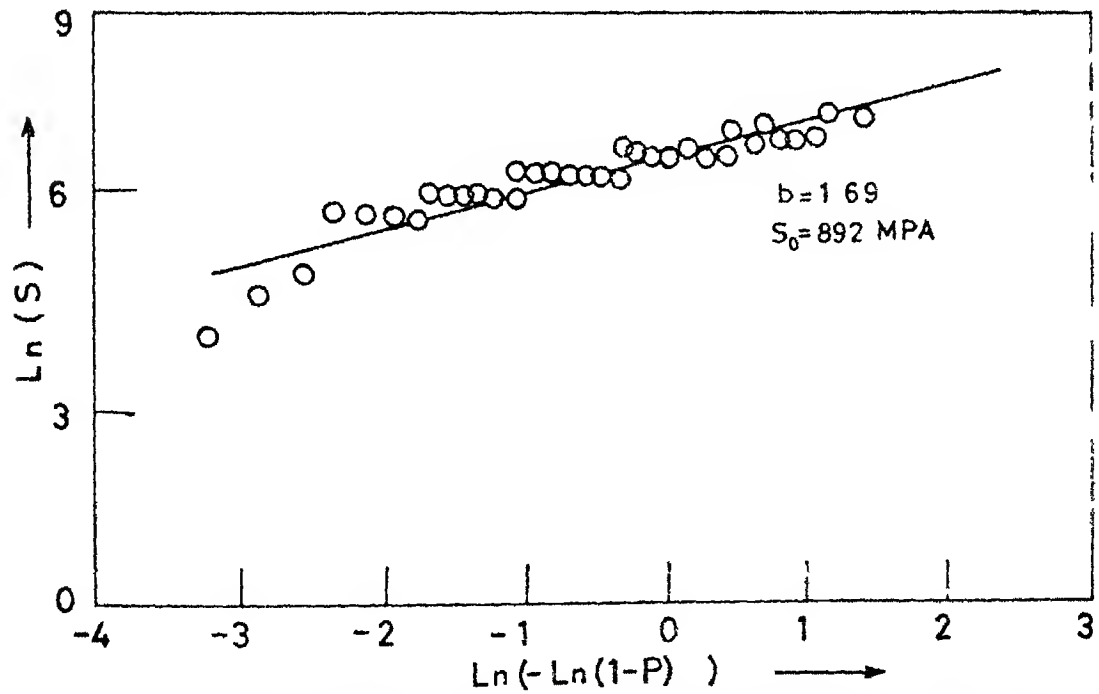

Fig 5 26 Regression analysis of observed strength (S) with failure probability (P) for virgin glass fibres (A1)

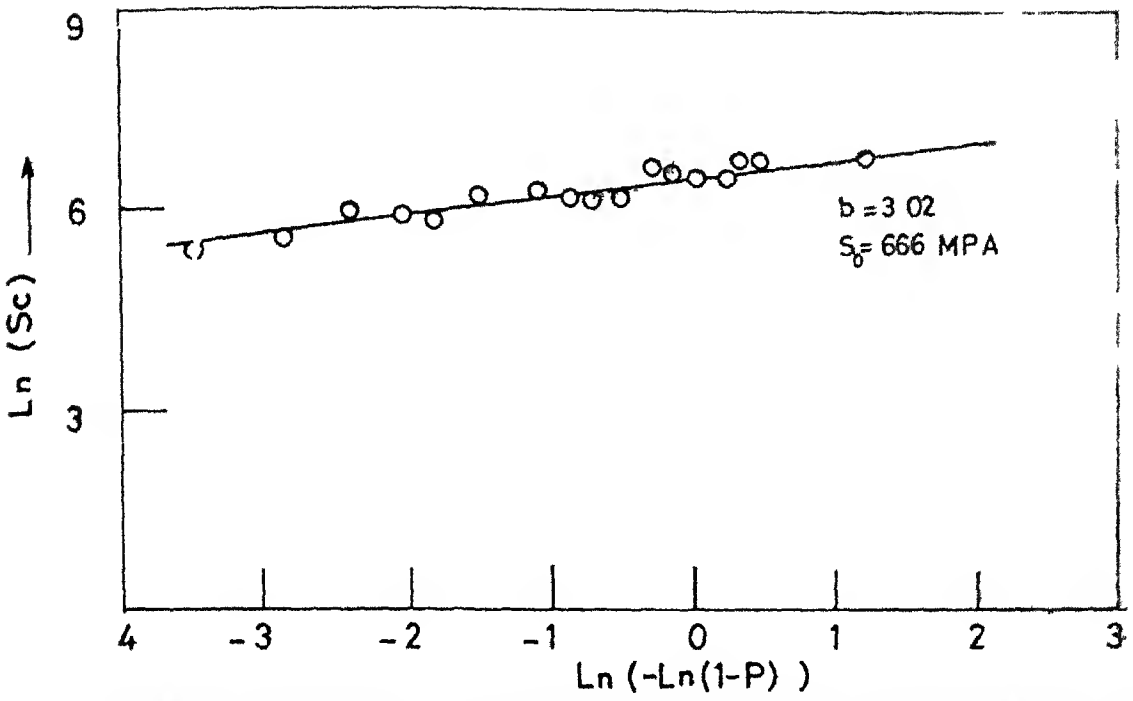

Fig 529 Regression analysis of calculated strength (Sc) with failure probability (P) for virgin glass fibres (A2)

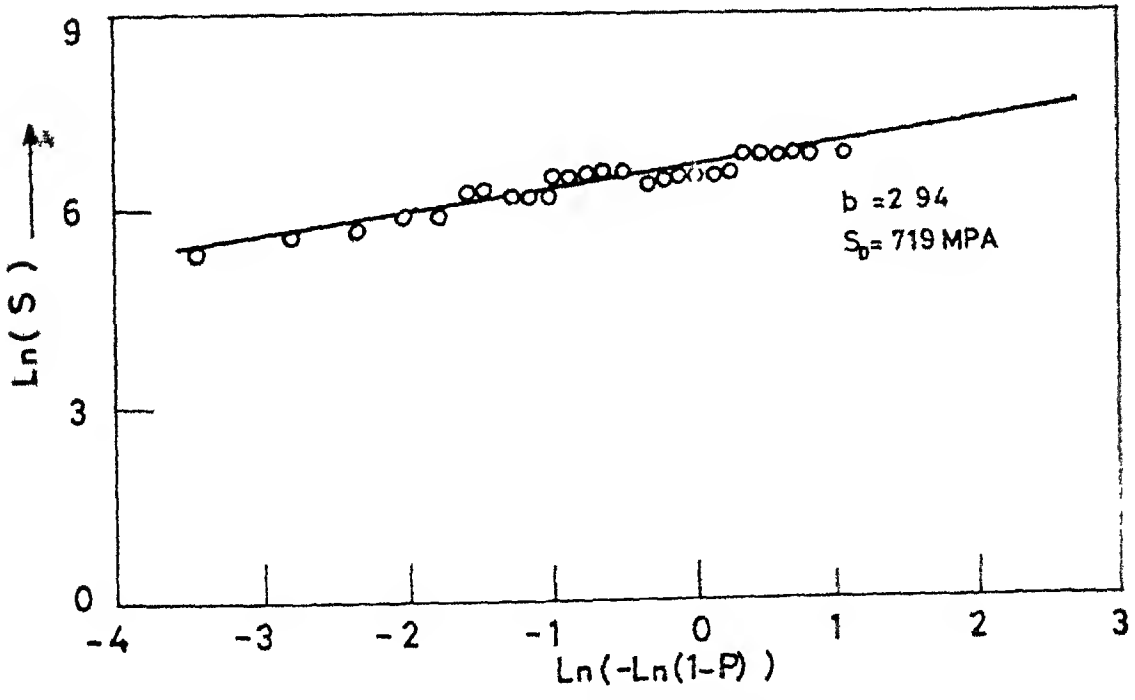

Fig 5 28 Regression analysis of observed strength(S) with failure probability(P) for virgin glass fibres (A2)

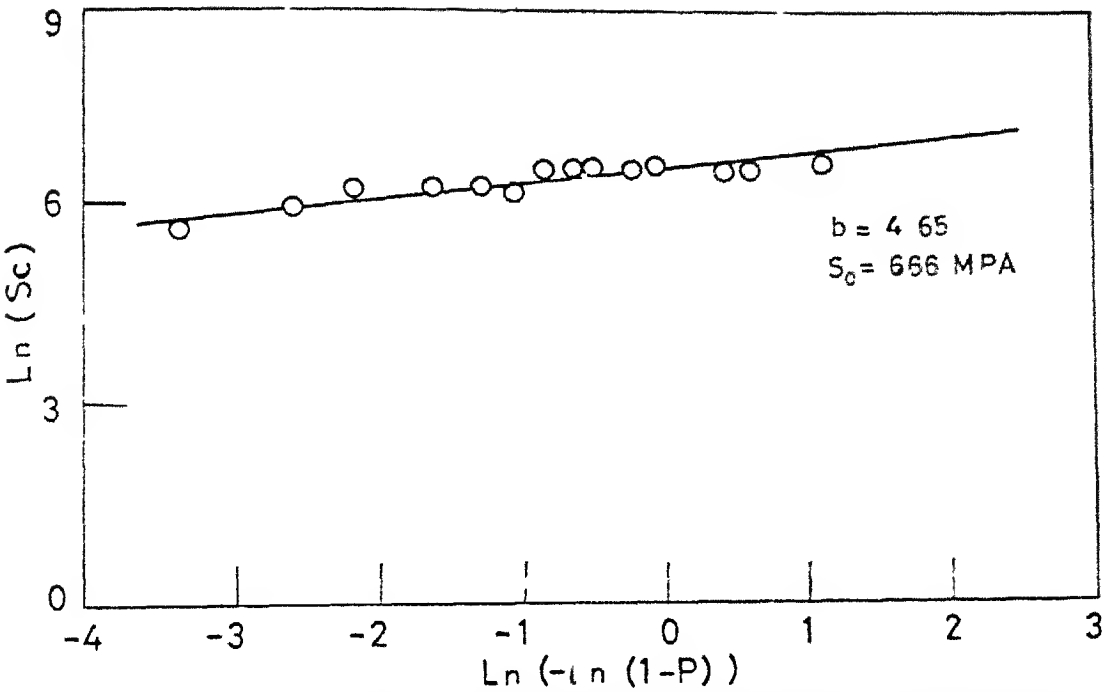

Fig 5 31 Regression analysis of calculated strength (Sc) with failure probability (P) for virgin glass fibres (A4)

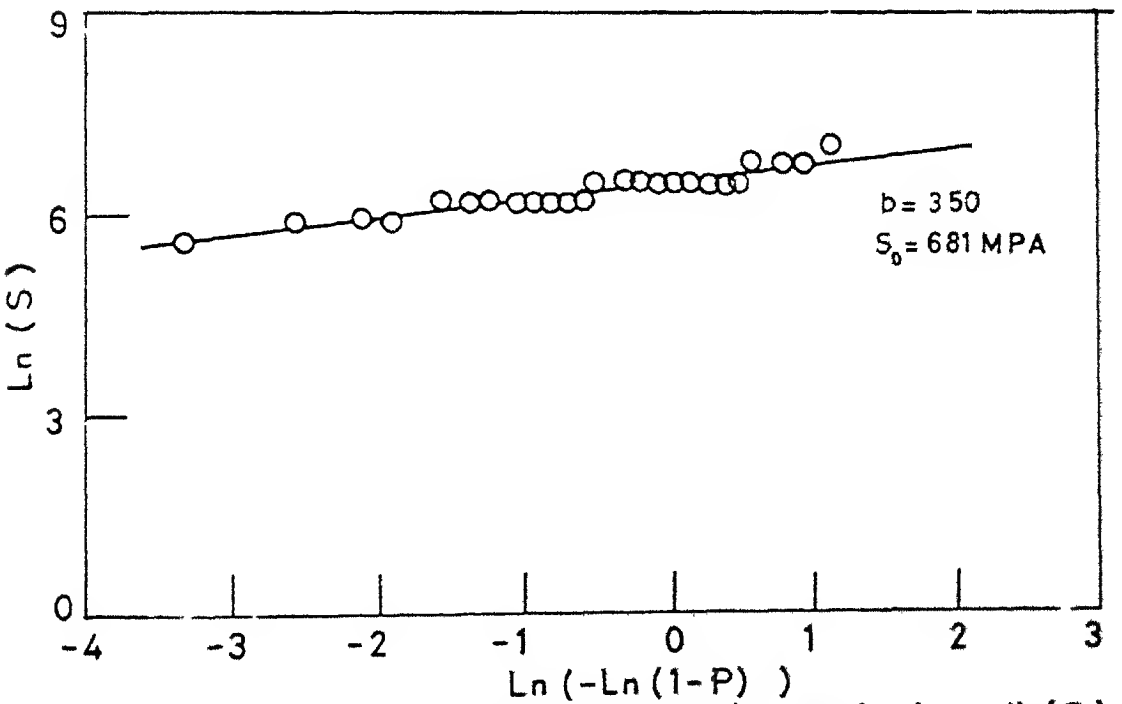

Fig 5 30 Regression analysis of observed strength (S) with failure probability (P) for virgin glass fibres (A4)

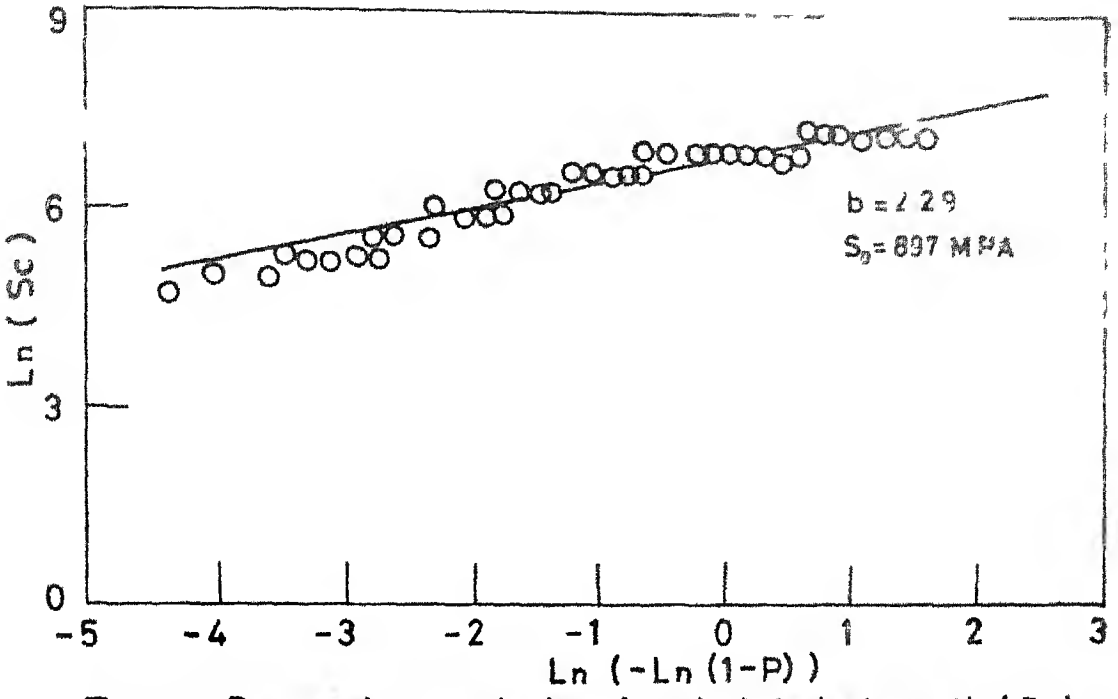

Fig 533 Regression analysis of calculated strength (Sc) with failure probability (P) for non virgin glass fibres (A1)

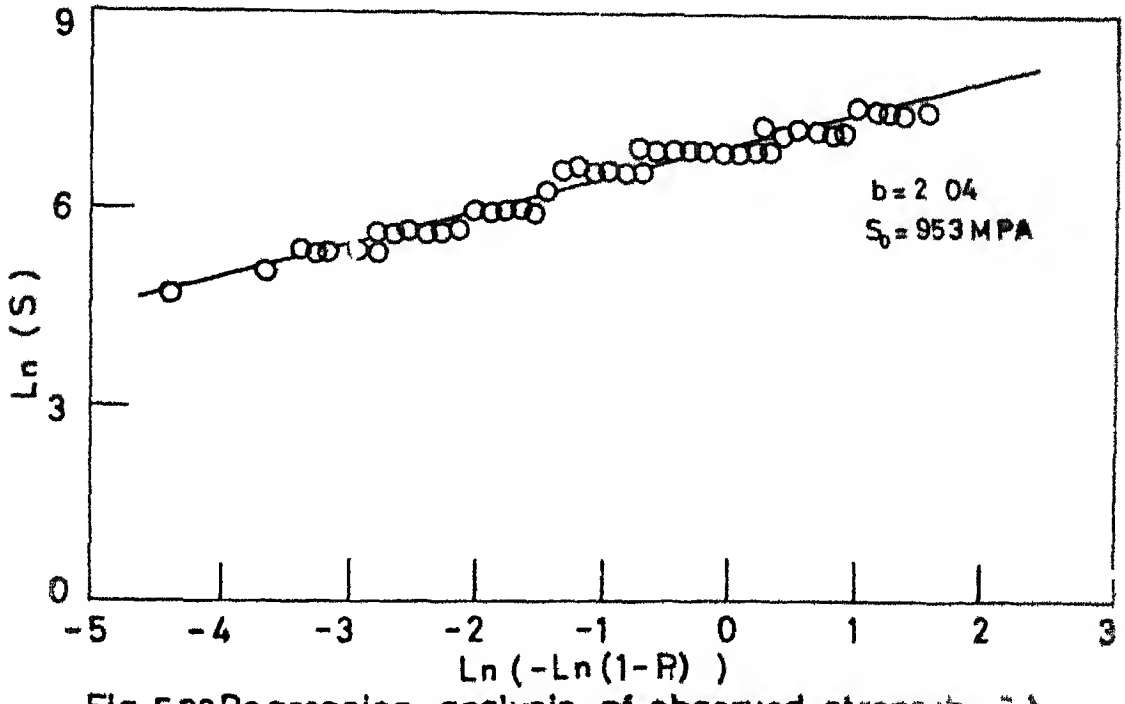

Fig 532 Regression analysis of observed strength (S) with failure probability (P) for non-virgin glass fibres(A1)

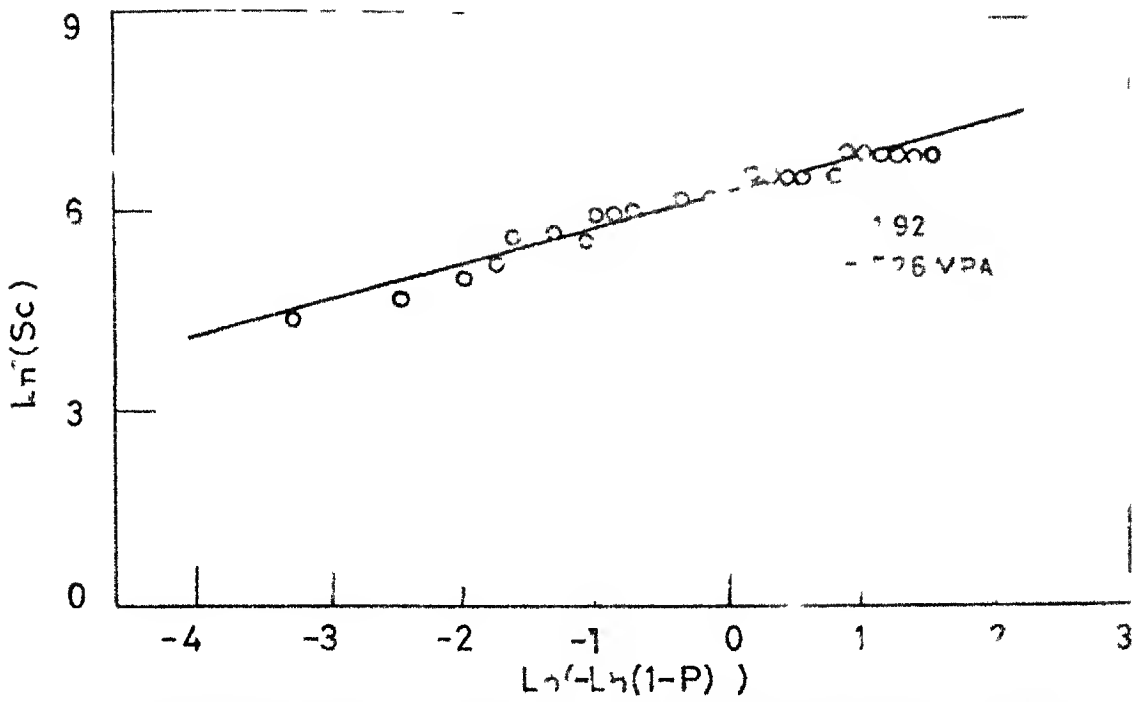

Fig 535Regression analysis of calculated strength(Sc) with failure probability(P) for non-virgin glass fibres(A2)

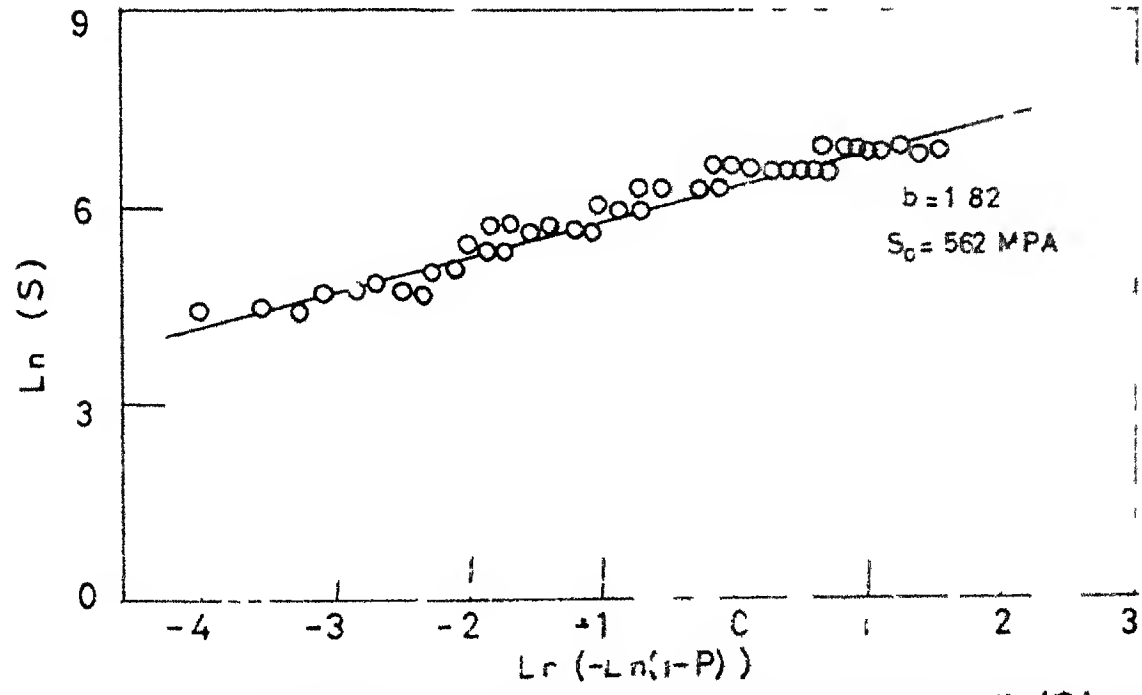

Fig 534 Regression analysis of observed strength (S) with failure probability (P) for non-virgin glass fibres (A2)

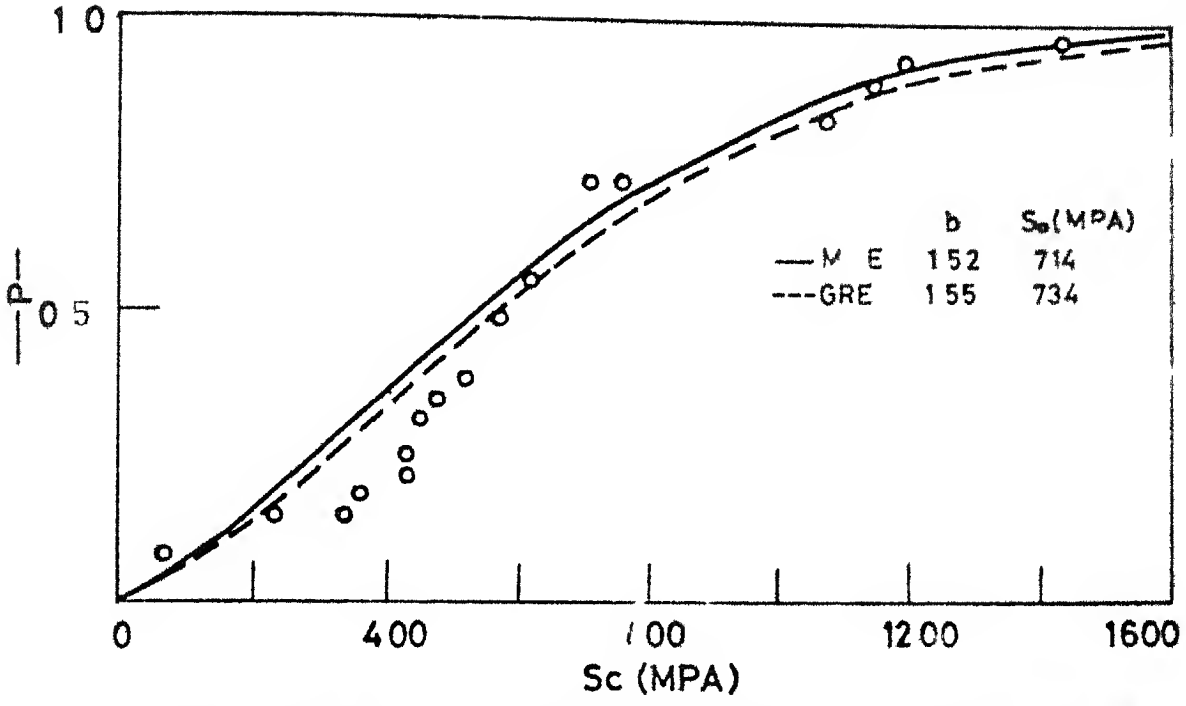

Fig 5 37 Variation of failure probability (P) with calculated strength (Sc) for virgin glass fibres (A1)

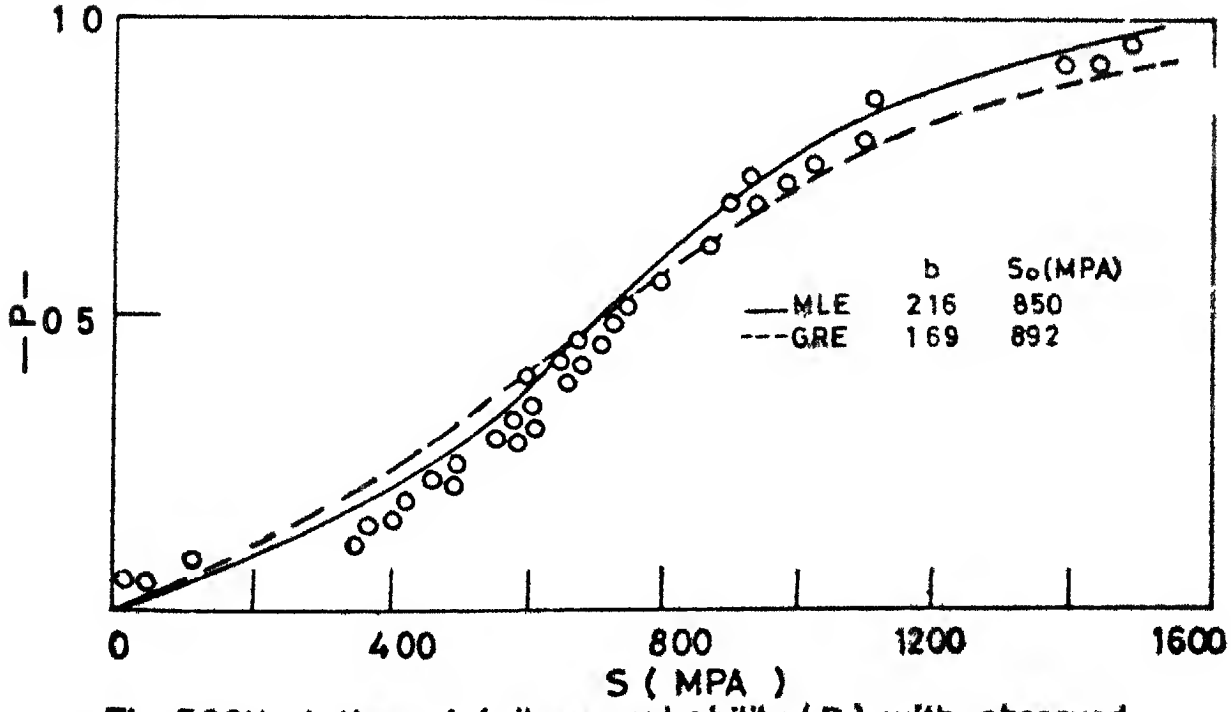

Fig 5 36 Variation of failure probability (P) with observed strength (S) for virgin glass fibres (A1)

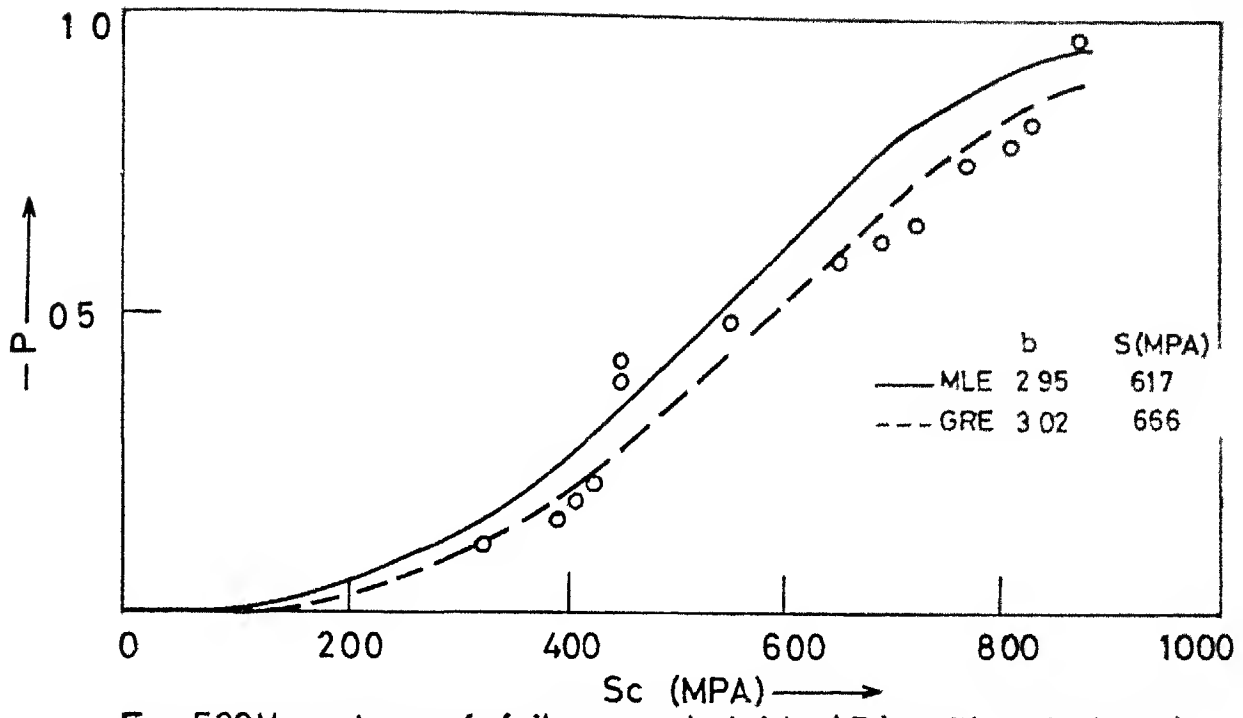

Fig 539Variation of failure probability (P) with calculated strength (Sc) for virgin glass fibres (A2)

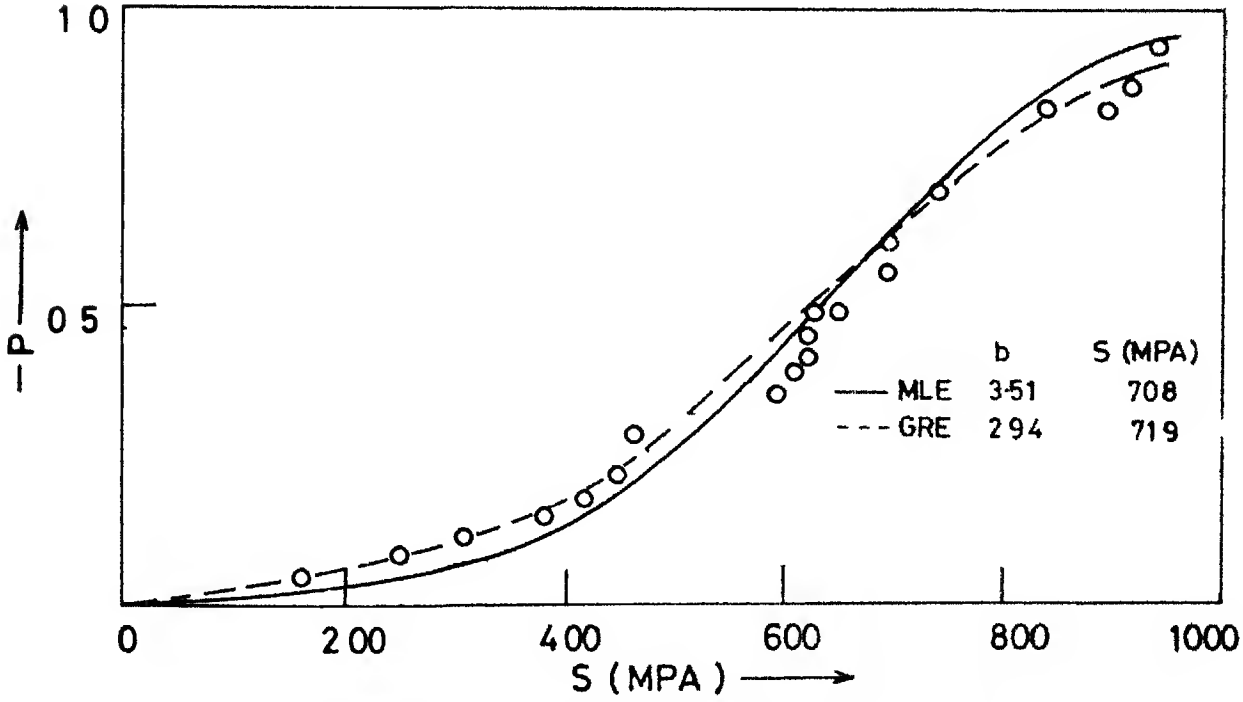

Fig 5 38 Variation of failure probability (P) with observed strength (S) for virgin glass fibres(A2)

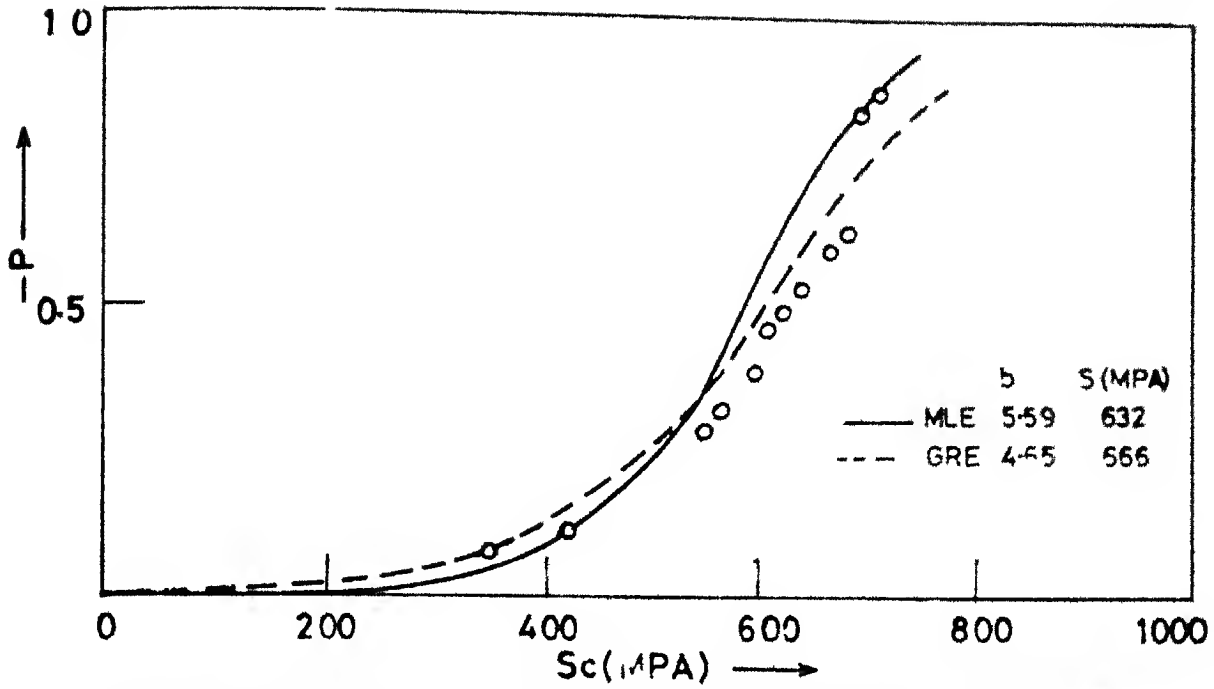

Fig 5.41 Variation of failure probability (P) with calculated - strength (Sc) for virgin glass fibres (A4)

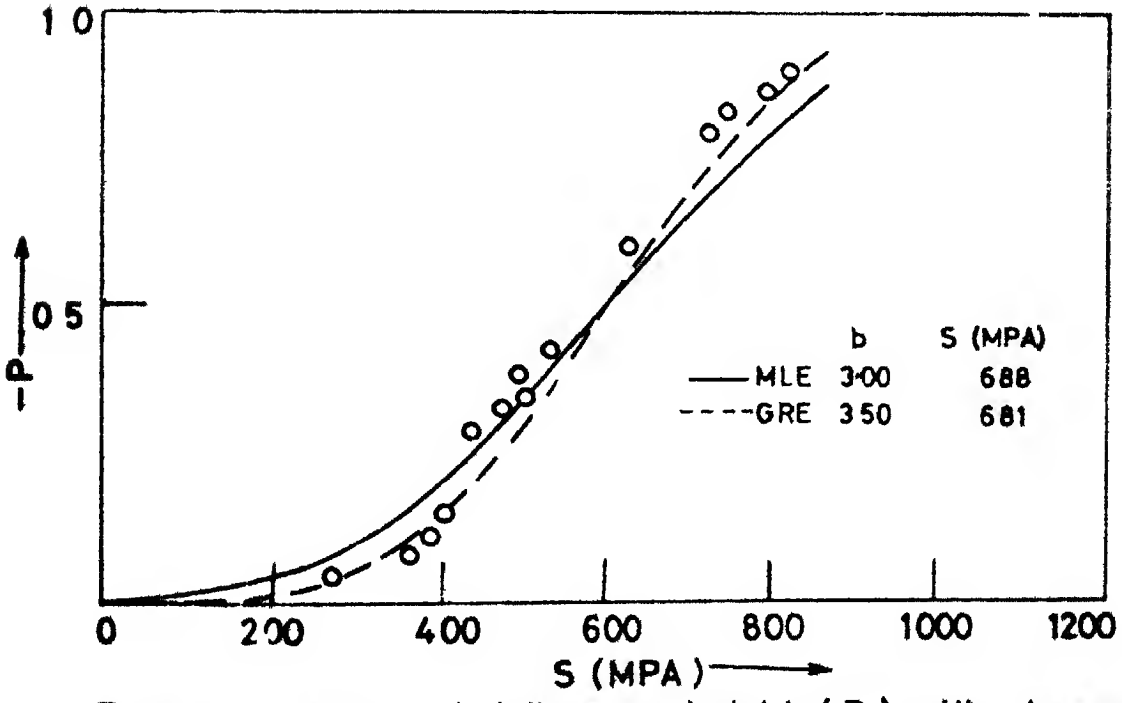

Fig 5.40 Variation of failure probability (P) with observed strength (S) for virgin glass fibres (A4)

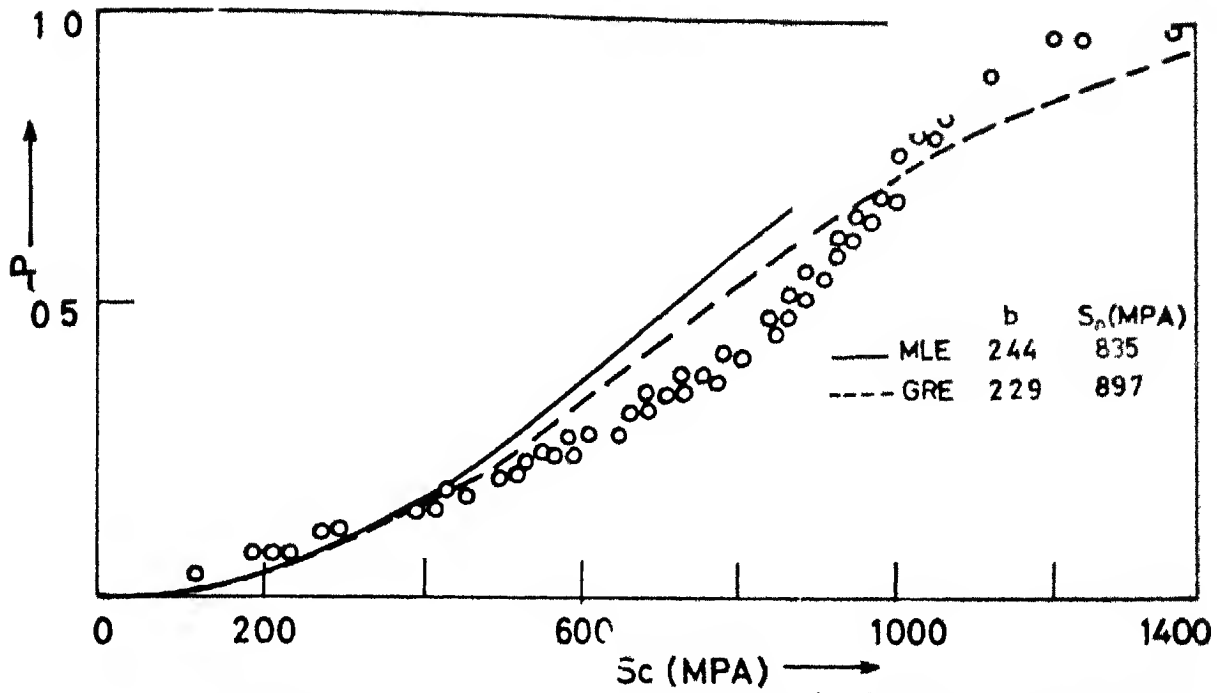

Fig 5 43 Variation of failure probability (P) with calculated - strength (Sc) for non-virgin glass fibres (A1)

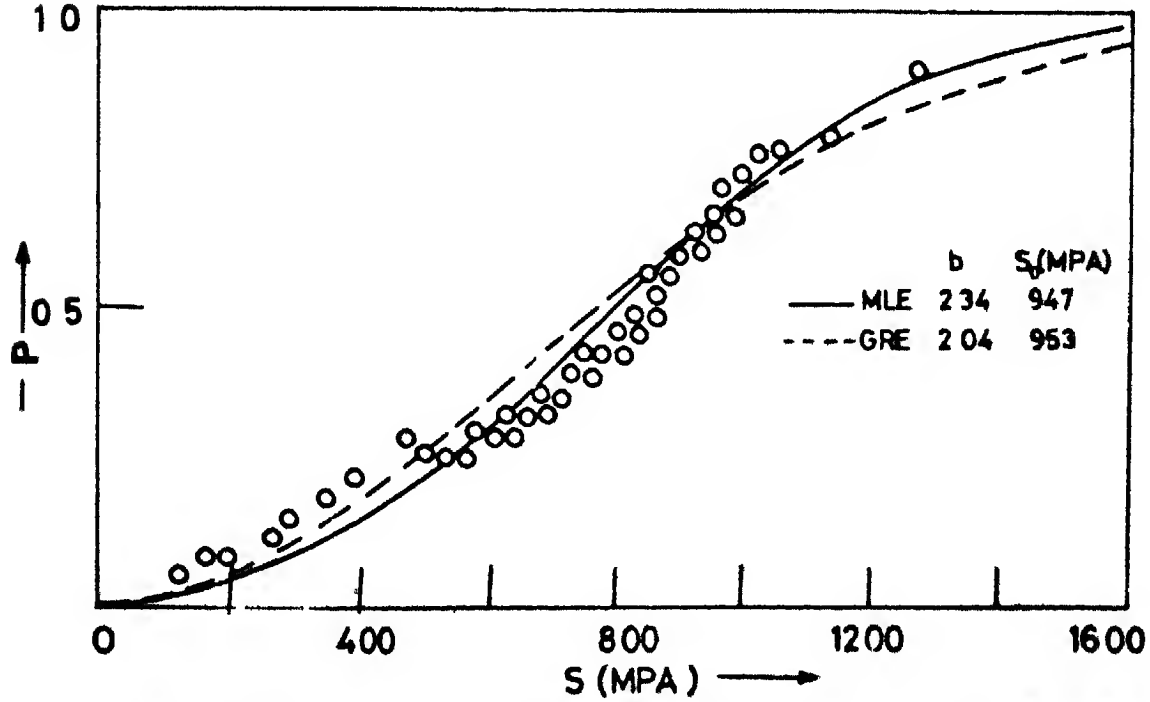

Fig 5 42 Variation of failure probability (P) with observed strength (S) for non-virgin glass fibres (A1)

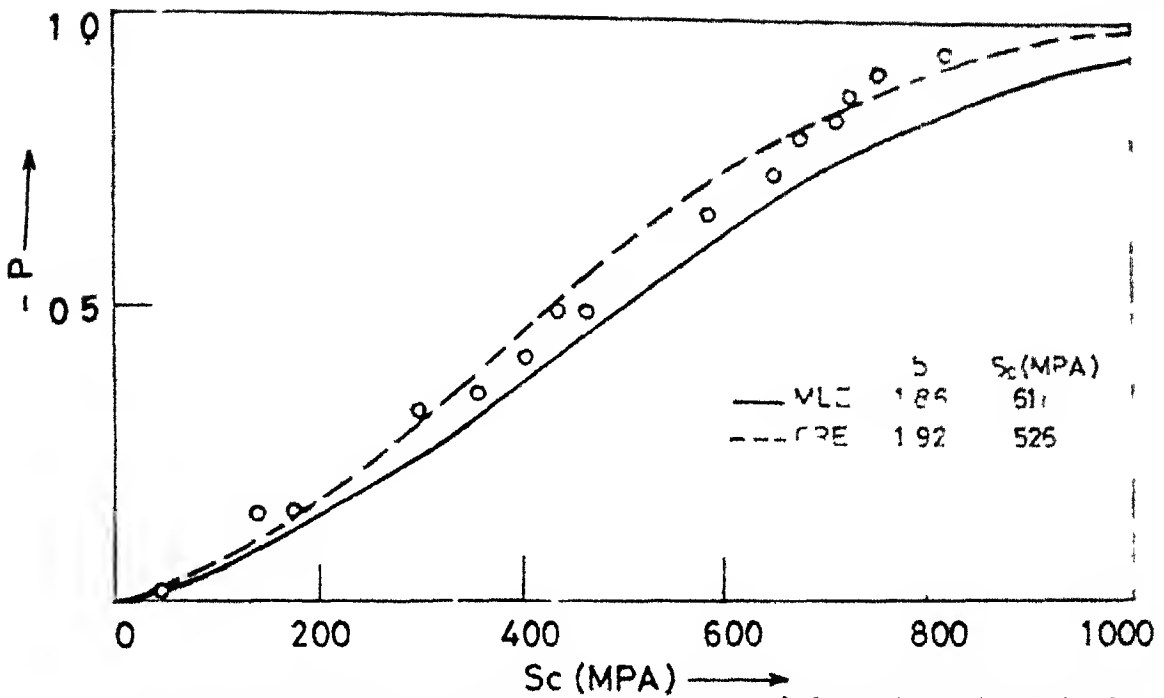

Fig 5 45 Variation of failure probability (p) with calculated-strength (Sc) for non-virgin glass fibres (A2)

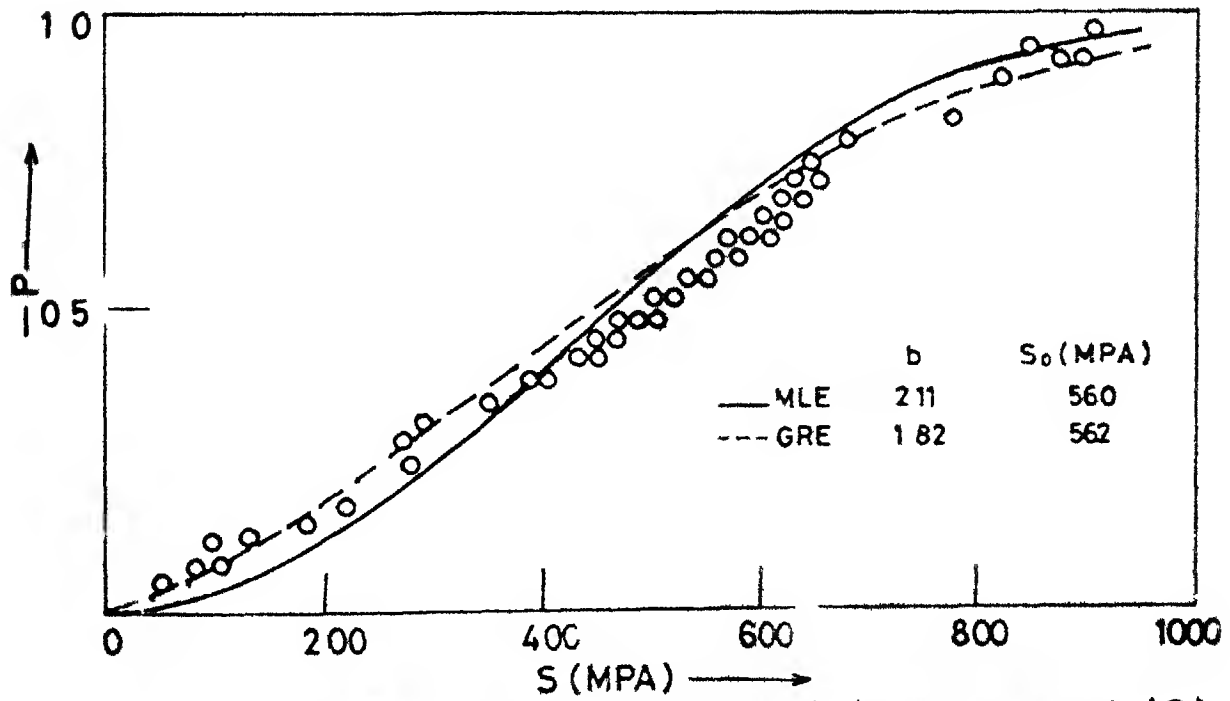

Fig 5 44 Variation of failure probability (P) with strength (S) for non-virgin glass fibres (A2)

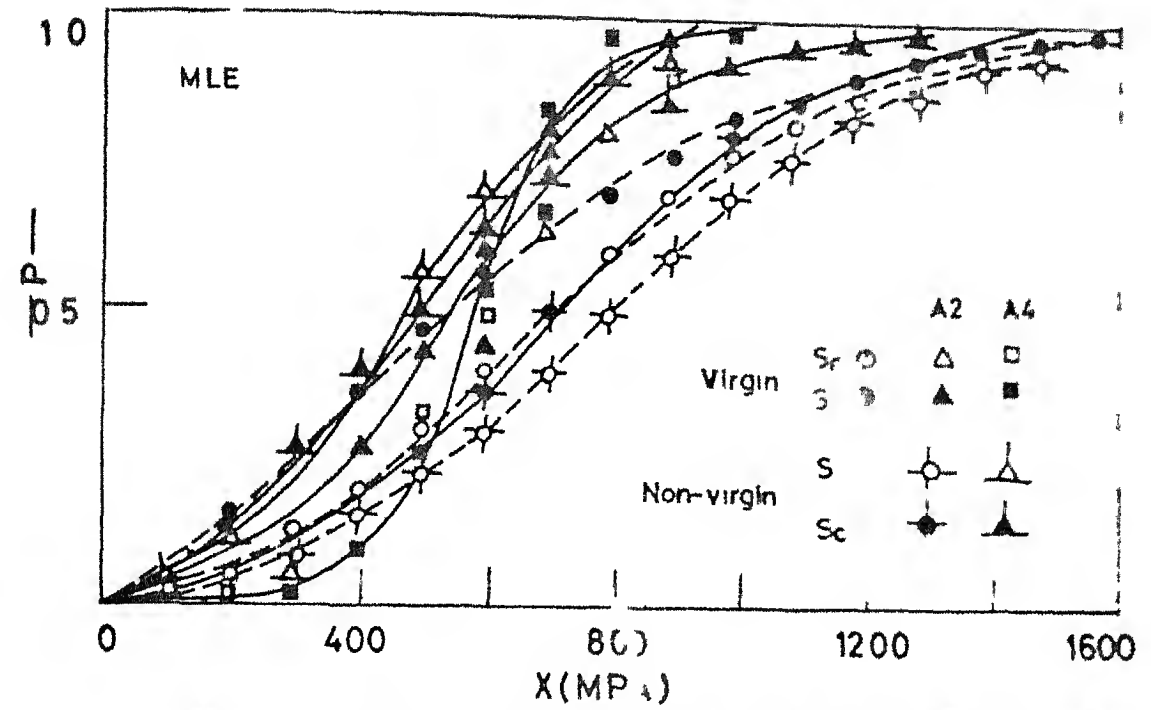

Fig:547Comparison of failure probability distributions of observed strength (S) and calculated strength (Sc) for virgin (A1, A2 A4) and non-virgin glass fibres (A1 A2) (MLE)

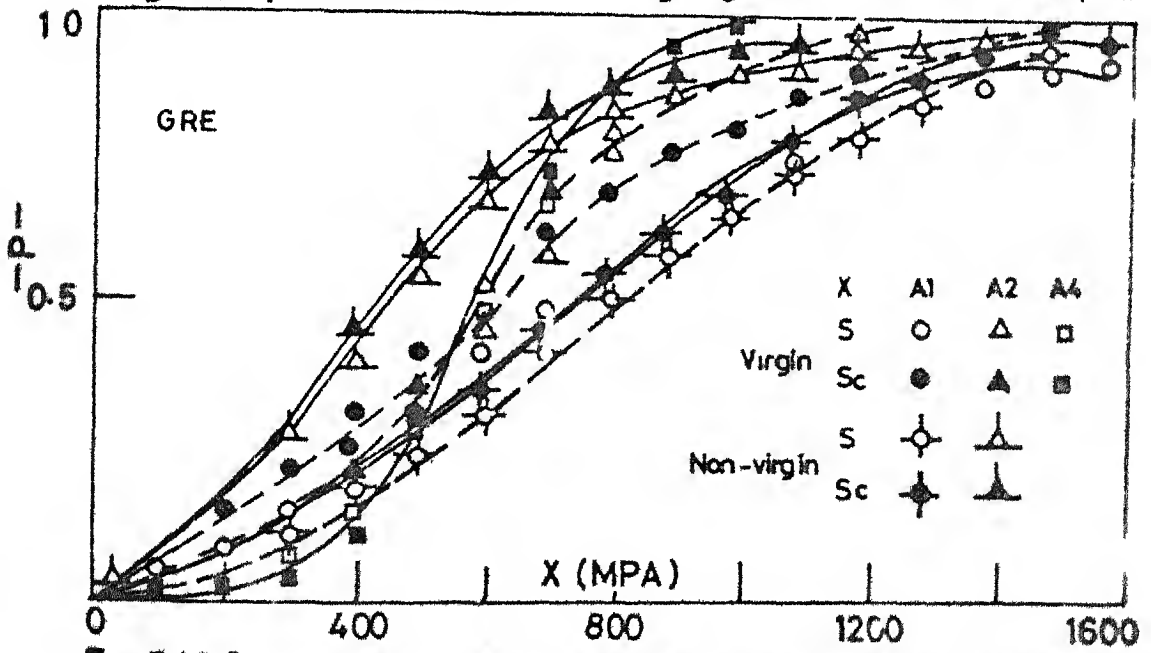

Fig:546 Comparison of failure probability distributions of observed strength (S) and calculated strength (Sc) for virgin (A1, A2, A4) and non-virgin glass fibres (A1, A2) (GRE).

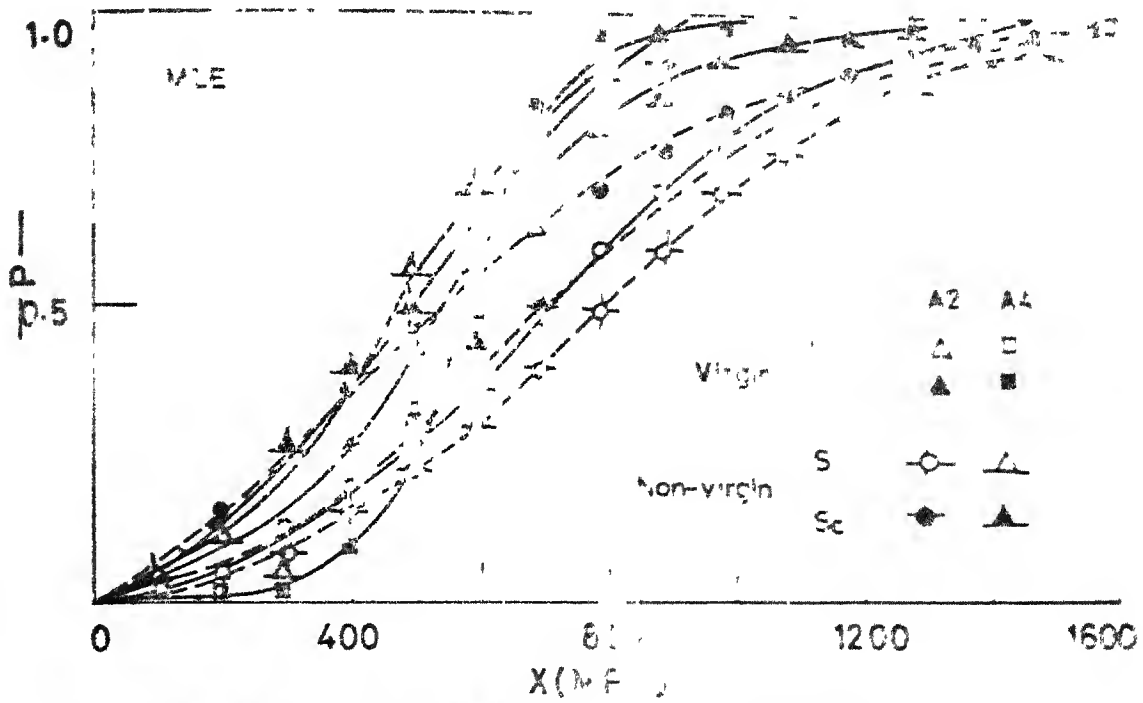

Fig:547Comparison of failure probability distributions of observed strength (S) and calculated strength (Sc) for virgin (A1, A2, A4) and non-virgin glass fibres (A1, A2) (MLE).

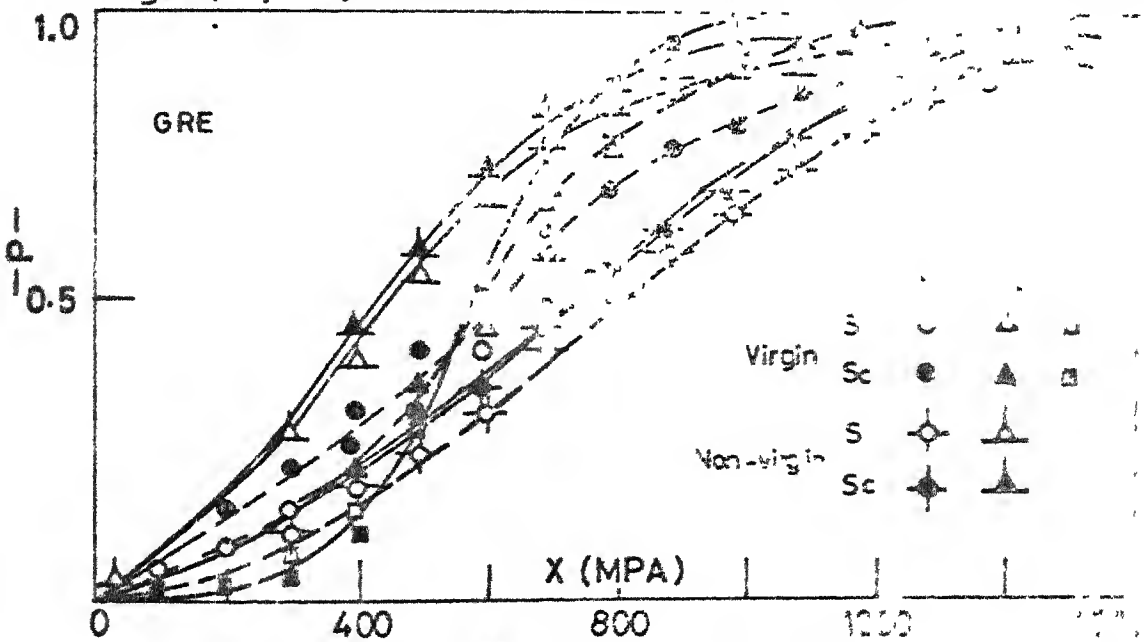

Fig:546 Comparison of failure probability distributions of observed strength (S) and calculated strength (Sc) for virgin (A1, A2, A4) and non-virgin glass fibres (A1, A2) (GRE)

technique and MLE technique are shown in figures 5.46 and 5.47 respectively.

As shown in section 2.10.6.2 mean ($\bar{S}$) and variance (Var (S)) of Weibull's distribution are given by equations (2.58) and (2.59) respectively while coefficient of variation (V_p) is given by equation (2.60) .

The values of mean ($\bar{S}$ and $\bar{S}_c$) deviation in mean given by square root of variance ($d\bar{S}$ and $d\bar{S}_c$) and coefficient of variance (V_p) for both S and S_c corresponding to Weibull's parameters as obtained by regression and MLE technique for both virgin and non-virgin samples are summarised in Table 5.4 and Table 5.5.

Similar analysis has been performed for both sets of S and S_c and corresponding statistical parameters have been found out directly by equations 2.30 and 2.31. These are summarised in Table 5.6.

5.2.3 Fracture Surface:

Glass fibres have been subjected to fracture surface studies. Samples have been prepared and characterised by scanning microscope (ISI-60) as described in section 2.10.7. Representative fracture surfaces of A1, A2 are shown in figures 5.48 and 5.49 respectively. Four typical fracture surfaces of A4 are shown in figures 5.50, 5.51, 5.52 and 5.53 respectively.

One remarkable feature of A4 fibres is the presence of [illegible] of diameters ranging from .1 μm to 1.5 μm. Such holes are

Table 5.3 : Weibull's parameters by MLE Technique.

Sl.No.	Set	S		S_c	
		b	S_o(MPa)	b	S_c(MPa)
1	VA1	2.16	850	1.52	714
2	VA2	3.51	708	2.95	617
3	VA4	3.00	688	5.59	632
4	NVA1	2.34	947	2.44	835
5	NVA2	2.11	560	1.86	611

Table 5.4 : Mean, dispersion and coefficient of variation for S and S_c for both virgin and non-virgin glass fibres (GRE Technique).

Sl.No.	Set	S			S_c		
		$\bar{S}$(MPa)	$d\bar{S}$(MPa)	V_p (S)	$\bar{S}_c$(MPa)	$d\bar{S}_c$(MPa)	$V_p(S_c)$
1	VA1	796	483	.61	661	438	.66
2	VA2	642	237	.37	595	214	.36
3	VA4	612	196	.32	608	152	.25
4	NVA1	844	433	.51	795	370	.47
5	NVA2	500	285	.57	467	253	.54

Table 5.5 : Mean, dispersion and coefficient of variation for S and S_c for both virgin and non-virgin glass fibres (MLE Technique).

Sl.No.	Set	S			S_c		
		$\bar{S}$(MPa)	$d\bar{S}$(MPa)	$V_p(S)$	$\bar{S}_c$(MPa)	$d\bar{S}_c$(MPa)	$V_p(S_c)$
1	VA1	753	365	.49	644	433	.67
2	VA2	637	204	.32	551	204	.37
3	VA4	615	221	.36	584	121	.21
4	NVA1	839	383	.46	741	324	.44
5	NVA2	496	245	.50	543	304	.56

Table 5.6 : Mean,dispersion and coefficient of variation for both S and S_c for both virgin and non virgin glass fibres

Sl.No.	Set	S			S_c		
		$\bar{S}$ (MPa)	$d\bar{S}$ (MPa)	$V_p(S)$	$\bar{S}_c$(MPa)	dS_c(MPa)	$V_p(Sc)$
1	VA1	766	360	.47	652	439	.67
2	VA2	637	211	.33	548	214	.39
3	VA4	616	212	.34	582	137	.24
4	NVA1	872	474	.54	788	350	.44
5	NVA2	498	248	.50	544	302	.56

Fig 5 48 Fracture surface of A1 glass-fibre (SEM) .

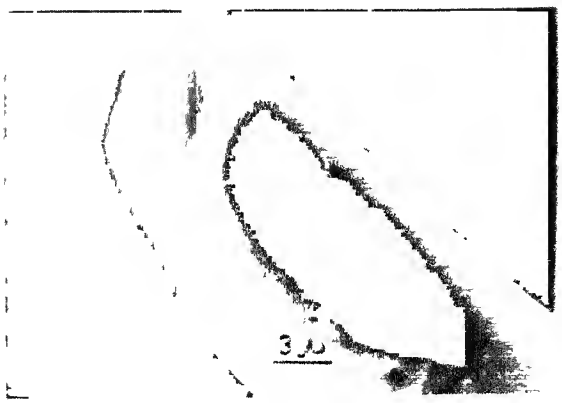

Fig 5 49 Fracture surface of A3 glass-fibre (SEM).

Fracture surface of A4 glass-fibre (SEM)

Fig 5 51 Fracture surface of A4 glass-fibre (SEM)

Fig 5 52 Fracture surface of A4 glass-fibre (SEM)

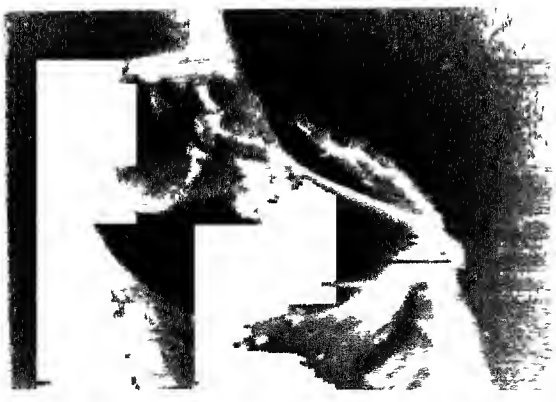

Fig 5 53 Fracture surface of A4 glass-fibre (SEM)

not observed in case of A1 and A2. Another interesting feature of fracture surfaces is the increasing frequencies with which the fracture path is observed to change as the aluminium content is increased. Thus in A4 in nearly all the cases a part of fracture surface is nearly perpendicular to the tensile axis while remaining part is quite parallel to it. This is most clearly indicated in figures 5.50, 5.51 and 5.53 by arrows.

5.2.4 Susceptibility to Chemical Attack:

When glass fibres are treated with 1% HF solution, they show a marked difference in chemical susceptibility. Figures 5.54, 5.55 and 5.56 show typical scanning micrographs of A1, A2 and A4 fibres respectivily when they have been treated with HF solution for 20 seconds.

For A1 fibres there is a severe, wide spread attack by acid while the attack on A2 fibres may be described as 'inter granular' kind in which region between blocks of material are attacked preferably. A4 fibre are found to be the least affected. These fibres are still largely intact. They however show only a light nearly uniform etching.

5.3 Discussion:

The young's modulus for a given glass fibre may be obtained by two methods as described in section 5.2.1. The two estimators $\bar{E}$ and E_R may be found out. This is obvious from Table 5.1 that E_R is always greater than $\bar{E}$. The value of $\frac{dE_R}{E_R}$ is found to be less than the value of $\frac{d\bar{E}}{\bar{E}}$ in almost all the cases. This implies

(a) (b)

Fig 5 54 SEM micrograph

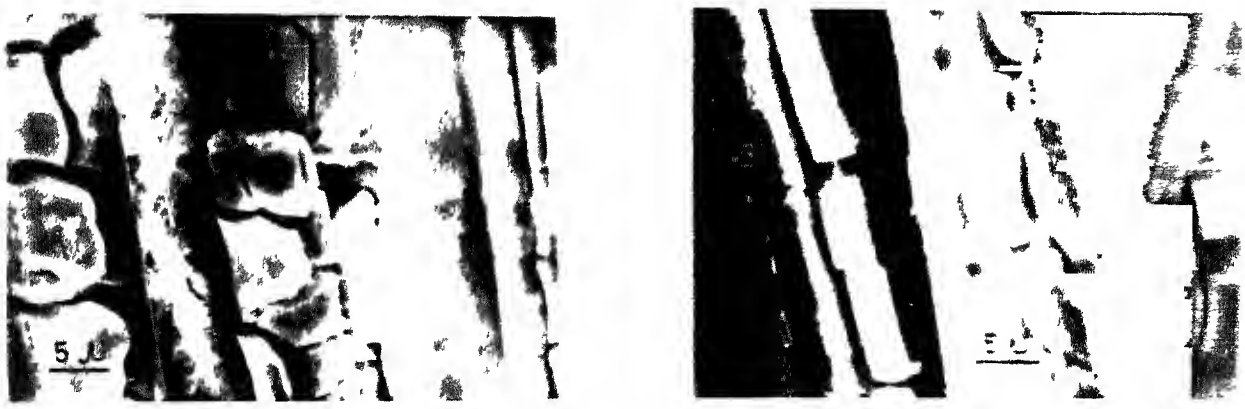

(a) (b)

Fig 5 55 SEM micrograph of etched A2 glass fibres.

(a)

Fig 5 56 SEM micrograph of etched A4 glass fibres.

that dispersion of E_R is smaller than that of $\bar{E}$. It is proposed that E_R is a better estimator of young's modulus than $\bar{E}$ for a given set of glass fibres. The reason for such a propostion is that regression of strength with strain for a given set of data provides a linear relationship which effectively represents the hypothetical stress versus strain curve for the given material. Thus slope of this line ought to represent the true young's modulus of the material. There is no similar logic based upon the physics of the problem in support of the calculated $\bar{E}$ which thus merely represents a statistical average of some parameter having dimensions similar to that of young's modulus. The further confirmation to above conclusion comes from the effect of the presence of aluminium particle on the young's modulus of glass fibres. While there is decrease in $\bar{E}$ with increase in aluminium percentage correspondingly there is a definite increasing trend of E_R. The latter behaviour is expected for any such composite material.

The large scatter in the observed strength arises from two sources. One is the surface flaws which arise due to various(a) intrinsic reasons and (b) processing effects. The other results from the errors made during strength measurement. The error arises predominantly from the diameter measurement made by an electronic comparator such as Accutron. Sometimes during sample preparation more than one fibre get stuck together which can not be resolved with naked eye. Only during fracture this gets resolved. Thus various procedural steps bring in extraneous errors in measure-

ments of strength and strain. The error involved in strain are insignificant while those in strength(S) are substantial. Thus distribution of S which has been referred to as observed strength really does not represent the true set of strenth data for a given glass fibre. So a better representative picture is obtained from parameter S_c. This is so because regression minimises in E_R the effect of extremities of data points in stress strain plane. As E_R expresses the best estimate of young's modulus where effect of extraneous errors in strength S and strain e has been averaged out and as the error in e is insignificant as compared to that in S hence S_c. Calculated by equation 5.1 is the more appropriate representatives of strength distribution reflecting the actual surface flaw distribution of glass fibres from S and S_c histograms it is clear that strength distribution becomes sharper in case of S_c than that for S.

Corresponding to S_c a new set of diameters D_c is found by equation 5.2. D_c represents the actual and effective distribution of diameters in the set of fibres tested, devoid of any extraneous error incroporated in diameter measurement.

Weibull's parameters may be determined by both graphical regression technique (GRE) and MLE technique. As obvious from the failure probability distributions f_1 and f_2 corresponding to parameters as obtained by GRE and MLE techniques respectively. Analysis with S gives values such that f_1 and f_2 invariably cross each other at some critical value of S being referred to as

S^*. For $S < S^*$, $f_1 > f_2$ while for $S > S^*$, $f_1 < f_2$. Similar analysis of S_c provides a remarkable defference as compared to that of S. For S_c, $f_1 < f_2$ in the entire range of S_c in almost all the cases except that of VA4 where f_1 and f_2 cross each other. Thus for same value of strength $S (> S^*)$ and Sc, MLE Technique provides estimators of b and S_o such that probability of failure is higher than that predicted by GRE. This ensures a better estimate for mean strength for safer designing. Hence MLE technique should be preferable to GRE technique for estimating weibull's parameters. This is reflected in the mean value of strength which is invariably found to be less for MLE technique as compared to that for GRE technique, as seen in Tables 5.4 and 5.5. Another remarkable outcome of this analysis is that mean strength $\bar{S}_c$ is found to be always less than mean strength $\bar{S}$ as is evident from Tables 5.4, 5.5 and 5.6. The deviation $d\bar{S}_c$ is always found to be less than $d\bar{S}$ in case of GRE, estimators (Table 5.4) and similar trend persists in most of the cases analysed by MLE technique (Table 5.5). Comparison of Tables 5.5 and 5.6 reveals that analysis done by the MLE technique provides mean strength values $\bar{S}$ and $\bar{S}_c$ and $Vp(S)$ and $Vp(S_c)$ which are almost equal to those obtained by simple arithmatic averaging of strength data. This further supports the superiority of MLE technique over GRE technique.

An increase in aluminium concentration in glass fibres results in the deterioration of observed strength ($\bar{S}$) in both virgin and non-virgin samples as is evident from Tables 5.4, 5.5 and 5.6. In case of $\bar{S}_c$, it is obvious from these tables that

minimum $\bar{S}_c$ occurs for VA_2 while it increases marginally for VA4. These observations suggest that aluminium particulates act as inclusions or stress concentrators, thereby reducing the mean strength.

This feature is reflected in the fracture surface micrographs as described in section 5.2.3. The complex surface morphology arises because of complex stress distribution due to the presence of hole and surface flaws nearest to the hole. Such duplex fracture surface morphology is not observed in case of A1. In case of A2 it is observed occasionally but in A4 such morphology is always observed. Presence of such a characteristic fracture surface can be taken to indicate the presence of stress concentrator like a hole or a particle inside the fibre even though such a feature may not be directly observable.

The holes in A4 fibres seem to be the sites where large Al particles are embedded in the fibre. These particles have either been dislodged during fracture process or they have caused the formation of small cylindrical cavities in the fibre during the fibre drawing process, so that particles may still be existing at the end of these cavities. In the latter case the holes represent a cross section through these cylindrical cavities.

The trend of $\bar{S}_c$ suggests that aluminium presence even at .5% level introduces the microheterogenities which act as stress concentrators and reduce the strength when aluminium concentration further increased to 7.5%, the $\bar{S}_c$ improves from its corre-

sponding value for .5% though some holes are also present. Whether these holes arise because of bigger aluminium particle getting dislodged during testing or during fiberisation process, in either case further deterioration of strength is expected. This suggests that microheterogeneities produced at atomic scale are the most probable cause for the lowering of strength.

From the present study a new technique has been established to evaluate young's modulus based on strength-strain regression analysis. The observed strength(S) does not represent the true distribution of surface flaws but another variable S_c is a better representation of strength distribution. Weibull's distribution represents the strength of glass fibres. The Weibull's parameters may be evaluated by graphical regression technique (GRE) or by maximum likelihood estimation technique. The latter technique is preferable as discussed above.

Aluminium particles decrease the strength while they increas the young's modulus of glass fibres. The microheterogeneities at atomic scale seem to be acting as stress concentrators. Bigger particles give rise to formation of holes whose diameters are of the order of a few microns. These give rise to formation of duplex fracture surfaces. Chemical susceptibility increases with increasing aluminium concentration.

Conclusion:

From the present investigations about electrical and mechanical behaviour of heterogeneous glass fibres, following conclusions are drawn.

(1) Glass fibres may be drawn from silica based compositions with sodium molar concentration varying in the range of 10 to 30%. Further the glass-metal composite, formed by melting aluminium powder with the glass batch, may be fiberised to give composite glass fibres. The aluminium fraction may be varied in the range of 0 to 10 mol%.

(2) Almost all of the sodium ions of these glasses may be replaced by silver by subjecting the glass fibres of such compositions to a sodium $\rightleftharpoons$ silver ion exchange treatment. This may be achieved by ion-exchanging the glass fibre specimens in a silver nitrate bath at 330°C for 36 hours.

(3) A.C. and D.C. electrical conductivity measurements may be made on these glass fibres, using silver paint as non blocking electrodes. Glass fibres having no metal particulates show ionic conductivity in which sodium ions are the charge carriers. The resistivity level is quite high ($\simeq 10^9 \Omega$ Cm at room temperature. The activation energy is about .8 eV. Conductivity increases with increasing amount of sodium concentration.

(4) Similar studies made on composite glass fibres reveal that higher concentration of aluminium in glass fibres ($\geqslant 5$ mol%)

increases the glass conductivity. The mechanism prevailing in lower temperature range is electron tunnelling while in higher temperature range (T > 120°C) ion migration predominates.

(5) Phase separation is seen in most of these glasses. Phase separation has been found to influence the electrical behaviour of these glasses in a significant manner. Glass transition temperature is also found to be sensitive to phase separation.

(6) Ion-exchanged glass fibres show an improvement by about two orders of magnitude in electrical conductivity as compared to that of the virgin fibres. The activation energy comes down to around .45eV. The maximum conductivity of 10^{-6}(ohm cm)$^{-1}$ at room temperature may be achieved by the ion exchange process.

(7) The charge carrier mechanism in ion-exchanged glass fibres is the migration of silver ions. The fraction of silver ions contributing to conduction mechanism are found to be of the order of 1%.

(8) The microstructure of ion-exchanged glass fibres shows phase separation. The disjointed regions of silver rich phase are scattered in the interconnected second phase having less than 1% of total silver content present in the glass. It is this interconnected phase which is responsible for electrical conduction.

(9) It has been established that an optimum combination of electric field and temperature brings a permanent micro-structural change in ion-exchanged glass fibres. This results in an increase of conductivity by many order of magnitudes. These electric fields are found to be quite low of the order of 1 volt/cm. With increasing temperature the value of critical electric field which brings about this transformation from low conducting state to high conducting state decreases. The initial glass composition too influences this critical electric field.

(10) The microstructural evidence suggests formation of links among the disjointed portions of silver rich phase under the combined influence of electric field and temperature. This makes silver ions, locked earlier in disjointed portion of silver rich phase, to move in the interconnected network of silver rich phase. Thus in high conducting state, it is the silver rich phase which predominantly contributes to silver ion migration.

(11) The activation energies in the high conducting state are very small, in some cases they tend to be negligibly small becoming almost zero. The highest conductivity of the order of 10^{-2} (ohm cm)$^{-1}$ may be achieved in this high conducting state.

(12) The presence of aluminium particles further increases the conductivity of ion-exchanged samples. Maximum effect has

been found when aluminium is present in small amount (.5 mol%). It is shown to influence the microstructure considerably.

(13) In high conducting state, aluminium particulates have a desirable effect. They further boost up the conductivity level. The value of conductivity is found to depend upon the amount of aluminium concentration in the ion exchanged glass fibres.

(14) It is for the first time that such a high state of electrical conduction could be achieved characterised by almost negligible activation energies. Without aluminium particles, highest conductivity of 2.5×10^{-2} $(\text{Ohm Cm})^{-1}$ has been achieved. Highest conductivity of 3×10^{-1} $(\text{Ohm C.m})^{-1}$ has been acomplished in the case of 5 mol% of ion-exchanged fibres containing aluminium particulates.

(15) Low value of activation energy and high value of conductivity at room temperature suggest that ion-exchanged glass fibres in both the states are most likely FIC . This further establishes a general route to prepare a family of new FIC from any silica based glass composition, viz. through the effect of sodium silver ion exchange on these glasses in their fibre form, followed by electric field induced morphological transformation.

Youngs modulus is found to increase with increasing aluminium concentration in the glass fibres. Strength invariably

decreases with increasing amount of aluminium. This suggests that microheterogeneties at atomic scale caused by the presence of aluminium particles act as stress concentrators. The presence of bigger aluminium particles results in the formation of holes (.1-1um diameter). The corrosion resistance increases with increasing aluminium arount.

(17) A new technique to estimate Youngs rodulus for glass fibres has been proposed, based on regression of strength strain data. Better representative parareter of strength has been suggested.

(18) Strength of glass fibres has been found to follow Weibull statistics. Weibull's parameters may be found out by GRE and MLE technique. The analysis suggests the superiority of MLE technique over GRE technique.

REFERENCES

1 (a) Abeles, B., Sheng P., Coutts M.D. and Arley Adv. Phys., 24, 407 1975)
(b) Abeles B., and Gittleman J.I, Appl. Opt. 15, 2328 (1976)

2. Aitken J. and Mac Crone R.K. (Materials Science Research, Vol. 9 'Mass Transport Phenomena in Ceramics' eds, A.R. Cooper and A.H. Heuer: Plenum Press(1975), (N.Y.).

3. Allan W.B. 'Fibre Optics', Theory and Practice'Plenum Press, 247 (1973) (N.Y.).

4. Anderson R. and Mc Crone R.K, J. of Non Cryst. Solids, Vol. 11, 1112 (1974).

5. Austin I.G. and Mott N.F. Adv. Phys. 18, 41 (1969)

6. Bacon F.R. , Glass Ind. 49, 430-46, 494-9, 544-9 (1968).

7. Bartholomew R.F. and Garfinkel H.M. 'Chemical Strengthening of Glass' in Glass , Science and Technology (ed) D.R. Uhlmann and N.J. Kreidel (1980) Academic Press (N.Y.).

8. Bartholomew R.F. and Garfinkel H.M. 'Non Crystalline Solids' (ed.) G.H. Frischat, 459-461 (1977). Trans. Techn. Publ. , Aedermannsdorf,(Switzerland).

9. Basu B., Maiti H.S. and Paul A. 1Bull. Mater.Sci., 5 , 21 (1983)

10. Baynton P.L., Rawson H and Stanworth, J.E. Trans. Electrochem. Soc. 104, 237-40 (1956).

11. Biefield R.M., Johnson R.T. and Banghman R.J., J. Electrochem. Soc., 125, 179 (1978) .

12. Blackman L.C. F., Proctor B.A., Smith J.W. and Taylor J.F., The Chartered Mechanical Engineer Jan. 45-51 (1977).

13. Borino F., Lazzari M., Leonardi A., Rivalta B. and Scrosati B., J. Sol. St. Chem., 20, 315 (1977).

14(a). Brungs, M.P. and Mc Cartney E.R., Phys. Chem. Glasses 16, 44 (1975).

15. Bundy F.P. and Dunn K.J., J. Chem. Phys. 71, 1550 (1979)

16. Burnett D.G. and Douglas R.W., Phys. Chem. Glasses 11, 125(1970).

17. Cahn, J.W., Trans. AIME 242, 166(1968).

18. Cahn J.W. and Hilliard J.E., J. Chem. Phys. 31, 688 (1959).

14.(b) Bottcher C.J.F. and Bordewijk, Theory of Electric Polarisation Vol. I, II 2nd ed (Elsevier NY 1978).

19.(a). Chakravorty D. Appl. Phys. Lett. 24, 62 (1974,.
19.(b)Chakravorty D., Bull. Mater. Sci. 6,(2, May,193-200 (1984).

20. Chakravorty D. in'Preparation and Characterisation of Materials (eds.) J.M. Honig and C.N.R. Rao 515 (1981) Academic Press (N.Y.).

21. Chakravorty D., Bandyopadhyay A.K. and Nagesh V.K., J. Phys. D, 10, 2077 (1977).

22. Chakravorty D. Bhatnagar R and Sharma B., Mat. In Engineering, 2, (3) (1981).

23. Chakravorty D. and Chakrabarty S. J. Non-Cryst. Solids, 38,39, 295(1980).

24. Chakravorty D., Harnahalli A.R. and Kumar D., Phys. Status Solidi 51,275(1979a)

25. Chakravorty D., Keshavram B.N., Venkateswaran A., J. Mat. Sci. 14, 2991 (1979).

26. Chakravorty D. and Murthy C.S. J. Phys. D9, L162 (1975).

27. Chakravorty D., Shuttleworth A and Gaskell P.H. J. Mat. Sci., 10, 79 (1975).

28. Chakravorty D., Tiwari A.N., Goel P.S. Phys. Chem. Glasses, 13, 91-93(1972).

29. Chandresekhar G.V. and Shafer M.M., Extended Abstracts Electrochem. Soc., 260 (1978),(Seattle, Washington)

30. Charles R.J. J. Am. Ceram. Soc. 49, 55-62(1966).

31. Charles R.J., J. Am. Ceram. Soc. 47, 559 (1964).

32. Charles R.J., J. Am. Ceram. Soc. 46, 235(1963).
33(a)Charles R.J., J. Appl. Phys. 32, 115, (1961).
33(b)Cohen (1951)'Life Testing and Reliability Estimation' , Kale B.X and Sinha S.K., New Delhi, Wiley Eastern (1980).
34. Collins D.R., Schroder D.K., Sah C.T., Appl. Phys. Letters 8, 323-325(1966).

35. Compaan K. and Haven Y , Trans. Faraday Soc. 52, 786(1956).

36. Cooper A.R. and Krohn D.A., J. Am. Ceram. Soc. 52, 665 (1969).

37. Das G.C. and Chakravorty D., J. Phys. D15, 2255 (1982).

38. Das G.C. and Chakravorty D. J. Appl. Phys. 51, 3896(1980).

19.(c) Chakravorty, D., Chattopadhyaya S., Datta S., Khan S.K. Sengupta K and Bahadur D, J. of Mater. Sc. Lett. 3, 461-3 (1984).

40 (a) Datta S., Chakravorty D., J. of Mat. Sci. Letters 2 729-31 (1983).

40(b) Denton E.P., Rawson H and Stanworth J.E. Nature, 173, 1080-1 (1954).

41. Dong.Hi Lee and Mc Pherson R., J. Mat. Sci. 15, 25 (1980)

42. Doreau M. and Robert G. , Mater. Res. Bull. 15, 1499 (1980).

43. Doremus J. Am. Ceram. Soc., 67, N(7) July (1984)

44. Doremus R.H. and Tomozawa M., J. of Non Cryst. Solids 14, 54, (1974).

45. Doremus R. H. Glass Science, John Wiley and Sons (N.Y.), 44 (1973)

46. Doremus R.H. JPhys. Chem. Glasses, 10, 28 (1969).

47. Doremus R.H. J. Electrochem. Soc. 115, 181(1968a).

48. Doremus R.H. J. Phys. Chem. 68, 2212 (1964).

49. Dozier A.W., Wilson L.K., Frieble E.J. and Kinser D.L., J. Am. Ceram. Soc. 55, 373 (1972).

50. Eakins W.J., Glass/Resin Interface, Patent Survey, Patent list and General Bibliography, D.C. Bell and Richardson Inc. Hazardville, Conn., Plastics Tech. Eval. Center, Picalinny Arsenal, Dover J.J., Plastics Rpt. 18 Sept. (1964).

51. Ernsberger F.M., Glass Ind. 47, 422-427, 481-487-542-545, (1966).

52. Eschard G. and Manley B.N., Acta Electron, 14, 19-39 (1971).

53. Evans A.M., Williamson J.P.H. and Glasser F.P., J. Mat. Sci. 15, 2325 (1980).

54. Evastropev K.K., Veksler G.I. and Kondrateva B.S. Dokl. , Akad. Nauk. SSR, 215, 902(1974).

55. Frischart G.H. , Ionic Diffusion in Oxide Glasses, Trans. Tech. Publ. Aeder Mannsdorf, Switzerland (1976).

56. Fritzsche H, Amorphous and Liquid Semi conductors, (ed.) J. Tauc, Plenum , Chapt. 5 , 221 (1974).

57. Gardon R.'Thermal Tempering of glass' in Glass Science and Technology (ed.) D.R. Uhlmann and N.J. Krieidl , 145-213 (1980), Academic Press (N.Y.).

58. Garfinkel H.M., 'Membranes, Vol 1: Microscopic Systems and Models', (ed.) G. Eisenman , Dekker, 179-2[illegible] (1972, N.Y.) .

59. Garfinkel H.M., and King C.B. J. Am. Ceram. Soc. 53, 676 (1970).

60. Garfinkel H.M. J.Chem. Phys., 73 1766-1773 1969, .

61. Glass A.M., Nassau K and Negran T.J. , J. Appl. Phys. 49, 4808, (1979).

62. Glass A.M. and Nassau K. J. Appl. Phys. 51, 3756 (1980).

63. Graf. J. and Polbert R , Acta Electron 16, 11-22 1973).

64. Granqvist C.G and Buhrman R.A., J. Appl. Phys. 47, 220 (1976).

65. Griffish J.A. , Phil Trans. R. Soc. A221, 163-198 (1920 .

66. Gossink R.G., Philips Res. Repts. Suppl., 3 (1971).

67. Gupta M.C. and Ruoff A.L., J. Appl. Phys. 49, 5880 (1978, .

68. Hagenmuller P., Levasseur A, Lucat C., Roau J.M., and Villeneuve G., Fast Ion Transport in Solids (eds) P. Vashishta, G.K. Shenoy and J.N. Mundy 637 (1979) (North Holland, Elsevier).

69. Hahnert M., Silikttechn, 22, 241-246 (1971).

70. Hamim R.M. and Uhlmann D.R., Phys. Chem. Glasses, 11, 91 (1973).

71. Haller W., Blackburn D.H., Wagstaff F.E. and Charles R.J., J. Am. Ceram. Soc. 53, 34 (1970).

72. Hammel J.J. and Ohlberg S.M., J. Appl Phys., 36, 1442 (1965).

73. Hashin AZ. and Shtrikman S, J. Mech. Phys. Solids 11(2), 127-140 (1963).

74. Haven Y. and Stevels J.M. , Proc. Int. Congr. Glass 4th , 343-347 (1957)., Imprimerie Chaix, 20 rue Bergene, Paris.

75. Haven Y. and Verkerk B, Phys. Chem. Glasses 6, 38 (1965).

76. Helfferich F. , J. Phys. Chem. 66, 39 (1962).

77. Herous L., J. Appl. Phys. 29, 1639 (1958).

78. Hughes K. and Isard J.O. 'Phys. of Electrolytes' Vol.1 , (ed.) J.H. Hladic, 351-400 (1972) A.P. London.

78.(b) Hodge I.M., Ingram M.D. and West A.R., J. Electroanal Chem. 74, 125 (1976).

79. Irion M., Couzi M., Levasseur A., Pezu J.N., Bretous J.C., Solid State Chem. 31, 235 (1980).

80. Isard J.O. J. of Non Cryst. Solids. 4, 357 (1970).

81. Isard J.O. J. Non Cryst. Solids 1, 235 (1969).

82. Ivkin E.B. and Kolomiets B.T., J. Non Cryst. Solids 3, 41 (1970).

83. Jagla M. and Isard J.O. Mat. Res. Bull. 15, 1027 (1980).

84. James P.F., J. Mat. Sci. 10, 1802 (1975).

85. James P.F. and Mc. Millan P. ., Phil. Mag. 10, 963 (1963).

86. James P.F. and Mc. Millan P.J. Phys. Chem. Glasses 11, 59 (1970).

87. Jain H and Ngai K.L.'Proc. Workshop on Relaxation Phenomenon in Disordered Systems, Blacksburg V.A. July 1983 (U.S. Govt. Printing Office, 1985).

88. Kapany N.S.'Fibre Optics: Principles and Applications", (1967), Academic Press. (USA).
Kapany N.S. Scient. Am. 203, 72-81 (1960).

89. Kerreman G. and Tisenman G., Bull. Math. Biophys. 24, 213, (1962).

90. Kawamoto Y., J. Non Cryst. Solids 20, 393 (1976).

91. Kawazoe H., Hosono H. and Kanazawa T., J. Non Cryst. Solids, 2, 279 (1978).

92. Kawazoe H. Hosono H., Kokurai H, and Kanazawa T., J. Ceram. Society Japan 87, 237 (1979).

93. Kervawwez J.P. and Tomozawa M., J. Appl Phys. 51, 4391 (1980).

94. Kitao M., Jpn. J. Appl. Phys. 11, 1472(1972).

95. Kone A., Barreau B., Soudoct, J.L., and Ribes M., Mat. Res. Bull. 14, 393 (1979).

96. Kolomites B.T.,Phys. Stat. Solidi 7, 713 (1964).

97. Kulkarni A.R. 'Lithium ion conducting glassy solid electrolytes in the LiF-Li_2O-$Al(PO_3)_3$ systems, Ph.D. thesis submitted to IIT/ Kharagpur., (1984).

98. Kulkarni A.R. Maiti H.S. and Paul A. Glass formation and electrical conductivity in the system LiF-$Li_2O(PO_3)_3$, paper presented in 45th Annual Session of Indian Ceramics Society.

99. Kulkarni A.R. Maiti H.S. and Paul A., Bull Mater. Sci., 6 (2), 201-221 (1984).

100. Kristic, V.D., Philosophical Magazine A, 48 (5), 695-709 (1983).

101. Kristic, V.D., P.S. Nicholson, J. Am. Ceramic Soc. 60, 467 (1977).

102. Kristic V.D., Nicholson P.S. and Hoagland R.C., J. Am. Ceramic Soc., 64(9) 499-504 (1981).

103. Lamatos A.I. and Ubrowitz M., Phys. Rev. B3, 1791 (1971).

104. La Course J.C. In Introd. Glass Sci. Proc. Tutorial Symp. 1970 (ed.) L.D. Pye, 451-512 (1972). Plenum Press, (N.Y.).

105. Lawless W.N., Rev. Sci. Instr. 43, 1743 (1972).

106. Lecleach M. and Elmier J.F., J. Non Cryst. Solids 18, 265 (1975).

107. Levasseur A., Brethous J.C., Reau J.M and Hagenmuller P., Mat. Res. Bull. 14, 921 (1979).

108. Levasseur A. Brethous J.C., Hagenmuller P., Berge R. and Vignand , Solid State Commun. 32, 115 (1979b).

109. Levasseur A., Brethous J.C., Reau J.M. Hagenmuller P., Couzi M., Solid State Ionics 1, 117 (1980).

110. Levasseur A., Report EUR 707 F.R. Comm. European Communities Luxemberger, 40 (1981).

111. Levasseur A., Olazcuaga R., Kabla, M., Zahir M., Hagenmuller P., Couzi M., Solid State Ionics 2, 205 (1981).

112. Lavasseur A., Brethous J.C., Kabla, M., Hagenmuller P., Solid Stat. Ionics 5,651 (1981).

113. Levasseur A., Cales B., Reau J.M. and Hagenmuller P., Mat. Res. Bull. 13, 205 (1978).

114. Levasseur A., Kabla M. Brethous J.C. Reau J.M., Hagenmuller P., and Couzi M. Solid State Commun. 32, 939 (1979).

115 Linsley, G.S. Owen, A.E. and Hayatee F.M., J. Non Cryst., Solids 4, 208 (1970).

116. Loeweustein K.L.'The Manufacturing Technology of continuous Glass Fibres' (1973) Elsevier Scientific Company, Amsterdam Netherlands.

117. Loewenstein K.L., Phys. Chem. Glasses, 2,69 (1961).

118. Loewenstein K.L., Phys. Chem. Glasses 2, 119 (1961).

119. Loewenstein K.L. and Dowd J., Glass Technol., 9, 164 (1968).

120. Loewenstein K.L. and Parvin, Brit. Plastics Federation, 3rd Reinforced Plastics Conf. 12 (1962).

121. Mac Chesney J.B., 'Case History of Development of Optical fibres', Preparation and Characterisation of Materials (ed.) J.M. Honig and C.N.R. Rao 37-56 (1981), Academic Press (N.Y.).

122. Mac Dowell, J.F. and Beale J.H., J. Am. Ceram. Soc. 52, 17 (1969).

123. Mackenzie J.D., Proc. 10th Int. Congr. Glass, Kyoto, I.4, 71-81 (1974).

124. Mackenzie J.D. 'Electrical Conduction in Ceramics and glasses' Part B (ed.) N.N. Tallen, Marcel Deker, 559 (1974), (N.Y.).

125. Mackenzie J.D.'Modern Aspects of Vitreous State', Vol. 3 (1964), (ed.) J.D. Mackenzie, Butterworth London.

126. Malti H.S., Kulkarni A.R. and Paul A., 'Lithium Conducting Glassy Solid Electrolytes in the $LiF-Li_2O-Al(PO_3)_3$ system,' paper presented in 4th International Conf. on Solid State Ionics (1983) Grenoble, (France).

127. Majumdar A.J. and Ryder J.F. 'Glass Reinforcement of Cement Products', Glass Technology 9, (3), 78-84 (1968).

128. Malinin V.R., Evstropev K.K., Tsekhomskii V.A., J. Appl. Chem. USSR, 45, 172-174 (1972), Transl. from Zhur. Prikl., Khim. 45, 184-186 (1972).

129. Malugani J.P., Robert G., Solid State Ionics 1, 519 (1980).

130. Malugani J.P., Robert G., Mater. Res. Bull. 14, 1075 (1979).

131. Malugani J.P. Wasniewski A., Doreau Mand Robert G., C. R. Acad. Sci. 287, 455 (1978). (Paris).

132. Manfre G., Meeting Am. Ceram. Soc. Bedford Springs Pa., Oct. (1967).

133. Mansingh A., J. Phys. C9, 1209 (1976).

134. Mansing A, Tandon R.P. and Vaid J.K., J. Phys. Chem. Solids 36, 1267 (1975).

135. Mansingh A., J. Phys. C9, 1023 (1975).

136. Markov V.P. and Kepylov O.M., Glass Ceramics, 27, 723-725 (1970) (English Transl.).

137. Matousek, J., Silikaty 12, 73-79, 86-95 (1968), Matousek J., Nemec L: Sb.Vys. S.Y. Chem. Technol. Praze norg. Chem. Technol. B16, 99-117 (1973).

138. Magistics A., Chiodelli, A., and Carpani C.V., Z.Naturf. 31a, 974 (1976).

139. Mazurin O.V. and Strettsina E.V., J. Non Cryst. Solids, 11, 199 (1972).

140. Mc. Creight L.R. Rauch H.W., Sr. and Sutton W.H.,'Ceramics and Graphide Fibres and Whiskers (1965), Academy Press (N.Y.).

141. Mc Geehin P., and Hooper A., J. Mat. Sci. 12, 1 1977).

142. Mac Millan P.W., Glass Ceramics, 71 (1979) (Academic Press, London.) N.Y.)

143. Mc Millan P.W., Phys. Chem. Glasses 17, 193 (1976).

144. Minami T., Nambu H. and Tanaka M., J. Am. Ceram. Soc. 60, 467 (1977).

145. Minomura S. 'Amorphous Semi conductors, Technologies and Devices (ed.) Y. Harakawa 245(1982) (Amsterdam: North Holland).

146. Minomura S., High Pressure and Low Temperature Physics, (ed.) C.W. Chu and J.A. Woolam 483 (1978) (N.Y., Plenum).

147. Morley J.G. 'Reinforcing Metals with Fibres' New Scientist, 322, 122-125 Jan. 17 (1963).

148. Morley J.G. 'Strength of Glass Fibres' Nature 184,(4698), 1560 Nov. (1959).

149. Moriya Y. Warington D.H. and Douglas R. W., Phy. Chem., Glass 8, 19 (1967).

150. Mott N.F., Contemp. Phys. 19, 225-45 (1977).

151. Mott N.F. J. Non Cryst. Solids 1, 1-17, (1968).

152. Mott. N.F. Adv. Phys. 16, 49 (1967).

153. Mott N.F. and Davis E.A., Electronic Processes in Non Crystalline Solids Ist Ed. (1971). (Oxford Press).

154. Mozhi, T., Arul and Chakravorty D., J. Of Mat. Sc. Letters, 1, 426-428 (1982).

155. Murawski L., Chung C.H. and Mackenzie J.D., J. of Non Cryst. Solids, 32, 91 (1979).

156. Murawski L. and Gnowski O., Phys. Stat. Solidi (a), 24, K115 (1974).

157. Nakajima T. 'Annual report conference on Electrical Insulation and Dielectric Phenomena (1972-1971), Natl. Acad. Sci.

158. Nono Tsutomo, Oguchi Tamiyuku (Kanegafuchi Chemical Indus Co. Ltd. Pat. Applied E.P. 130575 (Cl. H01B1/08), 9 Jan. 1985, J.P. Applied.

159. Narasimham P.S.L. and Rao K.J. , J. Non Cryst. Solids 27, 225, (1978).

160. Nassau K., Glass A.M. and Olson D.W., J. Electrochem. Soc., 127, 2743 (1980).

161. Nassau K., and Glass A.M., J. Non Cryst. Solids 44, 97 (1981 b).

162. Nassau K., Cava R.J. and Glass A.M., Solid State Ionics 2, 153 (1981 a).

163. Nassau K., Wang C.A. and Grasso M., Jm. Ceram. Soc. 62, 74 (1979 a).

164. Nassau K., Wang C.A. and Grasso M., Jm. Ceram. Soc. 62, 503 (1979 b).

165 Neilson G.F., Phys. Chem. Glasses 10, 54 (1969).

166. Neilson G.F., Phys. Chem. Glasses 13, 70 (1972).

167. Nemilov S.V. and Galev I.S. , Inorg. Mater. 8, 294-297 (1972).

168. Nedov S., Gerasimova I., Kochukhorov, V. and Marinov I., J. Mat. Sci. 15, 1153 (1980).

169. Mimikawa H.'Researches of Electrochemical Laboratory, No. 757' (Agency of Industrial Sciences and Technology) (1975).

170. Niizeki , Nobukazu , Jpn. Annu. Rev. Electron Comput. Telecom. 11, 168-78 (1984).

171. Orowan E. Rep. Prog. Phys. 12, 185-232 (1949).

172. Otto K.,Phys. Chem. Glasses 7, 29, (1966).

173. Otto K. and Milberg M.E., J. Am. Ceram. Soc. 51, 326 (1968).

174. Ovshinsky S.R. , Proc. 7th Int. Conf. on Amorphous and Liquid Semiconductors (ed.) W.E. Spear, G.G. Stevenson, Dundee, 519 (1977).

175. Owen A.E. , J. Non Cryst. Solids 25, 370 (1977).

176. Owen A.E., Contemp. Phys. 11, 227-96 (1970).

177. Owen A.E., Prog. Ceram. Sc. Vol. 3, 77 (1963), Pergeron Press.

178. Owen A.E. and Robertson J.M., J. Non Cryst. Solids 2, 40, (1970).

179. Owen A.E. and Spear W.E. , Phys. Chem. Glasses 17, 174-92, (1976).

180. Parkyn Brian'Glass Reinforced Plastics' (ed.), Butterworth and Co., London 11-108 (1970).

181. Parkyn B., Fl. R. Soc. Arts Cal., 205-23 (1963).

182. Parthasarthy G and Gopal E.S.R., Bull. Mater. Sci. 6, (2), 231-242 (1984).

183. Pavlovskii V.K.'Steklobraznoe Sostoyanie 5,149-153 (1970).

184. Pfister G., Phys. Rev. Letts. 36, 271 (1976).

185. Pronkin A.A. , Sov. J. Phys. Chem. 4, 388 (1978).

186. Prasad E., Sayer M. and Vyas H.M., J. Non Cryst. Solids, 40, 119 (1980).

187. Proctor B.A. in CI 70, Fibres Concrete , The Concrete Society, 69-86 (1980), published by The Construction Press Ltd. Lancaster (U.K.)

188. Proctor B.A. and Yale B. Royal Society Dicussion Meeting, New Fibres and their composites, May (1978) (London) to be published in Proceedings of Royal Society.

189. Proctor B., Phys. Chem. Glasses 3, 7-27 (1962).

190. Provance J.D. and Huebner J.S., J. Am. Ceramic Society 54, 147 (1971).

191. Quinn R.K. and Seager C.H., J. Non Cryst. Solids 17, 386, (1975).

192. Rao K.J. and Elliott S.R. (1981) results to be published.

193. Ravaine D and Soucuet J.L. , Solid Electrolytes, General Principles Characterisation, Materials Application (ed., P. Hagenmuller and W. Van Gool 277, (1978) (N.Y., Acad. Press.

194. Ravaine D and Soucuet J.L., Phys. Chem. Glasses 18, 27, (1977).

195. Ravaine D and Soucuet J.L., Proc. 24th Meeting ISE Eindhoven (1973).

196. Rawal B.S. and Maccrone R.K., J. Non Cryst Solids 22, 347, (1978).

197. Rawson H., Properties and Applications of Glass (ed.) (1984' Elsevier Science Publishers, Amsterdam, Netherlands.

198. Riebling E.F., J. Chem. Phys. 55, 804 (1971).

199. Rockstad H.K., J. Non Cryst. Solids B-1C, 621 (1972).

200. Roskos T.G. et. al
'Interfacial Properties of an Amine-modified Silane and its Preformed Polymer at E glass surfaces' SPE Trans., 2, (4) 326-331 Oct. (1962).

201. Russel K.C., 'Phase Transformations' (ed.) H.I. Aronson (Amer. Soc. Metals ' distributed by Chapman and Hall, 219, (1970) (London).

202. Ryabov V.A. and Kupfer V.V., Glass Ind. 51, 268, 271 (1970).

203. Ryabov V.A., Semenov N.I. and Paplauskao A.B, Glass Technol. 13, 168-170 (1972).

204. Sakai N. and Fritzsche H., Phys. Rev. B15, 973 (1977).

205. Sayer M., and Mansingh A. Phys. Rev. B6, 4629 (1972).

206. Sayer M., Reeves J.M. and Rosenblatt C., J. Appl. Phys. 42, 2857 (1971).

207. Schaeffer H.A. and Heinze R , Glastech. Ber, 47, 199 (1974).

208. Schonhorn H., Kurkjian C.R., Jaegar, R.E. Vazirani H.N., Albarino R.V. and Di Marcella F.V, Appl. Phys. Lett. 29, 7.2 (1976).

209. Sehonhorn H., Vazirani H.N. and Frisch H.L., J. Appl. Phys. 49 (7), 3703-6,July (1978).

210. Seager C.H., Emin D. and Quinin R.K., Phys. Rev. B10, 4746, (1973).

211. Segawa H., J. Phys. Soc. Jpn. 36, 1087 (1974).

212. Seward, T.P., Uhlman. D.R. and Turnbull D.R., J. Am. Ceram. Soc. 51, 634 (1968).

213. Shaw R.R. and Uhlmann D.R., J. Non Cryst. Solids 5, (3) 237-263 (1971).

214. Simmons J.H., Maceda, P.B., Napollitano, A. and Haller W.K., Discuss Faraday Soc. No. 50155-165 (1970).

215. Simmons J.H., Mills S.A. and Napolitano A., J. Am. Ceram. Soc. 57, 109, (1974).

216. Smedly S.I. and Angell C.A., Solid State Commun. 27,21 (1978).

217. Smith J.W. and Walker, T.W.D., Application of glass fibre Cement 174-188 (1980).'CI80 Fibrous Concrete, The Concrete Society published by The Construction Press Ltd. Lancaster (U.K.).

218. Smithard M A.and Dupreer , Phys. Status Solidi, A11, 695, (1972).

219. Souquet J.L., Kone A.and Ribes M., J. Non Cryst. Solids 38, 39, 307 (1980).

220. Srinivasan G.R., Colella R., Macedo P.G. and Volterra V., Phys. Chem. Glasses, 14, 90, (1973).

221. Srinivasan G.R., Sarkar A., Gupta, P.K. and Mercedo P.B., J. Non Cryst. Solids 20, 141 (1976).

222. Srinivasan G., Tweer I., Macedo P.B., Sarkar A. and Haller W., J. Non Cryst. Solids 6, 221 (1971).

223. Srivastava A., M.Tech. Thesis (1978), IIT/ Kanpur.

224. Srivastava A. and Chakravorty D., J. of Instution of Engineers (1979) (India) 59, I3, Journal IDJE 59, 104-107.

225. Stephanie C., Kunz, J. Am. Ceramic Soc. 66 (4), C73 (1983).

226. Stevels J.M. 'The Electrical Property of Glasses'[Handbuch der Physic] Vol. XX., (ed.) S.W. Flugge 350 (1957) (Springer-Verlog, Berlin).

227. Stookey S.D., Glastech. Ber. V. International Glass Congress 32K, Heft V. (1959).

228. Sundar H.G.K. and Rao K.J., J.C.S.I., 76, 1617 (1980).

230. Takahashi T. and Yamamoto O, Chem. Phys. Lett. 135 (1979).

231. Takamori T and Tomozawa M., J. Am. Ceram. Soc. 62, 373, (1979).

232. Takamori T and Tomozawa M. J. Am. Ceram. Soc. 61, 509, (1978).

233. Takamori T and Tomozawa M.J. Am. Ceram. Soc. 59, 377, (1976).

234. Taylor H.E., J. Soc. Glass Tech. 43, 124T (1959).

235. Taylor H.E., J. Soc. Glass Tech. 41, 350T (1957).

236. Taylor H.E., Trans. Farad. Soc. 52, 873 (1956).

237. Terai R.H. and Hayami R , J. Non-Cryst. Solids 18, 217, (1975).

238. Thomas W.F. , Phys. Chem. Glasses 1, 4 (1960).

239. Tomozawa M.and Takamori T, J.Am. Ceram. Soc. 63, 276 (1980).

240. Tomozawa M., J. Am. Ceram. Soc. 61, 444 (1978).

241. Tomozawa M. and Takamori T., J. Am. Ceram. Soc. 60, 301, (1977).

242. Tomozawa M.'Treatise on materials science and technology' (eds.) M. Tomozawa and R.H. Doremus, 12, 283 (1977). (N.Y.) Acad. Press.

243. Tomozawa M. Mac Crone R.K. and Herman H, Phys. Chem. Glasses 11, 136 (1970).

244. Trap. H.J.L, Acta Electron 14, 41-77 (1971).

245. Tsuchiya T. and Moriya T.,Glass Ceram. Bull 22, 55, (1975).

246. Tuller H.L. Button D.P. and Uhlman D.R., J. Non Cryst. Solids, 40, 93 (1980).

247. Varshneya A.K. , J. Am. Ceram. Soc. 58, 106 (1975).

248. Vaughan J.G., Perry C.H. and Kinsor D.L. Phys. Chem. Glasses 18, 87 (1977).

249. Venkateswaran A. M. Tech. Thesis (1979), IIT Kanpur

250. Washington D., Duchenois V, Polaert R and Beasley R.M., Acta. Electro. 14, 201-24(1971).

251. Weatall H.H., Nature, 223, 959 (1969).

252. Weibull W. , J. Appl. Mech. 18, 293 (1951).

253. Weinberg Mc and Neilson G.F., J. Mat. Sci. 13,1206 (1978).

254. Wiederhorn S.M., 'Mat. Sci. Res' 3, 503-25 (1966) (eds.) W.W. Kriegel and H. Palmour (N.Y.) Plenum Press.

255. Wiederhorn S.M., J. Am. Ceram. Soc. 53, 486-489 (1970).

256(a) Wojnarovits I., J. Am. Ceram. Soc, 66, (12), 896-8 (1983).
256(b) Wong J. and Angell C.A., Glasses: Structure by Spectroscopy (M. Dekker, N.Y. (1976).

257. Zarzycky J., C.R. Acad. Sci. Paris, Ser.C. 278(8),487-90(1974).

258. Zarzycki J. and Naudin F., Phys. Chem. Glasses 8, 11 (1967).

259. Zarzycki J. and Naudin F., J., Non Cryst.Solids, 1, 215, (1969).

260. Zvanut C., Contract Report No. 28-D P.118 'Ceramic and Graphite Fibres and Whiskers'' (ed.) Mc Creight L.R., H.W. Rauch., Sr, and W.H. Sutton Academic Press (1965), (N.Y.).